

Order N°: 4066

THESIS

Presented at

UNIVERSITY BORDEAUX I

DOCTORAL SCHOOL OF CHEMICAL SCIENCES

By

Sana AHMAD

TO OBTAIN THE DEGREE OF

DOCTOR

SPECIALITY: ORGANIC CHEMISTRY

PREPARATION AND CHARACTERIZATION OF CYCLOPENTADIENYL TITANIUM-BASED ORGANIC- INORGANIC HYBRID MATERIALS

Defended on: **30th September 2010**

After approval of:

A. VIOUX , Professor, University Montpellier 2	Referee
F. RIBOT , Researcher CNRS, LCMCP, University Paris 6	Referee

In front of a jury composed of:

L. SERVANT , Professor, University Bordeaux 1	President
A. VIOUX , Professor, University Montpellier 2	Referee
F. RIBOT , Researcher CNRS, LCMCP, University Paris 6	Referee
B. BUJOLI , Director of research CNRS, University of Nantes	Examiner
T. TOUPANCE , Professor, University Bordeaux 1	Examiner
B. JOUSSEAUME , Director of research CNRS, University Bordeaux 1	Examiner

Dedication

This thesis is dedicated to my parents,
my brother and my sisters,
for their love and support

Acknowledgement

This work has been carried out in the materials group, Institute of Molecular Sciences, University Bordeaux 1. It would not have been possible without the contribution of a lot of people.

First of all I would like to thank Prof. Laurent Servant, head of doctoral school of chemistry, for presiding my thesis jury. I am also grateful to him for his help in interpreting the infrared and Raman spectroscopic results. I would like to pay my regards to Prof. André Vioux, University Montpellier 2 and Dr. François Ribot, University Paris 6 who generously provided time, energy and valuable suggestions in evaluating my thesis as a referee. Special thanks to Dr. Bruno Bujoli, University of Nantes, for his time and encouraging remarks about my work.

I would like to express my sincere appreciation to Dr. Bernard Jousseume, director of research CNRS, for his generosity, time and continuous involvement in the project. Without his encouragement and support this work would not have been possible. I cannot forget his help both in and out of the lab to facilitate my stay in Bordeaux.

I am grateful to Prof. Thierry Toupance for co-supervising my thesis and being a member of my jury. I gained a lot from him during several discussions we had in these three years. In spite of his busy schedule, he was always interested in my work which helped me tremendously.

I would like to thank a lot of people who were involved in this project: Madam Odile Babot (ISM) for doing nitrogen sorption-desorption and thermogravimetric analysis on my samples. Her ready availability and gentle behavior facilitated the timely understanding of the results; Prof. Cécile Zakri (CRPP) for the powder X-ray diffraction analysis on my hybrid samples; Dr. Guy Campet (ICMCB) for the X-ray diffraction analysis on TiO₂ samples; Madam Christine Labrugère (ICMCB) for the XPS measurements on thin films.

I cannot forget Dr. Joachim Brötz, TU Darmstadt, for welcoming me to Darmstadt and facilitating my integration in the group. His involvement in the X-ray diffraction analysis of thin films deserves special appreciation. I would also like to thank Madam Ulrike Kunz for taking TEM images of TiO₂ powders.

Although I had many acquaintances during my PhD, I also formed some true and long lasting friendships including Laetitia Renard, Fauzia Allama, Ludmila Cojocar, Michael Ramin, M. Tamez Uddin and Suvendu Sekhar Dey. I would especially like to thank Laetitia for her help throughout my stay in the lab whether it is regarding my work or it concerns my French language limitations.

In a general manner I would like to thank all members of materials group for their generosity and cooperation and for maintaining a very competitive yet friendly environment in the group.

GENERAL INTRODUCTION

The possibility of combining the dissimilar properties of organic and inorganic components in one material has been an old challenge in industrial development. This field of science has been probably inspired by nature's remarkable ability to combine these entirely different components at nanoscale allowing the construction of smart natural materials e.g., mollusk shells, bone, etc. In industry, however, the main challenge is to synthesize hybrid combinations that keep or enhance the best properties of each of the components while eliminating or reducing their particular limitations. Hence the properties of these materials are not the sum of the individual contributions of both phases. These unique combinations, called organic-inorganic hybrid materials, propose unlimited combinations of components to create versatile materials with known and some unknown properties. Their uses in optics, electronics, mechanics, membrane, catalysis, etc. have given better results than the pure individual components¹.

The nature of the interface between the two components that has a very important role, is generally used to divide these materials into two distinct classes:

In **class I**, organic and inorganic components are embedded and only weak bonds (hydrogen, van der Waals etc.) give the cohesion to the whole structure.

In **class II** materials, the two phases are linked together through strong chemical bonds (covalent or ionic-covalent bonds).

Although the development of these organic-inorganic hybrid materials has been going on for centuries, a turning point was reached with the emergence of sol-gel science that opened a gateway to whole classes of new materials. The mild reaction conditions offered by the sol-gel process allow the introduction of organic molecules inside an inorganic network without decomposition. Inorganic and organic components can hence be mixed at the nanometric scale, in virtually any ratio leading to so-called hybrid organic-inorganic materials that are extremely versatile in their composition, processing and optical and mechanical properties.

So far class II materials have been developed mostly with silicon due to easy preparation of its precursors and stability of silicon-carbon bond during hydrolysis in sol-gel process. These materials have shown a high degree of organization either by self-assembly² or by the use of surfactants³. Some self-assembled tin-based materials⁴ have been developed as well. However, this field of science has not been studied with transition metals due to the fragile nature of transition metal-carbon bond towards hydrolysis. Hybrid materials using oxygen bridges between metal and carbon have only been described up to now. Hence there is a lot of potential for further development in this area.

In our research, we are interested in the preparation of well-organized titanium-based hybrid materials having a defined organic network, a homogeneous distribution of the metal

throughout the material and titanium-carbon bonds to link both networks. The problem of instability of titanium-carbon bond can be overcome by using strong organic ligands like cyclopentadienyl ligands, that instead of forming a σ -bond, held the metal using a π -bond instead that is reasonably stable towards hydrolysis.

The first goal of the project is the synthesis of di(cyclopentadienyltitanium) precursors with some organic groups acting as a spacer between the two cyclopentadienyl groups. The organic groups should play an important role in the self-assembly of the nanostructures. The nature of these groups would be varied in order to study their effect on the organization of the materials. The cyclopentadienyl groups should carry the metal equipped with three hydrolysable groups. The **2nd chapter** of the thesis explains the synthesis of various di(cyclopentadienyltitanium) precursors.

The next part of the project involves the hydrolysis of these precursors in a sol-gel process leading to the required hybrid materials after condensation. The inorganic network should consist of Ti-O-Ti bonds connected to the organic network through carbon-titanium π -bonds. The **3rd chapter** of the present work summarizes the mode of preparation and the complete characterization of these materials.

The unique properties of nanocrystalline titanium dioxide make it a very useful material in various applications including pigments, photocatalysis, photovoltaic applications etc. The **4th chapter** of the thesis describes the thermolysis of the prepared hybrid materials to synthesize nanocrystalline titanium dioxide as powders or films.

¹ (a) Kickelbick, G., *Hybrid Materials: Synthesis, Characterization and Applications*, Wiley-VCH, Weinheim, **2007** (b) Gomez-Romero, P.; Sanchez, C., *Functional Hybrid Materials*, Wiley-VCH, Weinheim, **2004** (c) Sanchez, C.; Julián, B.; Belleville, P.; Popall, M. *J. Mater. Chem.* **2005**, *15*, 3559

² (a) Moreau, J. J. E.; Vellutini, L.; Wong Chi Man, M.; Bied, C.; Bantignies, J. L.; Dieudonne, P.; Sauvajol, J. L. *J. Am. Chem. Soc.* **2001**, *123*, 7957 (b) Moreau, J. J. E.; Vellutini, L.; Wong Chi Man, M.; Bied, C. *J. Am. Chem. Soc.* **2001**, *123*, 1509 (c) Muramatsu, H.; Corriu, R. J. P.; Boury, B. *J. Am. Chem. Soc.* **2003**, *125*, 854

³ (a) Fujita, S.; Inagaki, S. *Chem. Mater.* **2008**, *20*, 891 (b) Hatton, B.; Landskron, K.; Whitnall, W.; Perovic, D.; Ozin, G. A. *Acc. Chem. Res.* **2005**, *38*, 305

⁴ (a) Sanchez, C.; Ribot, F.; Lebeau, B. *J. Mater. Chem.* **1999**, *9*, 35 (b) Elhamzaoui, H.; Jousseume, B.; Riague, H.; Toupance, T.; Dieudonné, P.; Zakri, C.; Maugey, M.; Allouchi, H. *J. Am. Chem. Soc.* **2004**, *126*, 8130 (c) Elhamzaoui, H.; Jousseume, B.; Toupance, T.; Zakri, C.; Biesemans, M.; Willem, R.; Allouchi, H. *Chem. Commun.* **2006**, 1304

SUMMARY

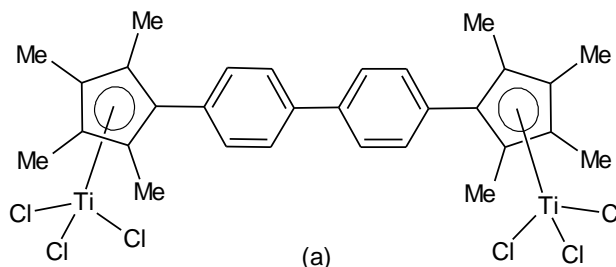
Chapter I: Literature review	5
1. Organic-inorganic hybrid materials	7
2. Sol-gel process	10
3. Silicon-based hybrid materials	19
4. Tin-based hybrid materials	27
5. Transition metal-based hybrid materials	31
6. Conclusion	33
Chapter II: Synthesis of di(cyclopentadienyltitanium) precursors	39
1. Synthesis of dicyclopentadienyl ligands	40
1.1. Synthesis of the ligands with linear aromatic spacers	43
1.2. Synthesis of the ligands with mixed aryl-alkyl spacers	47
1.3. Synthesis of the ligands with long lateral chains containing spacers	49
2. Synthesis of dititanium complexes	52
2.1. Syntheses of di(cyclopentadienyltriisopropoxytitanium) complexes	54
2.2. Syntheses of di(cyclopentadienyltrichlorotitanium) complexes	56
2.3. Syntheses of di(cyclopentadienyltrimethyltitanium) complexes	58
2.4. Syntheses of di(cyclopentadienyltribenzyltitanium) complexes	59
2.5. Syntheses of monocyclopentadienyltitanium complexes	60
3. Conclusion	63
Chapter III: Preparation of titanium-based hybrid materials	67
1. Preparation of hybrid materials with linear spacers	68
1.1. Hybrid materials from di(cyclopentadienyltriisopropoxytitanium) precursors	68
1.2. Hybrid materials from di(cyclopentadienyltrimethyltitanium) precursors	81
1.3. Hybrid materials from di(cyclopentadienyltribenzyltitanium) precursors	94
2. Preparation of hybrid materials with lateral chains	98
3. Conclusion	103
Chapter IV: Preparation of titanium dioxide from titanium-based hybrid materials	107
1. Introduction	108
2. Preparation of titanium dioxide powders	110
3. Preparation of titanium dioxide thin films	117
4. Conclusion	124
Chapter V: Experimental section	131
1. Experimental section related to chapter II	134
1. Experimental section related to chapter III	162
2. Experimental section related to chapter IV	164

List of abbreviations

XRD:	X-ray diffraction analysis
TGA:	Thermogravimetric analysis
SEM:	Scanning electron microscopy
TEM:	Transmission electron microscopy
HRTEM:	High resolution transmission electron microscopy
XPS:	X-ray photoelectron spectroscopy
BET:	Brunauer-Emmett-Teller
FT-IR:	Fourier transform infrared
TiO₂:	Titanium dioxide
UV:	Ultraviolet
RT :	Room temperature
THF :	Tetrahydrofuran
NMR:	Nuclear magnetic resonance
ppm:	Parts per million
Hz:	Hertz
J:	Coupling constant
Me:	Methyl group
OH:	Hydroxyl group
Oi-Pr:	Isopropoxy group
OR:	Alkoxy group
h:	Hour
min:	Minute

Nomenclature

Compound (a) has been named as $[\mu\text{-}[1,2,3,4,5\text{-}\eta\text{:}1',2',3',4',5'\text{-}\eta\text{-}][1,1'\text{-biphenyl}]\text{-}4,4'\text{-diylbis}(2,3,4,5\text{-tetramethyl-}2,4\text{-cyclopentadien-1-ylidene})]]\text{hexachlorodititanium}$ according to IUPAC nomenclature. However a simpler name also reported in the Chemical Abstract is 4,4'-biphenylene(2,3,4,5-tetramethylcyclopentadienyl)di(titanium trichloride). This simpler name was used as model for naming all the compounds prepared in this work.



CHAPTER I. LITERATURE REVIEW

The ever ongoing industrial development along with the desire for new functions generate an enormous demand for novel materials. Classical materials such as metals, polymers or ceramics cannot fulfill all requirements for various new applications. The idea of improving the properties of a pure substance by mixing it with another one has been known for centuries. The most common example is the group of composites in which a basic structural unit is incorporated into another component named the matrix. Generally the resulting materials show better mechanical properties than the original matrix. Examples are inorganic fiber-enhanced polymers in which the structural building blocks that are inorganic in nature are incorporated into a polymeric matrix. It has also been established that a reduction in size of both inorganic and organic units can lead to more homogeneous materials with better tunable properties. In that case where the level of mixing of the two components is at the nanometer or molecular level, the term hybrid material is used instead of composite material. This reduction in the domain size produces materials that show characteristics of both original phases and even new properties¹.

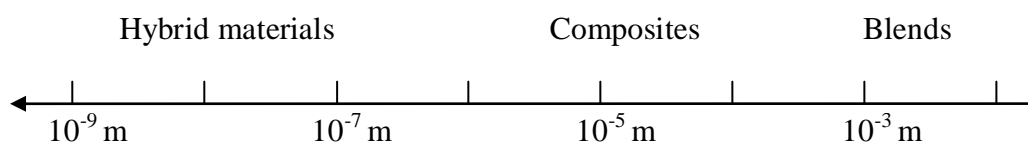


Figure I-1: Domain size in hybrid materials

The origin of hybrid materials, however, did not take place in the chemical laboratory but in nature. A lot of natural materials consist of inorganic and organic building blocks distributed on the macromolecular or nanoscale. In most cases the inorganic part provides mechanical strength and overall structure to the natural objects while the organic part serves to bind the inorganic building blocks. Typical examples of such materials are bone and nacre (Figure I-2).



Figure I-2: The iridescent nacre inside a Nautilus shell (Example of hybrid material)

The process of combining the properties of organic and inorganic components into a novel composite material was carried out as early as in ancient times. At that time the production of bright and colorful paint was the driving force to try different combinations of dyes and inorganic pigments. Maya blue is an example of such man-made materials. Ancient Maya fresco paintings are characterized by bright blue colors that had been miraculously preserved for about 12 centuries². Maya blue is actually a man-made hybrid organic-inorganic

material in which molecules of the natural blue indigo are encapsulated within the channels of a clay mineral known as palygorskite. It is a true example of hybrid materials which combines the resistance of an inorganic network and the color of an organic pigment in one material having properties well beyond those of a simple mixture of its components³.

Since the beginning of the industrial era, some coloring agents or inorganic charges have been dispersed in organic components (solvents, surfactants, polymers, etc.) to improve their optical and mechanical properties. However, the concept of organic-inorganic hybrid material exploded very recently with the development of soft inorganic chemistry process, also called sol-gel process. This process, which will be explained later in detail, allows the production of inorganic materials at low temperature and hence preserves the organic part of the material.

Organic-inorganic hybrids can be applied in many areas of material chemistry because they are simple to process and are amenable to design on the molecular scale. Currently there are four major research topics in the synthesis of organic-inorganic materials: (a) their molecular engineering, (b) their nanometer and micrometer-sized organization, (c) the transition from functional to multifunctional hybrids, and (d) their combination with bioactive components¹.

I. Definition: organic-inorganic hybrid materials

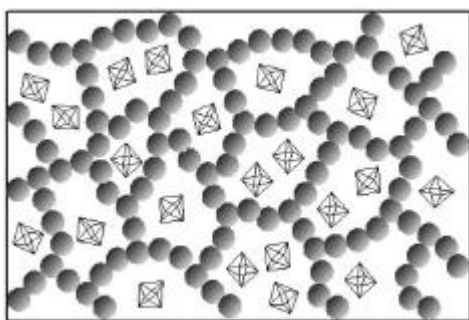
A hybrid material is generally defined as a material that includes organic and inorganic moieties blended at the molecular scale.

A tentative classification of hybrid materials based on the interactions connecting the inorganic and organic species has been proposed⁴.

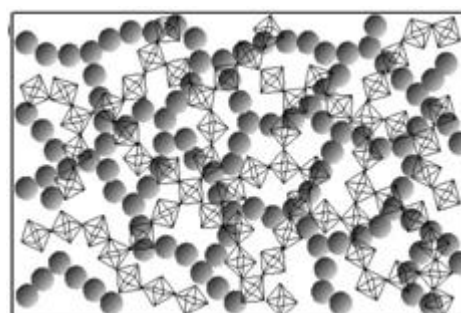
In **Class I hybrid materials**, organic and inorganic components are embedded and only weak bonds (hydrogen, van der Waals or ionic bonds) give the cohesion to the whole structure.

In **Class II hybrid materials**, part of the two phases are linked together through strong chemical bonds (covalent or ionic-covalent bonds).

Class I hybrids

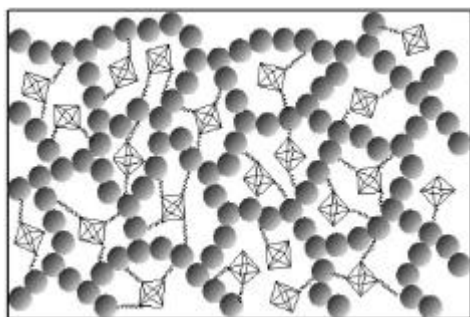


(a) Blends

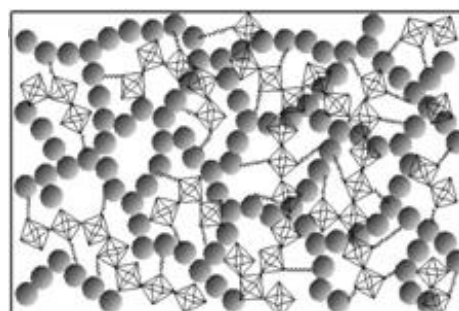


(b) Interpenetrating networks

Class II hybrids



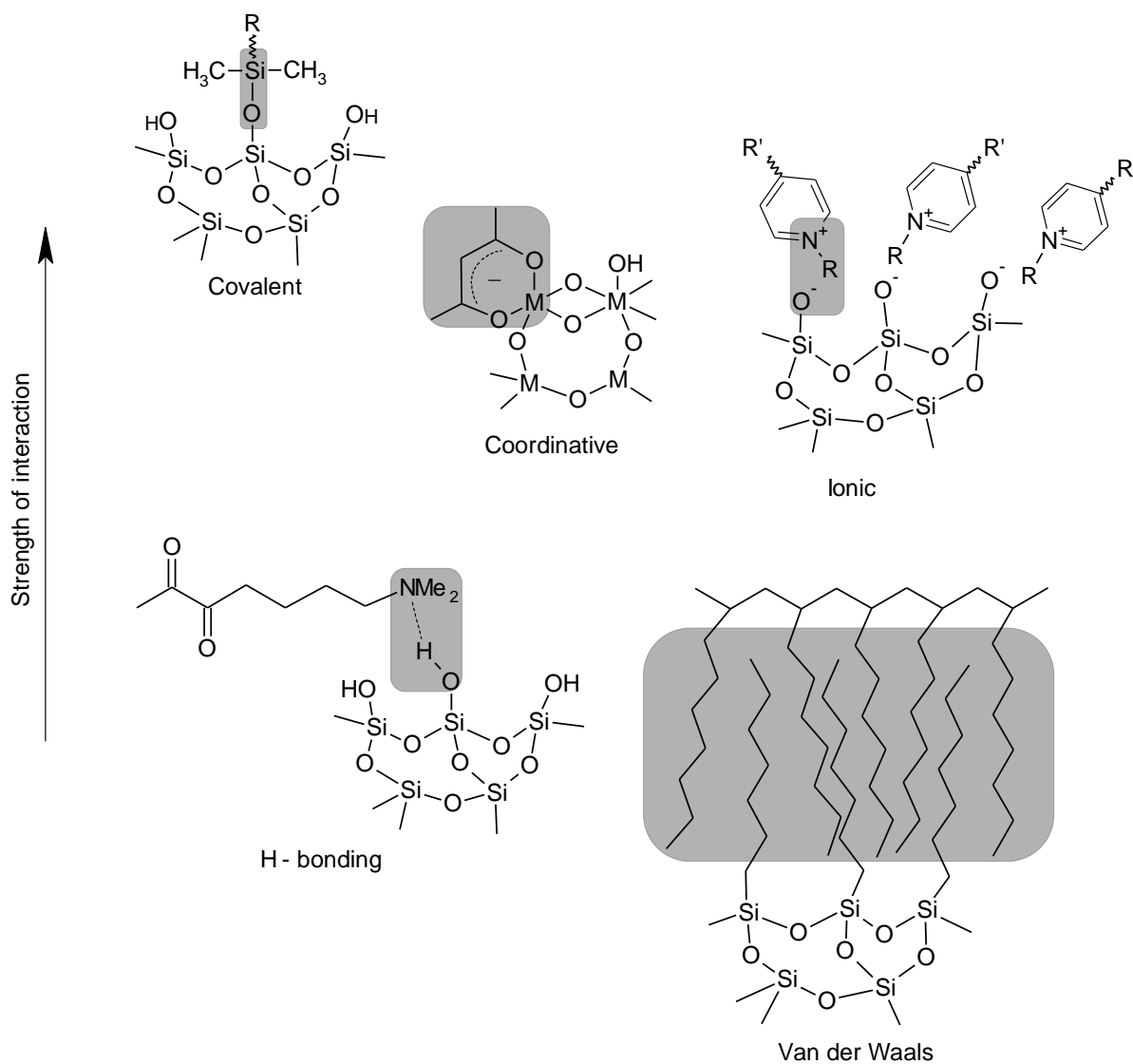
(c) Building blocks covalently connected



(d) Covalently connected polymers

Figure I-3: Different types of hybrid materials (Figure taken from reference 1)

Because of the gradual change in the strength of chemical interactions it becomes clear that there is a steady transition between weak and strong interactions (Figure I-4).

**Figure I-4:** Relative strength of various interactions in hybrid materials

Type of interaction	Strength (kJmol ⁻¹)	Range	Character
Van der Waals	ca. 50	Short	Nonselective, non directional
H-bonding	5 - 65	Short	Selective, directional
Coordination bonding	50 - 200	Short	Directional
Ionic	50 - 250*	Long	Nonselective
Covalent	350	Short	Predominantly irreversible

Table I-1: Different chemical interactions and their relative strength

*Depending on solvent and ion solution; data for organic media.

Some examples for class I and class II materials are⁵:

Class I

- organic dyes in inorganic matrices (Maya blue)
- organic monomers embedded and polymerized in porous inorganic matrices
- inorganic particles embedded in polymers
- polymers filled with inorganic particles generated in-situ
- simultaneous formation of interpenetrating organic and inorganic networks

Class II

- hybrids using organically modified polysilsesquioxanes based on
 - sequential synthesis of inorganic and organic networks
 - polyfunctional alkoxy silanes
 - alkoxy silanes functionalized polymers
- hybrids based on transition-metal oxide networks

The different possibilities of composition and structure of hybrid materials are given in Table I- 2.

Matrix:	crystalline ↔ amorphous
	organic ↔ inorganic
Building blocks:	molecules ↔ macromolecules ↔ particles ↔ fibers
Interaction between components:	strong ↔ weak

Table I-2: Different possibilities of composition of hybrid materials

Two different strategies are mainly used to prepare hybrid materials:

- Well-defined organic and inorganic building blocks react with each other to form the final hybrid material. In this case the precursors still, at least partially, keep their original identity.
- In situ formation of the components: one or both structural units are formed from the precursors that are transformed into a novel structure, as a network for instance.

As previously discussed the chemistry of hybrid materials has progressed very recently with the development of soft chemical process, well-known as the sol-gel route, for the preparation of these materials.

II. Sol-Gel Process

The sol-gel route consists of the formation of a polymeric structure by polycondensation of small molecules in solution. It is a low temperature synthetic route which allows to obtain new materials with non-traditional physical and chemical properties⁶. Usually the reaction results in a homogeneous and pure three-dimensional cross-linked network. It is particularly interesting for the formation of glassy and ceramic materials at temperatures much lower than the conventional techniques. Thus inorganic materials and organic-inorganic hybrid materials can be processed to form nanoparticles, coatings, fibers, or bulk materials⁷ (Figure 1-5).

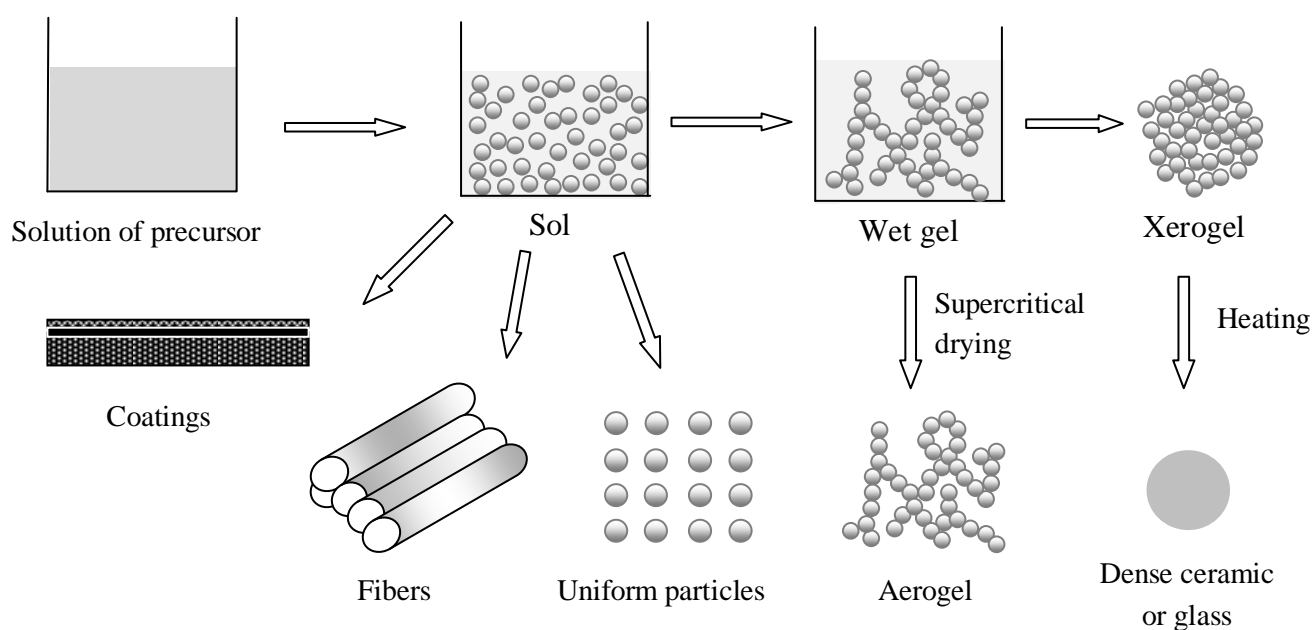


Figure I-5: Shape of the various products available through processing by sol-gel technology

The sol-gel process involves several steps: evolution of inorganic networks, formation of colloidal suspension (sol) and gelation of the sol to form a network in a continuous liquid phase (gel). The texture (porosity) and the morphology of the final material depend on the nature of thermal treatment used for drying the sol or the gel.

By definition *sols* are dispersions of colloidal particles in a liquid. *Colloids* are solid particles with diameters of 1-100 nm⁸. A *gel* is an interconnected, rigid network with pores of submicrometer dimensions and polymeric chains the average length of which is greater than a micrometer.

The term "gel" represents a variety of substances that can be classified in the following categories⁹:

- well-ordered lamellar structures
- covalent polymeric networks, completely disordered
- polymer networks formed through physical aggregation, predominantly disordered

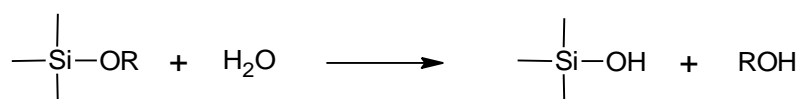
- particular disordered structures

The silicon based sol-gel chemistry has been developed the most; therefore it is used as a model system to explain the fundamental reactions. Unlike some other metal-carbon bonds, silicon-carbon bond is highly stable towards hydrolysis, a crucial step in the sol-gel process. Therefore it is possible to easily incorporate a large variety of organic groups in the formed network by using organically modified silanes.

Mainly, $R_{4-n}SiX_n$ compounds ($n=1-4$, $X=OR'$, halogen) are used as molecular precursors in which the Si-X bond is labile towards hydrolysis. In the following, alkoxy silanes, $R_{4-n}Si(OR')_n$, will be used to describe the main reactions involved during the sol-gel process.

II.1. Hydrolysis

Hydrolysis constitutes the first step of the sol-gel process in which Si-OR bond is hydrolyzed into an unstable silanol (Si-OH) and the corresponding alcohol is produced (Scheme I-1).



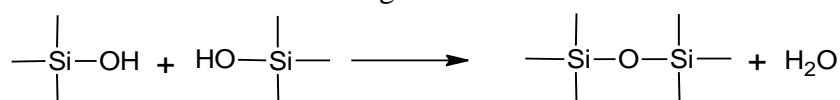
Scheme I-1: Schematic representation of hydrolysis

II.2. Condensation

The unstable silanols (Si-OH) then condense together to form siloxane bridges (Si-O-Si) which serve as the inorganic network. The reaction can proceed in two manners, oxolation and alkoxolation.

II.2.1. Oxolation

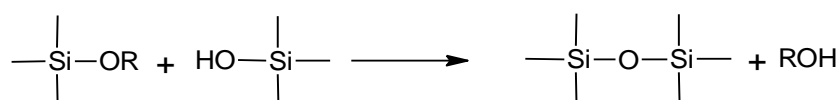
In this case two silanols condense together and release water as a secondary product.



Scheme I-2: Schematic representation of homocondensation

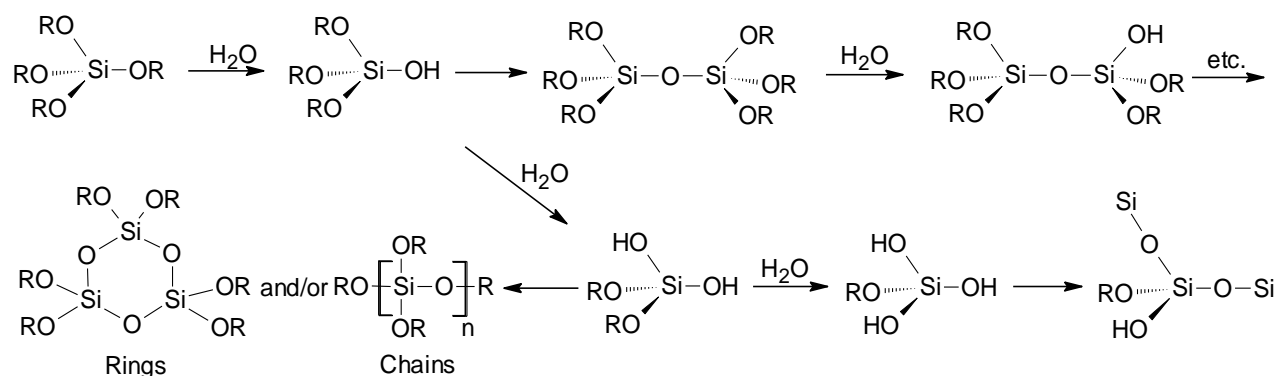
II.2.2. Alkoxolation

Heterocondensation involves the reaction of a silanol group with an alkoxy group yielding an alcohol molecule as a secondary product.



Scheme I-3: Schematic representation of heterocondensation

In the first steps of the condensation reaction, oligomers and polymers as well as cycles are formed. They subsequently result in colloids, hence forming the sol. Solid particles in sol then undergo crosslinking reactions and form the gel. A model system starting from a tetraalkoxysilane is shown in Scheme I-4 explaining the fundamental reactions in the sol-gel process.



Scheme I-4: Fundamental reaction steps in the sol-gel process based on tetraalkoxysilanes

As silicon alkoxides are not water miscible, the reaction is therefore carried out in an organic solvent. In order to increase the hydrolysis rate, a catalyst is added that could be either nucleophilic or electrophilic in nature.

II.3. Role of catalysis in the sol-gel process

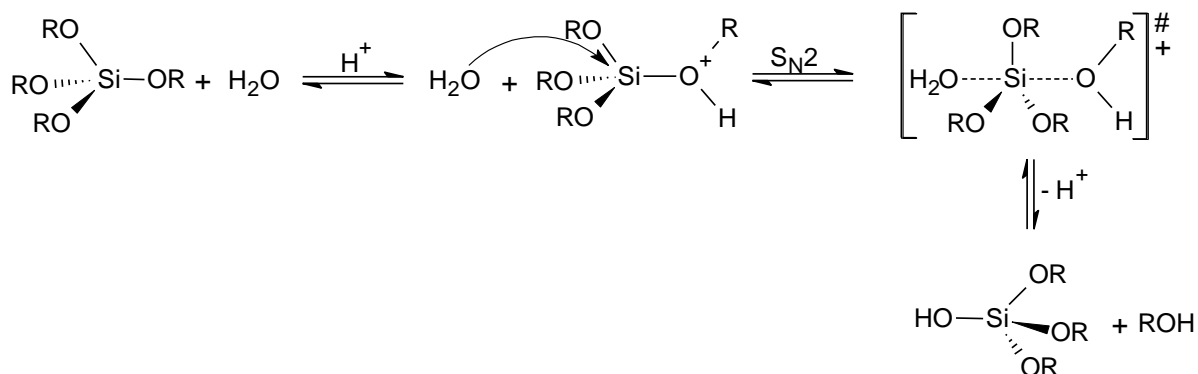
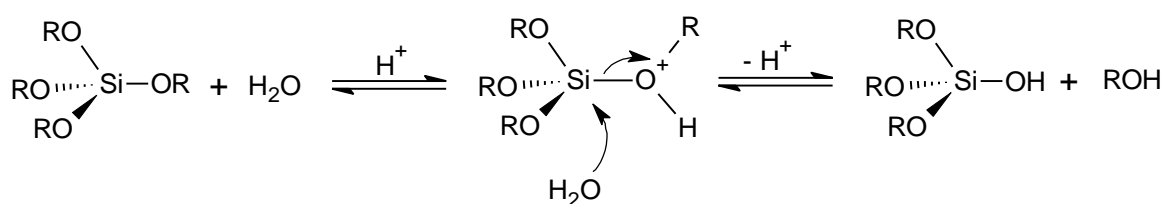
The catalysts play an important role in the sol-gel process by controlling the rate of hydrolysis and condensation. Compounds having an acidic or basic character are mostly used; however, sometimes salts are employed as well. The most commonly used catalysts are mineral acids (HCl , H_2SO_4 , HNO_3 etc.), alkali metal hydroxides ($NaOH$), ammonium hydroxide (NH_4OH), and fluoride ions (HF , NH_4F etc.).

All strong acids are very efficient, whereas weaker acids require longer reaction times to achieve the same extent of reaction. With weaker bases such as ammonium hydroxide and pyridine, measurable rate of reaction is attainable only if large concentration of base is used¹⁰.

II.3.1. Hydrolysis with an electrophilic catalyst

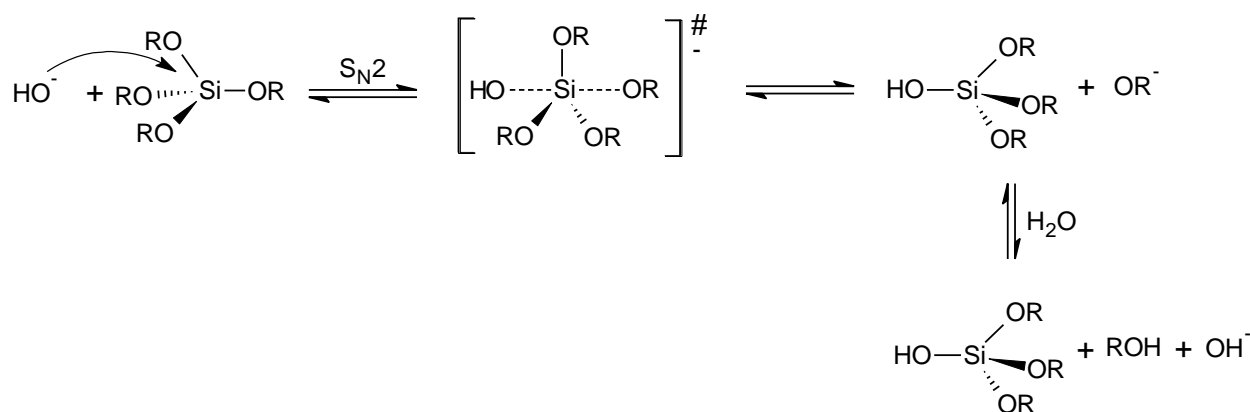
An electrophilic catalyst attacks preferably at the ligand having a high electron density and increases the rate of hydrolysis. As a result the condensation takes place between long and linear polymer chains and the monomer, resulting in a less branched inorganic network with low porosity.

The mechanism for acid-catalyzed sol-gel process could be either S_N2 (Scheme I-5) or S_{Ni} (Scheme I-6). The protonation of the alkoxy group makes it a better leaving group while making silicon more electrophilic in nature. The last step consists of the elimination of a proton to regenerate the catalyst¹¹.

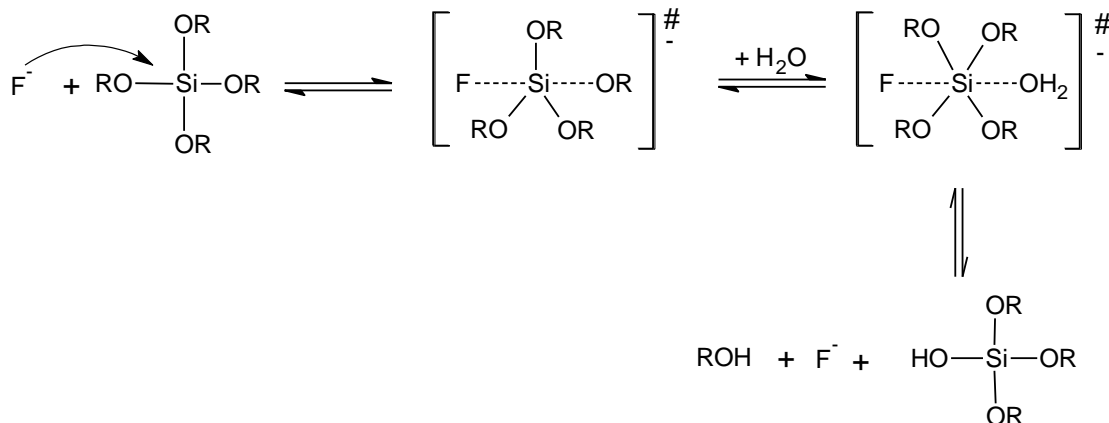
Scheme I-5: S_N2 mechanism of hydrolysis in acidic mediaScheme I-6: S_Ni mechanism of hydrolysis in acidic media

II.3.2. Hydrolysis with a nucleophilic catalyst

A nucleophile-catalyzed hydrolysis proceeds slower than an electrophile-catalyzed hydrolysis at an equivalent catalyst concentration. The reaction starts by the attack of a hydroxyl group (nucleophile) at the silicon atom having a low electron density. Again an S_N2 type of mechanism has been proposed in which the hydroxyl group replaces the alkoxy group which should result in inversion of configuration at the silicon tetrahedron (Scheme I-7).

Scheme I-7: S_N2 mechanism of hydrolysis in basic media

The fluoride ion is also used as a nucleophilic catalyst. The first step consists of the attack of the fluoride ion on the silicon atom resulting in the formation of a pentavalent intermediate. In the next step, the fluorinated intermediate is hydrolyzed to produce the required silanol and to regenerate the catalyst (Scheme I-8).



Scheme I-8: S_N2 mechanism of hydrolysis with fluoride ion

II.4. $\text{H}_2\text{O}/\text{Si}$ Molar ratio (R_a)

The water to precursor ratio is also an important parameter in controlling the rate of hydrolysis in the sol-gel process. The most obvious effect of the increased value of R_a is the acceleration of the hydrolysis reaction. Additionally higher values of R_a cause more complete hydrolysis of monomers before significant condensation occurs. Applying a lower R_a value would lead to a final material with unhydrolyzed alkoxy groups¹⁰.

II.5. Role of catalysis on the rate of condensation

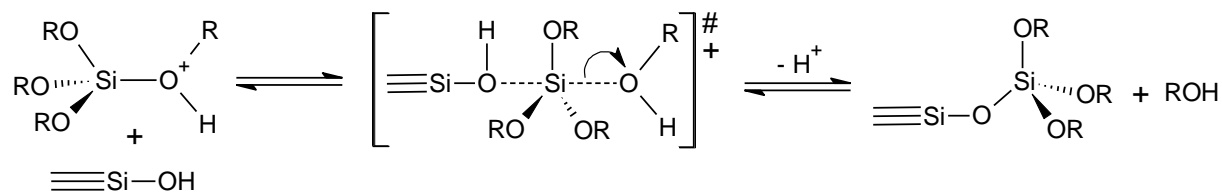
The polymerization to form siloxane bonds occurs by either an alcohol or water producing condensation reactions. The rate of the reaction is dependent on the pH of the reaction medium. In polymerizations below pH 2, the condensation rates are proportional to the proton concentration. Because the solubility of silica is rather low below pH 2, the formation and aggregation of silica particles occur in the same time and the growth of a network is reduced after particles exceed 2 nm in diameter. Thus the developing gel networks are composed of exceedingly small primary particles¹.

Between pH 2 and pH 6, the rate of dimerization is low. However, once dimers form, they react preferentially with monomers to form trimers, which in turn react with monomers to form tetramers and so on. The solubility of silica in this pH range is again low and particle growth stops when the particles reach 2-4 nm in diameter.

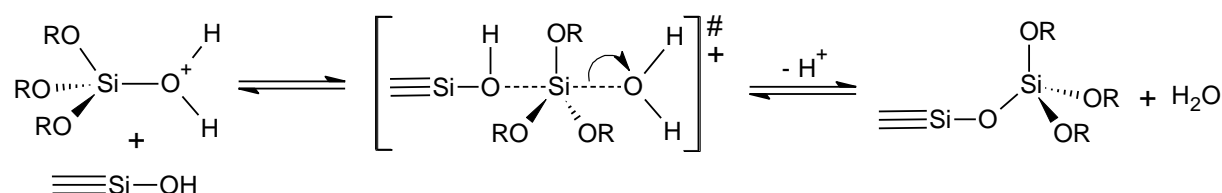
Above pH 7, growth occurs primarily by the addition of monomers to the more condensed particles rather than by particle aggregation. As the solubility of silica particles is high at this pH range, particles grow in size and decrease in number as highly soluble small particles dissolve and reprecipitate on larger less soluble particles. Particle size is thus mainly dependent on temperature, higher temperatures producing larger particles.

II.5.1. Condensation with an electrophilic catalyst

A S_N2 mechanism has been proposed for the condensation of silanols in the presence of an electrophilic catalyst (acid). The silanol replaces either the alkoxy (Scheme I-9) or the hydroxyl group (Scheme I-10) of the neighboring alkoxide which results in the formation of a dimer with inversion of configuration at the silicon tetrahedron. Either alcohol or water is produced as a secondary product in the reaction. The subsequent hydrolysis followed by condensation results in the formation of linear less branched polymers with low porosity.



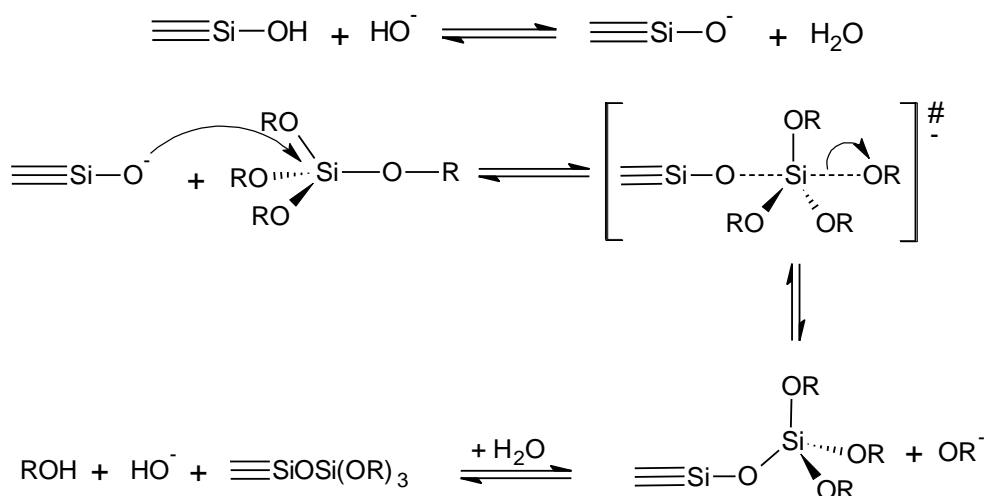
Scheme I-9: S_N2 mechanism of heterocondensation in acidic media



Scheme I-10: S_N2 mechanism of homocondensation in acidic media

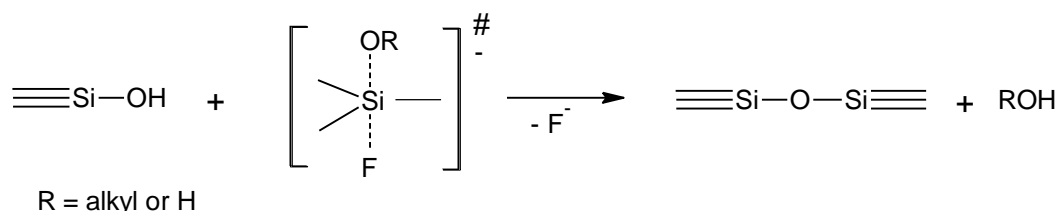
II.5.2. Condensation with a nucleophilic catalyst

The most widely accepted mechanism for a nucleophile-catalyzed condensation involves the attack of a deprotonated silanol on a neutral silanol or silicon alkoxy. The reaction involves a pentacoordinated transition state, similar to that of a S_N2 mechanism (Scheme I-11).



Scheme I-11: Mechanism of condensation in basic media

In the case where a fluoride ion is used as a catalyst, the first step is the fast reversible formation of a pentacovalent intermediate. The next step is the reaction of the silanol on the hypervalent silicon intermediate leading to the nucleophilic substitution. The result is the elimination of the catalyst along with a water (or alcohol) molecule and the formation of required Si-O-Si bridge (Scheme I-12). A well-branched polymer with high porosity is usually obtained after nucleophile-catalyzed condensation.



Scheme I-12: Mechanism of condensation with fluoride ions

II.6. Effect of substituents

The substituents on the silicon atom play a key role in controlling the rate of the reaction. Generally large substituents decrease the reaction rate due to steric hindrance. The electronic nature of the substituents also plays a crucial role in increasing or decreasing the reactivity of silicon. Under basic catalysis, the more the silicon is electrophilic in nature, the more the reaction with the nucleophile is favored. Hence electron-attracting groups increase the hydrolysis reaction.

In case of acidic catalysis, the leaving group is activated by protonation. Electron donating groups increase the electron density on silicon as well as on neighboring oxygens making it more basic in nature. It increases the acceptability of a proton by alkoxy groups and hence favors the hydrolysis reaction¹².

It should be noted that in both cases the reactivity of silicon is dependent on the number of alkoxy groups attached to it. During the course of the reaction, the electron density on silicon decreases due to polycondensation. As a result an increase in its reactivity towards hydrolysis in basic media and a decrease in acidic media is observed¹³.

In addition, the substituents play a major role in the solubility of the precursor in the solvent employed.

II.7. Effect of solvent

Polar protic solvents (methanol, formamide) favor the hydrolysis reaction in acidic medium. They stabilize the intermediates that are formed during the reaction by hydrogen bonding. In case of basic hydrolysis, however, they cannot be used as they protonate the attacking nucleophile and inhibit the reaction. In this case aprotic polar solvents are preferable. They not only stabilize the charged transition state but also solvate the attacking nucleophile¹⁴.

II.8. Aging

The transition from a sol to a gel is called the gelation point. It is the point at which links between sol particles are established to such an extent that the sol transforms into a solid called a gel. While reaction rates and physical changes slow down in the gel state, one must remember that the system is still dynamic. That is the reason why it has to be kept still for a certain period of time until a final stage is reached. This process is called aging.

II.9. Drying

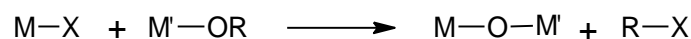
In the last step the solvent is evaporated from the gel to obtain the required material. In this drying process material acquire a more compact structure and the associated crosslinking leads to an increased stiffness.

Drying of the obtained gels, even at room temperature, produces glass-like materials named xerogels. *Xerogels* are porous, usually transparent materials which, when heated at the glass vitrification temperature (ca. 1200 °C), turn into the regular glass, identical with classical glasses obtained by melting.

Drying of the gels under supercritical conditions where the distinction between liquid and vapor no longer exists produces highly porous *aerogels*¹⁵.

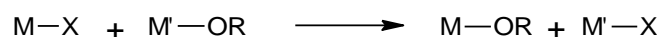
III. Non-hydrolytic sol-gel process

Non-hydrolytic sol-gel chemistry has been developed over the past fifteen years to control the hydroxylation and condensation reactions during sol-gel process in order to get a microstructural control over the final oxide material¹⁶. The process involves the reaction of a metal halide and an oxygen donor such as an alkoxide, an ether, an alcohol etc. to form an inorganic alkoxide under exclusion of water. The by-product of the reaction is usually an alkyl halide the structure of which depends on the nature of the oxygen donor molecule (Scheme I-13).



Scheme I-13: General reaction involved in non-hydrolytic sol-gel process

A ligand exchange side reaction can take place during the process which results in the modification of the course of the reaction as well as the structure of the products (Scheme I-14).



Scheme I-14: Side reaction involved in non-hydrolytic sol-gel process

Several examples of non-hydrolytic sol-gel process have been reported in the literature mainly based on silicon, aluminium and titanium precursors. In addition to inorganic metal

salts and metal alkoxides, the list of potential precursors also includes metal acetates and metal β -diketonates. The reaction is catalyzed by Lewis acids, such as iron (III) chloride that is the most commonly used catalyst, although other catalysts can be used as well. As most of the precursors are liquids, this technique is potentially solvent-free. The chemistry of non-hydrolytic sol-gel process for the formation of organic-inorganic hybrid materials is, however, less developed compared to the hydrolytic sol-gel chemistry due to more difficult experimental conditions. The reaction is usually carried out either in sealed tubes under pressure or under ambient pressure in flowing nitrogen.

Non-hydrolytic sol-gel synthetic routes can be classified into two main families: 1) the surfactant-controlled approach; 2) the solvent-controlled approach

III.1. Surfactant-controlled approach

The surfactant-controlled approach involves the use of a stabilizing ligand to transform the precursors into the final material at a temperature ranging from 250 to 350°C. The most popular strategy is the hot injection method, where the reagents are injected into a hot surfactant solution. Synthesis of semiconductor nanocrystals is a successful example of this methodology¹⁷.

III.2. Solvent-controlled approach

The solvent-controlled approach involves the use of a common organic solvent which acts as a reactant as well as a control agent for particle growth, enabling the synthesis of highly pure nanomaterials in surfactant-free medium¹⁸.

Surfactant-controlled approach	Solvent-controlled approach
Advantages	
Good control over crystal size and shape	Low amount of organic impurities
Narrow size distribution	No toxicity issues
Low agglomeration tendency	Good accessibility of the nanoparticles surface
Limitations	
Large amount of organic impurities	Less control over crystal size and shape
Toxicity of surfactants	Broader size distributions
Complex reaction mixtures	Formation of agglomerates
Restricted accessibility of the nanoparticle surface	

Table I-3: Advantages and limitations of surfactant-controlled and solvent-controlled non-hydrolytic sol-gel process

In comparison to the above mentioned technique, the solvent controlled approach is simpler because the initial reaction mixture consists of only two components, the metal oxide precursor and an organic solvent. It not only simplifies the characterization of the final reaction solution, but also helps in the elucidation of the reaction mechanism. The temperature range for the reaction is usually 50 to 200°C, much less than the temperature range of surfactant-controlled approach. Table I-3 summarizes some of the prominent advantages and limitations of both routes.

Advantages and inconveniences of the sol-gel process

The process presents several advantages over classical techniques for the preparation of inorganic materials or organic-inorganic hybrid materials.

First of all the reaction conditions are mild that allows the formation of materials (glass, ceramics, etc.) at ambient temperature while classical techniques require heating up to 1000°C¹¹. It is especially advantageous when glass contains volatile elements like boron oxide (B₂O₃).

The conditions for the production of oxides are so mild that we can incorporate organic molecules as well. Hence it opens a new field of organic-inorganic hybrid materials with completely original properties and interesting applications in various fields.

It is possible to control the texture and morphology of the materials by controlling the rate of hydrolysis/condensation or by the addition of templates¹⁹.

There are, however, certain inconveniences of this process as well. The high price of alkoxide precursors as well as the use of a large amount of organic solvent in the process are not desirable in industrial applications. One kilogram of sol-gel glass costs 100 times more than the same glass prepared by classical techniques²⁰.

Another problem is the control of reaction rates in the case of certain metals, especially transition metals. In this case the reaction is too fast that results in the loss of morphological and structural control over the final oxide material. Some organic additives like carboxylic acids, diketones or functional alcohols that act as chelating agents can be involved to control the rate of reaction²¹.

IV. Silicon-based hybrid materials

In principle, organic-inorganic hybrid materials can be prepared from any metal in combination with an organic moiety. However due to synthetic problems (stability of metal-carbon bond in sol-gel process, availability of precursors, cost, etc.) until now silicon-based materials have been prepared and studied the most. Their applications in various fields of science have been investigated and it has opened a new area of research for material scientists. Some of the silicon-based materials reported in the literature are described here.

IV.1. Silicon-based class I hybrid materials

These materials are generally prepared by the addition of inorganic charges in organic polymers in order to improve their properties like mechanical strength, thermal stability, etc. while preserving their advantages (flexibility, low density, etc.). Only weak non-covalent interactions (van der Waals, hydrogen bonding etc.) exist between the organic and the inorganic moieties.

These materials can be prepared by either of the following methods.

IV.1.1. Generation of inorganic charges within an organic polymer

Tetraethoxysilane (TEOS) and tetramethoxysilane (TMOS) are mostly used as precursors for creating an inorganic network within an organic polymer. Some linear polymers like poly(N,N-dimethacrylamide), poly(methyl methacrylate) (PMMA), poly(vinylpyrrolidone) (PVP), poly(acrylic acid) (PAA), poly(vinyl acetates) (PVAc) and poly(vinyl-alcohol) (PVA)²² have functional groups that can form hydrogen bonds with silanol groups and hence are used. The properties of the final material depend on the relative proportion of both species. Glass transition temperature of the polymer is increased when it is polymerized with a tetraalkoxysilane and a porous structure is usually obtained.

IV.1.1. Simultaneous generation of both networks

Most of the organic polymers are not soluble in tetraalkoxysilanes and therefore cannot be used to prepare materials by the above-described route. A lot of monomers are, however, quite soluble in them and can be used directly in the sol-gel process. Both organic and inorganic polymerizations take place simultaneously and their rate has to be controlled carefully. No covalent bonds exist between organic and inorganic species and both networks are held together by hydrogen bonding and van der Waals interactions only. Most commonly used monomers for this type of reaction are acrylic, acrylamide and acrylates²³, while tetra(acryloxyethoxy)silane is used instead of TEOS to generate the inorganic network. The resulting hybrid materials are transparent and have a good mechanical resistance²⁴.

IV.2. Silicon-based class II hybrid materials

The physical properties of the above-mentioned materials can be improved by decreasing the size of organic and inorganic domains in order to increase their interfacial surface. This can be done by placing both organic and inorganic functions in the same molecular precursor. As the silicon-carbon bond remains stable during the sol-gel process, trialkoxyorganosilanes are perfect to reach this goal. After sol-gel process, the resulting material contains a Si-O-Si network connected to the organic network via stable Si-C bonds. Some other elements like phosphorous, germanium and tin can also be used; however, due to extensive studies on organosilicon chemistry and ready availability of various precursors, silicon-based class II hybrid chemistry has been developed the most.

The most common way to introduce an organic group into an inorganic silica network is to use trialkoxyorganosilane molecular precursors or oligomers of general formula $R'_n\text{Si}(\text{OR})_{4-n}$ with $n = 1, 2, 3$. The role of the organic moiety depends on its nature. In case R' is a non-hydrolysable group (alkyl, phenyl, etc.) it has a network modifying effect. On the other hand it serves as a network former when it can react either with itself (epoxy, vinyl, etc.) or with other monomers. Polymeric components can also be introduced in hybrid materials by using functionalized macromonomers of general formula $(\text{RO})_3\text{Si}-R'-\text{Si}(\text{OR})_3$. Some examples of these trialkoxysilyl-functionalized polymers are given in Table I-4³.

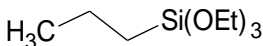
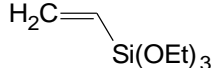
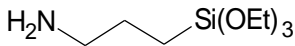
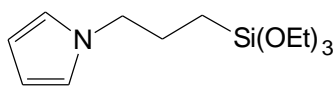
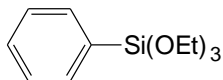
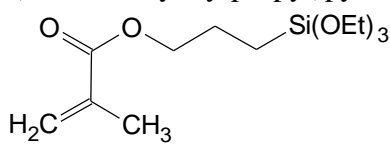
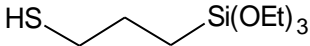
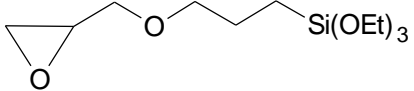
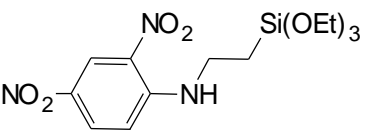
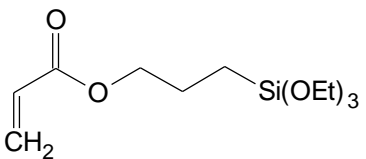
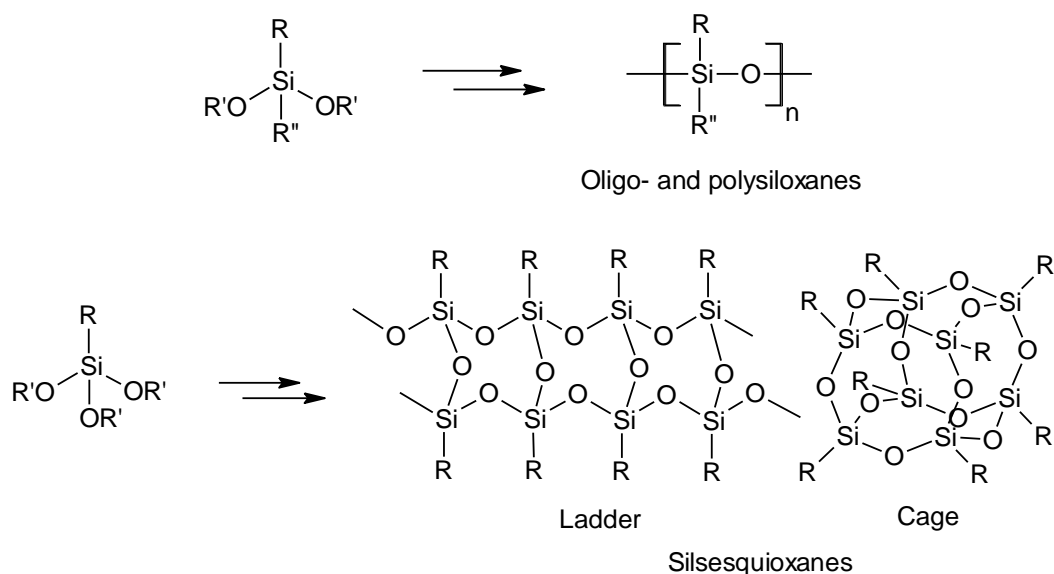
Network modifiers	Network formers
 Triethoxypropylsilane	 Triethoxyvinylsilane
 (3-Aminopropyl)triethoxysilane	 N-(3-Triethoxysilylpropyl)pyrrole
 Triethoxyphenylsilane	 Triethoxy(methacryloxypropyl)silane
 Triethoxy(3-mercaptopropyl)silane	 Triethoxy(3-glycidoxypropyl)silane
 3-(2,4-Dinitrophenylamino)propyltriethoxysilane	 Triethoxy(3-acryloxypropyl)silane

Table I-4: Some examples of network formers and network modifiers

In addition, organically functionalized trialkoxysilanes can also be used for the formation of 3-D networks giving so called *silsesquioxanes* (general formula $R\text{-SiO}_{1.5}$). Generally a 3-D network can only be obtained if three or more hydrolysable bonds are present in a molecule. Two such bonds generally result in linear products and one bond leads only to dimers or allows a modification of a preformed network by the attachment to reactive groups on the surface of the inorganic network (Scheme I-15)



Scheme I-15: Formation of different structures during hydrolysis and condensation reactions depending on the number of hydrolysable groups attached to silicon¹

IV.2.1. Hybrid materials having bridging spacers

These materials are prepared from precursors having two hydrolysable sites (mostly trialkoxysilyl groups) separated by an organic spacer²⁵. Hence the organic network is well defined and the inorganic network is formed by various hydrolysis and condensation steps in the sol-gel process. This arrangement offers exceptional opportunities to combine the important properties of both organic and inorganic worlds and to create some entirely new compositions with truly unique properties. Bridged polysilsesquioxanes are an example to this type of materials.

The unique properties of these materials come from the bridging organic spacer which is attached to the inorganic network by Si-C bonds. It can vary from aliphatic long chains to rigid aromatic rings and results in a change in the physical and chemical properties of the resulting material like porosity, optical clarity, refractive index, thermal stability, hydrophobicity etc. Due to this control over bulk properties of the final material, numerous examples of this class of materials have been reported in literature and have found various applications in optical devices²⁶, catalyst supports²⁷, and ceramic precursors²⁸.

A general structure of bridged polysilsesquioxanes prepared from bridged trialkoxysilyl precursors is shown in Figure I-6.

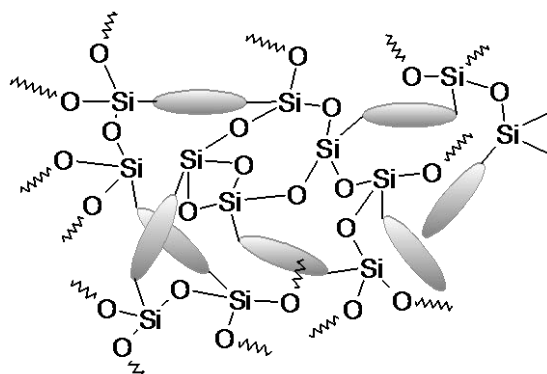
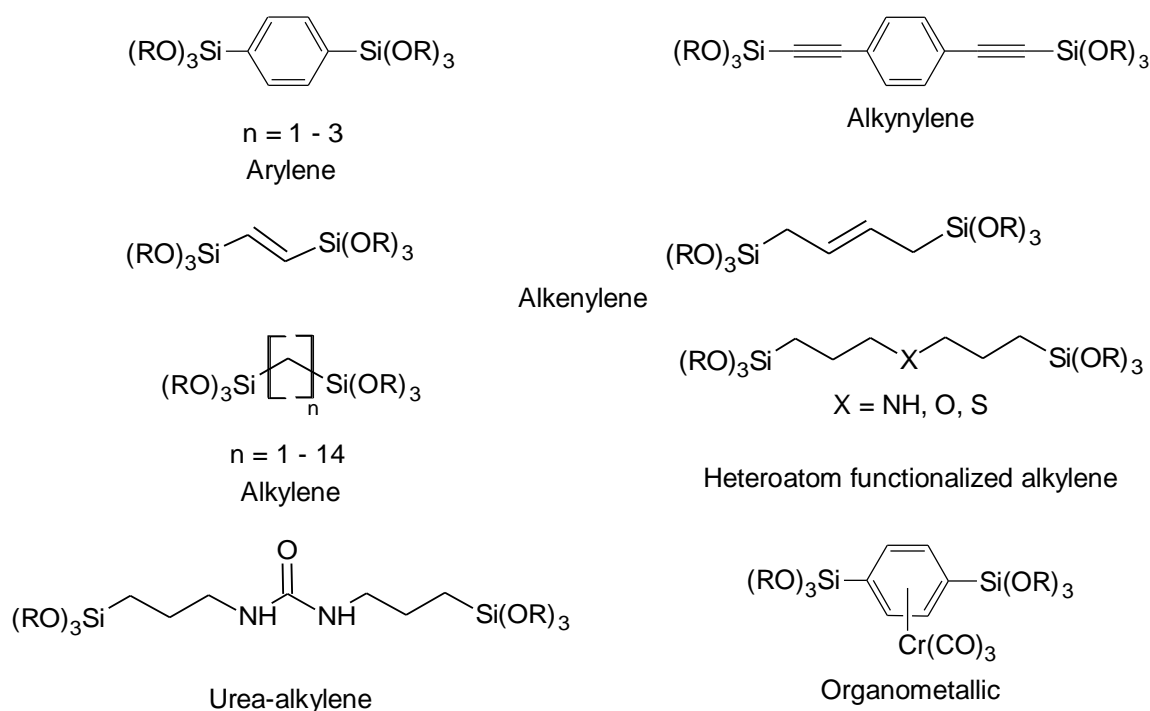


Figure I-6: Bridged polysilsesquioxane gel

IV.2.2. Nature of precursor

Based on the type of bridging organic groups, the precursors for the preparation of hybrid materials can be divided into two major groups: (i) precursors having rigid organic spacer like arylene²⁹, alkynylene³⁰ and olefinic³¹ groups; (ii) precursors having flexible organic spacer like alkylenes ranging from 1 to 14 methylene groups in length³².

A variety of functional groups have been introduced in the spacers like amines³³, ethers³⁴, sulphides³⁵, phosphine³⁶, urea³⁷, azobenzenes³⁸ etc. In addition, bridging groups have included organometallics in which the metal atom is part of the bridge as in a ferrocenyl-bridged monomer³⁹ or pendant to the bridge as in the η^6 -arenechromiumtricarbonyl complex⁴⁰ (Figure I-7).



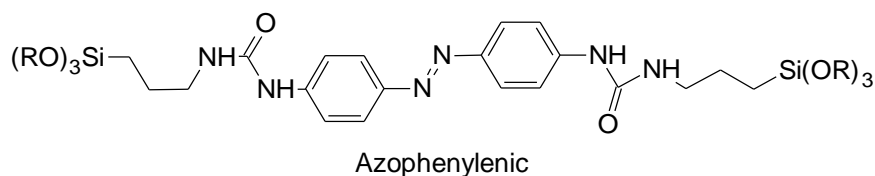
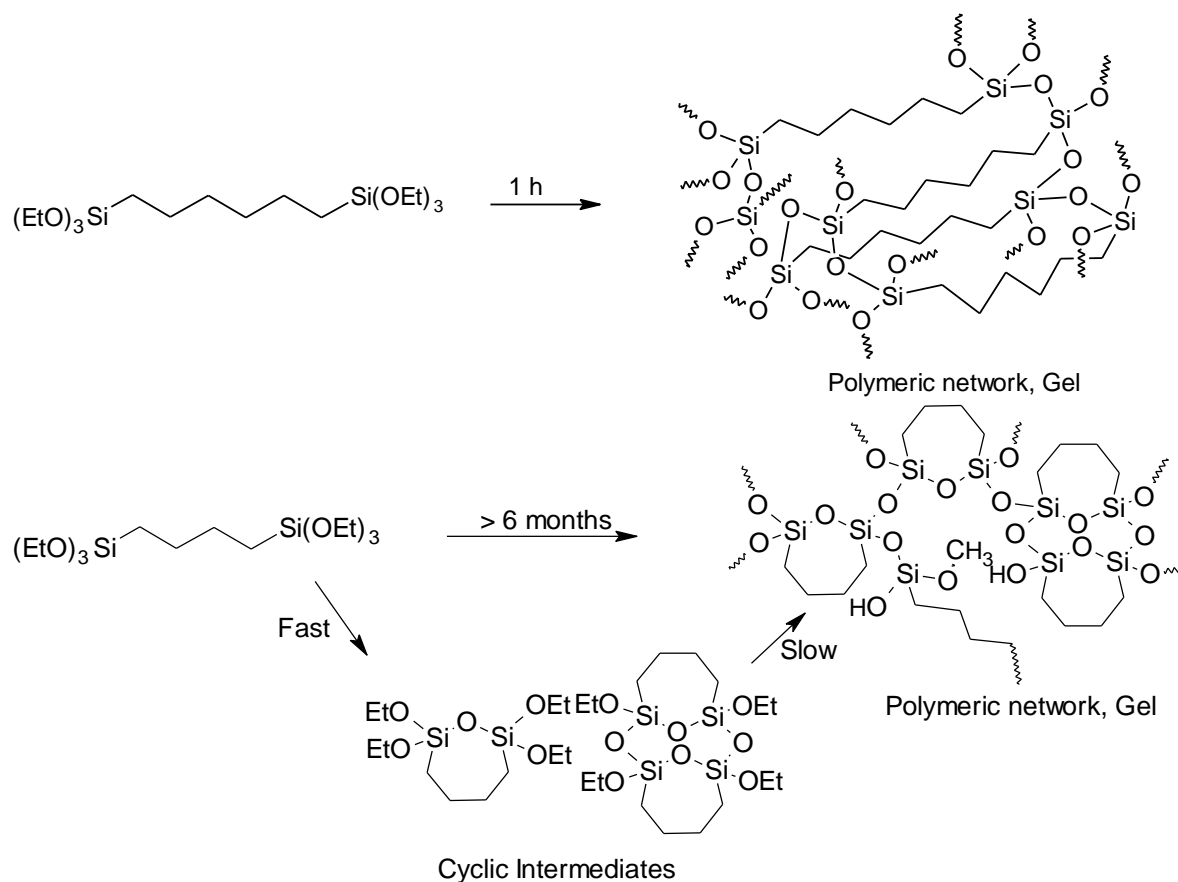


Fig I-7: Various bridged polysilsesquioxane precursors

The nature of bridging organic groups has a significant role not only in defining the properties of the final material, but also on the rate of hydrolysis and condensation reactions leading to gels. Cyclization reactions can take place during the sol-gel process and can delay or even prevent the formation of gels in the case of siloxanes⁴¹ (Scheme I-16).



Scheme I-16: Effect of monomer structure on the gelation times as well as on the structures of the gel

IV.3. Structural Engineering

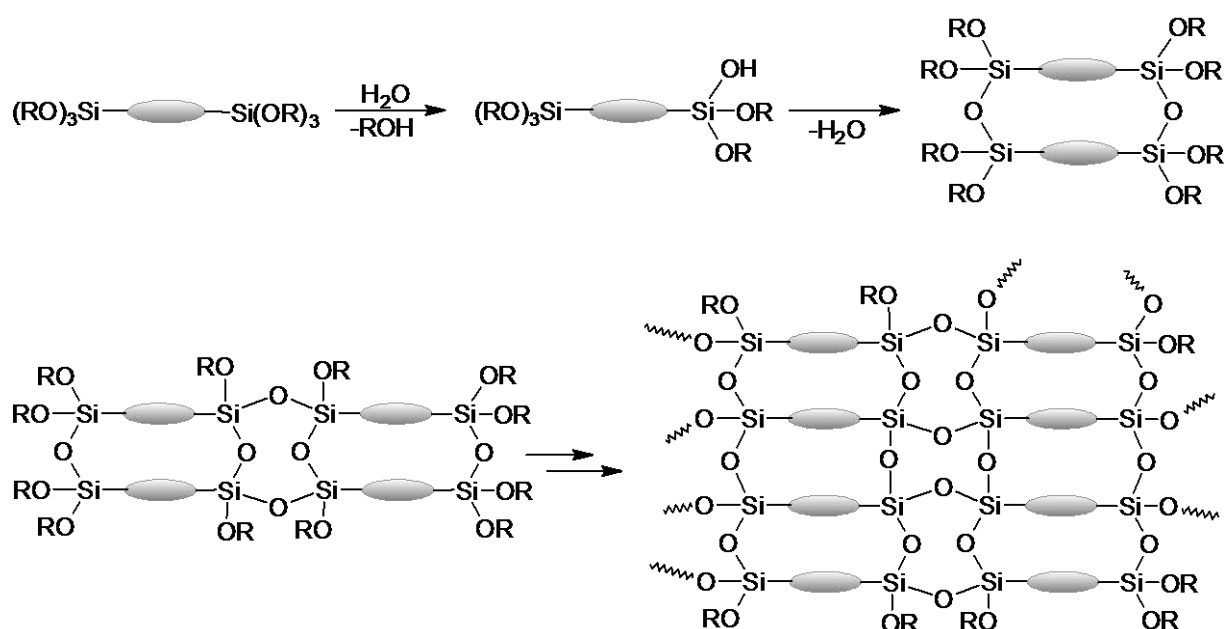
In order to prepare hybrid materials with specific properties for a particular application, they are being designed at several length scales, from molecular to macroscopic scale. There are various methods that can be used for processing at macroscopic level. Thin films and coatings are generally formed by spin-coating and dip-coating; fibers are formed by spinning techniques, etc. Control of nanometer structures is, however, a lot more challenging.

Many future technologies rely on well ordered hybrid materials from the micro- to the nanoscale.

Two different approaches are used to control structures to nanometer level: 1) self-assembly procedures; 2) template directed syntheses.

IV.3.1. Self-assembly

This approach relies on spontaneous self-organization of organic and inorganic species into a complex system that works against entropy. The factors that play an important role in self-assembly of a network are: the structure and shape of the building blocks, their interactions like attractive and repulsive forces, their interactions with solvents, the reaction environment, etc. A general example of well-organized bridged polysilsesquioxanes is shown in Scheme I-17 in which organic bridging groups self-assemble to give an organized structure through the sol-gel process⁴².



Scheme I-17: Proposed sol-gel polymerization mechanism of bridged monomers leading to well-ordered polysilsesquioxane nanostructures

For such supramolecular organization based on organic ligands, the non-bonding interactions should be relatively strong. Bridged polysilsesquioxanes with mesogenic bridging groups have shown some organization on thin films. So far, long chain alkylene bridging groups have not demonstrated ordered structures based on crystallization of alkylene chains^{31b,c}. However, if hydrogen bonding is introduced to the bridging group, it is possible to get supramolecular organization of the nanostructures. This can be done by incorporating bis-urea-alkylene groups or other organogelators⁴³. The introduction of bis-urea group into the bridging group permits the formation of strong hydrogen bonds between the organic bridging groups that are relatively independent of the siloxane network (Figure I-8).

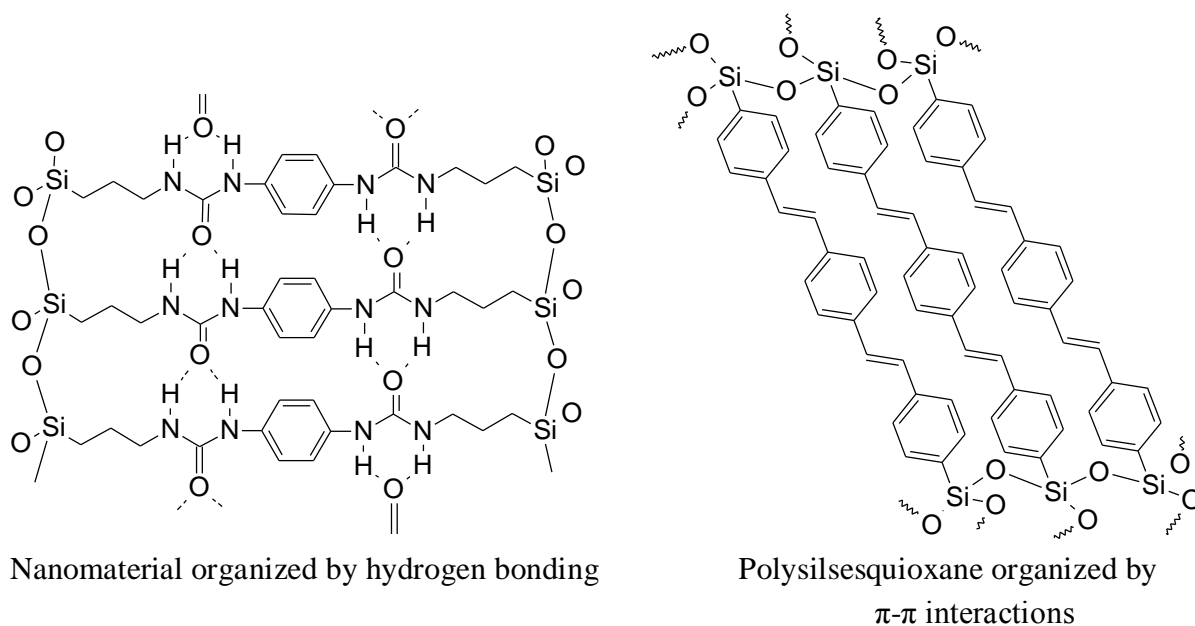
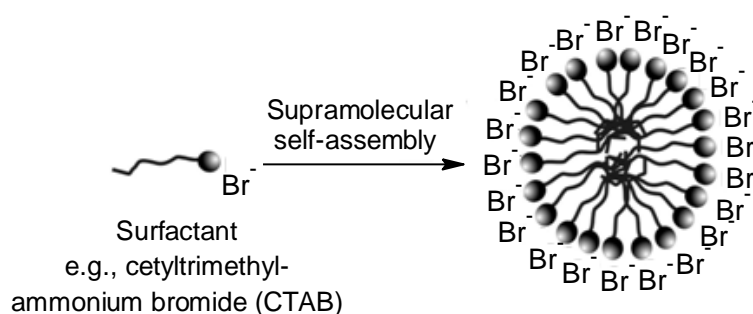


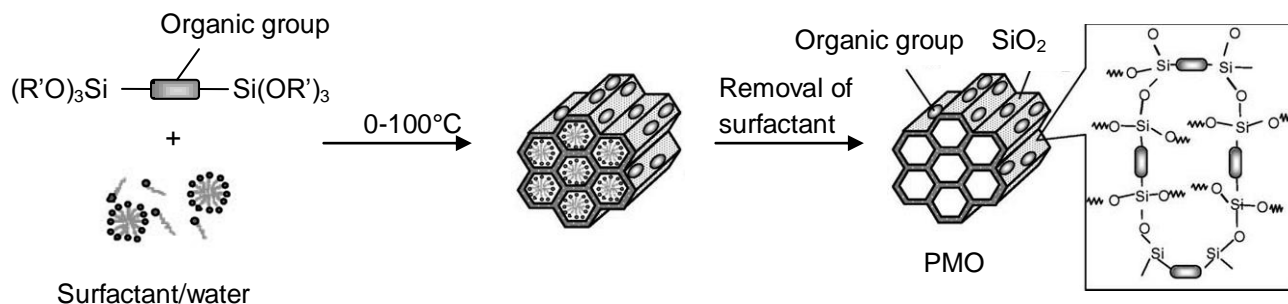
Figure I-8: Self-assembly in various hybrid materials

IV.3.2. Template-directed synthesis

Templates have been used to direct the formation of specific structures for a long time. Examples are the use of porogens for the formation of foam-like materials or single molecules that are employed in zeolite synthesis. In both cases templates are removed after forming pores in the material.

For the synthesis of hybrid materials, templates can be either preformed structures such as dendrimers or nanoparticles that form 2D or 3D ordered structures, or single molecules which then self-assemble into larger structures. The formation of the structures depends on various parameters, like concentration of the surfactant, temperature and pH of the solution, etc. The resulting structures consist of hydrophobic and hydrophilic regions and the interfaces between them direct the organization of the material. An example of this strategy to prepare bridged polysilsesquioxane materials from disilylated organic precursors is shown in Scheme I-18. The resulting periodic mesoporous organosilicas (PMOs) have a highly ordered mesostructure with well-defined hexagonal or cubic structures, uniform pore distributions and high surface areas⁴⁴.





Scheme I-18: Template-directed synthesis of well-ordered mesoporous material (Figure taken from reference 44)

A variety of organic groups have been incorporated to increase the functionality of PMOs, thus making them useful for practical applications. The nature of organic groups ranges from simple alkylene chains⁴⁵ to unsaturated or arylene groups⁴⁶ and to very large organometallic complexes⁴⁷.

V. Tin-based hybrid materials

Like silicon, tin also forms stable covalent bonds with carbon that can survive the hydrolysis reaction in the sol-gel process. It has a vacant 5d orbital which facilitates the hydrolysis and condensation reactions by showing different coordination states in the transition state of the reaction. However, due to difficulties in preparing organotin precursors, tin-based hybrid material chemistry has not progressed as much as silicon-based chemistry.

Two types of tin-based hybrid materials have been reported so far: 1) hybrid materials built from tin-oxo nanobuilding blocks, 2) hybrid materials having bridging organic spacers.

V.1. Hybrid materials built from tin-oxo nanobuilding blocks

As previously mentioned, the nanobuilding block approach is based on the combination of well-defined preformed polymetallic species, acting as nanobuilding blocks, that results in the formation of a hybrid material in which the components at least partially keep their identity. Tin-oxo clusters have been used as nanobuilding blocks to design new tin-based hybrid materials⁴⁸. The first step is the chemical modification of tin alkoxides or tin chlorides by reaction with suitable organic ligands (R) to $RSn(Oi-Pr)_3$, or $RSnCl_3$. Hydrolysis of these modified precursors leads to a well-defined tin-oxo cluster of general formula $[(RSn)_{12}(\mu_3-O)_{14}(\mu_2-OH)_6]^{2+}$ which can be used as a nanobuilding block to prepare hybrid materials (Figure I-9). Depending on the synthetic conditions, the positive charge 2^+ is balanced by different anions (OH^- , Cl^- , RSO_3^- , RCO_2^- , etc.). These charge-compensating anions (A^- in Figure I-10) are located at both cage poles, close to the hydroxyl groups which bridge the six-coordinate tin atoms.

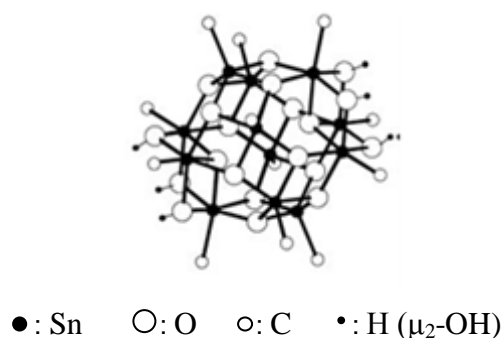


Figure I-9: Molecular structure of $[(\text{RSn})_{12}(\mu_3\text{-O})_{14}(\mu_2\text{-OH})_6]^{2+}$ [taken from reference 48(b)]

These clusters are good nanobuilding blocks for the synthesis of well-defined tin-oxo based hybrid materials. They can be linked to the organic network by two types of interaction: either by Sn-C covalent bonds or by electrostatic interactions with the charge compensating anions A^- or even both. In the first case, the organic moiety bound to tin should be polymerizable (i.e. R= butenyl, propyl methacrylate, propyl crotonate, 4-styryl, etc.). In the second case, charge compensating dianions must be able to bridge the clusters. This can be performed by using dicarboxylates, or α,ω -telechelic macromonomers terminated by carboxylic or sulfonic groups.

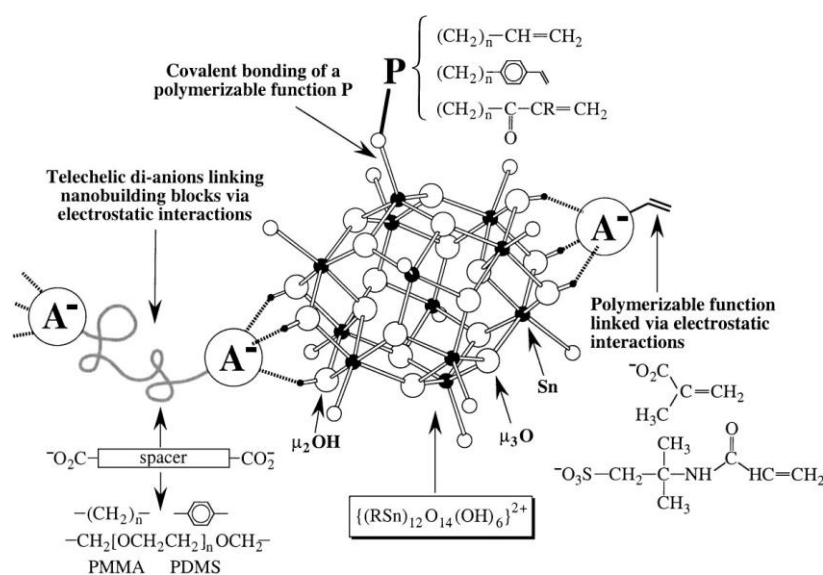


Figure I-10: Some of the possible strategies that can be used with the hybrid nanobuilding block $[(\text{RSn})_{12}(\mu_3\text{-O})_{14}(\mu\text{-OH})_6]^{2+}2A^-$ [taken from reference 48(a)]

An example of the first type of materials is observed when a tin oxo-hydroxo cluster surrounded by butenyl chains is formed by the hydrolysis of butenyl $\text{Sn}(\text{OAm}^t)_3$. The organic polymerization of these butenyl groups with azobis(isobutyronitrile) (AIBN) as a radical promoter results in the formation of a hybrid material in which tin-oxo clusters are connected to the organic network via Sn-C covalent bonds (Figure I-11)⁴⁹.

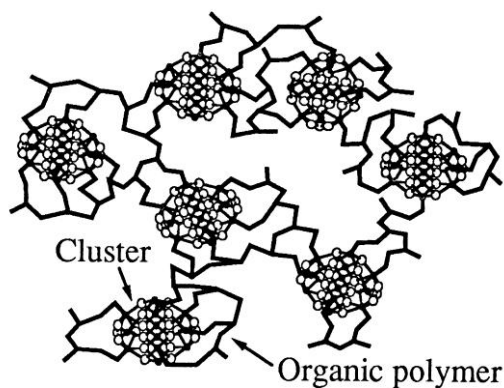
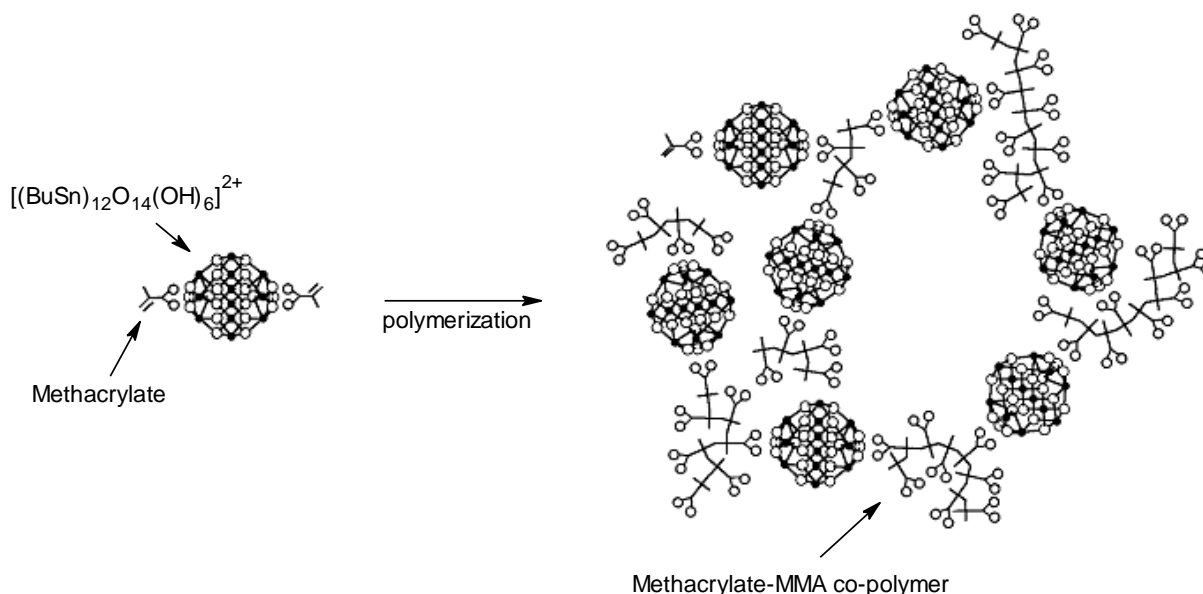


Figure I-11: Schematic structure for tin-based class II hybrid material (taken from reference 49)

In the case where the tin-oxo cluster is functionalized with methacrylate anions, polymerization of the methacrylate groups with methyl methacrylate (MMA) as co-monomer gives the required hybrid material as shown in Scheme 1-19. The inorganic cluster is linked to the organic network by electrostatic interactions and hydrogen bonding⁵⁰.



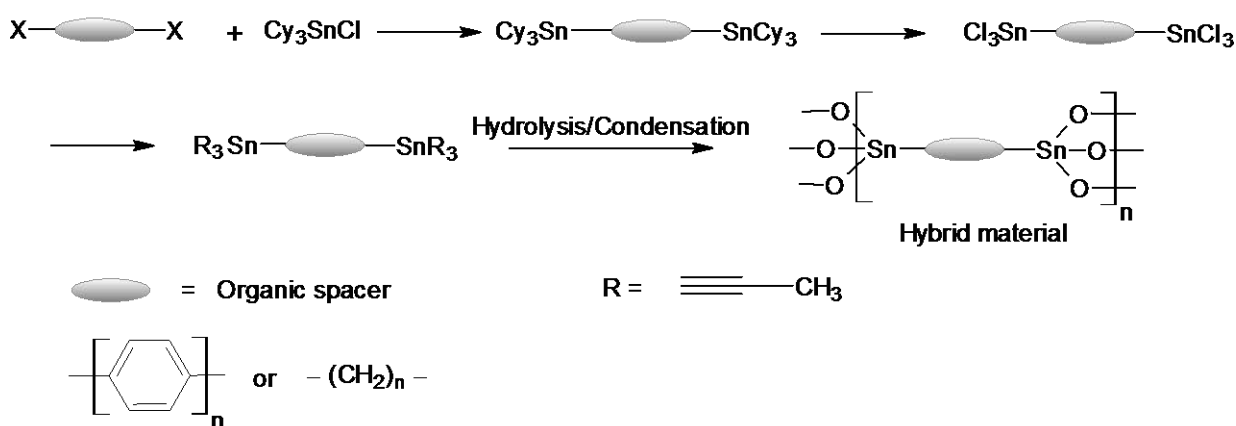
Scheme I-19: Schematic representations of hybrid material obtained by co-polymerizing $[(\text{BuSn})_{12}\text{O}_{14}(\text{OH})_6](\text{O}_2\text{C}-\text{C}(\text{CH}_3)=\text{CH}_2)_2$ and MMA (Scheme taken from reference 50)

Tin-oxo based hybrids were recently doped with spiroxazine dyes and europium complexes. In the first case the photocoloration process as well as the fading process were faster than in the conventional organic matrices. That has been explained by a free motion of the dye during the ring opening and closing reactions and by a non-stabilization of the open form by hydrogen bonding within the matrix⁵¹. In the second case, the tin-oxo based matrix includes a larger absorption spectrum and protects europium ions from quenching, that would maintain the life-times of the excited europium complexes⁵².

V.2. Hybrid materials having bridging organic spacers

Another strategy to prepare tin-based organized nanostructures that has given good results so far is to prepare materials having bridging organic spacers. The inorganic network is then formed by various hydrolysis and condensation reactions in the sol-gel process. It has been used in our laboratory to prepare well-organized tin-based bridged hybrid materials⁵³.

Organotin alkoxides would have been the usual precursors to prepare this type of materials. However due to difficulty in purification and isolation of certain alkoxides, organotin alkynides were used instead⁵⁴. After hydrolysis they give the same cluster of twelve tin atoms as is formed in the case of organotin alkoxides. The precursors for these materials consist of two tin atoms, equipped with hydrolysable groups and separated from each other through an organic spacer. A variety of spacers have been used ranging from long flexible aliphatic chains to rigid aromatic rings and their effect on the organization of the final materials has been studied. After hydrolysis, the hydrolysable alkynyl groups give an inorganic network based on Sn-O-Sn bonds connected to the organic network via Sn-C stable bonds. A general reaction scheme explaining a stepwise preparation of the materials is shown below.



Scheme I-20: Reaction scheme for the preparation of tin-based hybrid materials

X-ray diffraction analysis shows that the materials are well organized at the nanometer scale. The organic groups self-assemble by non-bonding interactions (via π -stacking, van der Waals interactions, etc.) and act as spacers between tin oxide (Sn-O-Sn) planes (Figure I-12).

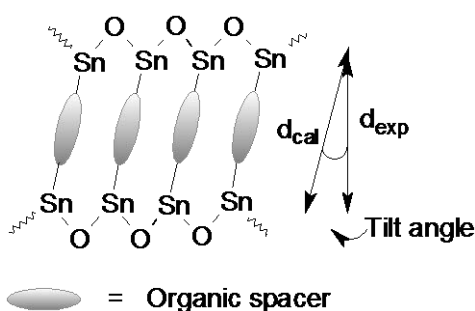
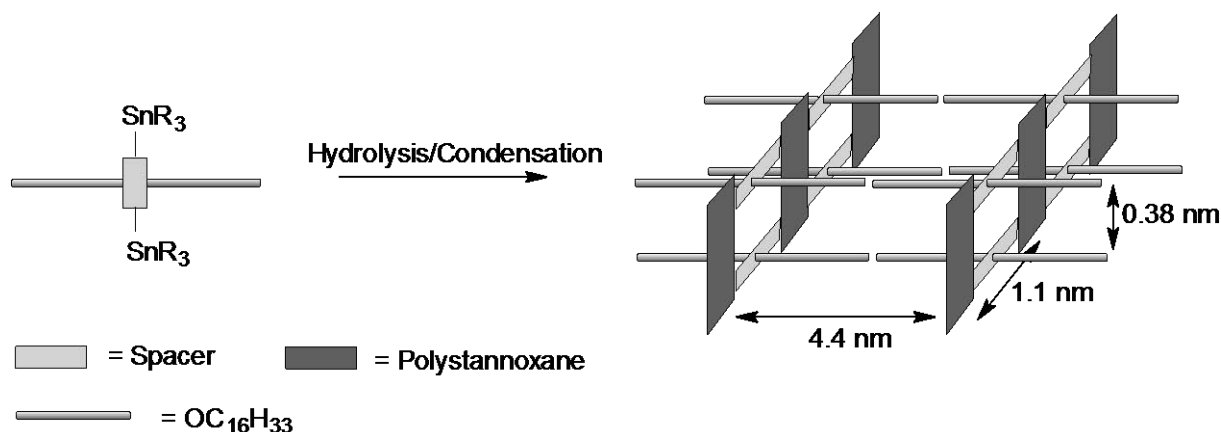


Figure I-12: Model of organization in tin-based organic-inorganic hybrid materials

Another type of organization has been observed when the bridging organic ligand contains lateral chains of 8 or 16 carbons⁵⁵. In this case the material is organized by the self-assembly of long aliphatic chains connected to the aromatic ring which is then connected to the inorganic network. There is no interdigitation of the aliphatic chains (Scheme I-21).



Scheme I-21: Organization of the hybrid material (perpendicular to the main chains)

VI. Transition metal-based hybrid materials

Transition metal-based hybrid nanosystems are promising for creating new nanomaterials with novel functionalities and controlled nanostructures. Their production, however, is limited due to synthetic problems. Transition metal alkoxides are far more reactive towards hydrolysis and condensation reactions than silicon alkoxides. The metals in these precursors are in their highest oxidation states surrounded by electronegative alkoxide ligands causing them to be more susceptible to nucleophilic attack. Another problem is the unsaturation of the coordination sphere of transition metals in these precursors. As a result, formation of oligomers via alkoxide or alcohol bridges or saturation of the coordination sphere by additional coordination of the alcohol molecules is observed.

One idea to overcome the above mentioned problems is to use organically functionalized bi- and multidentate ligands that show a better stability during the sol-gel reaction. These ligands also reduce the speed of the hydrolysis and condensation reactions by blocking the coordination sites (Figure I-13)¹.

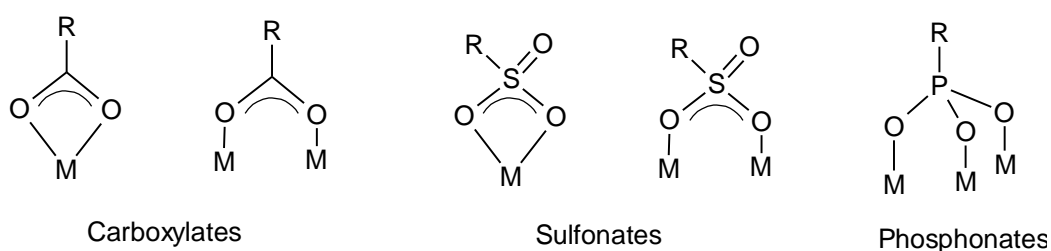


Figure 1-13: Typical coordination patterns between bi- and multidentate ligands and metals that can be used to make transition metal-based hybrid materials

Very limited work has been done so far on the development of transition metal based hybrid materials due to above mentioned inconveniences. Zirconium clusters functionalized with methacryl substituent $Zr_6(OH)_4O_4(OMc)_{12}$ ($OMc = \text{methacrylate}$) have been copolymerized with methyl methacrylate under radicalar initiation. Transparent glassy polymers resulted with improved thermal stability, due to the cross-linker properties of the cluster⁵⁶. Some titanium-based hybrid materials have been reported in the literature, also based on the metal-oxo nanobuilding block approach⁵⁷. For instance, the copolymerization of a four-titanium cluster $Ti_4O_2(OiPr)_6(OMc)_6$ with methyl methacrylate leads to hybrid materials where the clusters aggregate and show a kind of discotic structure. In another example, a larger cluster $[Ti_{16}O_{16}(OEt)_{24}(OEMA)_8]$, was copolymerized with dimethacryloxy-diethoxy-bisphenol A (CD-540)⁵⁸(Figure I-14). The resulting hybrid materials combine optical transparency and a very positive reinforcement of their mechanical properties. Moreover, the formation of blue domains resulting from the formation of mixed valence Ti^{3+} - Ti^{4+} centers by UV irradiation offers possibilities for optical information storage. TEM experiments performed on films of this hybrid reveal the presence of aggregates with size ranging from 100 to 400 nm which is the upper limit for optical transparency⁵⁹.

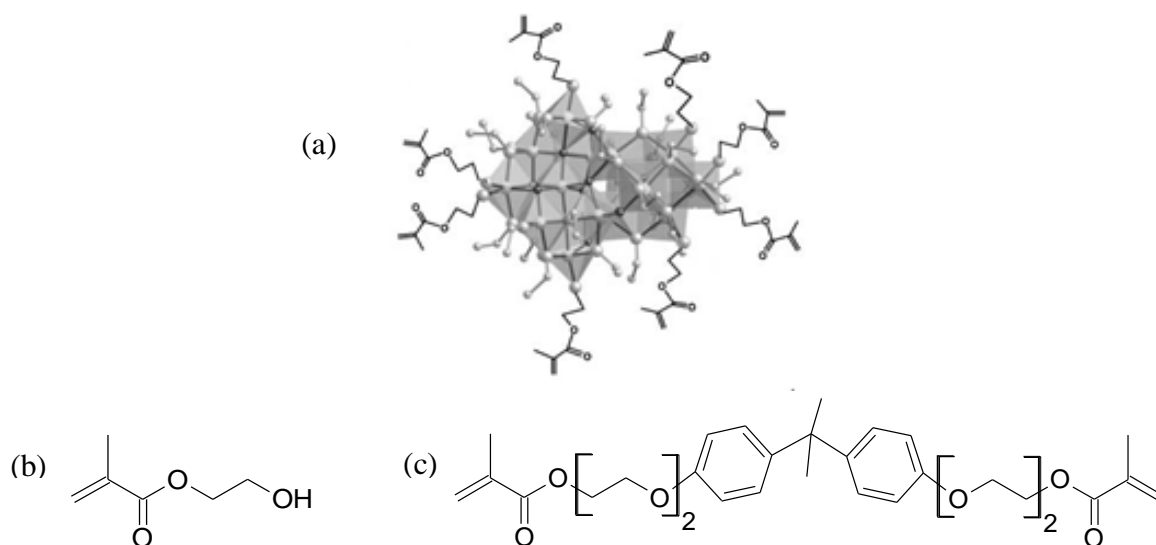


Figure I-14: (a) $[Ti_{16}O_{16}(OEt)_{24}(OEMA)_8]$ (Figure taken from reference 58a) (b) HEMA [2-hydroxyethyl methacrylate $\{H_2C-C(CH_3)CO_2CH_2CH_2OH\}$] (c) CD-540 bis(methacryloxy-diethoxy)bisphenol A

Similarly functional titanium oxo-clusters $Ti_{16}O_{16}(OEt)_{32-x}(OPhCH=CH_2)_x$ with $x=4$ or 16, have been synthesized and copolymerized with styrene. The resulting hybrid nanomaterials present three-dimensional networks in which the inorganic phase is covalently linked to the organic matrix through Ti-O-C bonds⁶⁰. Again TEM experiments show the presence of aggregates with a size of 100-250 nm. The amount of titanium is limited to 2.5% (by weight), either 0.6% of Ti (by mol).

Titanium-oxo clusters such as $\text{Ti}_6\text{O}_4(\text{OR})_8(\text{C}_6\text{H}_5\text{COO})_8$ ($\text{R}=\text{Et}, \text{Pr}, \text{Bu}$) (Figure I-15) have been added into a silicon-based organic-inorganic host material (ORMOCER) including diphenylsilanediol and trimethoxy(methacryloxypropyl)silane to tune its properties like refractive index⁶¹. More sophisticated silicon-titanium mixed clusters were also used. They were prepared by incorporation of a titanium atom in a silsesquioxane where the silicon atoms bear a vinyl substituent. Such clusters with high titanium content ($\text{Si}/\text{Ti} = 1/0.75$) can be obtained by a non-hydrolytic sol-gel route from chlorotrimethylsilane, titanium tetrachloride and diisopropylether⁶². These modified silsesquioxanes could not self-polymerize because of a too high steric hindrance. Fortunately they could cocondense with styrene to result in a new polymer with titanium content below 1%. They were subsequently adsorbed on an ordered silica matrix and used as catalyst for the epoxidation of olefins with success⁶³.

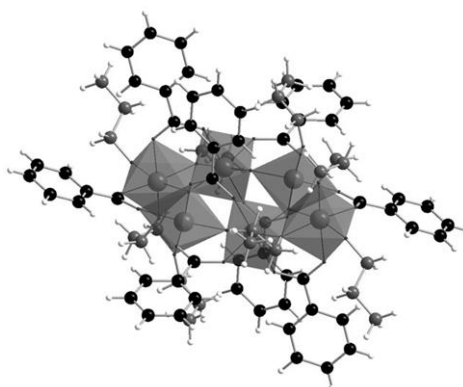


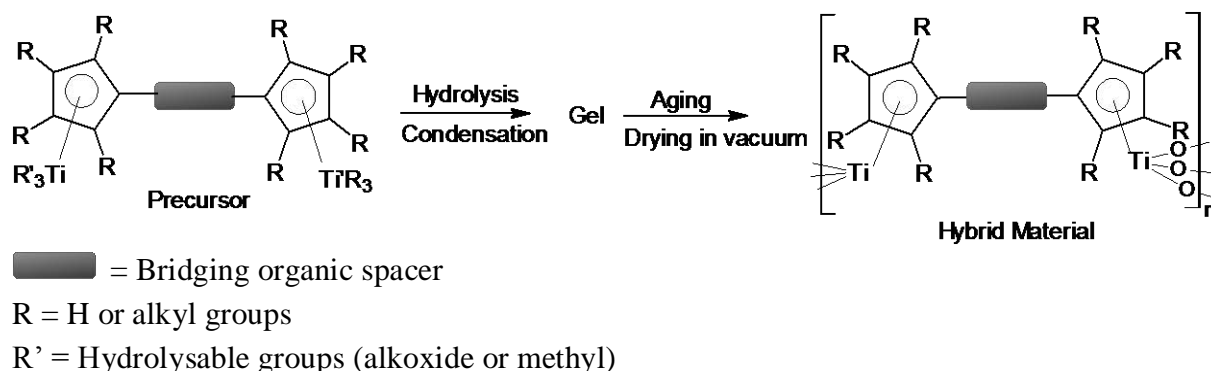
Figure I-15: Molecular geometry of $\text{Ti}_6\text{O}_4(\text{OPr}^n)_8(\text{OOCC}_6\text{H}_5)_8$ based on X-ray scattering (Figure taken from reference 61)

VII. Conclusion

Titanium-based hybrid nanomaterials reported in the literature are thus constituted of an inorganic network which is mainly formed of undefined or preformed oxo-clusters and of an organic network not so well defined as it is obtained by in-situ polymerization. The link between both networks is provided by titanium-oxygen bonds. Up to now, no titanium-based organic-inorganic hybrid materials with titanium-carbon bonds has been described, as metal-alkyl or metal-aryl bonds used for this purpose in silicon and tin hybrid materials are not stable in the case of titanium compounds. Moreover no titanium-based organic-inorganic hybrid nanomaterials has shown the same self-organization as exists in hybrid nanomaterials based on silicon or tin except the case, reported very recently, of a crystalline highly porous titanium dicarboxylate where terephthalic acid links clusters of $\text{Ti}_8\text{O}_8(\text{OH})_4$ ⁶⁴.

In our research, we are interested in the synthesis of well-organized titanium-based hybrid materials having a defined organic network, a homogeneous distribution of the metal throughout the material and titanium-carbon bonds to link both networks. This goal can be achieved by using precursors where a strong bond between the metal and the organic ligand induces a good stability, and where the organic ligand has two sites of coordination leading to a well-defined organic network. As has been discussed before, carbon-titanium σ -bond is not

stable towards hydrolysis which is a crucial step of sol-gel process. However certain ligands, like cyclopentadienyl ligands, form quite stable carbon-titanium π -bonds that can survive the reaction conditions and hence are chosen for this purpose. The first step of this work consists of synthesizing organic ligands having two cyclopentadienyl groups separated by different spacers. The next steps are the complexation of the two cyclopentadienyl groups with titanium by forming a carbon-titanium π -bond followed by the introduction of three hydrolysable groups. The inorganic network obtained by the hydrolysis of these groups will consist of a Ti-O-Ti network. The formation rate of the network could be adjusted by tuning the nature of hydrolysable groups (alkoxide, methyl, etc.) in order to build a perfectly mixed inorganic network. The organic network consisting of cyclopentadienyl ligands, separated by a spacer would ensure a homogeneous distribution of the metal throughout the material. Rigid or semi-rigid aromatic spacers would induce the self-assembly of the organic network by π -stacking. The modification of the organic network i.e., spacer or substituents at cyclopentadienyl group, would allow to control the properties of these materials, modifying their organization, porosity, specific area, thermal stability etc. This new concept could be extended to the other transition metals giving stable π -bonds with organic groups. The resulting materials are expected to find interesting applications in optics (transparent protective layers, mesoporous titanium oxide for photovoltaic cells) and catalysis (efficient low-leaching catalysts).



Scheme I-22: Reaction scheme for the preparation of titanium-based hybrid materials

Crystalline titanium dioxide is one of the most attractive metal oxide for technical and industrial applications because of its remarkable physicochemical properties which combine chemical inertia, mechanical hardness, electronic conductivity, transparency to visible light, and large surface area. The thermolysis of the hybrid materials proposes a new route to produce mesoporous titanium dioxide with controlled properties as powders and as thin films. Creation of these semi-conducting nanomaterials with controlled porosity and high surface area is particularly interesting for photovoltaic applications.

-
- ¹ Kickelbick, G., *Hybrid Materials: Synthesis, Characterization and Applications*, Wiley-VCH, Weinheim, **2007**
- ² Olphen, H. V. *Science* **1966**, *154*, 645 (b) Yacaman, M. J.; Rendon, L.; Arenas, J.; Serra, M. C. *Science* **1996**, *273*, 223 (c) Gómez-Romero, P.; Sanchez, C. *New J. Chem.* **2005**, *1*, 57
- ³ Sanchez, C.; Julian, B.; Belleville, P.; Popal, M. *J. Mater. Chem.* **2005**, *15*, 3559
- ⁴ (a) Judeinstein, P.; Sanchez, C. *J. Mater. Chem.* **1996**, *6*, 511 (b) Gomez-Romero, P. *Adv. Mater.* **2001**, *13*, 163
- ⁵ Haas, K.-H. *Adv. Eng. Mater.* **2000**, *2*, 571
- ⁶ (a) Novak, B. M. *Adv. Mater.* **1993**, *5*, 422 (b) Mark, J. E. *Poly. Eng. Sci.* **1996**, *36*, 2905 (c) Mascia, L. *Trends Polym. Sci.* **1995**, *3*, 61 (d) Loy, D. A.; Shea, K. J. *Chem. Rev.* **1995**, *95*, 1431 (e) Hench, L. L.; West, J. K. *Chem. Rev.* **1990**, *90*, 30
- ⁷ Schotter, G. *Chem. Mater.* **2001**, *13*, 3422
- ⁸ Davis, J. T.; Rideal, E. K., *Interfacial Phenomena*, Academic Press, New York, **1963**
- ⁹ Flory, P. J., *Principles of Polymer Chemistry*, Cornell University Press, Ithaca, NY, **1953**;
Chapter IX
- ¹⁰ Aelion, R.; Leobel, A.; Eirich, F. *J. Am. Chem. Soc.* **1950**, *72*, 5705
- ¹¹ Brinker, C. J.; Scherer, G. W., *Sol-Gel Science, The Physics and Chemistry of Sol-Gel Processing*, Academic Press, New York, **1990**
- ¹² Brinker, C. J. *J. Non-Cryst. Solids* **1988**, *100*, 31
- ¹³ Klein, L. C. *Ann. Rev. Mater. Sci.* **1985**, *15*, 227
- ¹⁴ Artaki, I.; Zerda, T. W.; Jones, J. *J. Non-Cryst. Solids* **1986**, *81*, 381
- ¹⁵ Loy, D. A.; Russick, E. M.; Yamanaka, S. A.; Baugher, B. M.; Shea, K. J. *Chem. Mater.* **1997**, *9*, 2264
- ¹⁶ Vioux, A.; Leclercq, D. *Heterogeneous Chem. Rev.* **1996**, *3*, 65 (b) Corriu, R. J. P.; Leclercq, D. *Angew. Chem. Int. Ed. Eng.* **1996**, *35*, 1420 (c) Vioux, A. *Chem. Mater.* **1997**, *9*, 2292 (d) Jun, Y. W.; Choi, J. S.; Cheon, J. *Angew. Chem. Int. Ed.* **2006**, *45*, 3414 (e) Hay, J. N.; Raval, H. M. *Chem. Mater.* **2001**, *13*, 3396 (f) Ching, S.; Welch, E. J.; Hughes, S. M.; Bahadoor, A. B. F. *Chem. Mater.* **2002**, *14*, 1292 (g) Niederberger, M. *Acc. Chem. Res.* **2007**, *40*, 793 (h) Niederberger, M.; Antonietti, M., *Nanomaterial Chemistry: Recent Developments and New Directions*, Wiley-VCH, Weinheim, **2007**
- ¹⁷ Mello Donega, C.; Liljeroth, P.; Vanmaekelbergh, D. *Small* **2005**, *1*, 1152
- ¹⁸ Pinna, N.; Niederberger, M. *Angew. Chem. Int. Ed.* **2008**, *47*, 5292
- ¹⁹ Sayari, A.; Hamoudi, S. *Chem. Mater.* **2001**, *13*, 3151
- ²⁰ Livage, J. *Revue Verre* **2000**, *6*, 1
- ²¹ (a) Hubert-Pfalzgraf, L.G. *Coord. Chem. Rev.* **1998**, *178-180*, 967, (b) Livage, J., Henry, M., Sanchez, C. *Prog. Solid State Chem.* **1988**, *18*, 259
- ²² (a) Landry, C. J. T.; Coltrain, B. K.; Wesson, J. A.; Zumbulyadis, N.; Lippert, J. L. *Polymer* **1992**, *33*, 1496 (b) Landry, C. J. T.; Coltrain, B. K.; Brady, B. K. *Polymer* **1992**, *33*, 1486 (c) Landry, C. J. T.; Coltrain, B. K.; Landry, M. R.; Fitzgerald, J. J.; Long, V. K. *Macromolecules* **1993**, *26*, 3702

- ²³ (a) Ellsworth, M. W.; Novak, B. M. *Polym. Prepr.* **1992**, *33*, 1088 (b) Ellsworth, M. W.; Novak, B. M. *J. Am. Chem. Soc.* **1991**, *113*, 2756 (c) Novak, B. M. *Adv. Mater.* **1993**, *5*, 422 (d) Novak, B. M.; Davies, C. *Macromolecules* **1991**, *24*, 5481
- ²⁴ (a) Hajji, B.; David, L.; Gérard, J. F.; Pascault, J. P.; Vigier, G. *J. Polym. Sci. : Part B: Polym. Phys.* **1999**, *37*, 3172 (b) Matjeka, L.; Dusek, K.; Plestil, J.; Kris, J.; Lednicky, F. *Polymer* **1998**, *40*, 171 (c) Matjeka, L.; Plestil, J.; Dusek, K. *J. Non-Cryst. Solids* **1998**, *226*, 114 (d) Wojcik, A. B.; Klein, L. C. *J. Non-Cryst. Solids* **1994**, *2*, 115.
- ²⁵ (a) Loy, D.A.; Shea, K. J. *Chem. Rev.* **1995**, *35*,1421 (b) Corriu, R. J. P.; Leclercq. D. *Angew. Chem., Int. Ed.* **1996**, *35*, 1421 (c) Shea, K. J.; Loy, D. A. *Chem. Mater.* **2001**, *13*, 3306 (d) Shea, K. J.; Loy, D. A.; Webster, O. *J. Am. Chem. Soc.* **1992**, *116*, 6700 (d) Shea, K. J.; Loy, D.; Webster, G. *Chem. Mater.* **1989**, *1*, 572 (e) Corriu, R. J. P.; Moreau, J. J. E.; Thepot, P.; Wong Chi Man, M. *Chem. Mater.* **1992**, *4*, 1217
- ²⁶ Choi, M.; Shea, K. J. *Plast. Eng.* **1998**, *49*, 437
- ²⁷ (a) Lindner, E.; Schneller, T.; Auer, F.; Mayer, H. A. *Angew. Chem., Int. Ed.* **1999**, *38*, 2155 (b) Schubert, U. *New J. Chem.* **1994**, *18*, 1049 (c) Moreau, J. J. E.; Wong Chi Man, M. *Coord. Chem. Rev.* **1998**, *178-180*, 1073
- ²⁸ Corriu, R. J. P. *Angew. Chem., Int. Ed.* **2000**, *39*, 1376
- ²⁹ (a) Shea, K. J.; Loy, D. A.; Webster, O. *Chem. Mater.* **1989**, *1*, 572 (b) Small, J. H.; Shea, K. J.; Loy, D. A. *J. Non-Cryst. Solids* **1992**, *160*, 234 (c) Shea, K. J.; Loy, D. A.; Webster, O. *J. Am. Chem. Soc.* **1992**, *114*, 6700
- ³⁰ (a) Corriu, R. J. P. *Polyhedron* **1998**, *17*, 925 (b) Boury, B.; Corriu, R. J. P., Le Strat, V.; Delord, P.; Nobili, M. *Angew. Chem., Int. Ed.* **1999**, *38*, 3172 (c) Boury, B.; Corriu, R. J. P.; Le Strat, V.; Delord, P. *New J. Chem.* **1999**, *23*, 531 (d) Cerveau, G.; Chappellet. S.; Corriu, R. J. P.; Dabiens, B. *J. Organomet. Chem.* **2001**, *626*, 92 (e) Boury, B.; Corriu, R. J. P.; Muramatsu, H. *New J. Chem.* **2002**, *26*, 981
- ³¹ (a) Loy, D. A.; Carpenter, J. P.; Yamanaka, S. A.; McClain, M. D.; Greaves, J.; Hobson, S.; Shea, K. J. *Chem. Mater.* **1998**, *10*, 4129 (b) Corriu, R. J. P.; Moreau, J. J. E.; Thepot, P.; Wong Chi Man, M. *J. Mater. Chem.* **1994**, *4*, 987
- ³² (a) Oviatt, H. W. Jr.; Shea, K. J.; Small, J. H. *Chem. Mater.* **1993**, *5*, 943 (b) Loy, D. A. Buss, R. J.; Assink, R. A.; Shea, K. J.; Oviatt, H. *J. Non-Cryst. Solids* **1995**, *186*, 44 (c) Loy, D. A.; Carpenter, J. P.; Myers, S. A.; Assink, R. A.; Small, J. H.; Greaves, J.; Shea, K. J. *J. Am. Chem. Soc.* **1996**, *118*, 8501
- ³³ (a) Hobson, S. T.; Shea, K. J. *Chem. Mater.* **1997**, *9*, 616 (b) Dalton, L. R.; Harper, A. W.; Ghosn, R.; Steier, W. H.; Ziari, M.; Fetterman, H.; Shi, Y.; Mustacich, R. V.; Jen, A. K. Y.; Shea, K. J. *Chem. Mater.* **1995**, *7*, 1060
- ³⁴ Oviat, H. W. Jr.; Shea, K. J.; Kalluri, S.; Shi, Y.; Steier, W. H.; Dalton, L. R. *Chem. Mater.* **1995**, *7*, 493
- ³⁵ Zhu, D.; Van Ooij, W. J. *J. Adhesion Sci. Tech.* **2002**, *16*, 1235
- ³⁶ (a) Corriu, R. J. P.; Embert, F.; Gauri, Y.; Mehdi, A.; Reye, C. *Chem. Commun.* **2001**, 1116 (b) Embert, F.; Mehdi, A.; Reye, C.; Corriu, R. J. P. *Chem. Mater.* **2001**, *13*, 4542
- ³⁷ Li, C.; Wilkes, G. L. *Chem. Mater.* **2001**, *13*, 3663

- ³⁸ Liu, N.; Yu, K.; Smarsly, B.; Dunphy, D. R.; Jiang, Y-B.; Brinker, C. J. *J. Am. Chem. Soc.* **2002**, *124*, 14540
- ³⁹ Cerveau, G.; Corriu, R. J. P.; Costa, N. *J. Non-Cryst. Solids* **1993**, *163*, 226
- ⁴⁰ (a) Choi, K. M.; Shea, K. J. *Chem. Mater.* **1993**, *5*, 1067 (b) Choi, K. M.; Shea, K. J. *J. Am. Chem. Soc.* **1994**, *116*, 9052
- ⁴¹ Loy, D. A.; Carpenter, J. P.; Myers, S. A.; Assink, R. A.; Small, J. H.; Greaves, J.; Shea, K. *J. Am. Chem. Soc.* **1996**, *118*, 8501
- ⁴² Shea, K. J.; Moreau, J.; Loy, D. A.; Corriu, R. J. P.; Boury, B. *Functional Hybrid Materials*, Wiley-VCH, Weinheim, **2004**, 70
- ⁴³ (a) Moreau, J. J. E.; Vellutini, L.; Wong Chi Man, M.; Bied, C.; Bantignies, J. L.; Dieudonne, P.; Sauvajol, J. L. *J. Am. Chem. Soc.* **2001**, *123*, 7957 (b) Moreau, J. J. E.; Vellutini, L.; Wong Chi Man, M.; Bied, C. *J. Am. Chem. Soc.* **2001**, *123*, 1509 (c) Corriu, R.; Anh. N. T. *Chimie Moléculaire, Sol-Gel et Nanomatériaux* Les Editions de l'Ecole Polytechnique, **2008**, 124
- ⁴⁴ Fujita, S.; Inagaki, S. *Chem. Mater.* **2008**, *20*, 891 (b) Hatton, B.; Landskron, K.; Whitnall, W.; Perovic, D.; Ozin, G. A. *Acc. Chem. Res.* **2005**, *38*, 305
- ⁴⁵ (a) Asefa, T.; MacLachlan, M. J.; Coombs, N.; Ozin, G. A. *Nature* **1999**, *402*, 867 (b) Inagaki, S.; Guan, S.; Fukushima, Y.; Ohsuna, T.; Terasaki, O. *J. Am. Chem. Soc.* **1999**, *121*, 9611 (c) Melde, B. J.; Holland, B. T.; Blanford, C. F.; Stein, A. *Chem. Mater.* **1999**, *11*, 3302 (d) Asefa, T.; MacLachlan, M.; Grondey, H.; Coombs, N.; Ozin, G. A. *Angew. Chem., Int. Ed.* **2000**, *39*, 1808
- ⁴⁶ (a) Beleizao, C.; Gigante, B.; Das, D.; Alvaro, M.; Garcia, H.; Corma, C. *Chem. Commun.* **2003**, 1860 (b) Kuroki, M.; Asefa, T.; Whitnall, W.; Kruk, M.; Yoshina-Ishii, C.; Jaroniec, M.; Ozin, G. A. *J. Am. Chem. Soc.* **2002**, *124*, 13886 (d) Temtsin, G.; Asefa, T.; Bittner, S.; Ozin, G. A. *J. Mater. Chem.* **2001**, *11*, 3202 (e) Ishii, C. Y.; Asefa, T.; Coombs, N.; MacLachlan, M.; Ozin, G. A. *Chem. Commun.* **1999**, 2539 (f) Mizoshita, N.; Ikai, M.; Tani, T.; Inagaki, S. *J. Am. Chem. Soc.* **2009**, *131*, 14225
- ⁴⁷ Asefa, T.; Kruk, M.; MacLachlan, M.; Coombs, N.; Grondey, H.; Jaroniec, M.; Ozin, G. A. *J. Am. Chem. Soc.* **2001**, *123*, 8520
- ⁴⁸ (a) Sanchez, C.; Lebeau, B.; Ribot, F.; In, M. *J. Sol-Gel Sci. Tech.* **2000**, *19*, 31 (b) Sanchez, C.; Ribot, F.; Lebeau, B. *J. Mater. Chem.* **1999**, *9*, 35 (c) Ribot, F.; Veautier, D.; Guillaudeu S.; Lalot, T. *J. Sol-Gel Sci. Tech.* **2004**, *32*, 37 (d) Sanchez, C.; Soler-Illia, G. J. de A. A.; Ribot, F.; Grosso, D. *C. R. Chimie* **2003**, *6*, 1131 (e) Sanchez, C.; Soler-Illia, G. J. de A. A.; Ribot, F.; Lalot, T.; Mayer, C. R.; Cabuil, V. *Chem. Mater.* **2001**, *13*, 3061 (f) Ribot, F.; Veautier, D.; Guillaudeu, S. J.; Lalot, T. *J. Mater. Chem.* **2005**, *15*, 3973
- ⁴⁹ Sanchez, C.; Ribot, F., *New J. Chem.* **1994** *18*, 1007
- ⁵⁰ Ribot, F.; Banse, F.; Sanchez, C.; Lahcini, M.; Jousseau, B. *J. Sol-Gel Sci. Tech.* **1997**, *8*, 529
- ⁵¹ Ribot, F.; Lafuma, A.; Eychenne-Baron, C.; Sanchez, C. *Adv. Mat.* **2002**, *14*, 1496
- ⁵² Fan, W-Q.; Feng, J.; Song, S-Y.; Lei, Y-Q.; Zheng, G-L.; Zhang, H-J. *Chem. Eur. J.* **2010**, *16*, 1903

- ⁵³ (a) Elhamzaoui, H.; Jousseau, B.; Riague, H.; Toupance, T.; Dieudonné, P.; Zakri, C.; Maugey, M.; Allouchi, H. *J. Am. Chem. Soc.* **2004**, *126*, 8130 (b) Elhamzaoui, H.; Jousseau, B.; Toupance, T.; Zakri, C.; Biesemans, M.; Willem, R.; Allouchi, H. *Chem. Commun.* **2006**, 1304 (c) Elhamzaoui, H.; Jousseau, B.; Toupance, T.; Zakri, C. *J Sol-Gel Sci. Technol.* **2008**, *48*, 6
- ⁵⁴ (a) Jousseau, B.; Lahcini, M.; Rascle, M.-C.; Sanchez, C.; Ribot, F. *Organometallics* **1995**, *14*, 685 (b) Jousseau, B.; Riague, H.; Toupance, T.; Lahcini, M.; Mountford, P.; Tyrell, B. R. *Organometallics* **2002**, *21*, 4590 (c) Biesemans, M.; Willem, R.; Damoun, S.; Geerlings, P.; Lahcini, M.; Jaumier, P.; Jousseau, B. *Organometallics* **1996**, *15*, 2237 (d) Jaumier, P.; Jousseau, B.; Tiekink, E. R. T.; Biesemans, M.; Willem, R. *Organometallics* **1997**, *16*, 5124 (e) Biesemans, M.; Willem, R.; Damoun, S.; Geerlings, P.; Tiekink, E. R. T.; Lahcini, M.; Jaumier, P.; Jousseau, B. *Organometallics* **1998**, *17*, 90 (f) Jaumier, P.; Jousseau, B.; Lahcini, M.; Ribot, F.; Sanchez, C. *Chem. Commun.* **1998**, 369 (g) Lahcini, M.; Jaumier, P.; Jousseau, B. *Angew. Chem., Int. Ed.* **1999**, *38*, 402.
- ⁵⁵ Elhamzaoui, H.; Jousseau, B.; Toupance, T.; Zakri, C. *Dalton Trans.* **2009**, *23*, 4429
- ⁵⁶ Trimmel, G.; Fratzl, P.; Schubert, U. *Chem. Mater.* **2000**, *12*, 602
- ⁵⁷ (a) Fornasieri, G.; Rozes, L.; Le Calvé, S.; Alonso, B.; Massiot, D.; Rager, M. N.; Evain, M.; Boubekour, K.; Sanchez, C. *J. Am. Chem. Soc.* **2005**, *127*, 4869 (b) Soler-Illia, G. J. de A. A.; Rozes, L.; Boggiano, M. K.; Sanchez, C.; Turrin, C. O.; Caminade, A. M.; Majoral, J. P. *Angew. Chem. Int. Ed.* **2000**, *39*, 4250 (c) Kameneva, O. V.; Kuznetsov, A. I.; Smirnova, L. A.; Rosez, L.; Sanchez, C.; Kanaev, A.; Alexandrov, A. P.; Bityurin, N. M. *Doklady Physics* **2006**, *51*, 103 (d) Kameneva, O.; Kuznetsov, A. I.; Smirnova, L. A.; Rozes, L.; Sanchez, C.; Alexandrov, A.; Bityurin, N.; Chhor, K.; Kanaev, A. *J. Mater. Chem.* **2005**, *15*, 3380 (e) Dominguez-Espinosa, G.; Halamus, T.; Wojciechowski, P.; Skurska, M.; Zaborski, M. *J. Non-Cryst. Solids* **2009**, *355*, 496 (f) Soler-Illia, G. J. de A. A.; Scolan, E.; Louis, A.; Albouy, P. A.; Sanchez, C. *New J. Chem.* **2001**, *25*, 156 (g) Schubert, U. *Acc. Chem. Res.* **2007**, *40*, 730
- ⁵⁸ (a) Bocchini, S.; Fornasieri, G.; Rozes, L.; Trabelsi, S.; Galy, J.; Zafeiropoulos, N. E.; Stamm, M.; Gérard, J. F.; Sanchez, C. *Chem. Commun.* **2005**, 2600 (b) Trabelsi, S.; Janke, A.; Hässler, R.; Zafeiropoulos, N. E.; Fornasieri, G.; Bocchini, S.; Rozes, L.; Stamm, M.; Gérard, J. F.; Sanchez, C. *Macromolecules* **2005**, *38*, 6068
- ⁵⁹ Kuznetsov, A. I.; Kameneva, O.; Bityurin, N.; Rozes, L.; Sanchez, C.; Kanaev, A. *Phys. Chem. Chem. Phys.* **2009**, *11*, 1248
- ⁶⁰ Trabelsi, S.; Fornasieri, G.; Rozes, L.; Janke, A.; Mensch, A.; Sanchez, C.; Stamm, M. *J. Appl. Cryst.* **2006**, *39*, 656
- ⁶¹ Cochet, S.; Rozes, L.; Popall, M.; Sanchez, C. *Mat. Sci. Eng. C* **2007**, *27*, 1401
- ⁶² Crouzet, L.; Leclercq, D.; Mutin, P. H.; Vioux, A. *J. Sol-Gel Sci. Tech.* **2003**, *26*, 335
- ⁶³ Lorret, O.; Lafond, V.; Mutin, P. H.; Vioux, A. *Chem. Mater.* **2006**, *18*, 4707
- ⁶⁴ Dan-Hardi, M.; Serre, C.; Frot, T.; Rozes, L.; Maurin, G.; Sanchez, C.; Férey, G. *J. Am. Chem. Soc.* **2009**, *131*, 10857

**CHAPTER II. SYNTHESIS OF
DI(CYCLOPENTADIENYLTITANIUM) PRECURSORS**

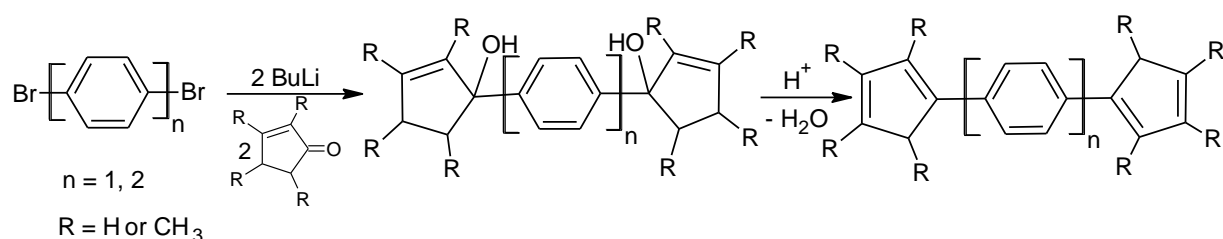
The first step of the project was the synthesis of suitable precursors able to allow the preparation of a new type of titanium-based hybrid materials where both networks are linked through strong titanium-cyclopentadienyl bonds. These compounds were chosen to be bis(polymethylcyclopentadienyltitanium) derivatives where the cyclopentadienyl groups are linked by different spacers and where the titanium atoms bear hydrolysable groups. It was important to get spacers of different lengths in order to allow the study of an eventual order in the corresponding materials. The presence of various hydrolysable groups was also important in order to change the rates of hydrolysis of the precursors, one of the factors influencing the kinetics of the formation of the hybrid materials.

I. Synthesis of dicyclopentadienyl ligands

The preparation of bis(polymethylcyclopentadienyl) ligands was the first goal of the project. Various synthetic routes have been reported in the literature to prepare these ligands with different spacers between the cyclopentadienyl groups and variable substituents on the ring.

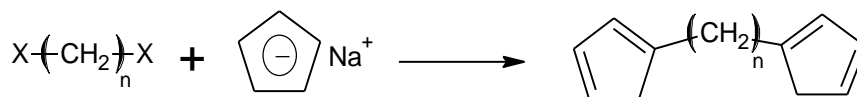
I.1. Literature review

The **nucleophilic reaction of spacers** is a very prominent route to synthesize dicyclopentadienyl ligands with variable spacers between the cyclopentadienyl groups¹. It is a two-step reaction which involves the nucleophilic attack of the lithium reagent derived from a dihalocompound on a cyclopent-2-enone to give a diol. The diol is used without further purification and its subsequent acid treatment results in the elimination of water leading to the dicyclopentadienyl ligands (Scheme II-1). This route has been used for the preparation of ligands with both aromatic and aliphatic spacers between the cyclopentadienyl groups. The starting materials are easy to get and the yield of the reactions is normally good making it a useful synthetic route for the preparation of the required ligands.



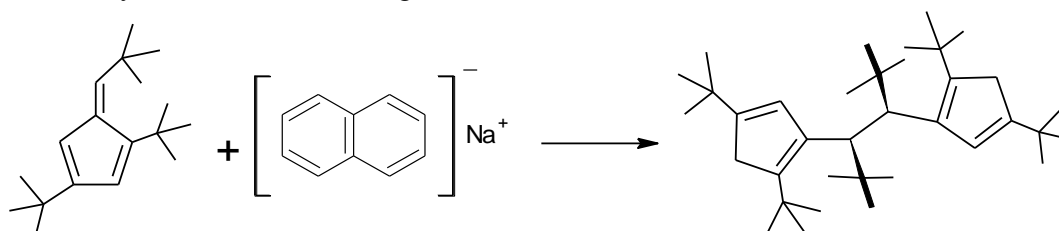
Scheme II-1: Nucleophilic reaction of spacers

An alternative method to prepare dicyclopentadienyl ligands with long alkyl or mixed aryl-alkyl spacers consists of **coupling a metallated cyclopentadiene** with a dihaloalkane². It is a one step reaction which results in the preparation of ligands in good yield. Cyclopentadienylsodium, the usual starting material, is a weak nucleophile which can easily substitute halogen atoms in aliphatic or mixed aliphatic-aromatic compounds like benzyl compounds (Scheme II-2). However it is not strong enough to be used with dihaloaromatic compounds. That is the reason why this synthetic route can only be utilized to prepare ligands with aliphatic or mixed aliphatic-aromatic spacers.



Scheme II-2: Nucleophilic reaction of cyclopentadiene

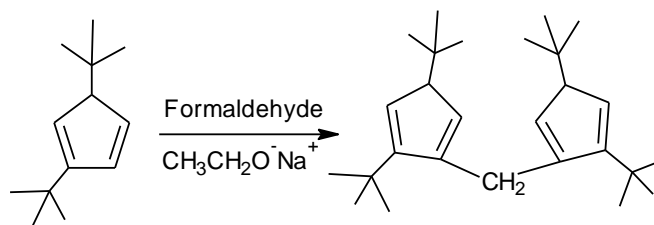
The **reductive dimerization** of fulvene is another synthetic route that leads to bridged dicyclopentadienyl ligands with short aliphatic spacers between the rings³. Reaction of 1,3,6-tri-tert-butylfulvene with sodium naphthalenide, followed by protonation of the disodium salt of the 1,2-dicyclopentadienylethane intermediate, results in rac-3,4-bis(1,4-di-tertbutylcyclopenta-1,3-dien-2-yl)-2,2,5,5-tetramethylhexane (Scheme II-3). A fulvene radical anion is the key intermediate, leading to the dimerization reaction.



Scheme II-3: Reductive dimerization

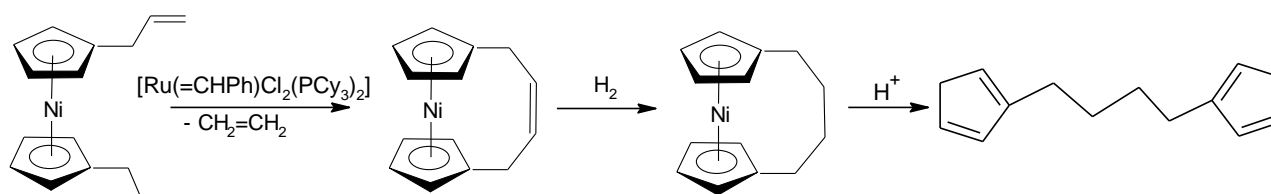
This reaction can potentially be used to prepare ligands with short aliphatic spacers and variable substituents on the ring.

Another synthetic route to prepare dicyclopentadienyl ligands with a short aliphatic spacer between the rings consists of the **addition of a cyclopentadienide anion to formaldehyde** (Scheme II-4). The yield of the reaction is, however, relatively low⁴.



Scheme II-4 : Reaction with aldehydes

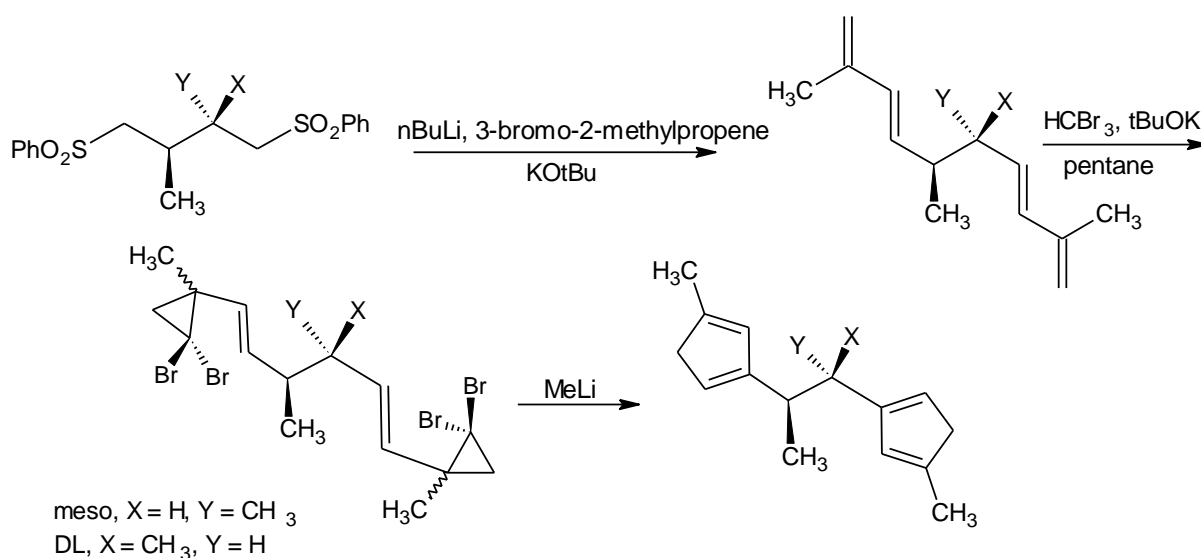
A ring closing **metathesis** reaction can also be considered. It has been used to prepare 1,1'-(2-buten-1,4-diyl)nickelocene⁵, which upon demetallation under acidic treatment leads to a dicyclopentadienyl compound having a long aliphatic spacer between the rings (Scheme II-5).



Scheme II-5 : Metathesis reaction

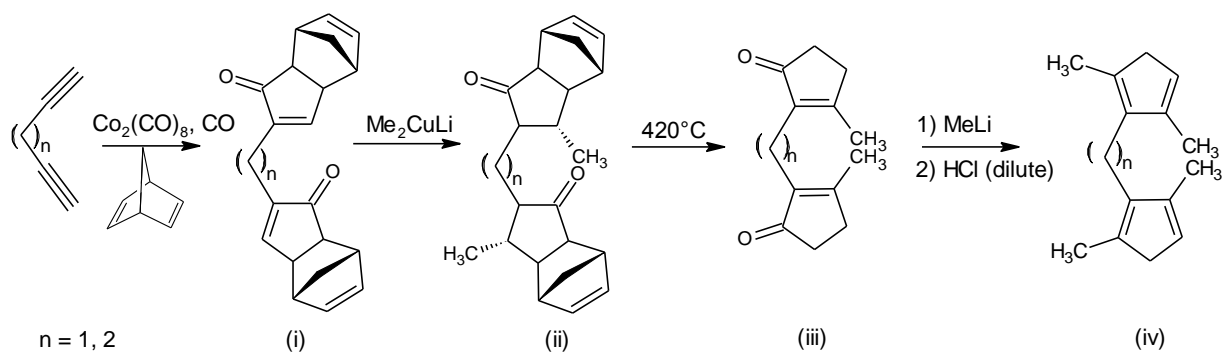
This synthetic route could in principle be applied to prepare ligands with longer aliphatic spacers. However, the use of an expensive catalyst, the multiple steps to reach the final product and the fewer yields make it less suitable for the preparation of the required ligands.

The **Skattebol rearrangement** is another example for the preparation of dicyclopentadienyl ligands with short aliphatic spacers. This two-step alkylation-elimination involves the formation of homoallylic sulfones which are treated with potassium tert-butoxide to afford tetraenes in meso and DL form. Subsequent cyclopropanation of tetraenes using Doering-Hoffmann conditions results in a diastereomeric mixture of the meso and DL tetrabromides in nearly quantitative yields. Addition of methyllithium to these thermally unstable tetrabromides leads to the Skattebol rearrangement that involves a ring expansion (Scheme II-6). The yield of the reaction is, however, moderate due to a competing side reaction involving the formation of terminal allenes⁶. Several steps are involved to reach the final dicyclopentadienyl compound and the starting materials are not commercially available.



Scheme II-6 : Skattebol rearrangement

The **Pauson-Khand reaction** is a useful method for the preparation of cyclopentenones by the cocyclization of an alkyne, an alkene and carbon monoxide. The cyclopentenones can then be easily converted to the cyclopentadienyl ligands in a next step (Scheme II-7). Dicyclopentadienylated ligands having a short aliphatic spacer and substituents on the carbon adjacent to the bridgehead carbon have been prepared using this synthetic route⁷. The Pauson-Khand reaction of 1,4-pentadiyne with norbornadiene leads to a tricyclic compound (i) which then reacts with Me₂CuLi to give a 1,4-addition product (ii). The thermal treatment of (ii) results in a retro-Diels-Alder reaction followed by a subsequent isomerization of double bonds to give the dicyclopentenone (iii). Further treatment of (iii) with MeLi and HCl gives a bridged dicyclopentadienylated ligand which has been used to prepare zirconium complexes used for the catalysis of ethylene-norbornene copolymerization. This preparation is, however, limited to trisubstituted cyclopentadienes and necessitates a thermolyzer.



Scheme II-7: Pauson-Khand reaction

Conclusion

According to the literature data presented above, the easiest way to get dicyclopentadienyl compounds separated by rigid spacers of variable nature and length seems the use of the nucleophilic reaction of the spacers on cyclopentenones. It requires fewer steps, involves easily available starting materials and leads to good yields of the products. This versatile method allows also to prepare dicyclopentadienyl ligands with different substituents on the cyclopentadienyl ring.

In the case of dicyclopentadienyl compounds with mixed aryl-alkyl spacers, the preparation involving a nucleophilic reaction of cyclopentadiene is the only one which authorizes structural variations of the spacers. However, it implies the use of reactive dihalides and either unsubstituted or tetramethylated cyclopentadienes to get symmetrical ligands.

I.2. Synthesis of the ligands with linear aromatic spacers

Various dicyclopentadienyl-substituted compounds with linear aromatic spacers were prepared. The nature of the spacer was changed from one phenyl group to two and three phenyl groups as well as to a bithiophenylene group. The cyclopentadienyl rings were substituted with two or four methyl groups to get more stable ligand-metal bonds.

A list of all the spacers is summarized in Table II-1.


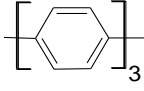
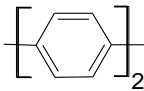
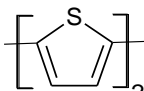
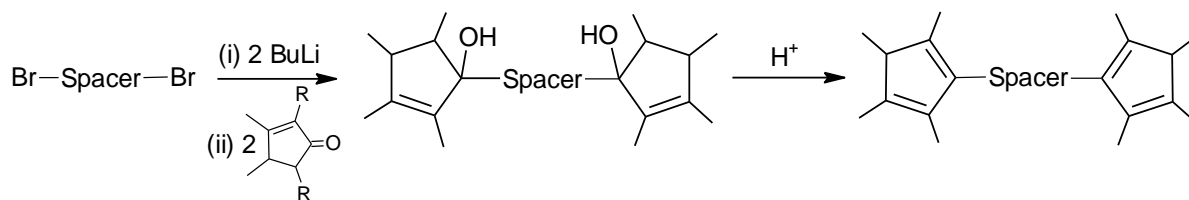
Rigid spacers	
	
	

Table II-1: Ligands with linear aromatic spacers

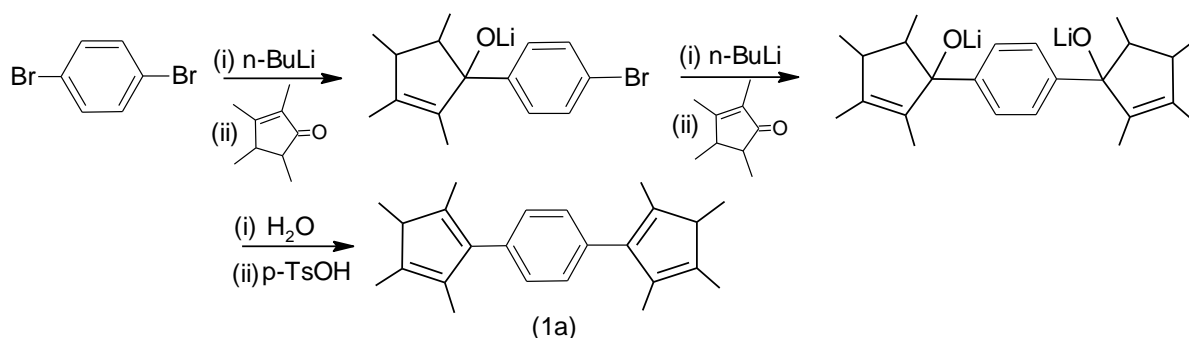
The synthesis of such compounds was achieved by the condensation of a bimetallic species, Grignard or lithium reagents, on 2,3,4,5-tetramethylcyclopent-2-enone, followed by dehydration of the formed diol. A general reaction scheme using a lithium reagent is given below.



Scheme II-8: General reaction scheme for the preparation of ligands

1.2.1. Synthesis of 1,4-bis(2,3,4,5-tetramethylcyclopentadienyl)benzene (1a)

The synthesis of 1,4-bis(2,3,4,5-tetramethylcyclopentadienyl)benzene was carried out following the two-step procedure described in the literature⁸ that avoids the formation of a monosubstitution compound, (2,3,4,5-tetramethylcyclopentadienyl)benzene, as a by-product. 1,4-Dibromobenzene was treated with one equivalent of n-BuLi to make the corresponding monolithium reagent that was then coupled with 2,3,4,5-tetramethylcyclopent-2-enone. The monosubstituted compound was next reacted with one equivalent of n-BuLi followed by its subsequent reaction with the ketone. After hydrolysis, it resulted in the formation of a diol. The acid treatment of the diol led to 1,4-bis(2,3,4,5-tetramethylcyclopentadienyl)benzene in 85% yield (Scheme II-9).



Scheme II-9: Synthesis of 1,4-bis(2,3,4,5-tetramethylcyclopentadienyl)benzene

Due to 1,5-sigmatropic hydrogen shift common in cyclopentadienyl compounds, six isomers can be formed.

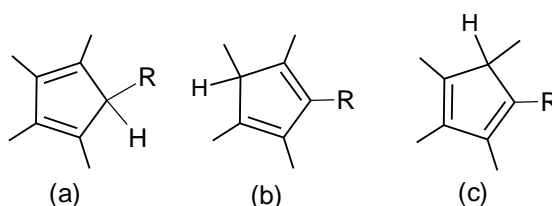
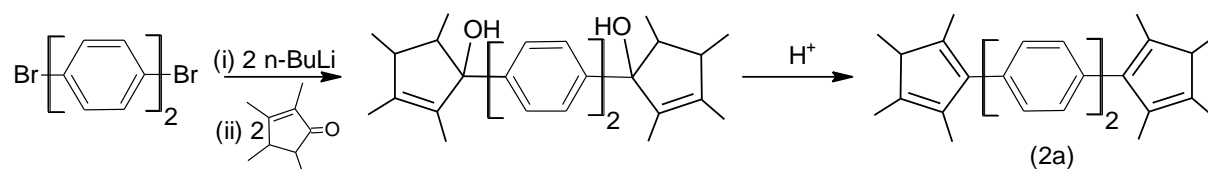


Figure II-1: Possible isomers of 1,4-bis(2,3,4,5-tetramethylcyclopentadienyl)benzene

The final product was characterized by ^1H , ^{13}C NMR, COSY and mass spectrometry. The 2D COSY spectrum indicates a weak long distance correlation of the allylic hydrogen with two methyl groups and not with the third one. This led to attribute the structure (b) for the ligand. A very small amount (<10%) of structure (c) is also formed as indicated by the ^1H NMR and GC-mass spectrometry. There is no peak in the NMR spectrum of the product that could be associated with structure (a). The reason for this dominance of isomers (b) and (c) over the other could be attributed to their better stability as their phenylene groups are conjugated to the double bonds.

1.2.2. Synthesis of 4,4'-bis(2,3,4,5-tetramethylcyclopentadienyl)biphenyl (2a)

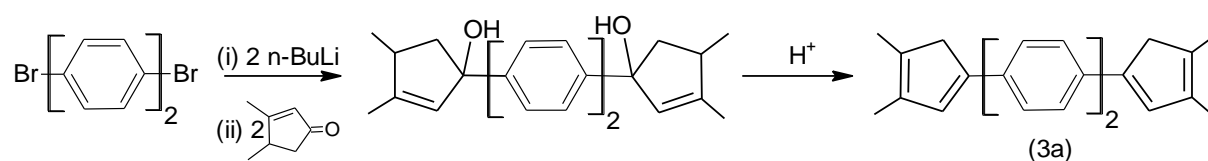
In order to study the effect of the length of the spacers on the self-assembly of the materials, the spacer was changed from a phenylene to a biphenylene group. The one-step dilithiation route reported by Do⁹ was followed instead of the stepwise monolithiation used for the preparation of 1,4-bis(2,3,4,5-tetramethylcyclopentadienyl)benzene. The treatment of 4,4'-dibromobiphenyl with two equivalents of *n*-BuLi resulted in the formation of a dilithiated reagent. It was then washed with diethyl ether to remove the monolithiated side product and the excess of *n*-BuLi. The subsequent coupling of this dilithiated reagent with two equivalents of 2,3,4,5-tetramethylcyclopent-2-enone resulted in the formation of a diol as a colorless oil which was used without further purification. The diol was treated with a catalytic amount of *p*-toluenesulfonic acid to afford the required ligand in 58% yield consisting of mainly one isomer (Scheme II-10).



Scheme II-10: Synthesis of 4,4'-bis(2,3,4,5-tetramethylcyclopentadienyl)biphenyl

1.2.3. Synthesis of 4,4'-bis(3,4-dimethylcyclopentadienyl)biphenyl (3a)

4,4'-Bis(3,4-dimethylcyclopentadienyl)biphenyl was prepared in order to study the effect of methyl substituents on the structure and properties of the corresponding hybrid material. When this compound is used as a ligand, the three cycles are almost coplanar¹⁰ while in the case of substitution on 2 and 5 positions of the cyclopentadienyl group, they are not because of the steric constraints brought by the methyl groups⁹. The dilithiated biphenyl reagent was thus reacted with 3,4-dimethylcyclopent-2-enone followed by its acid treatment (Scheme II-11). The product was obtained as a yellow solid in 57% yield.

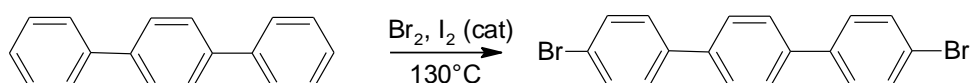


Scheme II-11: Synthesis of 4,4'-bis(3,4-dimethylcyclopentadienyl)biphenyl

A very prominent decrease in the solubility of the compound was observed with respect to 4,4'-bis(2,3,4,5-tetramethylcyclopentadienyl)biphenyl. The compound was very less soluble in all solvents and its ^1H NMR was taken in $\text{C}_2\text{D}_2\text{Cl}_4$ at 120°C . This effect could be attributed to a higher association of the molecules resulting from a more planar structure in (3a) than in (2a).

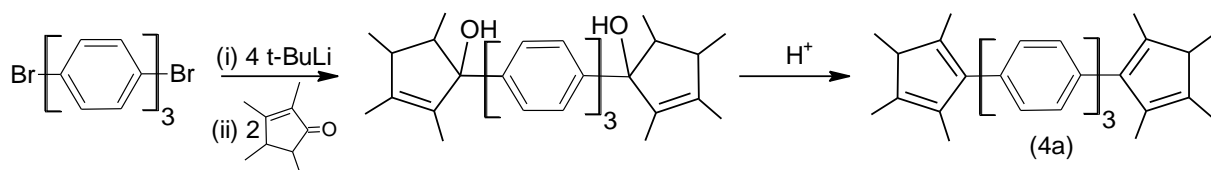
I.2.4. Synthesis of 4,4''-bis(2,3,4,5-tetramethylcyclopentadienyl)terphenyl (4a)

4,4''-Dibromoterphenyl was prepared by the bromination of terphenyl in the presence of iodine as a catalyst¹¹.



Scheme II-12: Synthesis of 4,4''-dibromoterphenyl

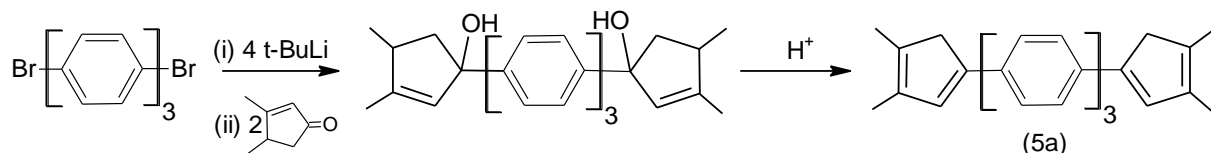
The lithiation of 4,4''-dibromoterphenyl was carried out with $t\text{-BuLi}$ ¹² followed by its coupling with 2,3,4,5-tetramethylcyclopent-2-enone to form the diol in one step. The diol was treated with p -toluenesulfonic acid without any purification and the required ligand was obtained in 45% yield (Scheme II-13). The comparatively lower yield of the ligand could be attributed to the lower solubility of the starting material in diethyl ether used for the reaction.



Scheme II-13: Synthesis of 4,4''-bis(2,3,4,5-tetramethylcyclopentadienyl)terphenyl

I.2.5. Synthesis of 4,4''-bis(3,4-dimethylcyclopentadienyl)terphenyl (5a)

The dilithiated terphenyl was reacted with 3,4-dimethylcyclopent-2-enone. The resulting diol was then treated with a catalytic amount of p -toluenesulfonic acid to furnish the required compound as a yellow powder in 43% yield (Scheme II-14).

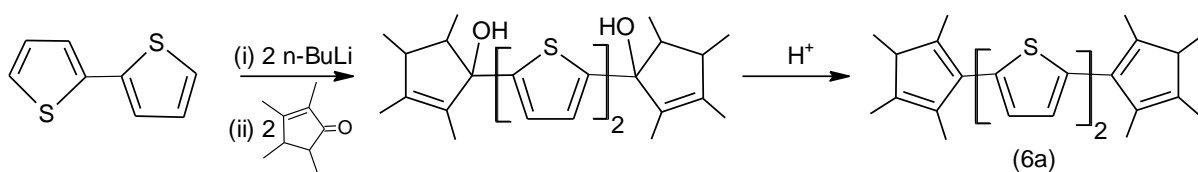


Scheme II-14: Synthesis of 4,4''-bis(3,4-dimethylcyclopentadienyl)terphenyl

The compound is practically insoluble in all solvents. It was characterized by ^1H NMR in $\text{C}_2\text{D}_2\text{Cl}_4$ at 120°C and high resolution mass spectrometry.

1.2.6. Synthesis of 5,5'-bis(2,3,4,5-tetramethylcyclopentadienyl)bithiophene (6a)

A ligand with a bithiophenylene spacer was then prepared as this spacer should potentially increase stacking interactions between the ligands by sulfur-sulfur interactions. A bis(tetramethylcyclopentadienyl) ligand with a thiophenylene spacer was reported recently and used in germanium, tin and iron chemistry¹³. A stepwise lithiation of 2,5-dibromothiophene followed by two successive additions of the ketone was carried out leading to 2,5-bis(2,3,4,5-tetramethylcyclopentadienyl)thiophene in only 10% yield. Instead of following this literature route, we used the usual one step procedure which consists of the addition of two equivalents of 2,3,4,5-tetramethylcyclopent-2-enone on the dilithiated spacer, followed by the dehydration of the resulting diol (Scheme II-15). As bithiophene can be easily lithiated at 5 and 5' positions by n-BuLi, bromination of the starting material to allow the lithiation reaction is not necessary. After extraction and purification steps, the required 5,5'-bis(2,3,4,5-tetramethylcyclopentadienyl)bithiophene was obtained as a yellow powder in 49% yield.

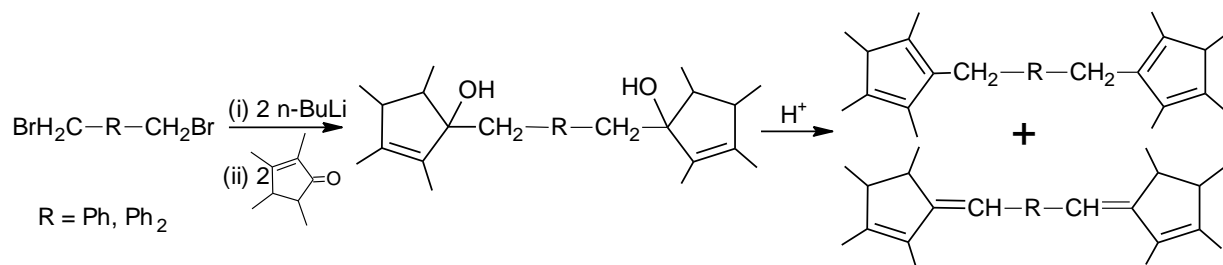


Scheme II-15: Synthesis of 5,5'-bis(2,3,4,5-tetramethylcyclopentadienyl)bithiophene

1.3. Synthesis of the ligands with mixed aryl-alkyl spacers

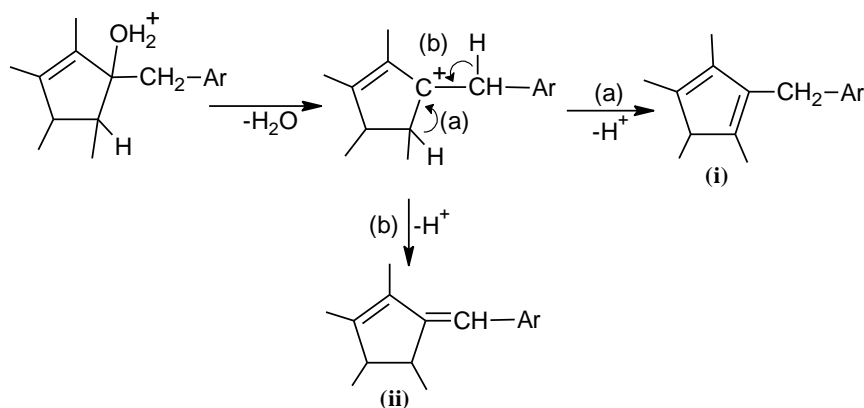
Dicyclopentadienyl compounds with mixed aryl-alkyl spacers were also prepared in order to bring some flexibility to the resulting materials and to induce some degree of freedom to allow them to self-assemble more easily.

The coupling of the dilithium reagent derived from the central unit with 2,3,4,5-tetramethylcyclopent-2-enone followed by its dehydration with p-toluenesulfonic acid resulted in the formation of the required ligand along with an exocyclic side product ($\approx 20\%$) (Scheme II-16).



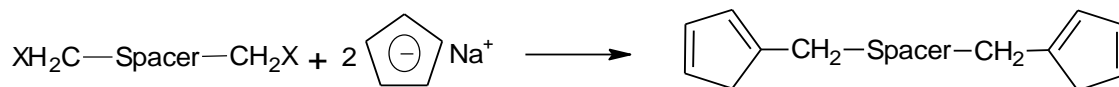
Scheme II-16: Synthesis of ligand with semi-rigid spacers

The exocyclic product is formed during the dehydration of the diol due to the availability of benzylic protons in the vicinity.



Scheme II-17: Mechanism of acid catalyzed dehydration leading to a mixture of regioisomers

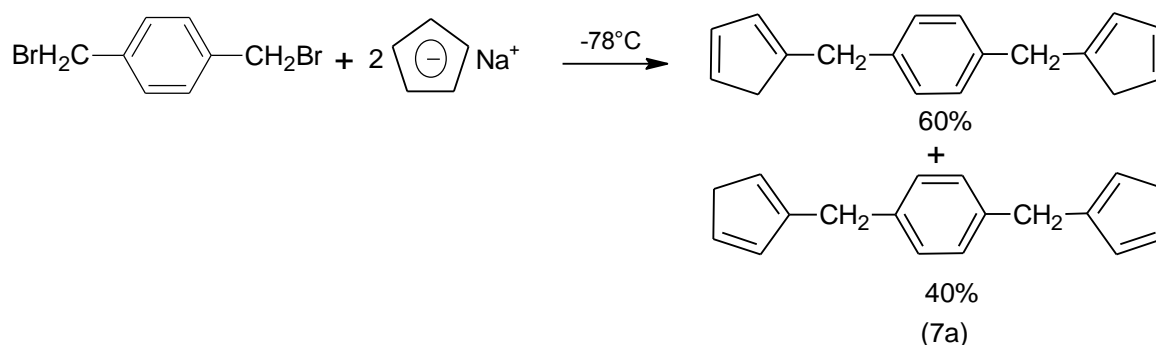
Similarly, a Barbier reaction where a simultaneous addition of benzyl halide and ketone on the metal is carried out resulted in the same mixture of products. All attempts to purify the ligand failed. Another synthetic route, the nucleophilic substitution of benzylic bromides by cyclopentadienylmetals, was then used^{2a,b}. With tetramethylcyclopentadienyllithium it did not give better results as, again, a mixture of isomers was obtained. However, with cyclopentadienylsodium the coupling with dihalocompounds occurred at lower temperature and did not involve any side products (Scheme II-18).



Scheme II-18: General reaction for the preparation of ligands with mixed aryl-alkyl spacers

1.3.1. Synthesis of 1,4-bis(cyclopentadienylmethyl)benzene (7a)

1,4-Bis(cyclopentadienylmethyl)benzene was prepared by reaction of 1,4-bis(bromomethyl)benzene with a stoichiometric amount of cyclopentadienylsodium at low temperature^{2a} (Scheme II-19).



Scheme II-19: Synthesis of 1,4-bis(cyclopentadienylmethyl)benzene

The ligand was obtained as a yellow oil in 30% yield. It was unstable at room temperature, where a Diels-Alder reaction between cyclopentadienyl groups takes place resulting in a polymeric material. The product was stored in dilute solution at -20°C . The

NMR spectrum of the product indicated the formation of a mixture of isomers due to a 1,5-sigmatropic hydrogen shift in about 60 : 40 ratio. The COSY spectrum showed that a correlation between allylic and benzylic protons exists in one of the isomers and is absent in the other one. Combining the results of 1D and 2D experiments, the above mentioned structures can be deduced. The possibility of a mixed isomer (Figure II-2) was rejected based on the integration of signals in ^1H NMR .

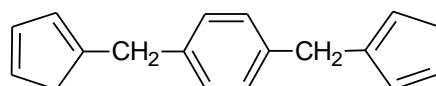
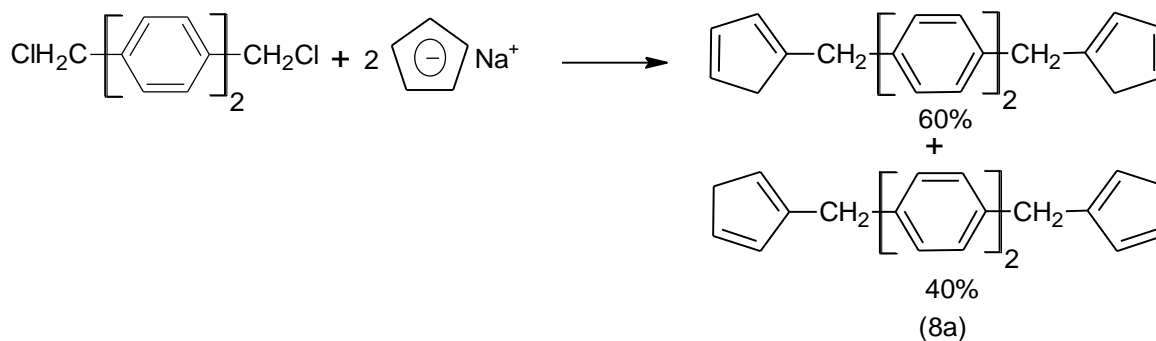


Figure II-2: Mixed double bond isomer

The product was used without further purification as both the isomers result in the same dilithiated reagent by reaction with *n*-BuLi in the next step.

1.3.2. Synthesis of 4,4'-bis(cyclopentadienylmethyl)biphenyl (8a)

The synthesis of 4,4'-bis(cyclopentadienylmethyl)biphenyl was carried out by the nucleophilic attack of cyclopentadienylsodium on 4,4'-bis(chloromethyl)biphenyl^{2h} (Scheme II-20). As chlorine is not as good leaving group as bromine, the reaction was carried out at room temperature instead of low temperature as in the previous case. The product was obtained as a white powder. It was more stable at room temperature and did not polymerize during the purification procedure. The yield of the reaction was, however, very low (9%).



Scheme II-20: Synthesis of 4,4'-bis(cyclopentadienylmethyl)biphenyl

The same mixture of isomers was obtained as for 1,4-bis(cyclopentadienylmethyl)-benzene which was used as such for the next step.

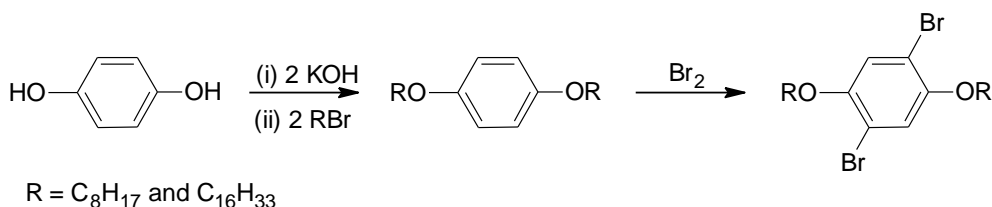
1.4. Synthesis of the ligands with long lateral chains containing spacers

The next objective of the project was to prepare dicyclopentadienyl ligands containing long lateral chains in the spacers. The presence of these chains could not only modify the physical properties of the precursors, as their solubility for instance, but could also result in a change in the organization of the materials as seen in tin-based hybrid materials¹⁴.

I.4.1. Synthesis of 2,5-bis(3,4-dimethylcyclopentadienyl)-1,4-bis(octyloxy)benzene (9a)

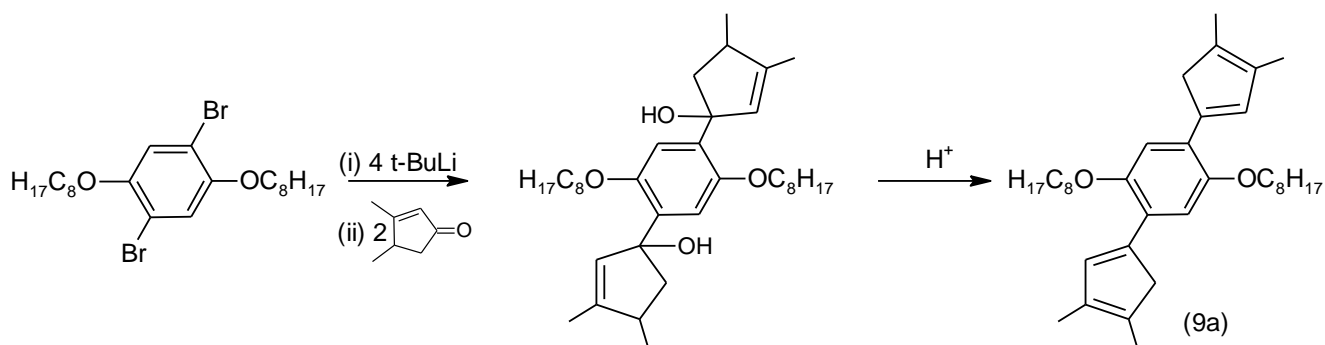
The octyloxy substituted ligand was prepared in the same manner as the unsubstituted ones.

In the first step, hydroquinone was treated with a haloalkane in basic media to furnish the dialkoxybenzene which was then brominated¹⁵.



Scheme II-21: Synthesis of 2,5-dibromo-1,4-bis(octyloxy)benzene

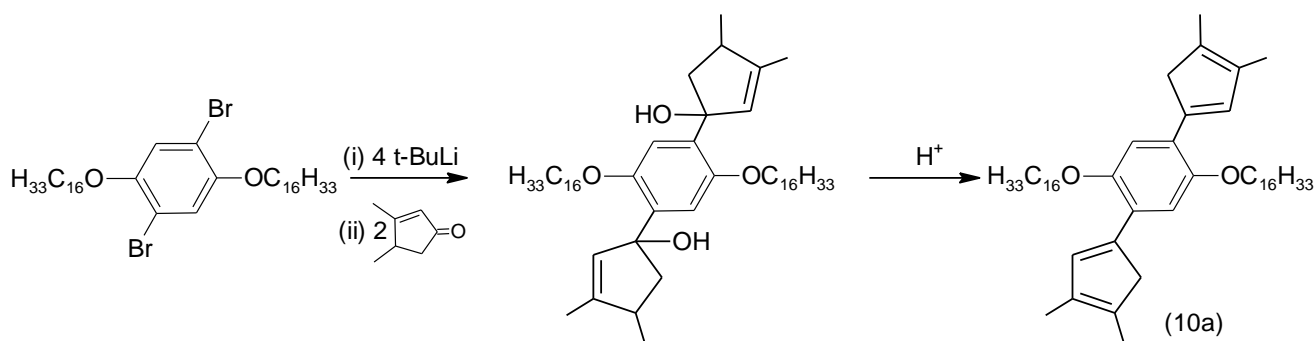
The dimetallation of 2,5-dibromo-1,4-bis(octyloxy)benzene with *t*-butyllithium in diethylether furnished the corresponding dilithiated reagent which was then reacted with 2,3,4,5-tetramethylcyclopent-2-enone. In this case, however, the expected diol was not obtained perhaps due to steric hindrance of the long alkyl chains. In order to reduce the steric hindrance and to facilitate the attack of the dilithiated derivative on the ketone, 2,3,4,5-tetramethylcyclopent-2-enone was replaced by 3,4-dimethylcyclopent-2-enone. The required diol was then obtained in good yield. It was not purified and was subsequently dehydrated at room temperature by treatment with a catalytic amount of *p*-toluenesulfonic acid (Scheme II-22). Recrystallization in toluene gave the dicyclopentadienyl ligand in 45% yield.



Scheme II-22: Synthesis of 2,5-bis(3,4-dimethylcyclopentadienyl)-1,4-bis(octyloxy)benzene

I.4.2. Synthesis of 2,5-bis(3,4-dimethylcyclopentadienyl)-1,4-bis(hexadecyloxy)benzene (10a)

The same route was used to synthesize the 2,5-bis(3,4-dimethylcyclopentadienyl)-1,4-bis(hexadecyloxy)benzene (scheme II-23). However, a small amount of the monosubstituted product was also obtained that was easily removed by recrystallization in toluene. The pure product was obtained in 48% yield. It was much less soluble in most of the solvents and its NMR was taken at higher temperature (55°C) in CDCl₃.



Scheme II-23: Synthesis of 2,5-bis(3,4-dimethylcyclopentadienyl)-1,4-bis(hexadecyloxy)benzene

I.5. Summary

A list of all the prepared dicyclopentadienyl ligands with various spacers and their starting materials is given in Table II-2.

	Starting materials	Ligands	Yield (%)
(1a)	 Available		85
(2a)	 Available		58
(3a)	 Available		57
(4a)	 Prepared		45
(5a)	 Prepared		43
(6a)	 Prepared		49

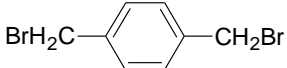
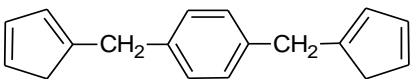
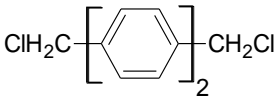
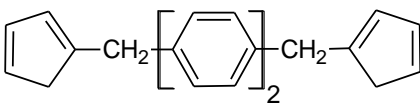
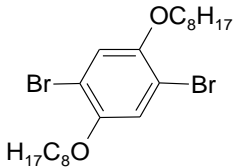
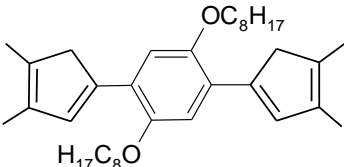
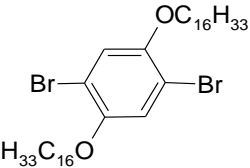
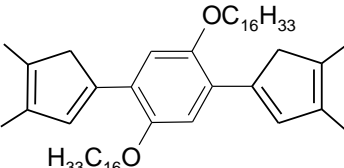
(7a)	 Available	 Available	30
(8a)	 Available	 Available	9
(9a)	 Prepared	 Prepared	45
(10a)	 Prepared	 Prepared	48

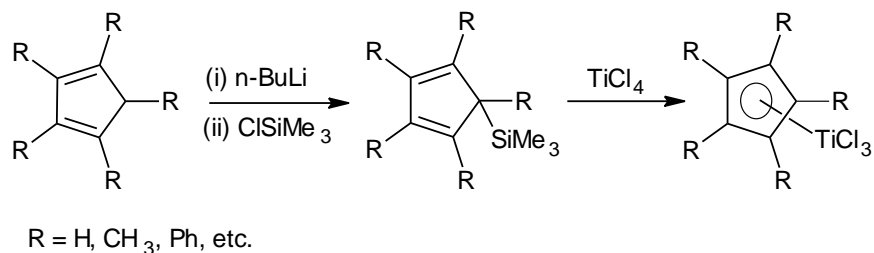
Table II-2: A summary of the prepared dicyclopentadienyl compounds and their starting materials

II. Synthesis of dititanium complexes

The next step is the introduction of the metal to these dicyclopentadienyl ligands which can be done by well-know literature routes.

II.1. Literature review

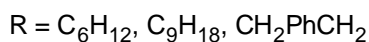
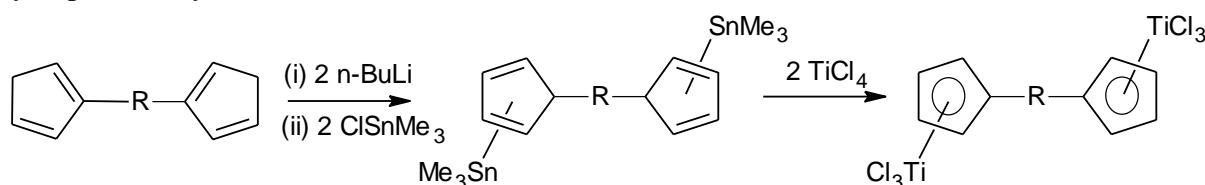
The most common route to bind a titanium metal to cyclopentadienyl ligands is a three-step reaction. The first step is the preparation of cyclopentadienyllithium salts, followed by their transmetallation into silylated compounds by reaction with chlorotrimethylsilane. In the last step, a reaction with titanium tetrachloride leads to trichlorotitanium complexes¹⁶ (Scheme II-24).



Scheme II-24: Synthesis of cyclopentadienyltitanium complexes through silylated derivatives

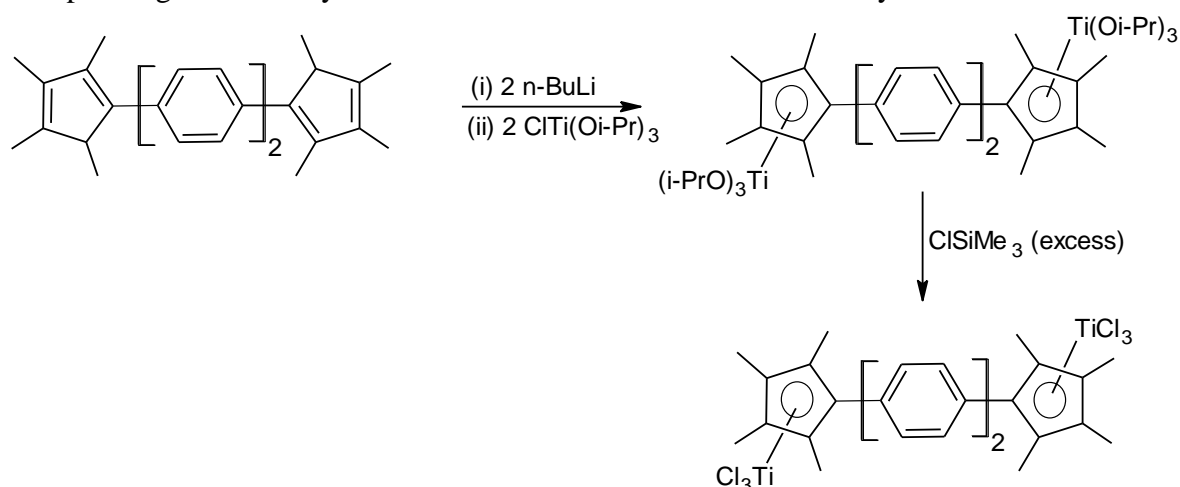
This method avoids the side reduction into titanium (III) species. It is a versatile route which is applicable to both substituted and unsubstituted cyclopentadienes. Later, if required, the trichlorides can be converted into the trialkoxides by reaction with a lithium alkoxide or an alcohol in the presence of triethylamine¹⁷. So far this method has been only used to prepare monocyclopentadienyltitanium complexes but it can be potentially applied to the synthesis of di(cyclopentadienyltitanium) complexes as well.

An analogy to the above mentioned route is to pass through stannylated derivatives¹⁸ instead of the silylated ones (Scheme II-25). Due to the more labile nature of the cyclopentadienyl-tin bond, the reaction with TiCl_4 is faster in this case.



Scheme II-25: Synthesis of di(cyclopentadienyltitanium) complexes through distannylated derivatives

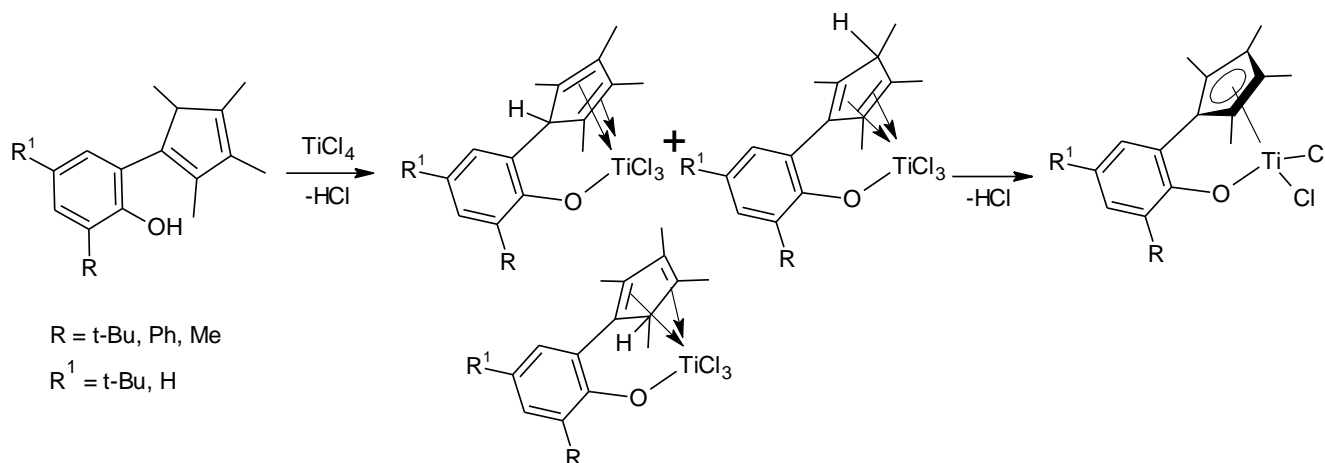
The reaction of cyclopentadienylmetal complexes with trialkoxychlorotitaniums has been developed for the synthesis of mono-¹⁹ or di(cyclopentadienyltrialkoxytitanium)^{9,20} complexes. It has the advantage of giving directly the alkoxides without isolating the corresponding chlorides. It is a two-step reaction in which cyclopentadienyllithiums or cyclopentadienylsodiums prepared from cyclopentadienes and $n\text{-BuLi}$ or $\text{NaH}^{2a, 2h}$ are treated with trialkoxychlorotitanium. It results in the formation of the required titanium complexes in good yield. An example of this route for the preparation of 4,4'-biphenylenebis(2,3,4,5-tetramethylcyclopentadienyl)di(triisopropoxytitanium) reported by Do⁹ is represented in Scheme II-26. If desired, the prepared titanium trialkoxides can be converted to the corresponding chlorides by treatment with an excess of chlorotrimethylsilane.



Scheme II-26: Synthesis of a di(cyclopentadienyltitanium) complex by reaction of a di(cyclopentadienyllithium) with a trialkoxychlorotitanium

This route has been used to prepare mono- or dicyclopentadienyl titanium complexes with or without substitution on the ring.

The use of cyclopentadienyl salts is not always necessary as it has been shown in a one-step synthesis of monocyclopentadienyltitanium complexes by addition of TiCl_4 to substituted cyclopentadienes. The presence of a side chain on the ring facilitates the reaction by coordinating the cyclopentadienyl group to the titanium atom and hence making the deprotonation easier (Scheme II-27).



Scheme II-27: Proposed mechanism for the direct synthesis of cyclopentadienyltitanium complexes

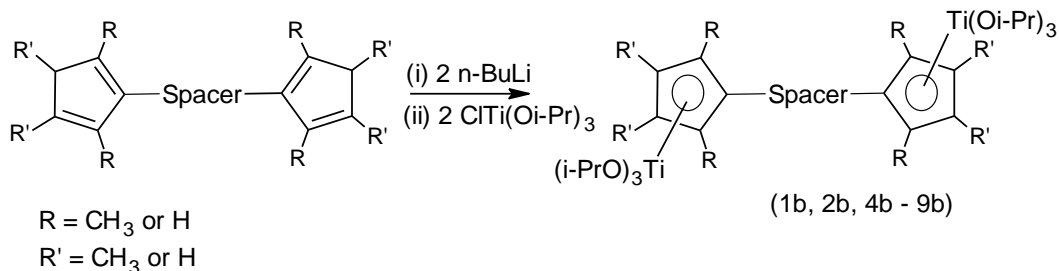
This route has been used for the synthesis of tetra- and pentamethylsubstituted cyclopentadienyltrichlorotitanium complexes. Unsubstituted cyclopentadienes, however, resulted in the formation of a black tar due to polymerization. This method is thus limited to the synthesis of polysubstituted cyclopentadienyl complexes only.

Conclusion

After a thorough literature study, the reaction of cyclopentadienylmetal complexes with trialkoxychlorotitaniums seems most appropriate to prepare the required compounds. This route has already been reported for the preparation of dimetallic complexes, works well for both substituted and unsubstituted cyclopentadienyl groups and involves less number of steps. The method involving silylated derivatives is well-developed but it involves two more steps to reach the targeted compound.

II.2. Syntheses of di(cyclopentadienyltriisopropoxytitanium) complexes

The reaction of a di(cyclopentadienyllithium) with chlorotriisopropoxytitanium, initially reported with a biphenylene spacer between the cyclopentadienyl rings, has been used to prepared the needed di(cyclopentadienyltriisopropoxytitanium) complexes⁹ (Scheme II-28). It was successfully extended to other ligands containing different spacers as well as to ligands having dimethyl substitution or no substitution on the cyclopentadienyl group (Table II-3).



Scheme II-28: General reaction for the syntheses of di(cyclopentadienyltriisopropoxytitanium) complexes

	Spacer	R	R'	Reaction time	Yield (%)
1b		CH ₃	CH ₃	3 days reflux	67
2b		CH ₃	CH ₃	3 days reflux	73
4b		CH ₃	CH ₃	3 days reflux	42
5b		H	CH ₃	3 days reflux	42
6b		CH ₃	CH ₃	2 days reflux	40
7b		H	H	24h RT	77
8b		H	H	24h RT	85
9b		H	CH ₃	4 days reflux	95

Table II-3: Conditions for the preparation of di(cyclopentadienyltriisopropoxytitanium) complexes

The reaction time varied depending on nature of the spacer and of the substituents on the cyclopentadienyl group. The addition of chlorotriisopropoxytitanium to the dilithium reagent of the ligand was carried out at 0°C. Then one night stirring at room temperature was enough for complexes having benzylic spacers and unhindered cyclopentadienyl groups. For all other complexes having methyl substituents on the ring, heating for 3 days was required to overcome the steric constraints. The complex with lateral chains required even longer reaction time. The expected product was obtained as a yellow powder after refluxing for 4 days. The

reaction involving 2,5-bis(3,4-dimethylcyclopentadienyl)-1,4-bis(hexadecyloxy)benzene (**10a**) remained incomplete even after 4 days of reflux. Similarly, a mixture of products containing mono- and disubstituted products was obtained when the reaction was carried out with 4,4'-bis(3,4-dimethylcyclopentadienyl)biphenyl (**3a**).

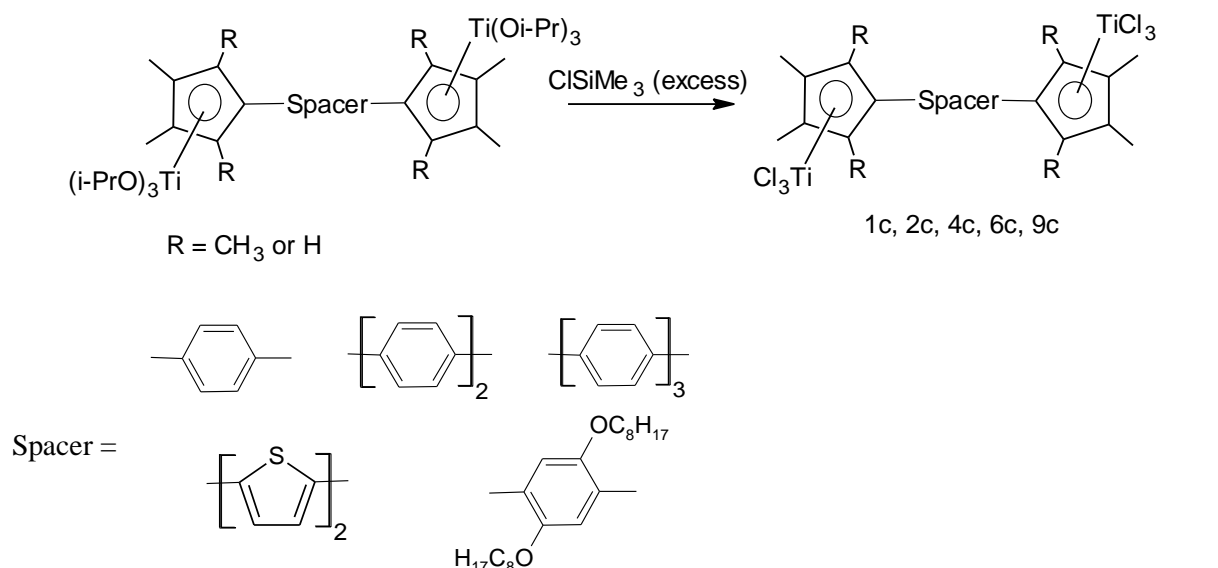
The complexes were extracted from the reaction mixture with pentane that led to yellow powders after evaporation of the solvent. Then they were washed with pentane to get rid of remaining chlorotriisopropoxytitanium. However, due to the very high solubility of these complexes in pentane and other solvents, a large amount of the products was lost during the washing and yields were low.

The complexes having benzylic spacers are viscous liquids and hence are the most difficult to purify. The purification was carried out by passing them several times through bio-bead columns using THF as the eluent.

These metal complexes are potential precursors for the hybrid materials as each titanium atom in the complex is endowed with three hydrolysable groups. However in order to study the influence of different hydrolysable groups on the rate of hydrolysis in sol-gel process and eventually on the organization of the materials, we decided to replace the isopropoxy groups with methyl groups. Direct conversion from the hexaisopropoxides to the hexamethyl complexes using MeLi resulted in a mixture of products that could not be separated. As a consequence, a two-step route was adopted that involves the conversion of the hexaisopropoxides into the corresponding hexachlorides and then to the hexamethyl complexes.

II.3. Syntheses of di(cyclopentadienyltrichlorotitanium) complexes

The conversion of di(cyclopentadienyltriisopropoxytitanium) compounds to the corresponding hexachlorides has been well described in the literature⁹. It involves a simple one-step reaction of the hexaisopropoxide with chlorotrimethylsilane as the chlorinating agent (Scheme II-29). The same reaction path was extended to all the complexes. An excess of chlorotrimethylsilane was added to a solution of di(cyclopentadienyltriisopropoxytitanium) in dichloromethane at 0°C and the reaction mixture was stirred at room temperature for 24h. A slow formation of red precipitates was observed during the course of the reaction. The resulting precipitates were washed with a mixture of pentane/dichloromethane (3/1) and characterized by NMR spectroscopy. However, in the case of 1,4-bis(octyloxy)phenylene-2,5-bis(3,4-dimethylcyclopentadienyl)di(triisopropoxytitanium) and 5,5'-bithiophenylenebis-(2,3,4,5-tetramethylcyclopentadienyl)di(triisopropoxytitanium), dichlorodimethylsilane was used instead of chlorotrimethylsilane to increase the rate of the chlorination reaction. The formed purple precipitates were washed with acetonitrile to give a good yield of the complexes (Table II-4).



Scheme II-29: General reaction for the syntheses of di(cyclopentadienyltrichlorotitanium) complexes

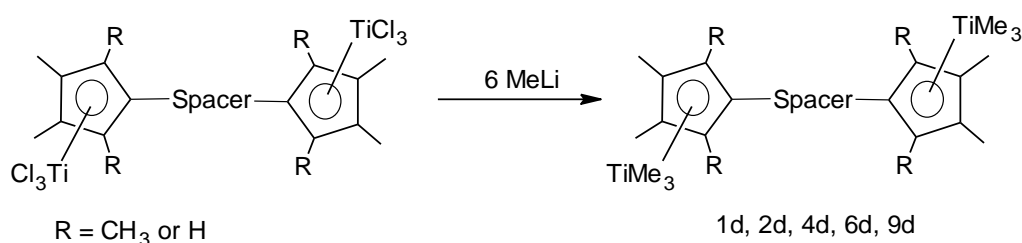
	Spacer	R	Chlorinating agent	Time	Color	Yield (%)
1c		CH ₃	ClSiMe ₃	24h RT	Red	84
2c		CH ₃	ClSiMe ₃	24h RT	Red	65
4c		CH ₃	ClSiMe ₃	24h RT	Red	87
6c		CH ₃	Cl ₂ SiMe ₂	48h RT	Violet	78
9c		H	Cl ₂ SiMe ₂	48h RT	Violet	65

Table II-4: Reaction conditions for the syntheses of di(cyclopentadienyltrichlorotitanium) complexes

All di(cyclopentadienyltrichlorotitanium) complexes are more stable in air than their corresponding hexaisopropoxides which facilitated their handling and purification. They are very less soluble in most of the solvents which on one side helped in their purification but on the other side made more difficult their characterization via NMR spectroscopy.

II.4. Syntheses of di(cyclopentadienyltrimethyltitanium) complexes

The syntheses of di(cyclopentadienyltrimethyltitanium) complexes were carried out by treatment of di(cyclopentadienyltrichlorotitanium) complexes with MeLi²¹ (Scheme II-30). The addition of MeLi was done at -78°C and the reaction mixture was stirred at low temperature for 1 h and then at room temperature for 3 h. 1,4-Bis(octyloxy)phenylene-2,5-bis(3,4-dimethylcyclopentadienyl)di(trimethyltitanium) (**9d**) and 5,5'-bithiophenylene-bis(2,3,4,5-tetramethylcyclopentadienyl)di(trimethyltitanium) (**6d**) were, however, less stable and the reaction was carried out at low temperature for 2 h only. Any increase in the reaction temperature resulted in the decomposition of the product. The products were extracted into toluene and the removal of toluene resulted in the required di(cyclopentadienyltrimethyltitanium) complexes as greenish yellow powders. These are very moisture and light sensitive in nature and all manipulations were carried out under nitrogen with the glassware wrapped with an aluminium foil.



Scheme II-30: General reaction for the syntheses of di(cyclopentadienyltrimethyltitanium) complexes

	Spacer	R	Yield (%)
1d		CH ₃	62
2d		CH ₃	71
4d		CH ₃	50
6d		CH ₃	95
9d		H	87

Table II-5: Results for the syntheses of di(cyclopentadienyltrimethyltitanium) complexes

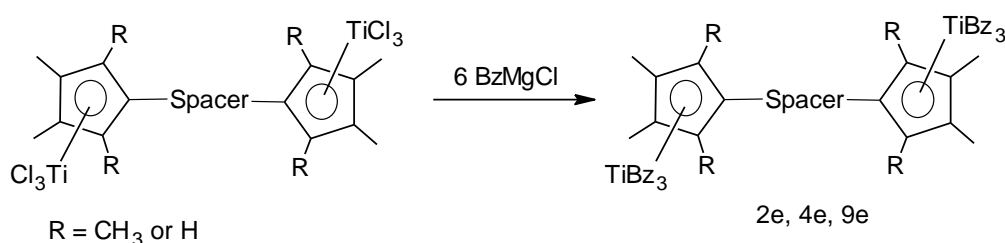
All the complexes were obtained in good yields and were characterized by ^1H and ^{13}C NMR spectroscopy. Due to the very high light and moisture sensitivity of the complexes, it was not possible to get good microanalysis results.

It has been reported in the literature that monocyclopentadienyltrimethyltitanium complexes are not only sensitive towards moisture and light but are thermally fragile too²². They decompose even at room temperature and have to be kept at low temperature through out the isolation and purification steps. Due to these handling problems, the synthesis of 1,4-phenylenebis(cyclopentadienylmethyl)di(trimethyltitanium) and 4,4'-biphenylenebis(cyclopentadienylmethyl)di(trimethyltitanium) with unsubstituted cyclopentadienyl groups was not attempted. 1,4-Bis(octyloxy)phenylene-2,5-bis(3,4-dimethylcyclopentadienyl)-di(trimethyltitanium) (**9d**) having two methyl groups substituents on cyclopentadienyl groups was, however, found thermally stable at room temperature to be isolated and characterized.

II.5. Syntheses of di(cyclopentadienyltribenzyltitanium) complexes

In order to further investigate the effect of the rate of hydrolysis on the organization and properties of the materials, the methyl groups of di(cyclopentadienyltrimethyltitanium) complexes were replaced by bulkier benzyl groups. It has been observed in the X-ray structure of pentamethylcyclopentadienyltribenzyltitanium that an agostic $\text{CH}_2\dots\text{Ti}$ interaction exists with one of the benzyl groups²³. Despite it is not sure that this interaction exists in solution, as only one peak for benzyl protons is observed in the ^1H NMR spectrum even at low temperature (-70°C), its presence should somehow shield the metal from attacking nucleophiles and hence increase the stability of the corresponding complex towards moisture. As a consequence, a decrease in the hydrolysis rate should result leading to a more controlled sol-gel process.

The di(cyclopentadienyltrichlorotitanium) complexes were treated with a slight excess of benzylmagnesium chloride at -78°C (Scheme II-31). The reaction mixture was stirred at low temperature for 1 h and then at room temperature for 3 h. Extraction into toluene and evaporation of the solvent resulted in the required di(cyclopentadienyltribenzyltitanium) complexes as red powders.



Scheme II-31: General reaction for the syntheses of di(cyclopentadienyltribenzyltitanium) complexes


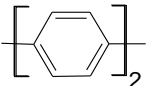
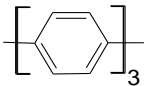
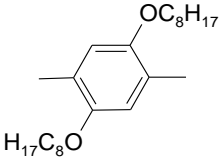
	Spacer	R	Yield (%)
1e		CH ₃	91
2e		CH ₃	95
4e		CH ₃	92
9e		H	92

Table II-6: Results for the syntheses of di(cyclopentadienyltribenzyltitanium) complexes

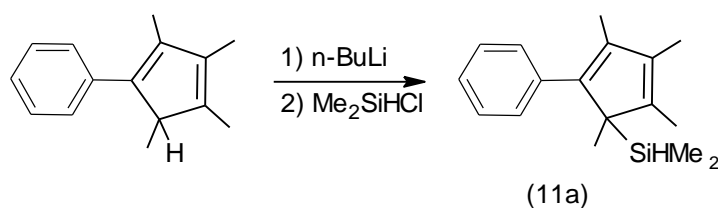
All the complexes were prepared in good yields. Although they are less sensitive to light than their corresponding hexamethyl complexes, still a change in color took place after long exposure to light due to the formation of decomposition products. All the manipulations were carried out in the dark by wrapping the glassware with an aluminium foil.

II.6. Syntheses of monocyclopentadienyltitanium complexes

To get reference compounds for spectroscopic studies on the materials derived from the above described precursors, we needed monomeric oxides with a phenyltetramethylcyclopentadienyl ligand. They were obtained by hydrolysis of trimethyl-(phenyltetramethylcyclopentadienyl)titanium as shown with a pentamethylcyclopentadienyl substituent of titanium²⁴.

II.6.1. Synthesis of dimethyl(phenyltetramethylcyclopentadienyl)silane (11a)

The synthesis of dimethyl(phenyltetramethylcyclopentadienyl)silane started by the treatment of phenyltetramethylcyclopentadiene with n-BuLi. The resulting monolithiated product was then reacted with chlorodimethylsilane and heated to 50°C for 1 h. Evaporation of the solvent resulted in dimethyl(phenyltetramethylcyclopentadienyl)silane in 94% yield (Scheme II-32).



Scheme II-32: Synthesis of dimethyl(phenyltetramethylcyclopentadienyl)silane

A mixture of isomers was obtained. It was characterized by ¹H NMR spectroscopy. A singlet at -0.4 ppm was attributed to two methyl substituents on silicon. However, only one

broad peak was observed at 1.5 ppm corresponding to methyl groups on the cyclopentadienyl ring instead of the four anticipated peaks (Figure II-3). This behaviour is expected in case of cyclopentadienylsilanes due to the fluxional nature of the cyclopentadienyl-silicon bond²⁵. A rapid intramolecular sigmatropic rearrangement takes place at room temperature and results in an averaging of hydrogen environments. That is why only one broad peak corresponding to methyl hydrogens on the ring is observed. In order to better characterize the cyclopentadienylsilane, a ¹H NMR spectrum was taken at low temperature (-60°C). Under this condition, although the rearrangement reaction does not stop completely, the molecules spend a reasonable time in one isomeric form that allows their observation.

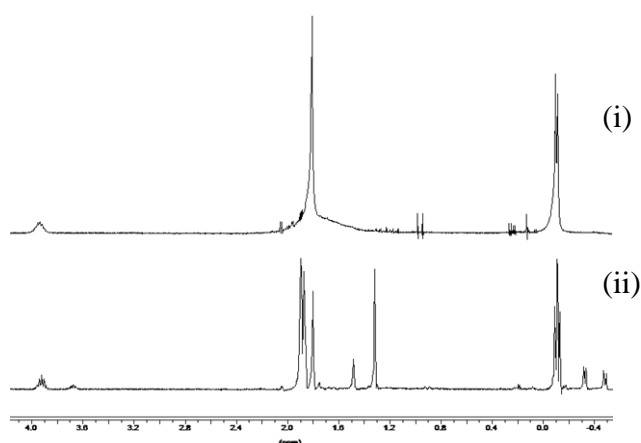


Figure II-3: ¹H NMR spectra of dimethyl(phenyltetramethylcyclopentadienyl)silane at different temperatures (i) room temperature (ii) -60°C

At -60°C, four prominent peaks were observed between 1.3-1.9 ppm corresponding to four unequivalent methyl groups linked to the cyclopentadienyl ring. An overlap of two doublets was seen at -0.1 indicating that the two methyl groups on silicon are not equivalent as well. A multiplet was observed at 3.95 ppm corresponding to the silyl proton as expected. This observation leads to propose the structure (a) for the major isomer (Figure II-4). A small amount of isomer (b) (about 22%, based on integration of the peaks) could also be identified in the spectrum.

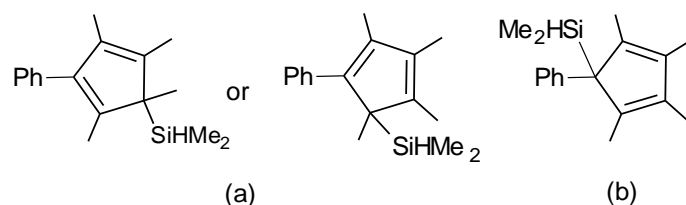
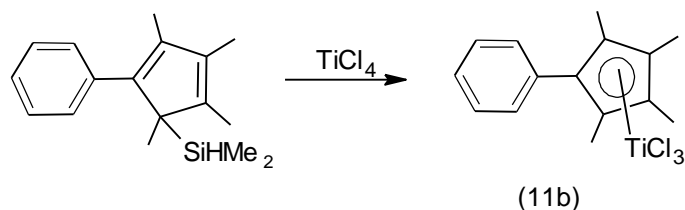


Figure II-4: Three possible isomers of the compound

II.6.2. Synthesis of trichloro(phenyltetramethylcyclopentadienyl)titanium (11b)

Dimethyl(phenyltetramethylcyclopentadienyl)silane (**11a**) was reacted with TiCl₄ at -78°C and then stirred at room temperature for 1.5 h. Removal of the solvent resulted in

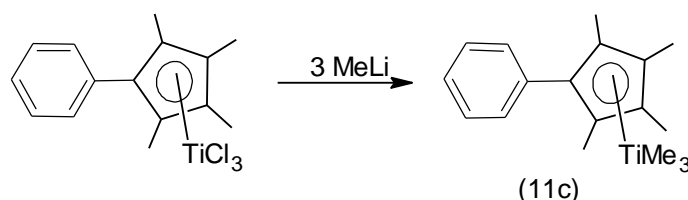
trichloro(phenyltetramethylcyclopentadienyl)titanium as a red crystalline compound in better yield (76%) than previously reported in literature²⁶ (Scheme II-33). The reason for this faster reaction with better yield results from the use of the more reactive dimethyl(phenyltetramethylcyclopentadienyl)silane as starting material instead of the corresponding trimethylsilane used previously.



Scheme II-33: Synthesis of trichloro(phenyltetramethylcyclopentadienyl)titanium

II.6.3. Synthesis of trimethyl(phenyltetramethylcyclopentadienyl)titanium (11c)

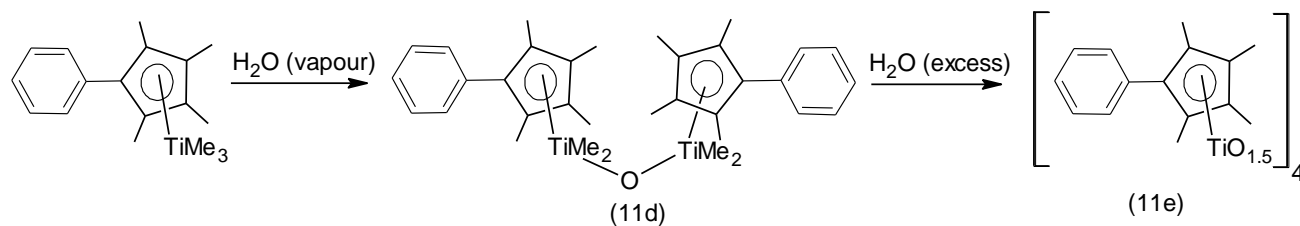
Trimethyl(phenyltetramethylcyclopentadienyl)titanium (**11c**) was synthesized by the alkylation of trichloro(phenyltetramethylcyclopentadienyl)titanium (**11b**) using methyllithium. The trichloride was reacted with methyllithium at -78°C and then stirred at room temperature for 2 h. The extraction of product with pentane and the removal of the solvent resulted in trimethyl(phenyltetramethylcyclopentadienyl)titanium as a greenish yellow powder in 81% yield (Scheme II-34). The compound was very sensitive to light and moisture and all the manipulations were carried out in inert environment covering the glassware with an aluminium foil.



Scheme II-34: Synthesis of trimethyl(phenyltetramethylcyclopentadienyl)titanium

II.6.4. Synthesis of hexa- μ -oxotetrakis(phenyltetramethylcyclopentadienyl)tetratitanium (11e)

The trimethyl(phenyltetramethylcyclopentadienyl)titanium (**11c**) complex was partially hydrolyzed under water vapour to lead to tetramethyl- μ -oxobis(phenyltetramethylcyclopentadienyl)ditanium (**11d**) in 86% yield (Scheme II-35). This partially hydrolyzed tetramethylated oxide was isolated as a green powder and was characterized by NMR spectroscopy.



Scheme II-35: Synthesis of hexa- μ -oxotetrakis(phenyltetramethylcyclopentadienyl)-tetratitanium

In the case where an excess of water was used, fully hydrolyzed hexa- μ -oxotetrakis(phenyltetramethylcyclopentadienyl)tetratitanium (**11e**) was obtained after 48 h. It was isolated and recrystallized in dichloromethane to give yellow crystals. The NMR spectrum of the crude product indicates the presence of the required product as a major fraction along with some uncharacterized oligomers which were separated by recrystallization. The yield was, however, about three times higher than previously reported from the triethylamine-catalyzed hydrolysis of trichloro(phenyltetramethylcyclopentadienyl)titanium.²⁶

III. Conclusion

A variety of di(cyclopentadienyltitanium) precursors for the preparation of titanium-based hybrid materials were synthesized. Various spacers linking the two cyclopentadienyl groups were used ranging from linear aromatic groups to long lateral chains containing groups. Similarly substituents on cyclopentadienyl groups were changed which resulted in a modification in the physical properties of the precursors. In order to study the effect of the rate of hydrolysis on the organization of the materials, the hydrolysable groups on titanium were also changed from isopropoxy to methyl and benzyl groups.

- ¹ (a) Al-Dulayymi, A.; Li, X.; Neuenschwander, M. *Helv. Chim. Acta.* **2000**, *83*, 1633 (b) Bunel, E. E.; Campos, P.; Ruz, J.; Valle, L.; Chadwick, I.; Ana, M. S.; Gonzalez, G.; Manriquez, J. M. *Organometallics* **1988**, *7*, 474 (c) Ritter, S. K.; Nöftle, R. E. *Chem. Mater.* **1992**, *4*, 872
- ² (a) Liu, X.; Sun, J.; Zhang, H.; Xiao, X.; Lin, F. *Eur. Polym. J.* **2005**, *41*, 1519 (b) Liu, X.; Sun, J.; Zhang, H.; Xiao, X.; Lin, F. *J. Appl. Polym. Sci.* **2006**, *99*, 2193 (c) Lee, D.; Lee, H.; Noh, S. K.; Song, B. K.; Hong, S. M. *J. Appl. Polym. Sci.* **1999**, *71*, 1071 (d) Jödicke, T.; Menges, F.; Kehr, G.; Erker, G.; Höweler, U.; Fröhlich, R. *Eur. J. Inorg. Chem.* **2001**, *8*, 2097 (e) Song, L.; Shen, J.; Wu, X.; Hu, Q. *Polyhedron* **1998**, *17*, 35 (f) Wegner, P. A.; Uski, V. A.; Kiestler, R. P.; Dabestani, S.; Day, V. W. *J. Am. Chem. Soc.* **1977**, *99*, 4846 (g) Wegner, P. A.; Uski, V. A. *Inorg. Chem.* **1979**, *18*, 646 (h) Sun, J.; Zhang, H.; Liu, X.; Xiao, X.; Lin, F. *Eur. Polym. J.* **2006**, *42*, 1259 (i) Carano, M.; Careri, M.; Cicogna, F.; D'Ambra, I.; Houben, J. L.; Ingrosso, G.; Maecaccio, M.; Paolucci, F.; Pinzino, C.; Roffia, S. *Organometallics* **2001**, *20*, 3478 (j) Mintz, E. A.; Pando, J. C.; Zervos, I. *J. Org. Chem.* **1987**, *52*, 2948
- ³ (a) Bragg, S.; Johnson, J. E. B.; Graziano, G. M.; Balaich, G. J.; Heimer, N. E. *Acta Cryst.* **2002**, *E58*, 1010 (b) Oku, A.; Yoshida, M.; Matsumoto, K. *Bull. Chem. Soc. Jpn.* **1979**, *52*, 524
- ⁴ Napoli, M.; Pragliola, S.; Costabile, C.; Longo, P. *Macromol. Chem. Phys.* **2006**, *207*, 304
- ⁵ Buchowicz, W.; Jerzykiewicz, L. B.; Krasinska, A.; Losi, S.; Pietrzykowski, A.; Zanello, P. *Organometallics* **2006**, *25*, 5076
- ⁶ Sutton, S. C.; Nantz, M. H.; Parkin, S. R. *Organometallics* **1993**, *12*, 2248
- ⁷ Lee, B. Y.; Kim, Y. H.; Won, Y. C.; Han, J. W.; Suh, W. H.; Lee, I. S.; Chung, Y. K.; Song, K. H. *Organometallics* **2002**, *21*, 1500
- ⁸ Meng, X.; Sabat, M.; Grimes, R. N. *J. Am. Chem. Soc.* **1993**, *115*, 6143
- ⁹ Lee, M. H.; Kim, S. K.; Do, Y. *Organometallics* **2005**, *24*, 3618
- ¹⁰ Rouzaud, J.; Castel, A.; Rivière, P.; Gornitzka, H.; Manriquez, J. M. *Organometallics* **2000**, *19*, 4678
- ¹¹ Wang, Z.; Heising, J. M.; Clearfield, A. *J. Am. Chem. Soc.* **2003**, *125*, 10375
- ¹² Shea, K. J.; Loy, D.; Webster, O. *J. Am. Chem. Soc.* **1992**, *114*, 6700
- ¹³ (a) Rouzaud, J.; Joudat, M.; Castel, A.; Delpech, F.; Riviere, P.; Gornitzka, H.; Manriquez, J. M.; Chavez, I. *J. Organomet. Chem.* **2002**, *651*, 44 (b) Southard, G. E.; Curtis, M. D. *Synthesis* **2002**, *9*, 1177
- ¹⁴ Elhamzaoui, H.; Jousseume, B.; Toupance, T.; Zakri, C. *Dalton Trans.* **2009**, *23*, 4429
- ¹⁵ Lightowler, S.; Hird, M. *Chem. Mater.* **2004**, *16*, 3963
- ¹⁶ (a) Llinás, G. H.; Mena, M.; Palacios, F.; Royo, P.; Serrano, R. *J. Organomet. Chem.* **1988**, *340*, 37 (b) Flores, J. C. Wood, J. S.; Chien, J. C. W.; Rausch, M. D. *Organometallics* **1996**, *15*, 4944 (c) Schwecke, C.; Kaminsky, W. *J. Polym. Sci.: Part A: Polym. Chem.* **2001**, *39*, 2805 (d) Royo, B.; Royo, P.; Cadenas, L. M. *J. Organomet. Chem.* **1998**, *551*, 293 (e) Christie, S. D. R.; Man, K. W.; Whitby, R. J.; Slawn, A. M. Z. *Organometallics* **1999**, *18*, 348
- ¹⁷ (a) Zhang, H.; Chen, Q.; Qian, Y.; Huang, J. *Appl. Organomet. Chem.* **2005**, *19*, 68 (b) Norura, K.; Naga, N.; Miki, M.; Yanagi, K. *Macromolecules* **1998**, *31*, 7588

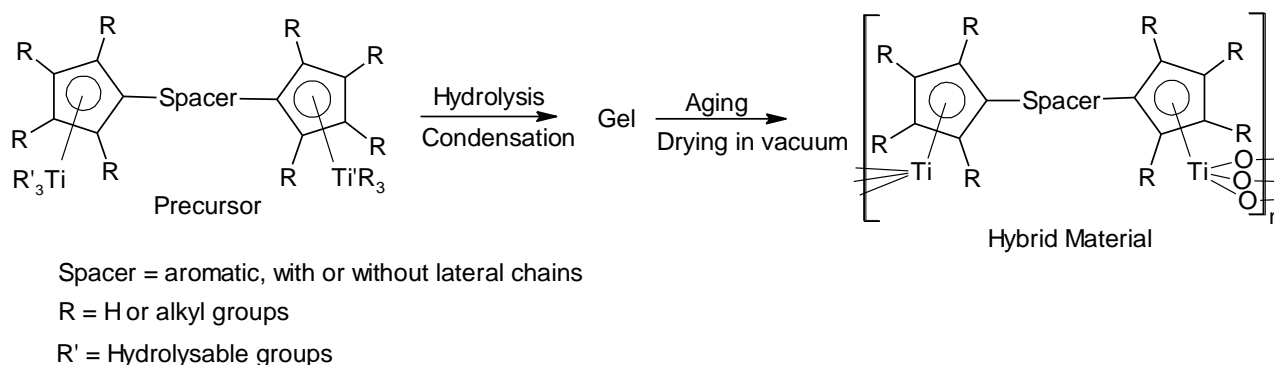
- ¹⁸ (a) Noh, S. K.; Kim, S.; Yang, Y.; Lyoo, W. S.; Lee, D. *Eur. Polym. J.* **2004**, *40*, 227 (b) Noh, S. K.; Jung, W.; Oh, H.; Lee, Y. R.; Lyoo, W. S. *J. Organomet. Chem.* **2006**, *691*, 5000
- ¹⁹ (a) Kucht, A.; Kucht, H.; Barry, S.; Chien, J. C. W.; Rausch, M. D. *Organometallics* **1993**, *12*, 3075 (b) Knjazhanski, S. Y.; Cadenas, G.; Garcia, M.; Pérez, C. M. *Organometallics* **2002**, *21*, 3094 (c) Barry, S.; Kucht, A.; Kucht, H.; Rausch, M. D. *J. Organomet. Chem.* **1995**, *489*, 195 (d) Booth, B. L.; Ofunne, G. C.; Stacey, C.; Tait, P. J. T. *J. Organomet. Chem.* **1986**, *315*, 143
- ²⁰ Kim, S. K. ; Kim, H. K. ; Lee, M. H.; Yoon, S. W. Han, Y.; Park, S.; Lee, J.; Do, Y. *Eur. J. Inorg. Chem.* **2007**, 537
- ²¹ Mena, M.; Royo, P.; Serrano, R. *Organometallics* **1989**, *8*, 476
- ²² McGrady, G. S. ; Downs, A. J. ; Hamblin, J. M. *Organometallics* **1995**, *14*, 3783
- ²³ Mena, M.; Pellinghelli, M. A.; Royo P.; Serrano, R.; Tiripicchio, A. *J. Chem. Soc., Chem. Commun.* **1986**, *14*, 1118
- ²⁴ (a) Blanco, S. G.; Gomez-Sal, P.; Carreras, S. M.; Mena, M.; Royo, P.; Serrano, R. *J. Chem. Soc., Chem. Commun.* **1986**, *21*, 1572 (b) Varkey, S. P.; Schormann, M.; Pape, T.; Roesky, H. W.; Noltemeyer, M.; Herbst-Irmer, R.; Schmidt, H-G. *Inorg. Chem.* **2001**, *40*, 2427 (c) Okuda, J. *Chem. Ber.* **1990**, *123*, 87
- ²⁵ (a) Davison, A; Rakita, P. E. *Inorg. Chem.* **1970**, *9*, 289 (b) McMaster, A. D.; Stobart, S. R. *Inorg. Chem.* **1980**, *19*, 1178 (c) Bonny, A.; Stobart, S. R. *J. Am. Chem. Soc.* **1979**, *101*, 2247 (d) Davison, A.; Rakita, P. E. *J. Am. Chem. Soc.* **1968**, *90*, 4479 (e) Jutzi, P.; Saleske, H.; Buhl, D.; Grohe, H. *J. Organomet. Chem.* **1983**, *252*, 29 (f) Lambert, J. B.; Lin, L.; Keinan, S. *Org. Biomol. Chem.* **2003**, *1*, 2559
- ²⁶ Björgvinsson, M.; Halldorsson, S.; Arnason, I.; Magull, J.; Fenske, D. *J. Organomet. Chem.* **1997**, *544*, 207



**CHAPTER III : PREPARATION OF
TITANIUM-BASED HYBRID MATERIALS**

Once the precursors of the hybrid materials were synthesized and well characterized, the next step of the project was their hydrolysis in a sol-gel process. Due to the quite fragile nature of the cyclopentadienyl-titanium bond, the hydrolysis was carried out under very mild conditions without any acidic or basic catalysts. THF was used as a solvent with most of the precursors in order to perform the hydrolysis in homogeneous medium. However, a comparative study of the effect of solvent on the properties of the final materials was done by carrying out the hydrolysis in biphasic medium using toluene as the solvent. The titanium to water ratio was kept at 1 to 3 while the solvent to the precursor ratio was kept at 20/1 (w/w). Most of the manipulations were carried out in an inert environment.

A mixture of water and solvent was added dropwise to a solution of the precursor at room temperature or below. The resulting solution was stirred for 10 minutes and then was allowed to settle down. It was left untouched for several days in order to make sure that the hydrolysis and condensation reactions were finished resulting in gelification. The gels were kept for aging and then were washed with THF, diethyl ether and petroleum ether after centrifugation to remove the oligomers. The resulting powder was dried under vacuum overnight and the required xerogels were obtained as yellow powders.



Scheme III-1: General reaction scheme for the preparation of hybrid materials

I. Preparation of hybrid materials with linear spacers

Various di(cyclopentadienyltitanium) precursors containing aromatic spacers without lateral chains were hydrolyzed in a controlled sol-gel process. Various hydrolysable groups on titanium were used in order to obtain the materials with the best suited properties as the difference in the rate of the cleavage of titanium-hydrolysable group bond can eventually have an influence on the organization of the materials.

I.1. Hybrid materials from di(cyclopentadienyltriisopropoxytitanium) precursors

I.1.1. Hydrolysis in homogeneous medium

In the first step, the di(cyclopentadienyltriisopropoxytitanium) precursors were hydrolyzed in THF using the reaction conditions described above. The reaction temperature

was reduced to -80°C for some of the precursors in order to slow down the hydrolysis. The resulting mixtures were stirred at this temperature for 30 min and then were allowed to warm up to room temperature. In the case of 4,4'-biphenylenebis(2,3,4,5-tetramethylcyclopentadienyl)di(triisopropoxytitanium) (**2b**), 4,4''-terphenylenebis(2,3,4,5-tetramethylcyclopentadienyl)di(triisopropoxytitanium) (**4b**) and 5,5'-bithiophenylenebis(2,3,4,5-tetramethylcyclopentadienyl)di(triisopropoxytitanium) (**6b**), yellow gels were obtained after 9-10 days which were then kept for aging for further 2 weeks. The gelification time was, however, much shorter for 4,4''-terphenylenebis(3,5-dimethylcyclopentadienyl)di(triisopropoxytitanium) (**5b**) that led to a gel after only 30 min (Table III-1).

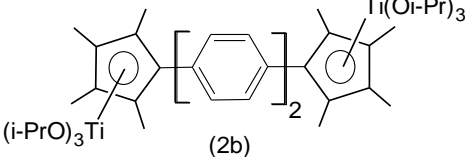
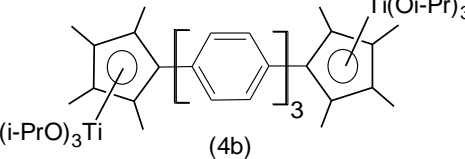
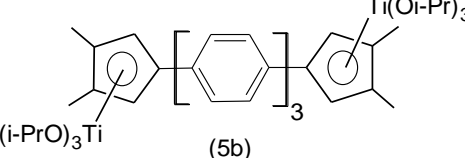
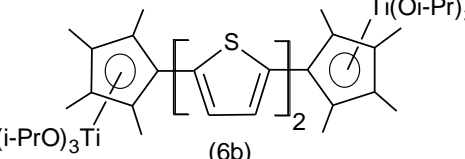
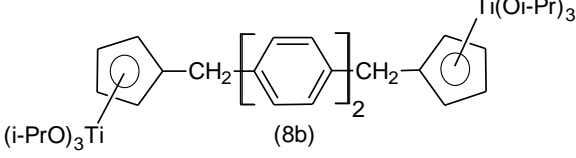
Hybrid Materials	Precursors	Temperature	Time*	Yield (%)
XPh2OR		-80°C	9 days	79
XPh3OR1		RT	9 days	88
XPh3OR2		RT	30 min	97
XTh2OR		-80°C	10 days	95
XBz2OR		RT	Rapid precipitation	73

Table III -1: Precursors and gelification time for xerogels

*Gelification time

When the hydrolysis was performed in air the gelification time of the materials was shorter and yellow gels were obtained only after 4 days in case of (**2b**) and (**4b**). However in order to carefully control the rate of hydrolysis, the reactions were performed under nitrogen for all the precursors. The corresponding gels were opaque which indicates that the particle size is larger than the optical transparency range ($< 400\text{ nm}$) resulting in light scattering.

The hydrolysis of 4,4'-biphenylenebis(cyclopentadienylmethyl)di(triisopropoxytitanium) (**8b**) to the corresponding hybrid materials was very rapid and immediate precipitation took place. The change in the conditions of the hydrolysis, e.g., low temperature (-80°C), changing the solvent or excess of solvent did not slow down the formation of the hybrid.

The resulting gels or precipitates were washed with THF, diethyl ether and pentane to remove oligomers and side products and then were dried under vacuum at 40°C overnight. The xerogels were obtained as yellow powders and were characterized by various techniques.



Figure III-1: Yellow opaque gel obtained after hydrolysis-condensation reactions (**XPh3OR2**)

The color and texture of the gels were independent of the spacer nature and the reaction conditions. Yellow opaque gels were obtained with all the precursors (Figure III-1) with the exception of 4,4'-biphenylenebis(cyclopentadienylmethyl)di(triisopropoxytitanium) (**8b**) that led to precipitates. However, the gelification time varied dramatically with the change in the substitution on the cyclopentadienyl rings. In the case of precursors containing cyclopentadienyl groups tetrasubstituted with methyl groups, the corresponding gels were obtained after 9-10 days. The time decreased to only 30 min in the case of disubstituted groups while precipitates were obtained rapidly in the case of unsubstituted rings. These differences can be explained, taking into account the steric hindrance caused by the substituted methyl groups to the attacking nucleophile. The result is a slower hydrolysis and then a time-consuming condensation step leading to longer gelification times. Changing the length or the nature of the spacer did not show a significant effect on the gelification time. Similarly although reducing the initial temperature of the reaction to -80°C decreases the rate of hydrolysis-condensation, it had no significant effect on the gelification time.

I.1.1.a. Spectroscopic studies

In order to check the complete cleavage of isopropoxy groups, infrared spectra of the xerogels were recorded. All the spectra were taken by dispersing the compounds in KBr pellets. The infrared spectra of the precursors and their corresponding xerogels are shown in Figure III-2.

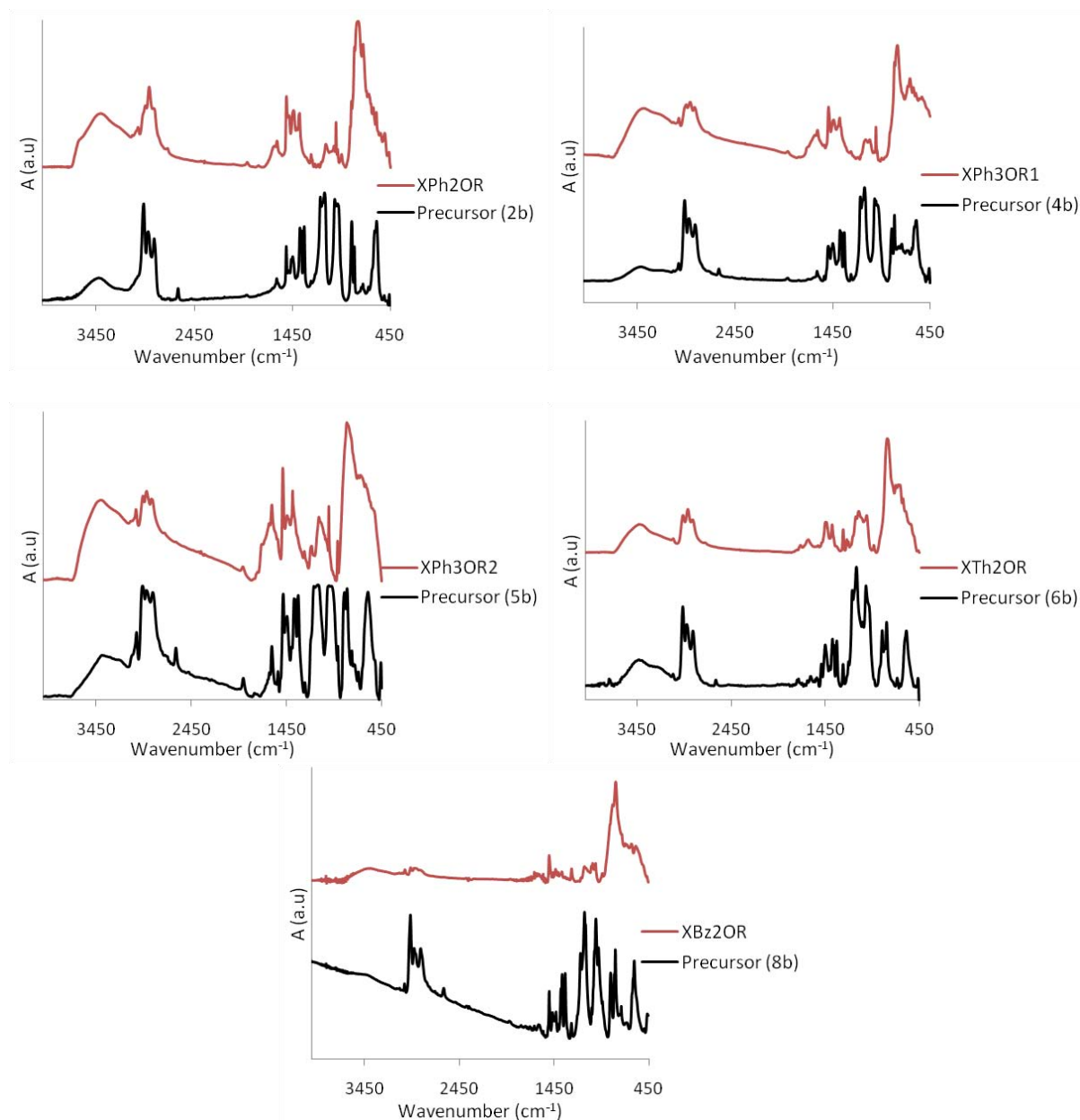


Figure III-2: Infrared spectra of the precursors and their corresponding hybrid materials

In the infrared spectrum of the precursors, a characteristic doublet was observed at $1360\text{--}1375\text{ cm}^{-1}$ due to the symmetric deformation of the gem-dimethyl structure of isopropoxides. Similarly, two strong doublets were observed around 1022 cm^{-1} and 1160 cm^{-1} that can be attributed to the skeletal C-C vibrations of isopropoxy groups¹. A disappearance of these characteristic bands was observed during hydrolysis with the passage of time. In the final materials these bands disappeared completely indicating a complete hydrolysis of the isopropoxy groups. Some new broad bands appeared between $450\text{--}850\text{ cm}^{-1}$ which indicates the formation of a Ti-O-Ti network as expected². A broad peak was observed in the infrared spectra of the xerogels around 3500 cm^{-1} which shows the presence of hydroxyl groups. The existence of this band can be justified in two ways. Either it is given by the water molecules entrapped in the xerogels in spite of the drying conditions used, or it indicates an incomplete

condensation of hydroxyl groups. It is possible that some of the hydroxyl groups could not condense due to geometrical constraints and as a result, some Ti-OH bonds could be present in the final material³. The rest of the peaks corresponding to $\nu_s(\text{C-H})$, $\nu_{as}(\text{C-H})$ etc. in the infrared spectrum of the precursors remained unchanged in the spectra of the xerogels indicating that some organics are preserved in the final material.

I.1.1.b. Microanalysis

The next step in the characterization of the xerogels was the determination of their elemental composition which was done by microanalysis. The results obtained for the xerogel **XPh2OR** as well as the calculated values are gathered in Table III-2.

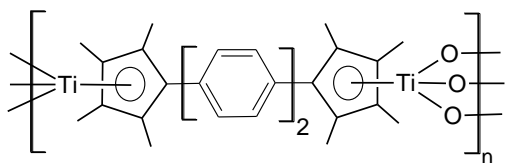
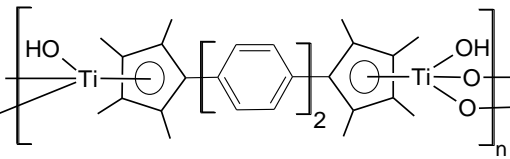
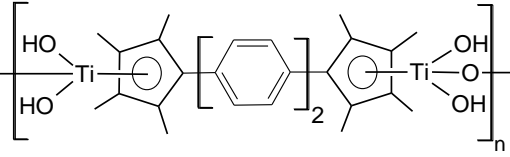
XPh2OR	Ti	C	H	O*
Experimental	16.2	62.1	6.0	15.8
Calculated for 	17.9	67.2	6.0	9.0
Calculated for 	17.3	65.0	6.1	11.6
Calculated for 	16.8	62.9	6.3	14.0

Table III-2: Theoretical and experimental elemental composition of xerogel **XPh2OR**

* Obtained by difference

The microanalysis results obtained for xerogel **XPh2OR** are presented in the first row. The value given for oxygen is obtained by the difference between one hundred and the sum of titanium, carbon and hydrogen percentages. It is based on the hypothesis that all the missing mass is made of oxygen and that there is no other element present in the sample. In the second row, the theoretical values calculated from the given formula are shown. They correspond to a fully condensed network, with 1.5 oxygen atoms per titanium atom. As it can be noticed, the fit between measured and theoretical value is not perfect. For titanium and carbon, differences are of 10% and 8% respectively. For oxygen the result of the comparison is even worse as a difference of 75% is found. For a better fit, the oxygen content of the theoretical structure must be increased by the introduction of oxygen atoms, either as water or in the form of hydroxyl group. This introduction is chemically significant as it is well known that water can

coordinate titanium atoms and as cyclopentadienylhydroxytitanium compounds have been reported in the literature⁴.

To chose between both hypotheses, we relied on the fact that no coordination water was reported in monocyclopentadienyltitanium oxides obtained under hydrolytic conditions⁵. In the described structures, the titanium atoms are tetracoordinated. In our case, the presence of hydroxyl groups would originate from steric hindrance preventing a full condensation of the hydroxyl groups. Under this hypothesis, new theoretical values are given in the third and fourth rows of Table III-2 with 2 and 2.5 oxygen atoms per titanium atom. As it can be noticed, the fit is far better than with the values of second row. The difference decreased from 10% to 4% for titanium, from 8% to 2% for carbon and from 75 to 13% for oxygen assuming 2.5 oxygen atoms per titanium atom in the structure as shown in the fourth row of the Table (II-2). The same is true for the other hybrid materials as well.

Based on the results of microanalysis, the proposed formulas for the materials are given in Table III-3.

Hybrid Material	Theoretical formula	Proposed formula
XPh2OR	$C_{30}H_{32}Ti_2O_3$	$C_{30}H_{32}Ti_2O(OH)_4$
XPh3OR1	$C_{36}H_{36}Ti_2O_3$	$C_{36}H_{36}Ti_2O(OH)_4$
XPh3OR2	$C_{32}H_{28}Ti_2O_3$	$C_{32}H_{28}Ti_2O(OH)_4$
XTh2OR	$C_{26}H_{28}S_2Ti_2O_3$	$C_{26}H_{28}S_2Ti_2O(OH)_4$
XBz2OR	$C_{24}H_{20}Ti_2O_3$	$C_{24}H_{20}Ti_2O(OH)_4$

Table III-3: Theoretical and proposed formulas for the hybrid materials

The molar ratios of H/Ti, C/Ti, O/Ti and spacer/Ti are given in Table III-4.

Hybrid		H/Ti	C/Ti	O/Ti	Spacer/Ti
XPh2OR	Theoretical	18.0	15.0	2.5	0.5
	Experimental	17.8	15.4	2.9	0.52
XPh3OR1	Theoretical	20	18.0	2.5	0.5
	Experimental	17.9	16.0	2.5	0.46
XPh3OR2	Theoretical	16	16	2.5	0.5
	Experimental	20.8	19.2	4.4	0.62
XTh2OR	Theoretical	16	13	2.5	0.5
	Experimental	15.3	13.1	-	0.51
XBz2OR	Theoretical	12	12	2.5	0.5
	Experimental	12.2	12.1	4.0	0.55

Table III-4: Theoretical and experimental molar ratios of elements

The spacer/Ti ratio is quite close to the theoretically calculated value for all xerogels. This observation leads us to assume that the proposed structures for the materials are correct and that both organic and inorganic parts are present in the final materials in good ratios.

I.1.1.c. Thermogravimetric analysis

The thermal stability and composition of the materials were studied by thermogravimetric analysis (TGA). A small mass loss was observed while heating the materials till 100°C owing to the removal of trapped water and solvent molecules. All the xerogels showed a prominent stability towards heat until 300°C after which the decomposition of the organic part started. A complete decomposition of the organic part was observed before 700°C (Figure III-3).

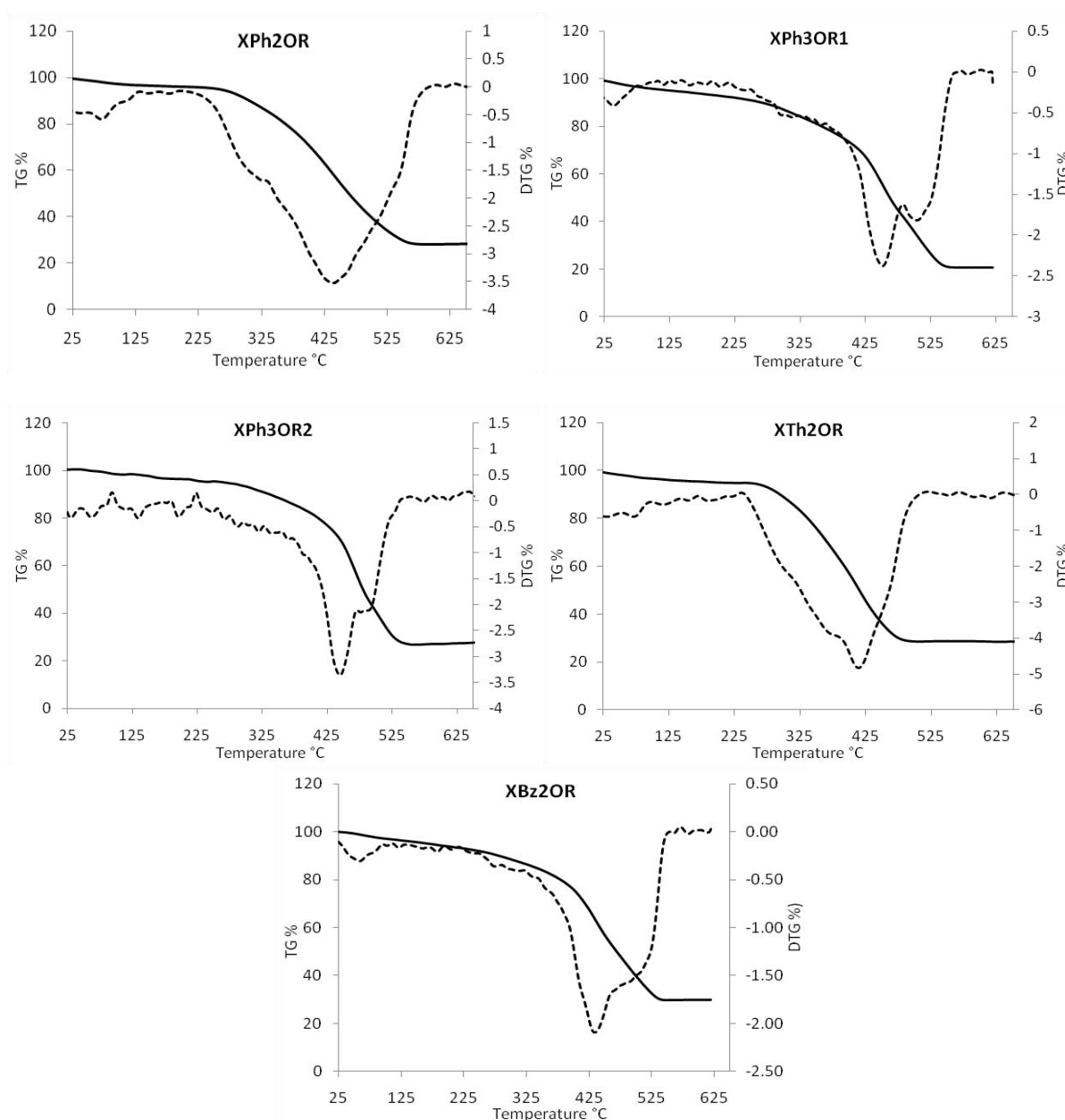


Figure III-3: TGA and DTG curves for the xerogels (in air)

The molecular weight of the xerogels can be calculated by using the following formula:

$$M = 160 \times \frac{100}{X} \text{ (g/mol)} \quad X = \text{Residual mass (\%)}$$

This formula is based on the assumption that at 700°C all the material is pyrolyzed to TiO₂.

Xerogel	Residual mass, X (%)	Molecular weight (g/mol)	Theoretical molecular weight (g/mol)
XPh2OR	27.9	573	572
XPh3OR1	25.5	628	648
XPh3OR2	26.7	599	592
XTh2OR	27.1	590	584
XBz2OR	29.8	536	488

Table III-5: Residual masses after complete pyrolysis of the xerogels, their corresponding molecular weights and the theoretical molecular weights

The theoretical molecular weights are calculated from the proposed formulas for the hybrid materials in the previous section, based on the microanalysis results. They are quite close to the molecular weights obtained from the TGA of the products that strengthens the predicted structures for the xerogels.

I.1.1.d. Textural Properties

The specific area of the xerogels was determined by nitrogen-sorption analysis BET⁶ and is given in Table III-6.

Xerogel	BET specific area (m ² /g)
XPh2OR	3.4
XPh3OR1	< 1

Table III-6: BET specific area of the xerogels

The prepared xerogels present negligible BET specific areas like the previously reported tin-based hybrid materials prepared in homogeneous medium⁷. The reason for this can be attributed to the presence of interactions between the aromatic spacers which results in the formation of a compact structure and to the lack of rigid Ti-O-Ti network due to the presence of two hydroxyl groups per titanium atoms. The same phenomenon has been observed in the case of silicon-based materials, where an increase in the length of the aliphatic spacer resulted in the formation of a non-porous material with low surface area⁸.

I.1.1.e. X-ray diffraction analysis

The X-ray diffraction analysis allowed us to study the organization of the nanostructures. The XRD patterns related to the prepared hybrids are presented in Figure III-4. The distances corresponding to the angles were calculated by using the Bragg's law:

$$d_{(\text{exp})} = \frac{\lambda}{2\sin\theta}$$

λ = Wavelength of the incident X-rays beam

θ = Diffraction angle

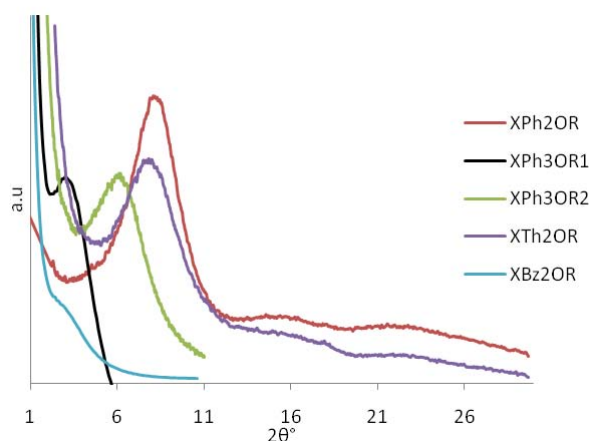


Figure III-4: X-ray diffraction analysis of xerogels

For **XPh2OR** a broad peak at 8.1° was obtained while the hybrid with an extra phenyl group **XPh3OR1** in the spacer presents a peak at a smaller angle 3.1° . In the case of **XPh3OR2** where the spacer carries two dimethylcyclopentadienyl groups, a peak at 6.1° was recorded. **XTh2OR** which holds two thiophene groups in the spacer gave a peak at 7.8° while **XBz2OR**, having a benzylic spacer between unsubstituted cyclopentadienyl rings presented a broader peak at 4.9° .

To check the influence of the temperature on the organization of the hybrid materials, 4,4'-biphenylenebis(2,3,4,5-tetramethylcyclopentadienyl)di(triisopropoxytitanium) (**2b**) was hydrolyzed both at room temperature and at -80°C and the resulting diffractograms are shown in Figure III-5. The hybrid prepared at room temperature showed a broad peak at 6.9° while the hybrid obtained after hydrolysis at -80°C showed a more intense peak at 8.1° . This observation can be explained by a slower hydrolysis and condensation reactions at low temperature giving enough time to the organic moieties to self-assemble via π -stacking. Encouraged by this result, the hydrolysis of other precursors was performed at low temperature and the organization of the corresponding hybrids was studied by X-ray diffraction. However, no significant difference could be detected in these cases indicating that the improvement obtained with (**2b**) could not be generalized.

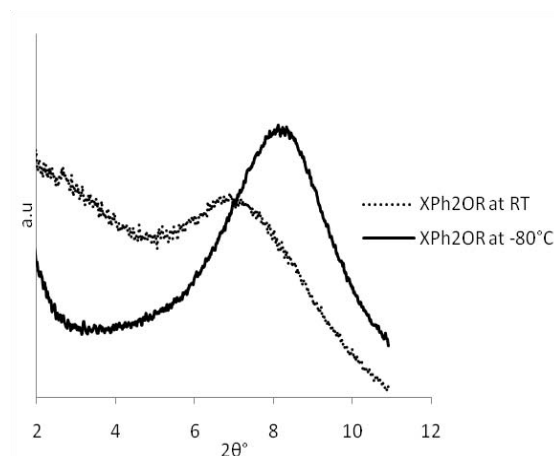


Figure III-5: X-ray diffractograms of xerogel **XPh2OR** prepared at -80°C and at RT

Hydrolysis was also carried out in slightly acidic media for **XBz2OR** but it resulted in the rupture of cyclopentadienyl-titanium bond rather than improving the organization.

These data obtained from the hydrolysis of titanium alkoxides show that the corresponding hybrid materials are not amorphous materials. Instead they are organized, the hybrids with the more rigid spacers showing the more intense peaks. However hybrids **XPh3OR1** and **XPh3OR2**, prepared from precursors with the same size, did not show the same repeating distance, i.e., 2.8 nm for **XPh3OR1** and 1.4 nm for **XPh3OR2**, making any attempt of interpretation difficult.

In order to get more reliable data, it was decided to change hydrolysis conditions.

I.1.2. Hydrolysis in heterogeneous medium

In order to study the effect of solvent on the organization of the materials, the hydrolysis of the precursors was carried out in biphasic medium using toluene as a solvent since it could change the kinetics of the hydrolysis-condensation process. A stoichiometric amount of water was added to the solution of the precursors in toluene and the reaction mixture was stirred at room temperature for 20 minutes. It was then left untouched for gelification. Yellow gels were obtained in the case of 4,4'-biphenylenebis(2,3,4,5-tetramethylcyclopentadienyl)di(triisopropoxytitanium) (**2b**) and 4,4''-terphenylenebis(2,3,4,5-tetramethylcyclopentadienyl)di(triisopropoxytitanium) (**4b**) after 12 h while yellow precipitates were formed with 4,4'-biphenylenebis(cyclopentadienylmethyl)di(triisopropoxytitanium) (**8b**). The reaction medium was aged for 3 weeks. After washing and drying of the products, yellow powders were obtained which were then characterized by FT-IR, TGA, XRD, and microanalysis.

A marked decrease in the gelification time of the materials was observed. When 4,4'-biphenylenebis(2,3,4,5-tetramethylcyclopentadienyl)di(triisopropoxytitanium) (**2b**) was hydrolyzed in THF, it gave a gel after 9 days while in toluene it took only 12 h. This difference can be explained by a slower reaction rate in THF due to surrounding of the metal

by the solvent molecules. Titanium being electron deficient can weakly coordinate with the oxygen of the THF molecules and hence could be shielded from the attacking nucleophiles. In the case of toluene, however, no such complexation is present and hence the hydrolysis-condensation process of unhindered metal precursors is very rapid. The same is true for the other precursors.

I.1.2.a. Microanalysis

The chemical composition of the resulting materials was determined by microanalysis. The molar ratios of H/Ti, C/Ti, O/Ti and spacer/Ti are given in Table III-7.

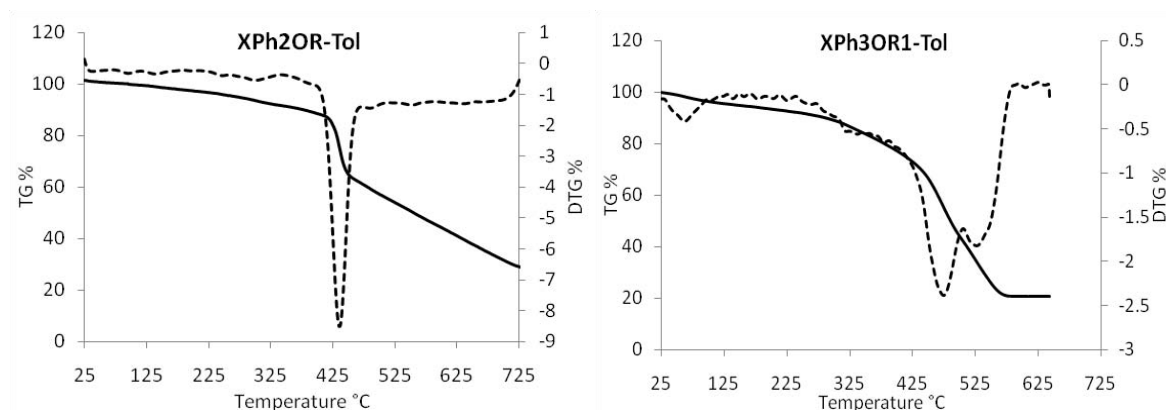
Hybrid		H/Ti	C/Ti	O/Ti	Spacer/Ti
XPh2OR-Tol	Theoretical	18.0	15.0	2.5	0.5
	Experimental	19.1	16.4	2.8	0.54
XPh3OR1-Tol	Theoretical	20.0	18.0	2.5	0.5
	Experimental	21.6	18.6	4.2	0.55
XBz2OR-Tol	Theoretical	12.0	12.0	2.5	0.5
	Experimental	12.2	11.6	4.5	0.55

Table III-7: Theoretical and experimental molar ratios of elements

Microanalysis results of the xerogels prepared in toluene showed no apparent change in the composition of the materials. The percentages of carbon and titanium were as usual slightly lower than the calculated values owing to the presence of extra oxygen. These values fit well when uncondensed hydroxyl groups are taken into account like previously considering 2.5 oxygen atoms per titanium atom. No change in the composition of the materials could be related to the change in the solvent.

I.1.2.b. Thermogravimetric analysis

The thermal stability of the materials was investigated by TGA and the results are shown in Figure III-6.



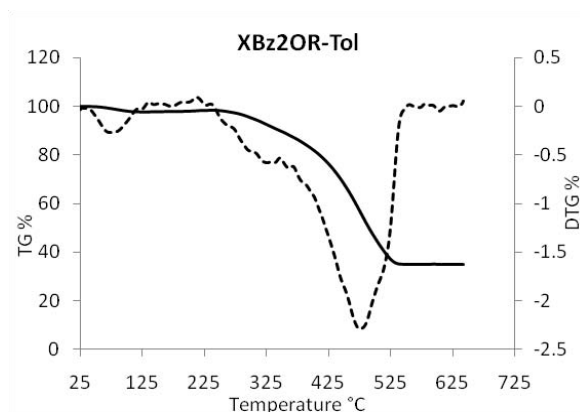


Figure III-6: TGA and DTG curves of xerogels (in air)

In each case, the xerogels are thermally stable up to 300°C, the main mass loss occurring above 400°C. The residual mass obtained after complete pyrolysis of the organic part allowed us to calculate the molecular weight of the xerogels.

Xerogel	Residual mass, X (%)	Molecular weight (g/mol)	Theoretical molecular weight (g/mol)
XPh2OR-Tol	28.3	565	572
XPh3OR1-Tol	21.9	730	648
XBz2OR-Tol	35.1	456	488

Table III-8: Theoretical and experimental molecular weights calculated from TGA

Again there is no apparent difference in the molecular weights of xerogels prepared either in THF or in toluene.

I.1.2.c. Textural Properties

The specific area of different xerogels was determined by nitrogen sorption analysis (BET) and is given in Table III-9.

Xerogel	Specific surface (m ² /g)
XPh2OR-Tol	5.1
XPh3OR1-Tol	< 1

Table III-9: Specific surface of the xerogels

As seen above, the xerogels show very low specific area. The change from the homogeneous to the heterogeneous media did not result in any change in the textural properties of the materials.

I.1.2.d. X-ray diffraction analysis

The X-ray diffraction analysis of the xerogel **XPh3OR1-Tol** gave no peak in XRD indicating that the material is completely amorphous. In the case of **XBz2OR-Tol**, a broad peak was recorded at 4.8° while for **XBz2OR** (in THF), it was at 3.4° . No apparent change was noticed when going from **XPh2OR** (in THF) to **XPh2OR-Tol** (Figure III-7).

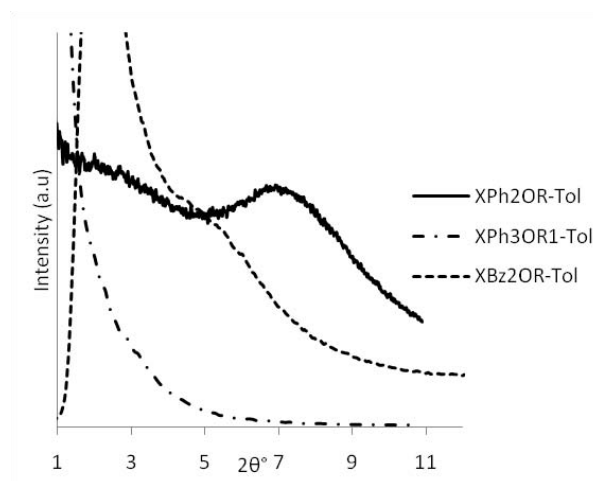


Figure III-7: X-ray diffraction analysis of xerogels prepared in toluene

The hybrid materials generated by hydrolysis in toluene showed compositions similar to those of the hybrid materials obtained in THF. However, X-ray data were different, as with **XPh3OR1-Tol** no organization was detected and with **XBz2OR-Tol** a change in the repetition length was noticed. That is why hydrolyses were conducted in THF instead of toluene for the continuation of this study.

The hydrolysis of di(cyclopentadienyltriisopropoxytitanium) complexes generated the expected hybrid materials from all the precursors both in THF and toluene. The resulting xerogels were thermally stable and their chemical composition matched with the theoretically calculated values. However some uncertainties were encountered in the study of organization of the nanostructures as the XRD results were not consistent, e.g., peaks were present or not in corresponding samples and shifts in the position of the peaks were observed as well. Due to these problems, it was difficult to predict a model for the nano-organization of the materials. In order to get more consistent and reproducible results, a chemical modification of the precursors was carried out. The isopropoxy groups were replaced by methyl groups in an attempt to control the hydrolysis and condensation reactions. Although it involved two extra steps to prepare the di(cyclopentadienyltrimethyltitanium) complexes from di(cyclopentadienyltriisopropoxytitanium) complexes, the assumed advantages were more appealing.

I.2. Hybrid materials from di(cyclopentadienyltrimethyltitanium) precursors

The hydrolysis of di(cyclopentadienyltrimethyltitanium) precursors was carried out in THF under nitrogen using a stoichiometric amount of water. The solvent to the precursor ratio was kept at 40/1 (w/w). An evolution of gas was observed during the addition of water indicating the hydrolysis of the methyl groups. Yellow gels were formed after 10-12 days for most of the precursors except 5,5'-bithiophenylenebis(2,3,4,5-tetramethylcyclopentadienyl)di(trimethyltitanium) (**6d**) which gave a suspension of yellow precipitates after 2 days (Table III-10). The resulting gels or suspensions were washed and dried after 3 weeks. They were then characterized by FT-IR, microanalysis, TGA, and XRD analysis.

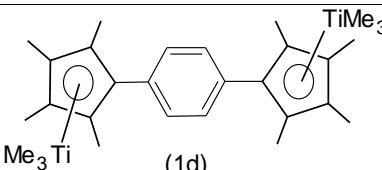
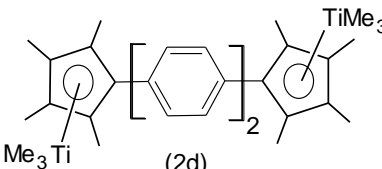
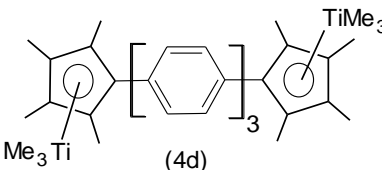
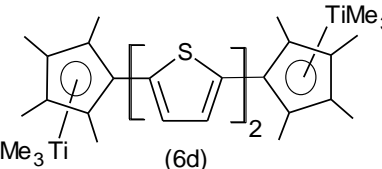
Xerogels	Precursors	Physical state	Yield (%)
XPh1Me	 (1d)	Yellow gel	70
XPh2Me	 (2d)	Yellow gel	77
XPh3Me	 (4d)	Yellow gel	80
XTh2Me	 (6d)	Yellow suspension	-

Table III-10: List of hybrid materials and their precursors

I.2.a. Spectroscopic studies

The completion of the hydrolysis process was probed by infrared spectroscopy. The spectra were recorded by taking the samples in the form of KBr pellets. Several broad bands were observed in the 450-800 cm^{-1} range owing to the formation of Ti-O-Ti network, as expected². The peaks around 2900 cm^{-1} corresponding to methyl groups [$\nu_s(\text{C-H})$, $\nu_{as}(\text{C-H})$] did not disappear completely in the resulting materials due to the presence of methyl substituents on the cyclopentadienyl rings. Several bands were observed around 1400 cm^{-1} corresponding to various C=C and C-H stretching and bending vibrations (Figure III-8).

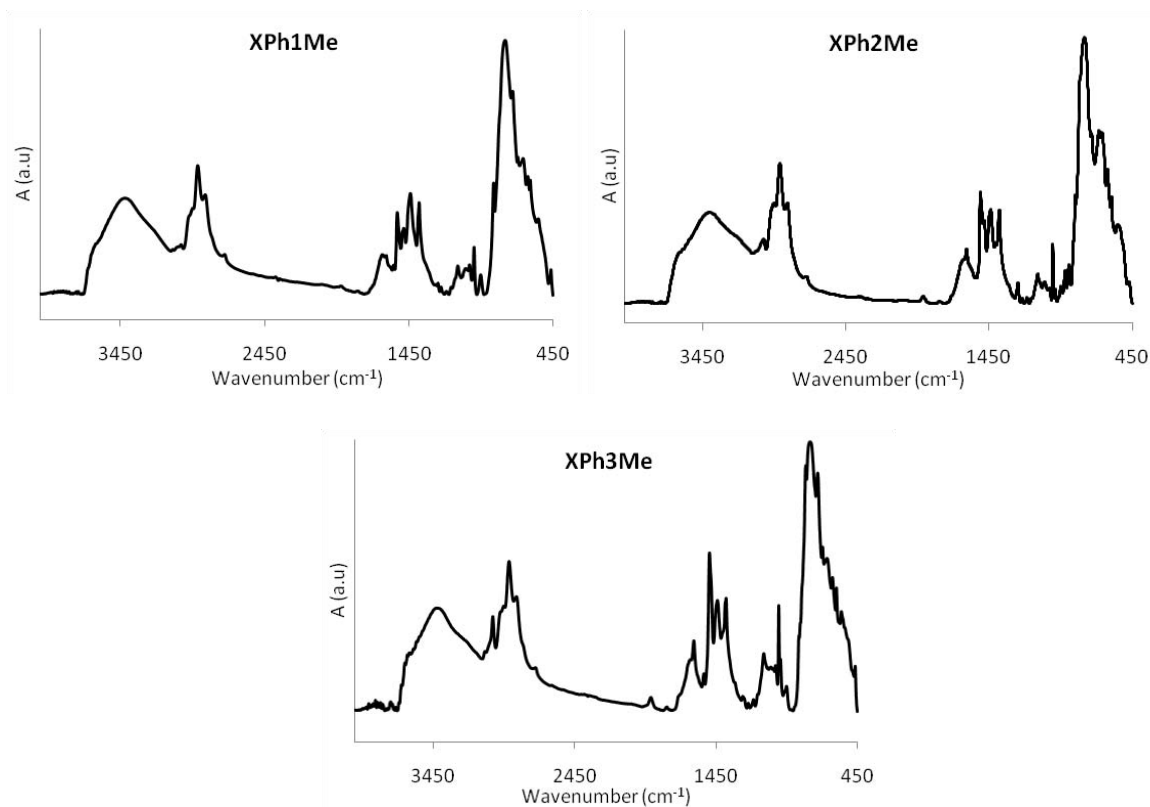


Figure III-8: Infrared spectra of the xerogels obtained by the hydrolysis of di(cyclopentadienyltrimethyltitanium) precursors

Study of the Cp-Ti bond*

General Overview

The next step in the characterization of the xerogels was to ensure the presence of the cyclopentadienyl-titanium bond, as it is the key-point for class II hybrid materials. The evidence about the retention of this bond in the materials could come from a combined study of infrared and Raman spectroscopy in the 200-600 cm^{-1} range as some literature data show that characteristic bands of Cp*-M, M-O and M-Me can be clearly evidenced in this region⁹.

To the best of our knowledge, very few data are available on di(cyclopentadienyltitanium) complexes and their corresponding oxides concerning infrared and Raman spectroscopies. This is why some simpler monocyclopentadienyl compounds were prepared in order to be used as reference compounds to conduct spectroscopic studies. The compounds we prepared are listed in Table III-11. The first reference compound was chosen to be pentamethylcyclopentadienyltrimethoxytitanium in order to obtain a simple spectrum with fewer peaks. Then we tried to design some more reference compounds whose structure was closed to our hybrid materials by introducing a phenyl group. The substituents on the metal were also changed from methyl to oxygen bridges in order to progressively mimic our hybrid materials. Pentamethylcyclopentadienyltrimethoxytitanium, is commercially available while the rest of them was synthesized and have been discussed in the previous chapter. The data obtained from the literature and the spectra of these reference compounds were then

compared to those of the materials. The Raman spectra were taken in solid state using a red laser beam (632 nm) while the infrared spectra were recorded in the form of CsI pellets.

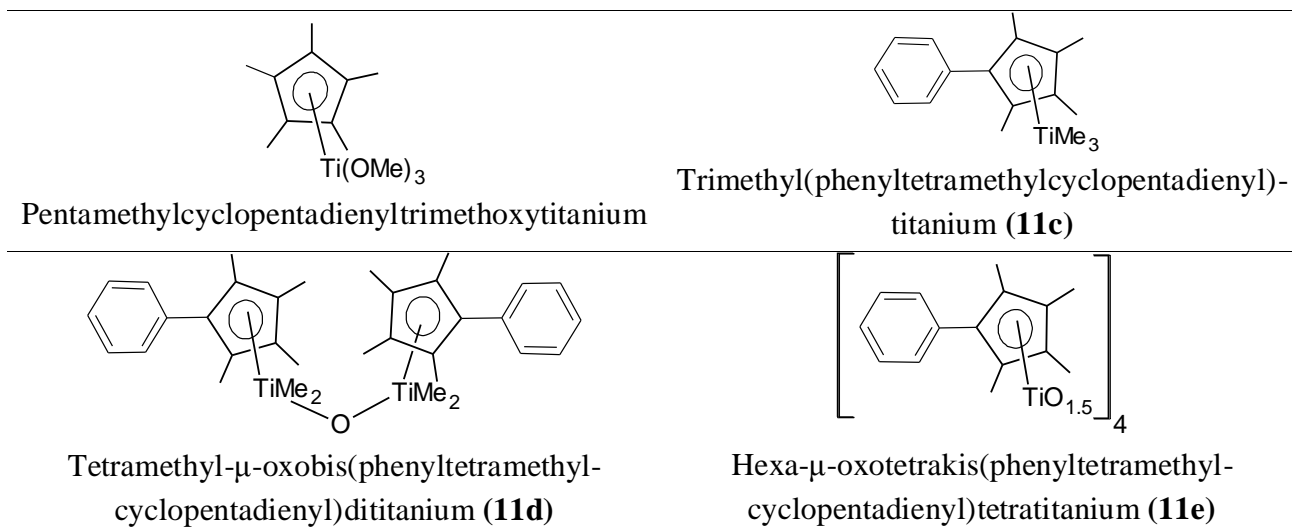


Table III-11: List of reference compounds used for the spectroscopic studies

The expected vibrational modes for cyclopentadienyl-titanium bonds are asymmetric and symmetric $\text{Cp}^*\text{-Ti}$ stretching, Cp^* ring tilt and Cp^* ring breath. Some additional bands due to Ti-O and Ti-Me stretching vibrations should be observed in this frequency range.

Spectra of reference compounds

The first reference compound was chosen to be pentamethylcyclopentadienyl-trimethoxytitanium [$\text{Cp}^*\text{Ti}(\text{OMe})_3$]. The Raman spectrum of this compound showed three prominent bands situated at 405.9 cm^{-1} , 571.8 cm^{-1} , and at 594.9 cm^{-1} (Figure III-9). The first was assigned to asymmetric Cp^* ring tilt and the later to Cp^* ring breath according to the values reported in literature for similar compounds¹⁰. The third band at 594.9 cm^{-1} could be due to Ti-O stretching vibration⁹.

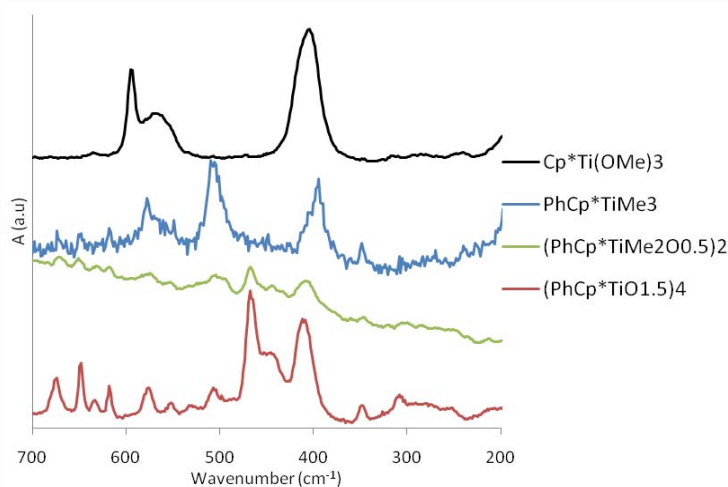


Figure III-9: Raman spectra of the reference compounds

The Raman band corresponding to $\nu(\text{Cp}^*\text{-Ti})$ is usually weak and sometimes is not observed at all. However, the presence of a band corresponding to Cp^* ring tilt indicates the existence of $\text{Cp}^*\text{-Ti}$ bond as this mode of vibration is absent in isolated cyclopentadienyl groups.

The important infrared and Raman bands observed between 200-600 cm^{-1} for all the reference compounds and their corresponding assignments to various bonds are given in Table III-12.

Compound	Infrared (cm^{-1})	Raman (cm^{-1})	Assignment
$\text{Cp}^*\text{Ti}(\text{OMe})_3$		405.9	Cp^* ring tilt ^{10a,b}
		571.8 (broad peak)	Cp^* ring breath ^{10c,d,e}
		594.9	$\nu(\text{Ti-O})^9$
$\text{PhCp}^*\text{TiMe}_3$ (10c)		394.9	Cp^* ring tilt
		509.4	$\nu(\text{Ti-Me})$
		578.7	Cp^* ring breath
$(\text{PhCp}^*\text{TiMe}_2\text{O}_{0.5})_2$ (10d)		408.9	Cp^* ring tilt
		468.4	$\nu(\text{Ti-O})$
		509.6	$\nu(\text{Ti-Me})$
		577.6 (weak)	Cp^* ring breath
$(\text{PhCp}^*\text{TiO}_{1.5})_4$ (10e)	305.6	312.8	$\nu_s(\text{Cp}^*\text{-Ti})$
		351.3 (weak)	$\nu_{as}(\text{Cp}^*\text{-Ti})$
	410.8	408.9	Cp^* ring tilt
	444.5	468.4	$\nu(\text{Ti-O})^{11}$
	506.2	506.7	$\nu_{as}(\text{Ti-O})^{12}$
	540.9		$\nu_{as}(\text{Ti-O})$
	593.0	580.5	Cp^* ring breath

Table III-12: Infrared and Raman spectra of the reference compounds

The Raman spectrum of $\text{PhCp}^*\text{TiMe}_3$ (**10c**) exhibits three prominent bands at 394.9, 509.4, and 578.7 cm^{-1} which can be attributed to Cp^* ring tilt, Ti-Me stretching and Cp^* ring breath respectively. Two small peaks at 349.8 and 308.3 cm^{-1} were observed as well which can be assigned to asymmetric and symmetric $\nu(\text{Cp}^*\text{-Ti})$ respectively according to the values reported in the literature^{10a,b}. The decrease of the band corresponding to Ti-Me bond was observed in the partially hydrolyzed complex $(\text{PhCp}^*\text{TiMe}_2\text{O}_{0.5})_2$ (**10d**) while a new band appeared concomitantly at 468.4 cm^{-1} , which should correspond to Ti-O bond stretching mode¹¹. The band corresponding to Cp^* ring tilt shifted from 394.9 cm^{-1} to 408.9 cm^{-1} in the partially hydrolyzed complex. This shift can be understood due to the change in the electronic

environment of the ring as a result of the replacement of one methyl group by oxygen. Due to fluorescence in the Raman spectra, the signal to noise ratio was not good and the bands corresponding to asymmetric and symmetric Cp*-Ti stretching were not visible. In the fully hydrolyzed complex $[(\text{PhCp}^*\text{TiO}_{1.5})_4]$ (**10e**) the band at 509.6 cm^{-1} attributed to the Ti-Me bond disappeared completely while another small band at 506.7 cm^{-1} became visible and was assigned to Ti-O bond. This band was difficult to observe in the spectrum of partially hydrolyzed complex due to an overlap with the Ti-Me band at 509.6 cm^{-1} . The band at 408.9 cm^{-1} corresponding to Cp* ring tilt was persistent which agrees well with our assigning of the bands. Other bands corresponding to Cp*-Ti, Cp* ring breath, etc. were observed as usual and are listed in Table III-12.

The perturbation in the Raman spectra of the compounds due to fluorescence created problems in the exact assignment of the bands to a particular bond. The intensity of the bands was low and some expected bands due to vibrations, e.g., $\nu_s(\text{Cp}^*\text{-Ti})$, $\nu_{as}(\text{Cp}^*\text{-Ti})$, were not observed at all. In order to be more certain about the assignment of the bands to particular bonds, infrared spectra of the compounds were taken as well. These both techniques are complementary to each other and should give us more information about the nature of the present bonds.

The infrared spectrum of $[(\text{PhCp}^*\text{TiO}_{1.5})_4]$ (**10e**) exhibits one prominent band at 410.8 cm^{-1} which can hence be easily assigned to Cp* ring tilt. A small peak was also observed at 593.0 cm^{-1} which corresponds to Cp* ring breath as has been seen in the Raman spectrum. Similarly bands corresponding to $\nu_s(\text{Cp}^*\text{-Ti})$, and $\nu(\text{Ti-O})$ were observed at 305.6 , 444.5 and 506.2 cm^{-1} respectively (Figure III-10).

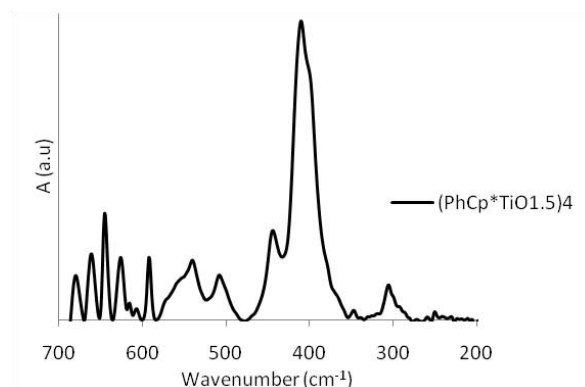


Figure III-10: Infrared spectrum of the reference compound $(\text{PhCp}^*\text{TiO}_{1.5})_4$ (**10e**)

After recording the spectra of the reference compounds we are able to assign the bands resulting from Cp* ring tilt (due to Cp*-Ti bond) at about $405\pm 10\text{ cm}^{-1}$, Cp* ring breath at about $585\pm 10\text{ cm}^{-1}$ and Ti-O at about 465 ± 20 in the infrared and Raman spectra of Cp^*TiX_n (X= halogens, alkoxides, etc.). It is reasonable to expect the bands at the same position in the prepared hybrid materials as there are not a lot of differences in the electronic environment of the cyclopentadienyl-metal bond. Some other factors like restricted freedom of rotation in the

materials compared to free molecules can, however, influence the profile and position of the bands.

Spectra of hybrid materials

We report the infrared and Raman spectra of three typical hybrid materials having linear spacers between the cyclopentadienyl rings. The Raman spectra were perturbed due to the presence of fluorescence. As a result, the signal-to-noise ratio was not good and intensity of the bands was low. In spite of this inconvenience, the Raman spectra of all three materials showed an expected band at 409.2 cm^{-1} which can be easily attributed to Cp*-Ti bond (Cp* ring tilt) as has been established previously. The expected weak band around $585\pm 10\text{ cm}^{-1}$ was not observed due to the fluorescence observed in the samples during the Raman studies. The infrared spectra of the materials showed a prominent band at 409.8 cm^{-1} which can easily be attributed to Cp* ring tilt. Two weak peaks around 302.8 and 464.8 cm^{-1} were observed and were assigned to $\nu_s(\text{Cp}^*-\text{Ti})$ and Ti-O bond respectively according to the previous results. A weak peak corresponding to Cp* ring breath was observed around $600\pm 10\text{ cm}^{-1}$ in all the materials (Figure III-11). Table III-13 summarizes the prominent infrared and Raman bands observed for all the hybrid materials.

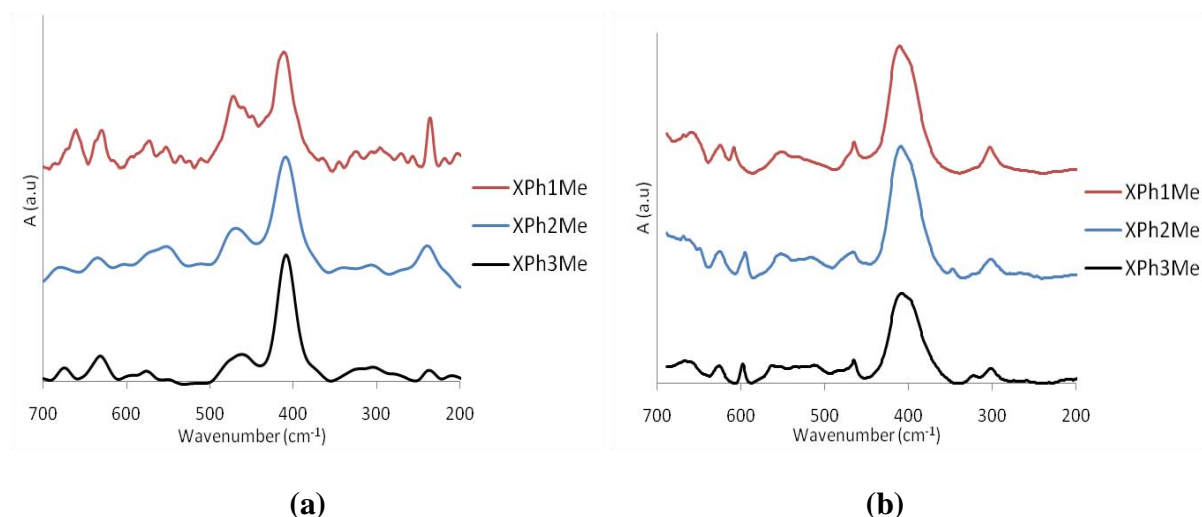


Figure III-11: (a) Raman spectra of the hybrid materials (b) Infrared spectra of the hybrid materials

Hybrid material	Infrared (cm^{-1})	Raman (cm^{-1})	Assignment
XPh1Me	302.8		$\nu_s(\text{Cp}^*-\text{Ti})$
	410.8	409.2	Cp* ring tilt ^{10a,b}
	464.8	473.2	$\nu(\text{Ti-O})^{11}$
	549.6		$\nu_{as}(\text{Ti-O})^{12}$
	608.4		Cp* ring breath ^{10c,d,e}
XPh2Me	302.7		$\nu_s(\text{Cp}^*-\text{Ti})$

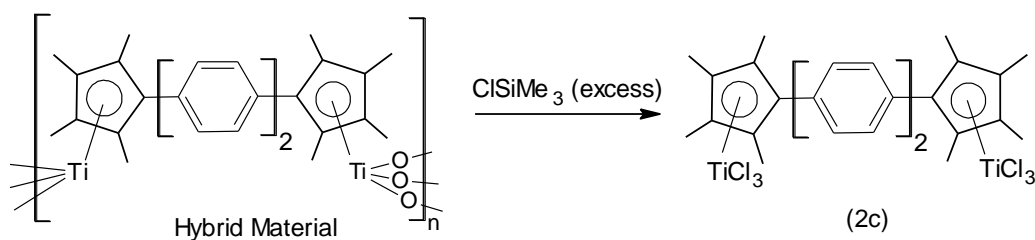
	409.8	409.2	Cp* ring tilt
	466.7	470.3	$\nu(\text{Ti-O})$
	551.5		$\nu_{\text{as}}(\text{Ti-O})$
	594.9		Cp* ring breath
XPh3Me			
	302.8		$\nu_{\text{s}}(\text{Cp}^*-\text{Ti})$
	409.8	407.6	Cp* ring tilt
	464.8	473.2	$\nu(\text{Ti-O})$
	562.2		$\nu_{\text{as}}(\text{Ti-O})$
	597.8		Cp* ring breath

Table III-13: Infrared and Raman spectra of the hybrid materials

Based on the above mentioned results of infrared and Raman spectroscopy, we can conclude that the cyclopentadienyl-titanium bond is maintained in the hybrid materials. Hence the prepared materials can be classified as class II hybrid materials in which the metal is connected to the inorganic network through stable C-Ti π -bonds.

Chemical evidence about the retention of Cp*-Ti bond

Another confirmation about the existence of a cyclopentadienyl-titanium bond in the hybrid materials came from a chemical treatment of the xerogels. The conversion of titanium oxides to the corresponding titanium chlorides by reaction with chlorotrimethylsilane has been reported in the literature¹³. Using the same methodology, a suspension of **XPh2Me** in dichloromethane was treated with an excess of chlorotrimethylsilane at room temperature in an inert environment. A color change from yellow to red was observed as a function of time. After completion of the reaction, the red product was washed and characterized by ¹H and ¹³C NMR. The expected 4,4'-biphenylenebis(2,3,4,5-tetramethylcyclopentadienyl)-di(trichlorotitanium) complex (**2c**) was obtained in almost quantitative yield.



Scheme III-2: Synthesis of 4,4'-biphenylenebis(2,3,4,5-tetramethylcyclopentadienyl)di(trichlorotitanium) complex (**2c**)

The synthesis of (**2c**) from the hybrid material is possible only if the cyclopentadienyl-titanium bond is retained in the material. The proposed structure of the material is thus correct. Hence it is another evidence for the existence of class II hybrid materials as required.

I.2.b. Microanalysis

The next step in the characterization of the xerogels is to determine their chemical composition by microanalysis. The microanalysis result for the xerogel **XPh2Me** are given in the Table III-14.

The results obtained for **XPh2Me** are shown in the first row while the theoretical results corresponding to a fully condensed material are shown in the second row. It can be seen that the difference between the experimental and the theoretical values is quite prominent. For carbon and titanium, it is not very significant (4% and 10% respectively) but for oxygen it is 50%. For a better understanding of the composition of xerogels, the oxygen content of the proposed structures should be increased. This can be done by introducing oxygen atoms in the form of hydroxyl groups as has been done previously with hybrids obtained after the hydrolysis of di(cyclopentadienyltriisopropoxytitanium) precursors. A better agreement is observed in the experimental and the calculated values by incorporating one oxygen atom in the structure due to an incomplete condensation of the hydroxyl groups. An even better fit is obtained by including two oxygen atoms per mole of the xerogel as shown in the fourth row of the Table. In this case the differences between the experimental and the calculated values are of 2%, 4% and 3% for carbon, titanium and oxygen respectively. The same is true for other hybrid materials except **XTh2Me**.

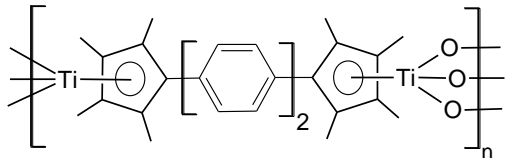
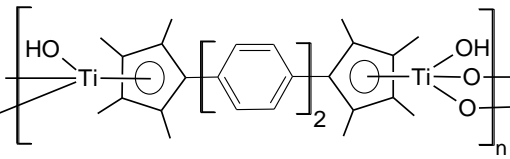
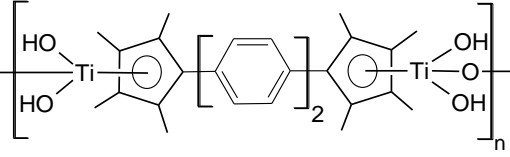
XPh2Me	Ti	C	H	O*
Experimental	16.1	64.4	6.0	13.5
Calculated for				
	17.9	67.2	6.0	9.0
Calculated for				
	17.3	65.0	6.1	11.6
Calculated for				
	16.8	62.9	6.3	14.0

Table III-14: Experimental and theoretical elemental composition of xerogel **XPh2Me**

* Obtained by difference

Based on the elemental composition obtained by microanalysis of the materials, the following formulas can be predicted.

Hybrid Material	Theoretical formula	Proposed formula
XPh1Me	$C_{24}H_{28}Ti_2O_3$	$C_{24}H_{28}Ti_2O(OH)_4$
XPh2Me	$C_{30}H_{32}Ti_2O_3$	$C_{30}H_{30}Ti_2O(OH)_4$
XPh3Me	$C_{36}H_{36}Ti_2O_3$	$C_{36}H_{36}Ti_2O(OH)_4$
XTh2Me	$C_{26}H_{28}Ti_2S_2O_3$	-

Table III-15: Theoretical and proposed formulas for the hybrid materials

The elemental compositions obtained for **XTh2Me** were quite different from the calculated values and showed a decomposition of the compound during hydrolysis. The reason for this can be attributed to the thermal fragility of the starting precursor i.e., 5,5'-bithiophylenebis(2,3,4,5-tetramethylcyclopentadienyl)di(trimethyltitanium) (**6d**), that resulted in the degradation of the product during either hydrolysis-condensation reactions or while aging for 3 weeks at room temperature. Other analysis results (TGA, XRD, etc.) for this xerogel are not discussed in the following parts of the chapter.

The theoretical and experimental molar ratios of H/Ti, C/Ti, O/Ti and spacer/Ti are given in the Table III-16.

Hybrid		H/Ti	C/Ti	O/Ti	Spacer/Ti
XPh1Me	Theoretical	16	12	2.5	0.5
	Experimental	18.0	14.1	2.7	0.56
XPh2Me	Theoretical	18.0	15.0	2.5	0.5
	Experimental	17.9	16.0	2.5	0.52
XPh3Me	Theoretical	20.0	18.0	2.5	0.5
	Experimental	21.6	19.5	3.0	0.54
XTh2Me	Theoretical	16.0	13.0	2.5	0.5
	Experimental	29.6	16.4	9.4	0.82

Table III-16: Theoretical and experimental molar ratios of elements

The spacer/Ti ratio is quite close to its theoretical value for all the materials except **XTh2Me** discussed before. This observation is consistent with our predicted structures for the hybrid materials and hence we can believe that both organic and inorganic parts are present in the final materials in good ratio.

I.2.c. Thermogravimetric analysis

The thermogravimetric analysis of the xerogels was carried out in air. All the materials showed very high stability towards heat. Only a negligible mass loss took place between 25-300°C owing to the removal of entrapped water and solvent molecules. The materials started degrading after 300°C and were completely pyrolyzed at 800°C (Figure III-12).

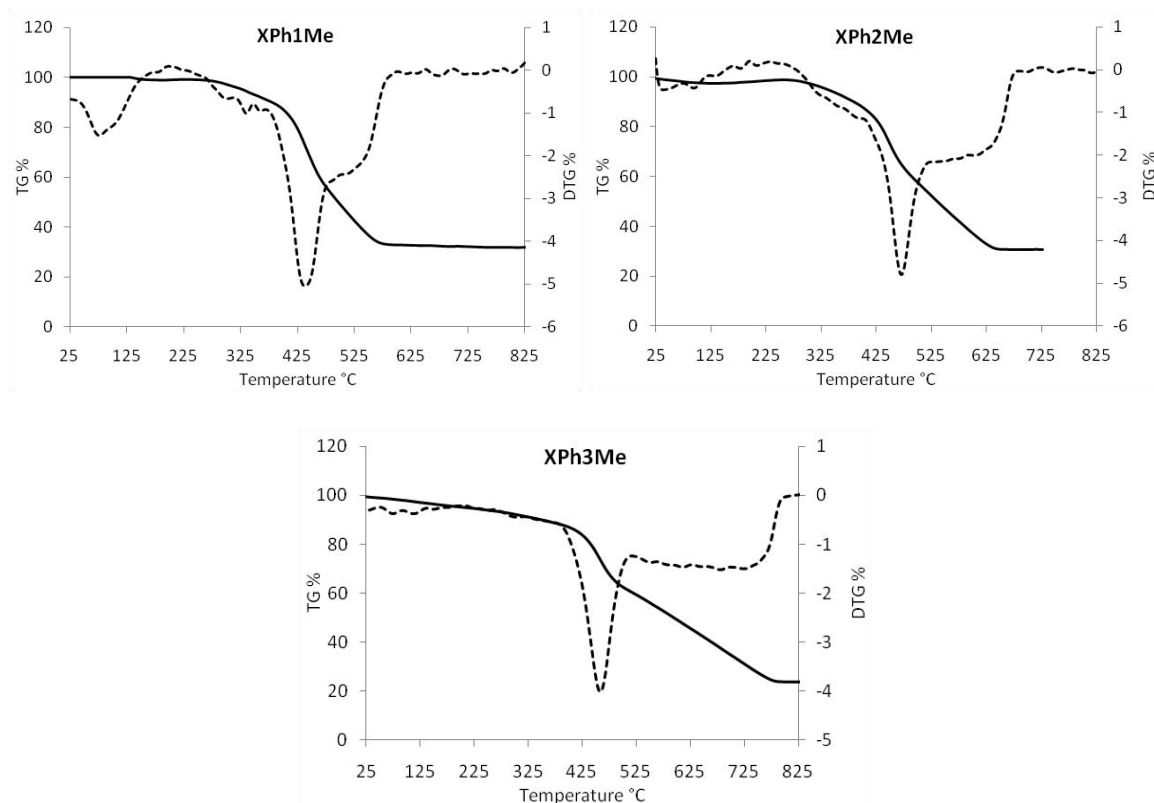


Figure III-12: TGA and DTG curves of the xerogels (in air)

The molecular weights of the xerogels calculated from the residual mass obtained after pyrolysis of the materials are given below.

Xerogel	Residual mass, X (%)	Molecular weight (g/mol)	Theoretical molecular weight (g/mol)
XPh1Me	32.2	497	496
XPh2Me	27.2	588	572
XPh3Me	24.6	650	648

Table III-17: Residual masses after complete pyrolysis of the xerogels, their corresponding molecular weights and the theoretical molecular weights

The molecular weights calculated for the xerogels are quite close to the calculated values based on the formulas proposed in the previous part of the discussion. Hence we can deduce that the microanalysis and the thermogravimetric analysis results are in good agreement and that they strengthen our predicted structures for the hybrid materials.

I.2.d. X-Ray diffraction analysis

Contrarily to what was reported above with alkoxide precursors, X-ray analysis of hybrids obtained from methylated precursors gave reproducible results. The hybrids were characterized by a main intense wide peak around 8.2° for all the samples. Two other less

intense peaks by 14.5° and 20° can be seen in some samples while a peak at 21.5° was observed in sample **XPh3Me** (Figure III-13).

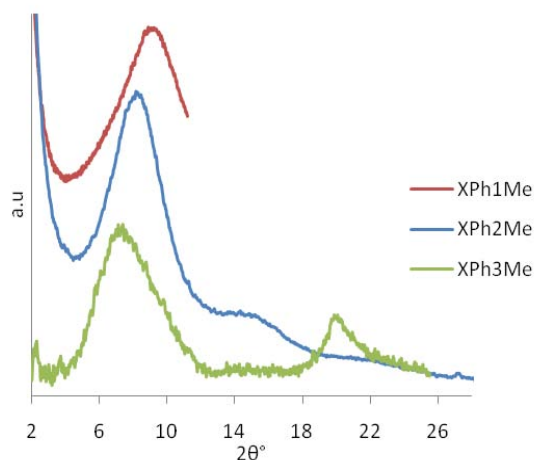


Figure III-13: X-ray diffractogram for xerogels **XPh1Me**, **XPh2Me** and **XPh3Me**

The presence of these peaks show that these titanium-based hybrids are organized at the nanometric scale and that the organization is independent of the size of the spacers, i.e., of the separation between metal atoms. Up to now, to the best of our knowledge, self-assembled hybrids have been organized according to a spacer-metal repeated pattern¹⁴. This phenomenon has been also highlighted in hybrids prepared in the presence of a surfactant inducing a hierarchical organization¹⁵. It has been explained by a slow condensation rate of the species with metal-hydroxyl bonds allowing the auto-organization process to take place. This rationalization has been achieved in two ways, in-situ crystallization¹⁶ and kinetic studies¹⁷ in the case of silicon- or tin-based hybrids.

In our case, the shape of the titanium-precursors differs from that of the studied silicon or tin precursors. The silicon or tin precursors can be considered as cylinders with the metal atoms standing at their ends that allows a tridimensional network to develop perpendicularly to the axis of the spacer with a close packing of the spacers. On the other hand all the structures of the dititanium complexes with rigid spacers^{13b,c} show an anti conformation, with both metal atoms on either side of the mean plane of the spacer. If it is assumed that this conformation is kept in the hybrid, and taking into account the steric constraints induced by the tetramethylcyclopentadienyl group, an organization of the hybrid analogous to that of silicon- or tin-based hybrid is difficult to conceive. The inorganic network can only develop in a parallel way to the mean plane of the spacer from each side of this plane that forbids the building of large planes of titanium oxide. According to this scheme, the peak by 8.2° could be attributed to the diffraction due to reflective planes made of spacers linked by Ti-O-Ti bonds. The interplanar distance corresponding to this peak, calculated according to Bragg's equation is equal to 1.08 nm. The peak at 21.5° which

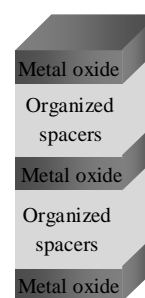


Figure III-14: Si- or Sn-based organized hybrid materials

corresponds to a distance of 0.41 nm is compatible to a π -stacking distance between a parallel arrangement of aromatic planes. A slightly larger distance than the previously reported values¹⁸ could result from the non planarity of the aromatic rings observed in the crystal structures of the similar dititanium compounds^{13b}. The spacial organization deduced from these values is depicted in Figure III-15.

The mean interplanar distance fits with a calculated value obtained by the addition of individual bond distances taken from the published crystal structures of polytitanium oxides. Tetramethylcyclopentadienyl-titanium bond is equal to 0.204 nm^{5,13b} and titanium-oxygen-titanium distance varies from 0.327 nm (PhMe₄CpTiO_{1.5})₄ to 0.359 nm in the dimer (PhMe₄CpTiCl₂)₂O⁵. The addition of these values leads to cyclopentadienyl-cyclopentadienyl distances from 0.735 to 0.767 nm. However, when the angles between bonds are taken in account, for instance in (PhMe₄CpTiCl₂)O₂ this distance is shortened to 0.569 nm, as the Cp-Ti-O angle is equal to 118° and the Ti-O-Ti angle to 169°. When the mean of these values is considered, it leads to an average distance of 0.660 nm between cyclopentadienyl groups, that, added to a π -stacking distance between aromatic planes of 0.41 nm, gives a repetition distance of 1.07 nm which falls in the range of the value found, 1.08 nm.

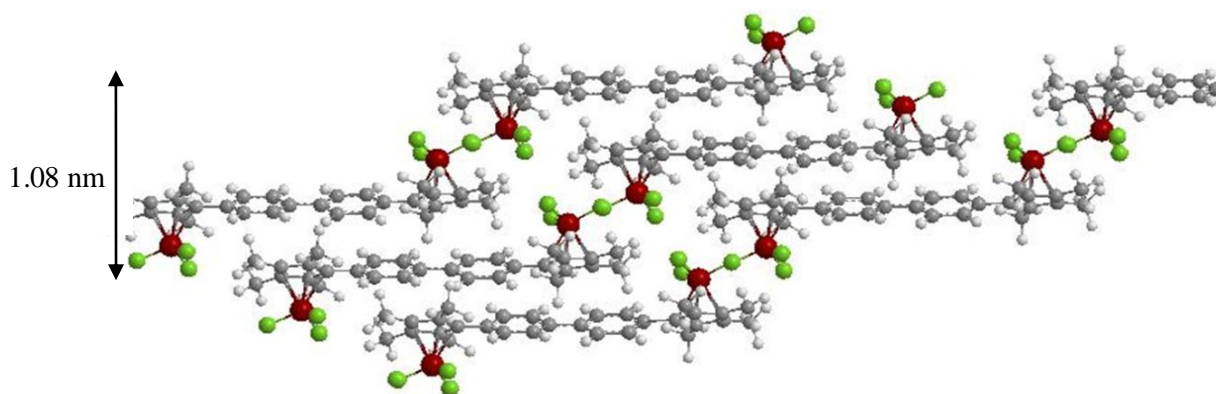


Figure III-15: Proposed structure for the organization of the materials

Up to now, a packing induced by Cp-Ti-O bonds and π -stacking has only been discussed, defining slices of the hybrid. The peak at 14° corresponding to a distance of 0.63 nm could help to explain how the slices are held together. For that we have to take into account the two hydroxyl groups attached to each titanium atom and their ability to form hydrogen bonds, that would result in the linkage of the slices together and the building of a 3D network (Figure III-16). The titanium-oxygen bond length in the known cyclopentadienyltitanium hydroxides is equal to 0.19 nm and the oxygen-oxygen distance in the alcohols, where there are strong hydrogen bonds is about 0.28 nm¹⁹. The titanium atoms would thus be 0.65 nm apart for a perfect hydrogen bonding, which is not far from the found value of 0.63 nm. In the case of such arrangement, the hydrogen atoms of the methyl group linked to the cyclopentadienyl ring would be in close contact as the distance between the center of the cyclopentadienyl ring and the plane defined by the hydrogen atoms is 0.30 nm. This value corresponds to a separation of 0.05 nm, that would make the methyl group too

close. However, a simple tilt of 7° of the cyclopentadienyl-titanium bond increases the separation to 0.11 nm and if the hydrogen bonding due to the hydroxyl-hydroxyl interaction is lower, then the proposed organization of the slices becomes likely.

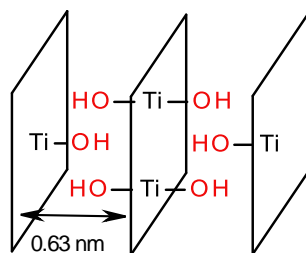


Figure III-16: Proposed structure for the 3D organization of the materials

It must be noted that the domain size, calculated from the peak at 8.2° is not so large (3.70 nm) and corresponds to about four associated dimers. However, these titanium-based hybrids show an irrefutable short range organization and the organization scheme we propose explains the main information of this X-ray study, the angle invariance of the main peaks despite variations of spacer length.

The above mentioned results show that the studied hybrid materials are organized as desired. To the best of our knowledge, the proposed organization has never been reported for hybrid materials.

I.2.e. Microscopy

The hybrid **XPh2Me** was studied by transmission electron microscopy (TEM) in order to detect an order in the material. The pictures show mainly a worm-like morphology. In some places a weak parallel lamellar structure of about 1.2 nm width can be distinguished. This value corresponds with the values calculated from XRD for the proposed stair-like structure for the materials.

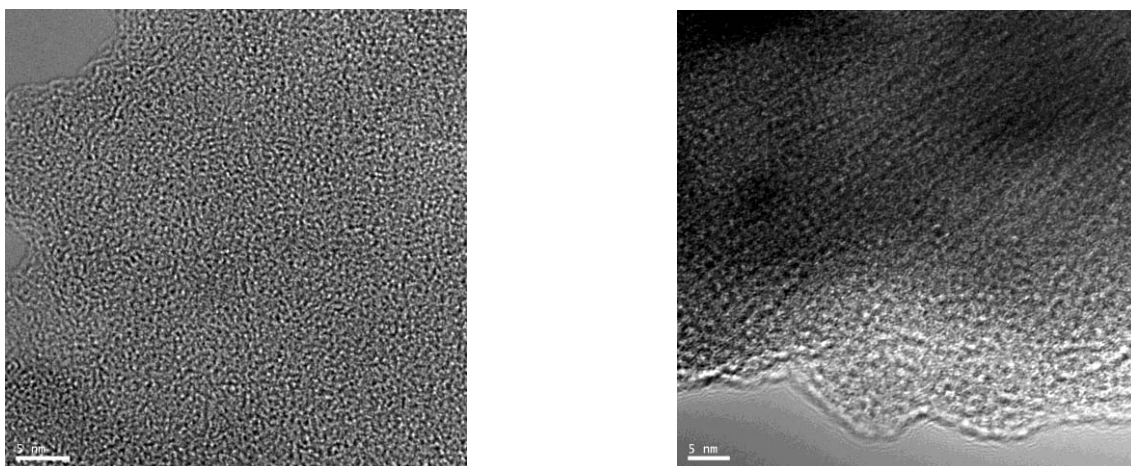


Figure III-17: High resolution TEM images for **XPh2Me**

In addition to the above mentioned observation, no metal aggregates were seen. The material looks very homogeneous with no TiO_2 crystallites indicating that the metal is homogeneously distributed throughout the material as desired.

I.3. Hybrid materials from di(cyclopentadienyltribenzyltitanium) precursors

Several self-assembled titanium-based hybrid materials have been prepared by hydrolysis of di(cyclopentadienyltrimethyltitanium) precursors. However, in order to further investigate the effect of hydrolysable groups on the composition and organization of the materials, di(cyclopentadienyltribenzyltitanium) precursors were used as well. The rate of hydrolysis of titanium-methyl and titanium-benzyl groups could be different and hence it could modify the properties of the corresponding hybrid materials.

The hydrolysis of di(cyclopentadienyltribenzyltitanium) precursors was carried out in THF under nitrogen using a stoichiometric amount of water. The solutions were left untouched for gelification for several days. The corresponding gels were washed with THF, diethyl ether and petroleum ether under centrifugation and then were dried under vacuum overnight.

The hydrolysis of 1,4-phenylenebis(2,3,4,5-tetramethylcyclopentadienyl)di(tribenzyltitanium) (**1e**) and 4,4'-biphenylenebis(2,3,4,5-tetramethylcyclopentadienyl)di(tribenzyltitanium) (**2e**) complexes resulted in the formation of yellow gels after several days (10-12 days). A color change from red to yellow was observed as the reaction proceeded indicating the hydrolysis of the benzyl groups. 4,4''-Terphenylenebis(2,3,4,5-tetramethylcyclopentadienyl)di(tribenzyltitanium) complex (**4e**), however, did not form a gel even after one month of hydrolysis. Analysis of the product obtained after evaporation of the solution showed a mixture of products indicating an incomplete hydrolysis-condensation reaction.

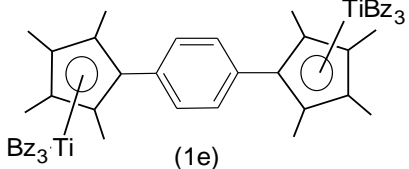
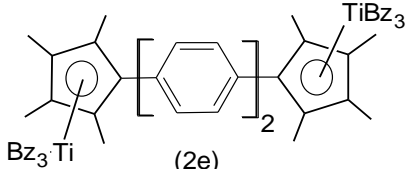
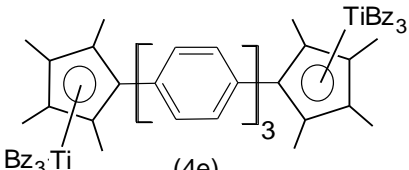
Xerogels	Precursors	Physical state	Yield (%)
XPh1Bz	 (1e)	Yellow gel	85
XPh2Bz	 (2e)	Yellow gel	74
XPh3Bz	 (4e)	Solution due to incomplete hydrolysis	-

Table III-18: List of hybrid materials and their precursors

I.3.a. Spectroscopic studies

The prepared xerogels were studied by infrared spectroscopy. Several broad bands were observed between $450\text{-}800\text{ cm}^{-1}$ which are characteristic of Ti-O-Ti network². Similarly a broad band was observed at 3400 cm^{-1} which represents a Ti-OH functional group and entrapped water molecules as discussed before. Some sharp peaks at $\approx 2910\text{ cm}^{-1}$ corresponding to $\nu_s(\text{C-H})$, $\nu_{as}(\text{C-H})$ etc. and at $\approx 1450\text{ cm}^{-1}$ corresponding to $\nu(\text{C}=\text{C})$, $\delta(\text{C-H})$, etc. were observed as usual indicating the presence of organic groups in the materials.

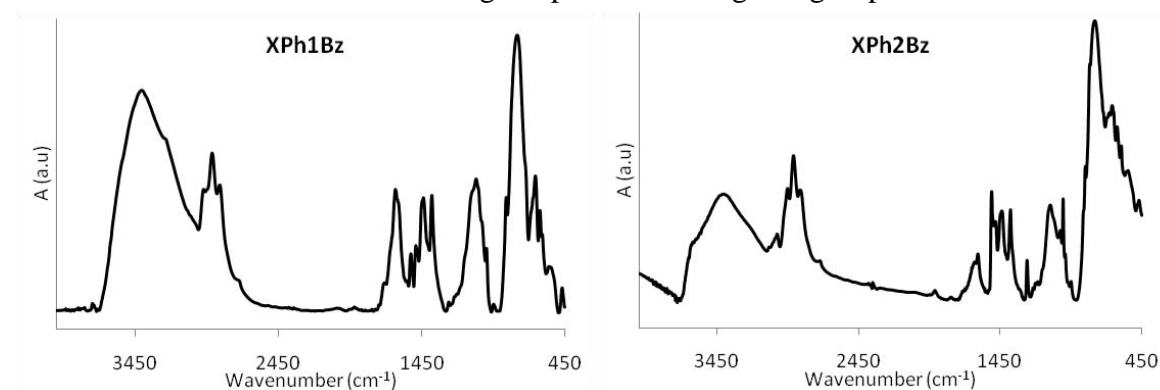


Figure III-18: Infrared spectra of xerogels **XPh1Bz** and **XPh2Bz**

I.3.b. Microanalysis

The next step in the characterization of the xerogels was to determine their chemical composition by microanalysis. The elemental composition obtained after microanalysis and the calculated values are given in Table III-19.

XPh2Bz	Ti	C	H	O*
Experimental	14.4	62.2	6.3	17.1
Calculated for				
	17.9	67.2	6.0	9.0
Calculated for				
	17.3	65.0	6.1	11.6
Calculated for				
	16.8	62.9	6.3	14.0

Table III-19: Experimental and calculated elemental composition of **XPh2Bz**

*Obtained by difference

The chemical composition of fully condensed materials presented in the second row is very different from the experimental values. A better fit was obtained between the experimental and the theoretical values by assuming four hydroxyl groups per mole of the material due to incomplete condensation as it has been discussed previously. In this case, the experimental percentages of carbon and hydrogen come close to the calculated values. Titanium and oxygen percentages are, however, still little far from the expected values.

Based on the microanalysis results, the following chemical formulas can be proposed for the xerogels.

Xerogels	Theoretical formula	Proposed formula
XPh1Bz	$C_{24}H_{28}Ti_2O_3$	$C_{24}H_{28}Ti_2O(OH)_4$
XPh2Bz	$C_{30}H_{32}Ti_2O_3$	$C_{30}H_{32}Ti_2O(OH)_4$

Table: III-20: Theoretical and proposed formulas for the xerogels

The theoretical and experimental molar ratios of H/Ti, C/Ti, O/Ti and spacer/Ti calculated by microanalysis results are given in Table III-21.

Xerogels		H/Ti	C/Ti	O/Ti	Spacer/Ti
XPh1Bz	Theoretical	16	12	2.5	0.5
	Experimental	17.8	13.4	4.3	0.60
XPh2Bz	Theoretical	18	15.0	2.5	0.5
	Experimental	20.9	17.3	3.6	0.58

Table III-21: Theoretical and experimental molar ratios of the elements

The above mentioned experimental molar ratios are not far from the calculated values that indicates that our predicted structures for the materials are correct. However, better results were obtained in case of materials prepared by the hydrolysis of di(cyclopentadienyltrimethyltitanium) precursors where the molar percentages of elements were closer to their expected values.

I.3.c. Thermogravimetric analysis

The thermal stability of the xerogels was studied by thermogravimetric analysis. Both materials showed good thermal stability until 300°C after which the decomposition of the organic part started. A small mass loss was, however, observed between 25-150°C corresponding to the removal of entrapped water and solvent molecules. All the organic part was decomposed before 600°C for **XPh1Bz** and 800°C for **XPh2Bz** (Figure III-19).

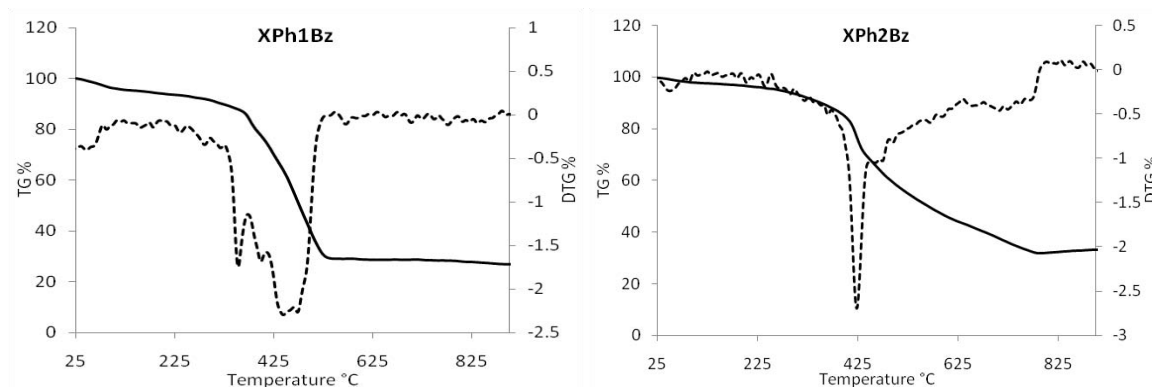


Figure III-19: TGA and DTG curves for **XPh1Bz** and **XPh2Bz** (in air)

The molecular weight of the xerogels were calculated from the residual mass obtained after pyrolysis of the materials. These calculations are based on the hypothesis that at 800°C all the matter is pyrolyzed to TiO_2 (Table III-22)

Xerogel	Residual mass, X (%)	Molecular weight (g/mol)	Theoretical molecular weight (g/mol)
XPh1Bz	29.8	537	496
XPh2Bz	29.1	550	572

Table III-22: Residual masses after complete pyrolysis of the xerogels, their corresponding molecular weights and the theoretical molecular weights

The molecular weight calculated for **XPh2Bz** is not very different from the theoretical value calculated from microanalysis results.

I.3.d. X-ray diffraction analysis

In the X-ray diffraction analysis, a prominent peak around 8.2° was observed for both materials. Two smaller peaks at 14.5° and 20.5° were also observed in the case of **XPh2Bz**.

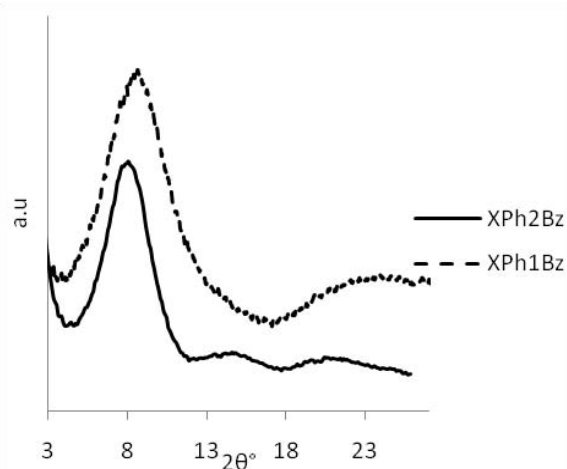


Figure III-20: X-ray diffractograms for xerogels

A comparison of the above mentioned results with the XRD results of the materials prepared from di(cyclopentadienyltrimethyltitanium) precursors shows that there is no difference in the position of the peaks and in the corresponding experimental distances between the planes. Hence the previously proposed model for the organization of the nanostructures fits here too. A stair-like structure which is independent of the size of the spacer is proposed. The distance corresponding to the peak at 8.2° is 1.08 nm which represents the spacing between the reflective planes consisting of spacers linked by Ti-O-Ti bonds. The inorganic network is built parallel to the mean plane of the spacers. Hence, a change in the hydrolysable groups did not modify the nature of organization. However a slight decrease in the domain sizes from 3.7 nm to 3.0 nm was observed.

Hybrid materials having aromatic spacers between the cyclopentadienyl groups were prepared from di(cyclopentadienyltribenzyltitanium) precursors. The X-ray diffraction analysis depicts that the materials are well organized as expected. The nature of organization was consistent with the proposed model for materials obtained from di(cyclopentadienyltrimethyltitanium) precursors. Hence a change in the hydrolysable groups did not affect the self-assembly of the nanostructures. However, better TGA and microanalysis results were obtained in case of materials prepared from methylated precursors.

II. Preparation of hybrid materials with lateral chains

In order to modify the organization in the materials, precursors carrying long lateral chains were hydrolyzed. These lateral chains can potentially auto-assemble to give a different type of organization as has been observed with tin-based materials²⁰. This methodology has also been successfully employed in case of π -conjugated organic polymers²¹ studied for their optical and electrochemical properties.

1,4-Bis(octyloxy)phenylene-2,5-bis(3,4-dimethylcyclopentadienyl)di(triisopropoxy-titanium) (**9b**) that carries eight-carbon lateral chains was used as the precursor as it is easy to synthesize with a limited number of steps. However, keeping in mind the previous results where better organized materials were obtained by the hydrolysis of di(cyclopentadienyltrimethyltitanium) and di(cyclopentadienyltribenzyltitanium) complexes, 1,4-bis(octyloxy)phenylene-2,5-bis(3,4-dimethylcyclopentadienyl)di(trimethyltitanium) (**9d**) and 1,4-bis(octyloxy)phenylene-2,5-bis(3,4-dimethylcyclopentadienyl)di(tribenzyltitanium) (**9e**) complexes were synthesized and hydrolyzed as well.

The first precursor (**9b**) was hydrolyzed in THF using the reaction conditions as previously described. The reaction temperature was, however, decreased to -80°C in an attempt to slow down the rate of the hydrolysis reaction. The reaction mixture was stirred at -80°C for 30 min and then was allowed to warm up to room temperature. A yellow gel was obtained after staying 30 min at room temperature. It was left untouched for aging for three weeks and then was washed and dried. The required xerogel (**XPhC8OR**) was obtained as a yellow powder. In the case of 1,4-bis(octyloxy)phenylene-2,5-bis(3,4-dimethylcyclopentadienyl)di(tribenzyltitanium) (**9e**) a yellow gel was obtained after 1 h while the

hydrolysis of 1,4-bis(octyloxy)phenylene-2,5-bis(3,4-dimethylcyclopentadienyl)di(trimethyltitanium) (**9d**) resulted in the formation of yellow precipitates after 1 h (Table III-23).

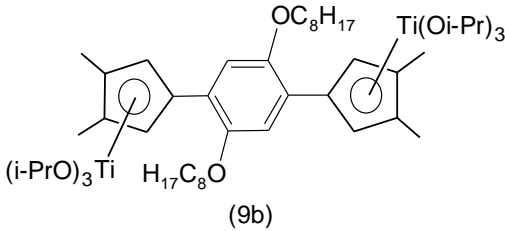
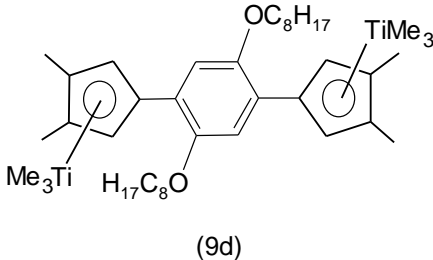
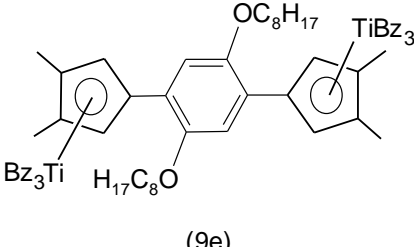
Xerogels	Precursors	Temperature	Gelification Time	Yield (%)
XPhC8OR	 <p>(9b)</p>	-80°C	1 h	82
XPhC8Me	 <p>(9d)</p>	RT	Precipitation	38
XPhC8Bz	 <p>(9e)</p>	RT	1 h	70

Table III-23: List of precursors and their corresponding xerogels

The characterization of xerogel **XPhC8Me** by FT-IR, microanalysis, TGA, and XRD analysis indicated a decomposition of the starting material during hydrolysis-condensation reactions. Again the reason can be attributed to high thermal instability of the precursor (**9d**). Therefore results for this xerogel are not shown in the next part of the discussion.

II.a. Spectroscopic studies

The hydrolysis and condensation reactions were studied via infrared spectroscopy. Appearance of broad bands between 450-800 cm^{-1} in the infrared spectra of the xerogels was observed as usual due to the formation of Ti-O-Ti network². Very prominent peaks around $\approx 2930 \text{ cm}^{-1}$ corresponding to $\nu_s(\text{C-H})$, $\nu_{as}(\text{C-H})$ etc. were observed in the materials owing to the presence of long alkyl chains and methyl substituents on the cyclopentadienyl groups. A broad peak corresponding to $\nu(\text{O-H})$ was obtained around 3450 cm^{-1} that should come from the uncondensed hydroxyl groups and water molecules as discussed previously. This peak is however, very intense in the spectrum of **XPhC8Bz** indicating that perhaps in addition to the

uncondensed hydroxyl groups, a large number of water molecules are entrapped in the nanostructure, and, in spite of the overnight drying, are not completely removed.

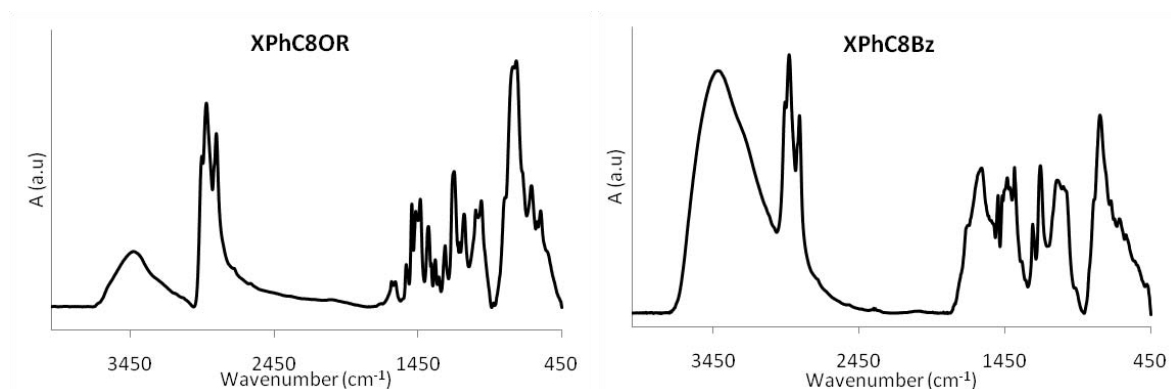


Figure III-21: Infrared spectra of hybrid materials carrying lateral chains

II.b. Microanalysis

The chemical composition of the xerogels was determined by microanalysis. Like previously described materials, the percentage of oxygen was higher than the calculated value for fully condensed material in both the xerogels. A better fit was obtained by considering a partial condensation reaction incorporating four hydroxyl groups per mole of the material. Hence the following formulas can be proposed for both the xerogels.

Hybrid Material	Theoretical formula	Proposed formula*
XPhC8OR	$C_{36}H_{52}Ti_2O_5$	$C_{36}H_{52}Ti_2O_3(OH)_4$
XPhC8Bz	$C_{36}H_{52}Ti_2O_5$	$C_{36}H_{52}Ti_2O_3(OH)_4$

Table III-24: Theoretical and proposed formulas for the xerogels

The molar ratios of H/Ti, C/Ti, O/Ti, and spacer/Ti calculated from microanalysis results are given below.

Hybrid		H/Ti	C/Ti	O/Ti	Spacer/Ti
XPhC8OR	Theoretical	28	18	3.5	0.5
	Experimental	30.2	19.7	3.8	0.54
XPhC8Bz	Theoretical	28	18	3.5	0.5
	Experimental	29.3	19.9	5.9	0.59

Table III-25: Theoretical and experimental molar ratios for XPhC8OR and XPhC8Bz

The above mentioned molar ratios are quite close to the calculated values indicating that the proposed formulas for the materials are correct. However, a better fit was observed in case of XPhC8OR compared to XPhC8Bz especially in O/Ti ratio.

II.c. Thermogravimetric analysis

The thermal stability of the xerogels was studied by thermogravimetric analysis. Both xerogels were stable until 200°C before which only the removal of small molecules (water and/or solvent) was observed. After 200°C, degradation of the organic part started and at about 500°C all the organic part had been pyrolyzed.

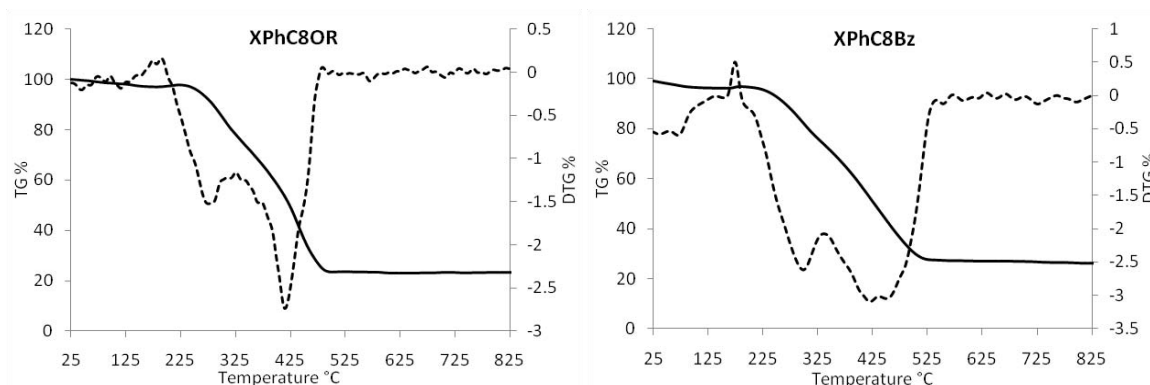


Figure III-22: TGA and DTG curves for xerogels (in air)

Based on the residual mass of TiO_2 obtained after complete combustion of the xerogels, molecular weights have been calculated and are compared to the theoretical masses calculated according to microanalysis results.

Xerogel	Residual mass, X (%)	Molecular weight (g/mol)	Theoretical molecular weight (g/mol)
XPhC8OR	23.2	690	696
XPhC8Bz	26.3	608	696

Table III-26: Residual masses after complete pyrolysis of the xerogels, their corresponding molecular weights and the theoretical molecular weights

The molecular weight obtained from TGA is very close to the theoretical molecular weight for xerogel **XPhC8OR** indicating that microanalysis and TGA results are in agreement and that the proposed formula for the material is correct. For xerogel **XPhC8Bz**, however, the difference in the calculated and experimental mass is quite significant. A higher residual mass obtained in TGA could indicate a partial rupture of Ti-C bond during either hydrolysis or later during washing and handling of the xerogel.

II.d. X-ray diffraction analysis

The X-ray diffractogram of both xerogels depicted one sharp peak around 4.7° . A broad peak at 17.9° for **XPhC8OR** and at 18.6° for **XPhC8Bz** was observed as well (Figure III-23).

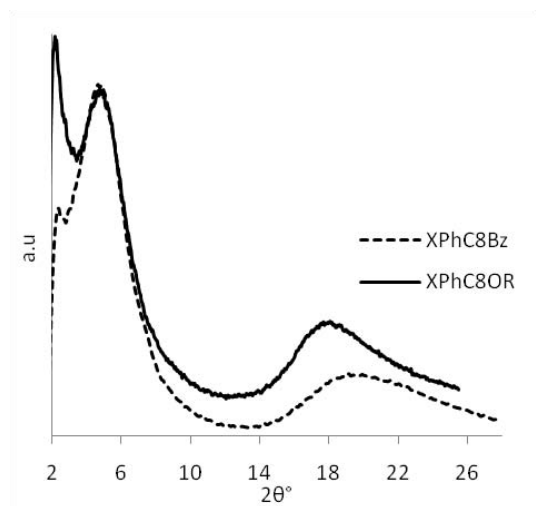


Figure III-23: XRD diffractogram for xerogels **XPhC8OR** and **XPhC8Bz**

The presence of these peaks shows that the materials are organized at nanometric scale. The position of the peak at low angle shows that the nature of organization, however, is not the same as for materials containing linear spacers. The peak at 4.7° corresponds to an interplanar distance of 1.88 nm. It is less than the distance measured for fully stretched lateral chains, 2.31 nm with a chain/spacer axis angle of 75.9° ²². However it is larger than the distance of 1.46 nm that can be measured in the crystal structure of a compound when the lateral chains are distorted²². So the distance of 1.88 nm is fully compatible with a structure where no interdigitation of the chains takes place (Figure III-24). The second broad peak by 18.3° corresponding to a distance of 0.48 nm is larger than the distances corresponding to alkyl chains fully packed by van der Waals interactions that are usually lying in the 0.43-0.37 nm range. However this difference could be explained by a loose packing of alkyl chains.

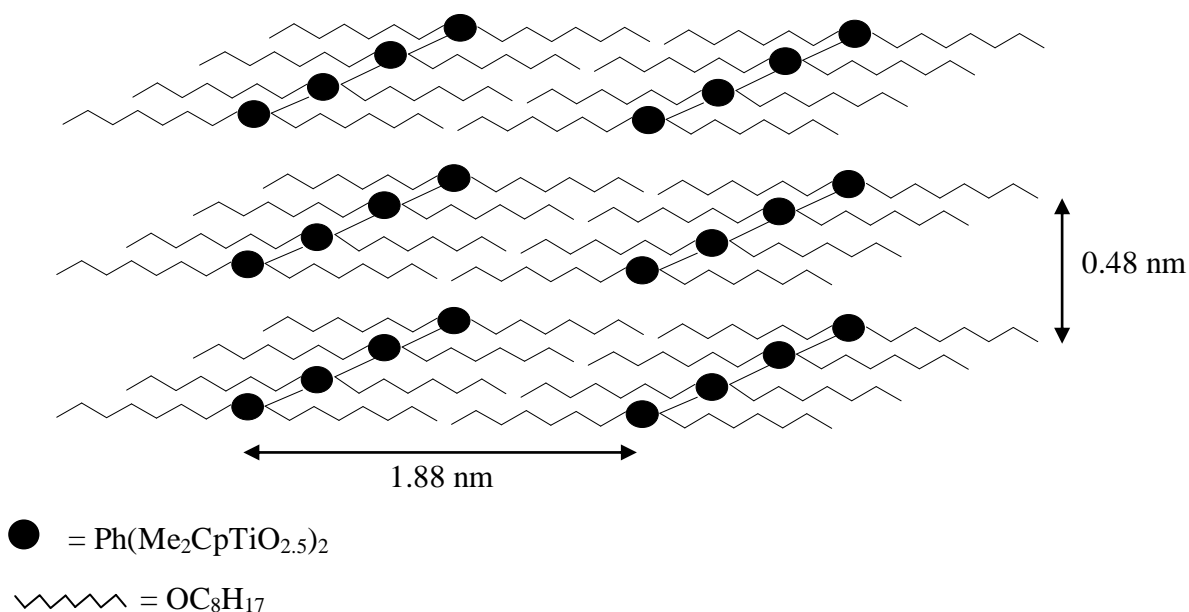


Figure III-24: Proposed model for the xerogels **XPhC8OR** and **XPhC8Bz**

A change in the hydrolysable group of the precursors from isopropoxy to benzyl had no influence on the position of the main peak indicating that the organization is independent of the nature of the hydrolysable groups.

III. Conclusion

Various self-assembled titanium-based class II hybrid materials have been prepared in which the inorganic network is connected to the organic network through stable titanium-carbon π -bonds. The mode of organization of the nanostructures depends on the spacer binding the dicyclopentadienyl groups. Linear aromatic spacers lead to materials having a stair-like structure in which the organic ligands are arranged via π -stacking. The length of the spacer has a little effect on the organization of the nanostructures. The structure of the materials obtained with spacers endowed with long lateral chains is governed by the length of the side chains. Microanalysis and thermogravimetric studies agree well with the proposed structures of the nanomaterials.

- ¹ (a) Burgos, M.; Langlet, M. *Thin Solid Films* **1999**, *349*, 19 (b) Lynch, C. T.; Mazdidasni, K. H.; Smith, J. S.; Crawford, W. J. *Anal. Chem.* **1964**, *36*, 2332
- ² Léaustic, A.; Babonneau, F.; Livage, J. *Chem. Mater.* **1989**, *1*, 248
- ³ Loy, D. A.; Beach, J. V.; Baugher, B. M.; Assink, R. A.; Shea, K. J.; Tran, J.; Small, J. H. *Chem. Mater.* **1999**, *11*, 3333
- ⁴ (a) Beweries, T.; Burlakov, V. V.; Peitz, S.; Arndt, P.; Baumann, W.; Spannenberg, A.; Rosenthal, U. *Organometallics* **2008**, *27*, 3954 (b) Hanna, T. E.; Lobkovsky, E.; Chirik, P. J. *Inorg. Chem.* **2007**, *46*, 2359 (c) Kickbusch, R.; Lentz, D. *Chem. Comm.* **2010**, *46*, 2118
- ⁵ (a) Björgvinsson, M.; Halldorsson, S.; Arnason, I.; Magull, J.; Fenske, D. *J. Organomet. Chem.* **1997**, *544*, 207
- ⁶ Brunauer, S.; Emmett, P. H.; Teller, E. *J. Am. Chem. Soc.* **1938**, *60*, 309
- ⁷ (a) Elhamzaoui, H. *Thesis University Bordeaux I* **2006** (b) Riague, E. *Thesis University Bordeaux I* **2003**
- ⁸ Oviatt, Jr. H. W.; Shea, K. J.; Small, J. H. *Chem. Mater.* **1993**, *5*, 943
- ⁹ Maslowsky, E. Jr. *Vibrational Spectra of Organometallic Compounds* **1977**, Wiley-Interscience, New York
- ¹⁰ (a) Samuel, E.; Ferner, R.; Bigorgne, M. *Inorg. Chem.* **1973**, *12*, 881 (b) Jiang, S.; Zhang, P.; Wang, Y. *Chem. Res. Chin. Univ.* **2000**, *16*, 341 (c) Malisch, W.; Jehle, H.; Möller, S.; Thum, G.; Reising, J.; Gbureck, A.; Nagel, V.; Fickert, C.; Kiefer, W.; Nieger, W. *Eur. J. Inorg. Chem.* **1999**, 1597 (d) Malisch, W.; Lankat, R.; Schmitzer, S.; Pinkl, R.; Posset, U.; Kiefe, W. *Organometallics* **1995**, *14*, 5622 (e) Bencze, E.; Lokshin, B. V.; Mink, J.; Herrmann, W. A.; Kühn, F. E. *J. Organomet. Chem.* **2001**, *627*, 55
- ¹¹ Bobrova, A. M.; Zhigun, I. G.; Bragina, M. I.; Fotiev, A. A. *J. Appl. Spectrosc.* **1968**, *8*, 96
- ¹² Moran, P. D.; Bowmaker, G. A.; Cooney, R. P.; Finnie, K. S.; Bartlett, J. R.; Woolfrey, J. L. *Inorg. Chem.* **1998**, *37*, 2741
- ¹³ (a) Nielson, A. J.; Shen, C.; Waters, J. M. *Polyhedron* **2006**, *25*, 2039 (b) Lee, M. H.; Kim, S. K.; Do, Y. *Organometallics* **2005**, *24*, 3618 (c) Kim, S. K.; Kim, H. K.; Lee, M. H.; Yoon, S. W.; Han, Y.; Park, S.; Lee, J.; Do, Y. *Eur. J. Inorg. Chem.* **2007**, 537
- ¹⁴ (a) Elhamzaoui, H.; Jousseau, B.; Riague, H.; Toupance, T.; Dieudonné, P.; Zakri, C.; Maugey, M.; Allouchi, H. *J. Am. Chem. Soc.* **2004**, *126*, 8130 (b) Elhamzaoui, H.; Jousseau, B.; Toupance, T.; Zakri, C.; Biesemans, M.; Willem, R.; Allouchi, H. *Chem. Comm.* **2006**, 1304 (c) Toupance, T.; de Borniol, M.; Elhamzaoui, H.; Jousseau, B. *Appl. Organomet. Chem.* **2007**, *21*, 514 (d) Elhamzaoui, H.; Jousseau, B.; Toupance, T.; Zakri, C. *J Sol-Gel Sci. Technol.* **2008**, *48*, 6 (e) Kapoor, M. P.; Yang, Q.; Inagaki, S. *J. Am. Chem. Soc.* **2002**, *124*, 15176
- ¹⁵ (a) Hatton, B.; Landskron, K.; Whitnall, W.; Perovic, D.; Ozin, G. A. *Acc. Chem. Res.* **2005**, *38*, 305 (b) Fujita, S.; Inagaki, S. *Chem. Mater.* **2008**, *20*, 891 (c) Mizoshita, N.; Imai, M.; Tani, T.; Inagaki, S. *J. Am. Chem. Soc.* **2009**, *131*, 14225
- ¹⁶ Dieudonné, P.; Wong Chi Man, M.; Pichon, B. P.; Vellutini, L.; Bantignies, J. L.; Blanc, C.; Creff, G.; Finet, S.; Sauvajol, J. L.; Bied, C.; Moreau, J. J. E. *Small* **2009**, *5*, 503

¹⁷ Elhamzaoui, H.; Jousseaume, B.; Toupance, T.; Zakri, C.; Maugey, M. *Langmuir* **2007**, *23*, 785

¹⁸ (a) Chen, Z.; Muller, P.; Swager, T. M. *Org. Lett.* **2006**, *8*, 273 (b) Ji, H. F.; Majithia, R.; Yang, X.; Xu, X.; More, K. *J. Am. Chem. Soc.* **2008**, *130*, 10056

¹⁹ McGregor, P. A.; Allan, D. R.; Parsons, S.; Clark, S. J. *Acta Cryst.* **2006**, *B62*, 599

²⁰ Elhamzaoui, H.; Jousseaume, B.; Toupance, T.; Zakri, C. *Dalton Trans.* **2009**, *23*, 4429

²¹ Hoeben, F. J. M.; Jonkheijm, P.; Meijer, E. W.; Schenning, A. P. H. J. *Chem. Rev.* **2005**, *105*, 1491

²² Elhamzaoui, H.; Jousseaume, B.; Toupance, T.; Allouchi, H. *Organometallics* **2007**, *26*, 3908



**CHAPTER IV : PREPARATION OF TITANIUM DIOXIDE
FROM TITANIUM-BASED HYBRID MATERIALS**

I. Introduction

Titanium dioxide has become one of the most attractive binary oxide for technical and commercial applications because of its remarkable physicochemical properties that include chemical inertia, mechanical hardness, electronic conductivity, transparency to visible light, and large surface area. It is the most stable oxide of titanium and can be obtained from either natural or synthetic sources.

Titanium dioxide is most importantly used as a white pigment¹, owing to its very high reflectance at visible and ultraviolet wavelengths. Its refractive index is so high that fine particles scatter light with almost total efficiency. For this reason it has found various applications including formulation of sun screens², paints, ointments, surface coatings, toothpastes³ etc. Another important application of titanium dioxide results from its high photoactivity. It participates in many photocatalytic reactions including oxidative degradation of organics⁴, reduction of metal ions⁵, and evolution of dihydrogen from water⁶. Similarly the use of dye-sensitized nanocrystalline nanoporous titanium dioxide electrodes deposited on conductive glass substrates has found widespread applications in the field of solar cells⁷.

Titanium dioxide exists naturally in three crystalline forms, anatase, brookite, and rutile, brookite being the rare one⁸. Out of these, anatase is generally regarded as the most active phase. Rutile is chemically the most stable form and its high reflective index allows more diffusion of light resulting in a better overall absorption of the system⁹. The anatase, on the other hand, presents better properties for electron transport.

Several ways of preparation of crystalline titanium oxide nanoparticles of different size and shapes are available¹⁰. The most common route is the sol-gel process that involves the hydrolysis of a titanium alkoxide followed by condensation¹¹. The reaction is normally acid-catalyzed¹² although base-catalyzed¹³ reactions have been reported as well. The titanium alkoxide-to-water ratio and the rate of hydrolysis reactions influence the development of Ti-O-Ti chains, low water content and slow hydrolysis rates favoring the formation of three dimensional polymeric skeletons with close packing. A thermal treatment is usually carried out after the hydrolysis-condensation reactions in order to increase the crystallinity of the TiO₂ particles. An example of base-catalyzed sol-gel route is the polycondensation of titanium alkoxide in the presence of tetramethylammonium hydroxide leading to highly crystalline anatase TiO₂ nanoparticles with different sizes and shapes¹⁴ (Figure IV-1a).

The use of micelles and inverse micelles is another method to synthesize TiO₂ nanomaterials¹⁵. An example of the route is the synthesis of shuttle-like crystalline TiO₂ nanoparticles by hydrolysis of titanium tetrabutoxide in the presence of acids in NP-5 (Igepal CO-520) cyclohexane reverse micelles at room temperature¹⁶.

A non-hydrolytic sol-gel process involving the reaction of titanium tetrachloride with a variety of different oxygen donor molecules, e.g., a metal alkoxide or an organic ether, can be used for the preparation of nanocrystalline titanium dioxide¹⁷. The Ti-O-Ti bridges are

formed by the condensation of Ti-Cl and Ti-OR. The alkoxide groups can be provided by titanium alkoxides or can be formed in situ by reaction of the titanium chloride with alcohols or ethers.

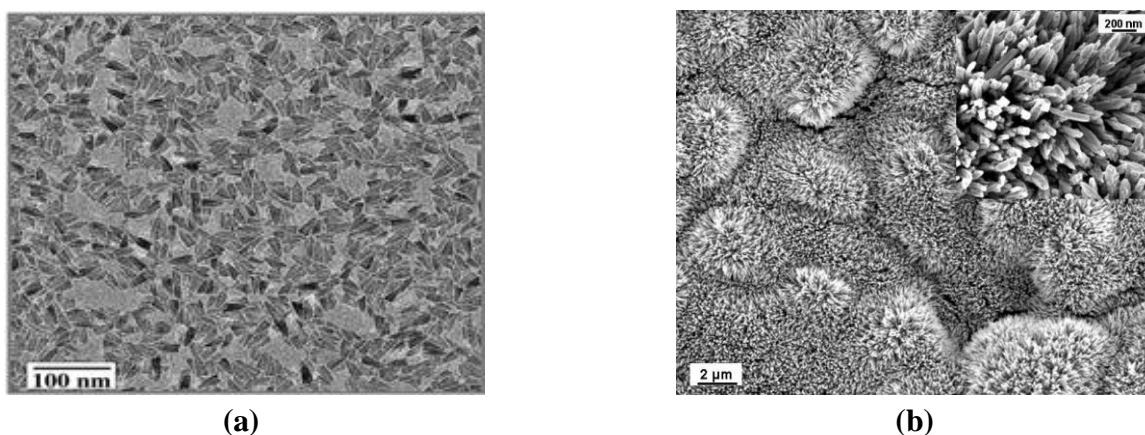


Figure IV-1: SEM images of (a) TiO₂ nanoparticles (Figure taken from reference 14a) (b) TiO₂ nanorods (Figure taken from reference 23)

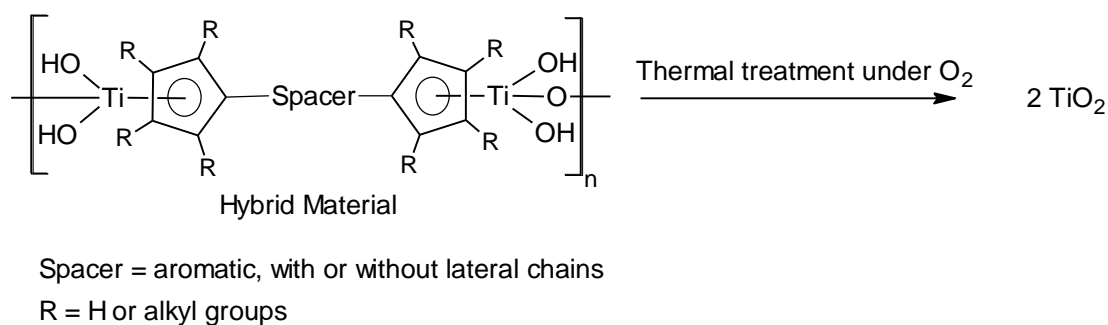
Other less common but effective routes for the synthesis of titanium dioxide particles or nanotubes include an hydrothermal treatment of titanium precursors carried out in autoclaves at controlled temperature and pressure¹⁸, solvothermal method¹⁹ (similar to the hydrothermal method but water is replaced by a nonaqueous solvent), direct oxidation of titanium metal²⁰, ultrasound²¹ or microwave²² irradiation of titanium precursors, etc. An example of the synthesis of titanium dioxide nanorods by the direct oxidation of titanium plate with a hydrogen peroxide solution is shown in Figure IV-1b²³.

Analogous to titanium dioxide powders, titanium dioxide thin films have attracted great attention in a variety of advanced applications as well due to their ability to be applied as coatings and their high surface area. Their uses in catalysis²⁴, membranes²⁵, biological supports²⁶, and environmental applications²⁷ are a constant research interest.

The most common route to prepare crystalline titanium dioxide thin films is the sol-gel process that involves the hydrolysis of a precursor of TiO₂, e.g., TiCl₄, Ti(OR)₄, etc., with or without additives. It is advantageous as it allows the simple production of high purity films at low cost. The amorphous particles formed after the hydrolysis-condensation reactions are crystallized either by thermal treatment²⁸, at high pressure²⁹ or by microwaves³⁰.

The calcination of the titanium-based hybrid materials discussed in the previous chapter proposes a new route to produce mesoporous titanium dioxide with controlled properties as powders and as thin films. The same strategy has been utilized to prepare SiO₂³¹ and SnO₂³² particles by thermal treatment of silicon-based and tin-based hybrid materials respectively. The crystal phase, porosity and crystallinity of the resulting materials could be controlled by changing the reaction conditions, especially calcination temperature. A high specific area brought about by small particles is desirable as it is beneficial to many applications. It facilitates interaction between devices and the interacting media, which mainly

occurs on the surface and strongly depends on the specific area of the material. Thus, the performance of TiO_2 -based devices is largely influenced by the size of the TiO_2 building units and their interactions at the nanometer scale.

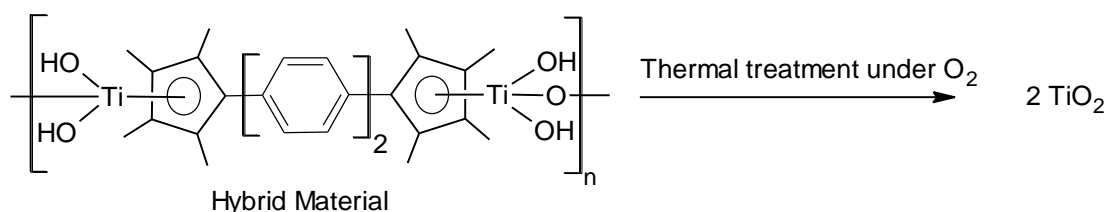


Scheme IV-1: Schematic representation of the synthesis of TiO_2 particles from titanium-based hybrid material

II. Preparation of titanium dioxide powders

The hybrid material containing a biphenyl group in the spacer (**XPh2Me**) that showed good chemical composition and better organization of the nanostructures and that is prepared in good yields was selected to prepare titanium dioxide powders by thermolysis. The choice of the reaction temperature was very important as annealing at low temperature would lead to incomplete conversion giving high carbon residues while a very high temperature would result in changes in the crystallographic forms and in the formation of aggregates, hence modifying the textural properties of the resulting material. The optimal calcination temperature was determined by studying the TGA curves of the xerogel (Figure III-12, chapter 3). A prominent mass loss was observed around 450°C which continued till 650°C where all the organic part was removed. Hence two different temperatures (450°C and 500°C) were chosen for calcinations in order to obtain titanium dioxide particles with controlled properties. Higher temperatures ($> 500^\circ\text{C}$) were avoided in order to get mesoporous materials with specific area as elevated as possible.

The xerogel **XPh2Me** was calcinated under oxygen flow at 450°C (**TiO_2 - 450°C**) or 500°C (**TiO_2 - 500°C**) for 4 h (Scheme IV-2). White powders were obtained in both cases that were then characterized by various techniques.



Scheme IV-2: Schematic representation of the preparation of titanium dioxide from the hybrid material (**XPh2Me**)

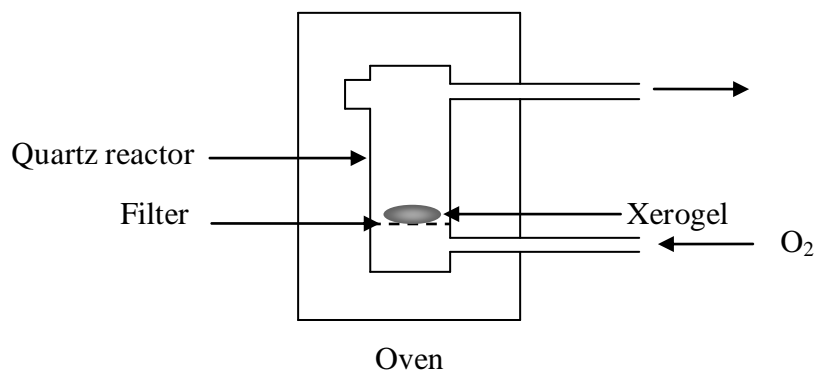


Figure IV-2: Pyrolysis of the xerogel to prepare TiO_2 particles

II.1. Spectroscopic studies

The infrared spectra of both samples prepared at 450°C ($\text{TiO}_2\text{-}450^\circ\text{C}$) and at 500°C ($\text{TiO}_2\text{-}500^\circ\text{C}$) were taken to ensure the complete removal of the organic part. The resulting spectra along with the starting hybrid material (**XPh2Me**) are given in Figure IV-3.

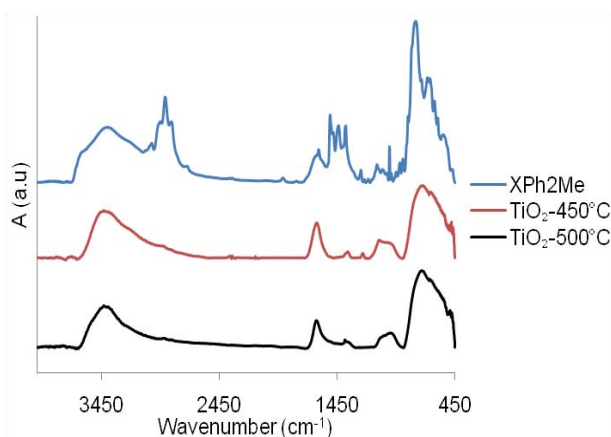


Figure IV-3: Infrared spectra of the xerogel and the prepared TiO_2 samples

A complete removal of the peaks around 2900 cm^{-1} corresponding to $[\nu(\text{C}_{\text{aryl}}\text{-H}), \nu_{\text{s}}(\text{C-H}), \nu_{\text{as}}(\text{C-H})]$ vibrations of the organic ligand was observed in $\text{TiO}_2\text{-}450^\circ\text{C}$ indicating that at 450°C the organic groups are either completely removed or their amount is negligible. Similarly, peaks around 1400 cm^{-1} corresponding to various $\text{C}=\text{C}$ and C-H stretching and bending vibrations of the ligand disappeared completely. There was, however, a small peak at 1080 cm^{-1} that can be explained by considering the presence of a small amount of remaining organics. There were two small peaks at 1250 cm^{-1} and 1380 cm^{-1} in both samples indicating the presence of a small amount of carbonates on the surface. The adsorption of carbon dioxide to the surface of titanium dioxide either during or after calcination could lead to the formation of these carbonates³³.

Expected broad bands between $450\text{-}800\text{ cm}^{-1}$ were observed that correspond to the presence of Ti-O-Ti network³⁴. A broad band around 3400 cm^{-1} due to $\nu(\text{O-H})$ and another around 1625 cm^{-1} due to $\delta(\text{O-H})$ were observed in both samples and can be associated with

the presence of hydroxyl groups. The presence of these bands indicates the existence of Ti-OH groups along with water molecules adsorbed during cooling of the samples.

Hence we can deduce that heating the xerogels at 450°C or 500°C removes almost all the organic groups resulting in the preparation of titanium dioxide powders. The surface of the resulting powders is, however, polluted by the presence of carbonates.

The Raman spectrum of the sample **TiO₂-500°C** showed a prominent peak at 150.0 cm⁻¹. Four small peaks at 197.6, 404.3, 521.4 and 642.4 cm⁻¹ were observed as well (Figure IV-4). All these peaks are characteristics of titanium dioxide in anatase crystalline phase³⁵. Three very small peaks were observed at 252.8, 323.3, and 369.0 cm⁻¹ indicating the presence of a small amount of brookite as well. However the amount of brookite phase was very low.

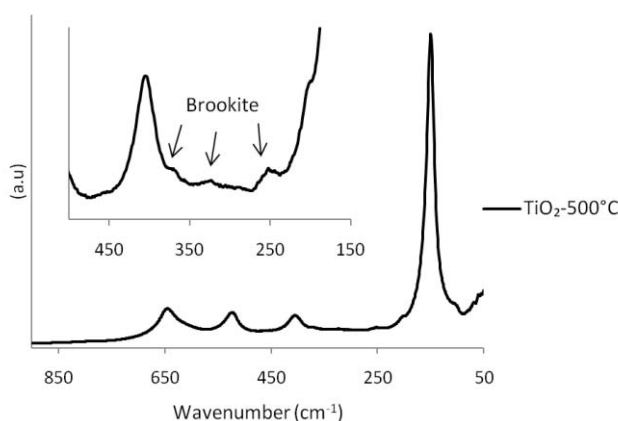


Figure IV-4: Raman spectrum of **TiO₂-500°C**

The crystallite size can be estimated by applying a phonon confinement model³⁶ to the main Eg Raman band observed at 150.0 cm⁻¹. The full width at half maximum or the shift of this peak compared to the standard value were used in this model to give a crystallite size of about 7.0 ± 0.5 nm.

II.2. Microanalysis

The chemical composition of the powders was determined by microanalysis. The percentages of carbon and hydrogen obtained for both powders are given in Table IV-1.

Sample	%C	%H
TiO₂-450°C	<0.3	0.59
TiO₂-500°C	<0.3	0.39

Table IV-1: Percentage composition of the TiO₂ samples prepared at different temperatures

The percentages of carbon and hydrogen are very low in both the samples prepared at different temperatures. Hence we can deduce that even at 450°C, almost all the organic groups have been decomposed leading to quite pure titanium dioxide.

II.3. Thermogravimetric analysis

The thermogravimetric analysis was performed in order to obtain information about the chemical composition of the prepared metal oxides. The TGA curves for both samples along with their starting material (**XPh2Me**) are given in Figure IV-5.

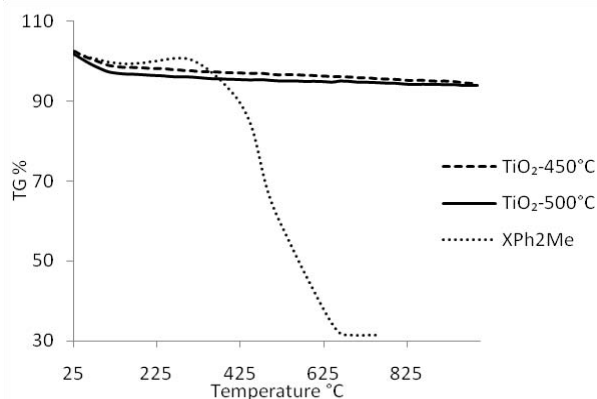


Figure IV-5: TGA curves for **XPh₂Me**, **TiO₂-450°C** and **TiO₂-500°C** recorded in air

In comparison with the xerogel **XPh₂Me**, both TiO₂ samples showed a high stability towards high temperature. A small mass loss (4-5%) was observed between 25°C to 100°C in the calcinated samples which could be associated with the removal of chemisorbed water molecules and carbonates. After that there was a minor mass loss till 1000°C at which all the organic part must have been pyrolyzed. This result clearly shows that most of the organic part of the xerogel has already been removed in the samples leading to a negligible mass loss during TGA. The residual mass of xerogel and the calcinated samples are given in Table IV-2.

Sample	Residual mass (%)
XPh₂Me	27.2
TiO₂-450°C	94.3
TiO₂-500°C	93.8

Table IV-2: Residual mass after thermal treatment of TiO₂ samples

II.4. Textural properties

The influence of calcination temperature on textural properties of the prepared TiO₂ particles was studied by nitrogen sorption analysis (BET). The nitrogen adsorption-desorption isotherms and the pore size distribution curves are given in Figure IV-6.

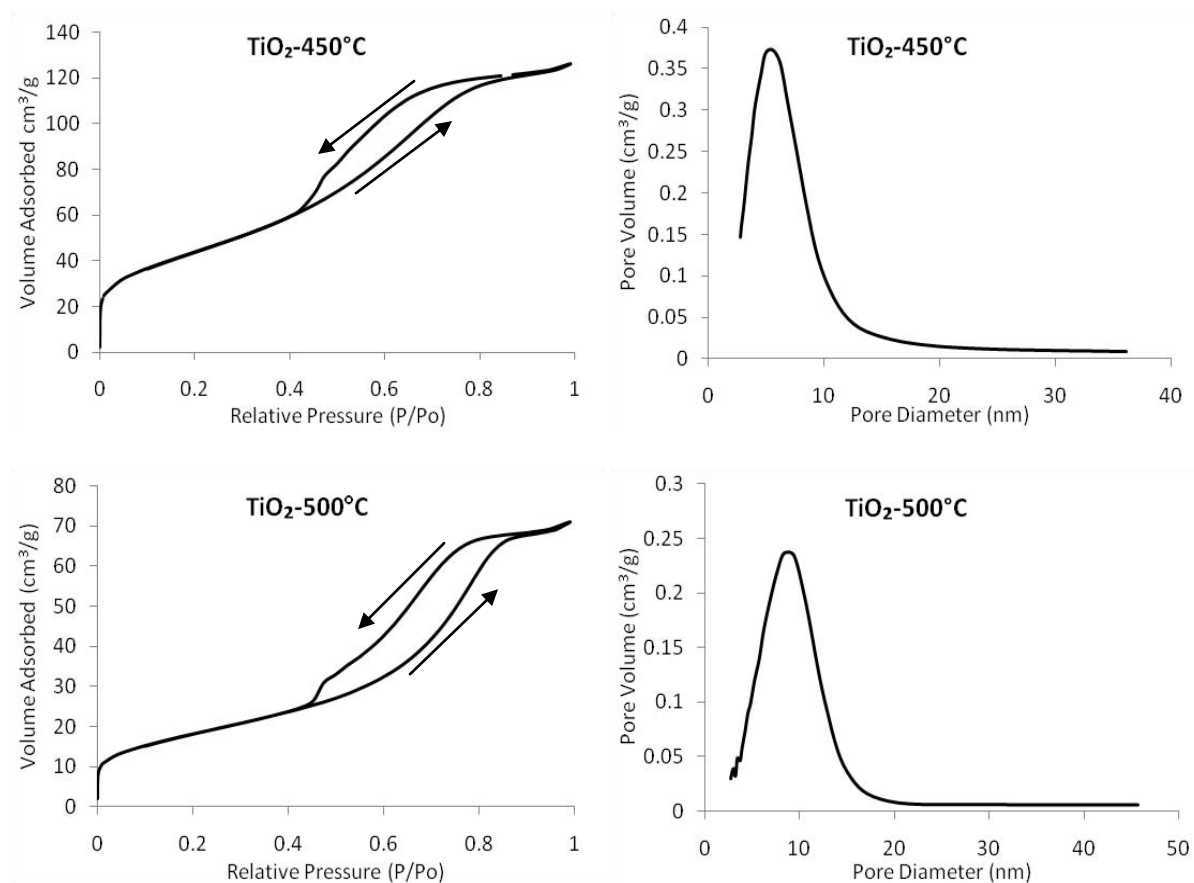


Figure IV-6: Nitrogen adsorption-desorption isotherms and pore size distributions (BJH adsorption) for **TiO₂-450°C** and **TiO₂-500°C**

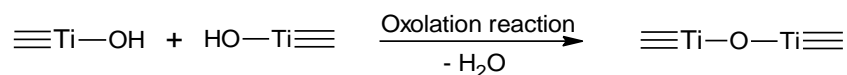
A type IV nitrogen adsorption-desorption isotherm with a type-H2 hysteresis loop was observed for **TiO₂-450°C** which is typical of mesoporous materials according to the IUPAC classification³⁷. A narrow pore size distribution based on the adsorption behavior with an average pore diameter of 5.1 nm was obtained. A marked increase in the specific area was observed after thermal treatment of the xerogel at 450°C, from $< 5 \text{ m}^2/\text{g}$ for xerogel **XPh2Me** to $158.0 \text{ m}^2/\text{g}$ for **TiO₂-450°C**. The value is quite high as desired and it has a potential to be used in TiO₂-devices as the average specific area of materials used in the known devices ranges between $100\text{-}150 \text{ m}^2/\text{g}$. A high value facilitates reaction/interaction between the devices and other media that mainly occurs on the surface and depends on the specific area.

TiO₂-500°C showed no significant change in the N₂ adsorption isotherms, a type IV isotherm with type-H2 hysteresis being observed as previously. However, the pore size distribution became broader and the mean pore diameter increased to 7.0 nm. Table IV-3 comprises the important textural characteristics of both samples calculated from nitrogen adsorption curves.

Samples	BET specific area (m ² /g)	Pore volume (cm ³ /g) (BJH adsorption)	Pore diameter (nm) (BJH adsorption)
TiO ₂ -450°C	158.0	0.17	5.1
TiO ₂ -500°C	65.2	0.10	7.0

Table IV-3: Textural properties of TiO₂-450°C and TiO₂-500°C

A significant decrease in the specific area from 158.0 m²/g to 65.2 m²/g was observed with the increase in the calcination temperature. Similarly cumulative pore volume also decreased while moving from 450°C to 500°C. This decrease in the specific area and pore volume with the increase in temperature can be explained by oxolation reaction (Scheme IV-3) that involves the formation of oxo-bridges between particles and is favored by high temperature. As a result, an increase in the size of the particles with low specific area and reduced pore volume was observed leading to a denser oxide.



Scheme IV-3: Schematic representation of oxolation reaction leading to large particle size

II.5. X-ray diffraction analysis (XRD)

The XRD analysis was used to determine the nature of phase and the crystallinity of the samples. Both samples prepared either at 450°C (TiO₂-450°C) or at 500°C (TiO₂-500°C) presented characteristic peaks of anatase phase [(101), (004), (200), (105), (204) planes etc.] (Figure IV-7). Some extra peaks at 27.5°, 36.1°, 41.3° etc. were also observed in the diffractogram of TiO₂-450°C corresponding to rutile phase (15-16 %). Interestingly, this high temperature stabilized phase was absent in the sample prepared at 500°C. Instead, a very small peak at 30.8° was observed indicating the presence of a minor quantity of brookite which is in accordance with the Raman spectrum of the sample discussed before.

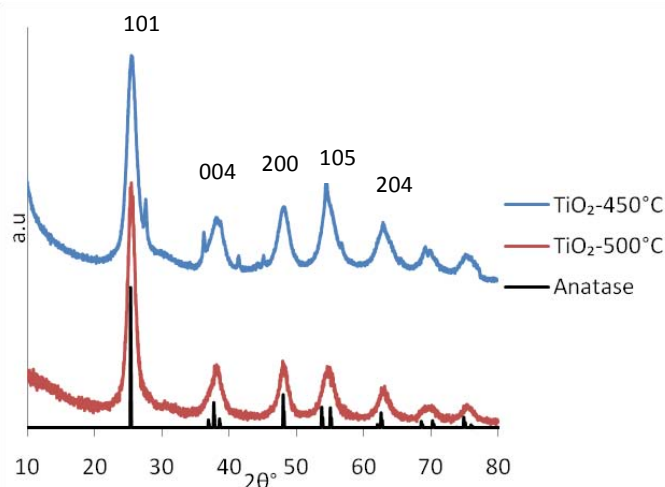


Figure IV-7: X-ray diffractogram of TiO₂-450°C, TiO₂-500°C and expected peaks for pure anatase phase

The presence of rutile at 450°C and its absence at 500°C is an unexpected result as an increase in temperature should favor the formation of this most stable phase of titanium dioxide. However, the unstability of rutile at intermediate temperatures and a higher stability of anatase when the crystal size is less than 11 nm could be a reason for this behaviour³⁸.

A prominent increase in peak intensity coupled with a sharpening of the peaks was observed as the temperature was increased from 450°C to 500°C that indicates a higher crystallinity of the titanium dioxide phase. The average crystallite size of the anatase phase was calculated by the Scherrer equation shown below using the TiO₂(101) reflexion peak.

$$D = k \frac{\lambda}{\beta \cos \theta}$$

where D is the crystallite size, k is a constant (= 0.9 assuming that the particles are spherical), λ is the wavelength of the X-ray radiation, β is the line width (obtained after correction for the instrumental broadening) and θ is the angle of diffraction. The results are given in Table IV-4.

Samples	Average crystallite size (nm)
TiO ₂ -450°C	5.4
TiO ₂ -500°C	6.7

Table IV-4: Average crystallite size of TiO₂-450°C and TiO₂-500°C

The average crystallite size for TiO₂-500°C is compatible with the size calculated from the Raman spectrum discussed previously. By combining the results of BET and XRD, we can deduce that small crystallites with large specific area were produced at 450°C while an increase in temperature to 500°C resulted in better crystallinity and larger particle size with a lower specific area. Hence a better compromise between the crystallite size and the specific area is achieved in the sample TiO₂-450°C. The results are comparable or even better with some of the values reported in the literature for the TiO₂ powders prepared in this temperature range using different titanium precursors^{11f}.

II.6. High resolution transmission electron microscopy (HRTEM)

In order to obtain further information about the crystallinity of the samples, high resolution transmission electron microscopy was performed on TiO₂-500°C. The technique allowed the direct visualization of the structure to reveal high degrees of order. The corresponding image is given in Figure IV-8.

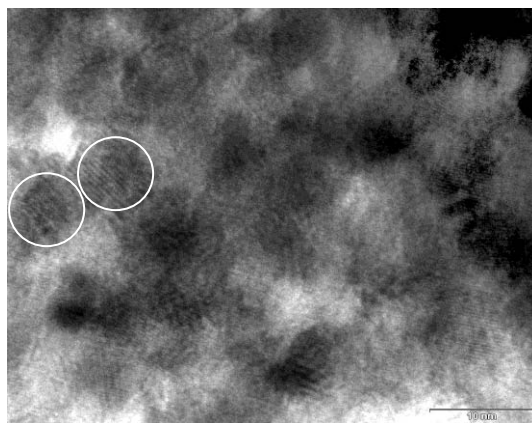


Figure IV-8: HRTEM image of $\text{TiO}_2\text{-}500^\circ\text{C}$ (Circles highlighting the crystallite size)

The image shows lattice planes with an interplanar distance of about 0.3 nm that corresponds to the 101 planes of anatase crystal structure. Almost spherical crystallites were observed the size of which closely matches the average crystallite size determined by X-ray diffraction analysis, i.e. 6-7 nm.

III. Preparation of titanium dioxide thin films

Once the preparation of crystalline titanium dioxide from the hybrid material was achieved, the next step was the preparation of titanium dioxide thin films. As the same methodology of calcination at high temperature was used, the first step was the preparation of hybrid thin films.

III.1. Preparation of hybrid films

The hybrid containing a biphenylene spacer between the cyclopentadienyl rings, **XPh2OR**, was selected for this purpose. The choice was made due to its easy synthesis, the high solubility of its precursor and its good nanostructural organization in powder form. After several attempts to prepare homogeneous films of a reasonable thickness, it was found that a smooth film was obtained after spin-coating a solution of 4,4'-biphenylenebis(2,3,4,5-tetramethylcyclopentadienyl)di(triisopropoxytitanium) (**2b**) in chloroform (650 mg/2.5 mL of the solvent) on a glass slide at a speed of 2000 rotation/min (Figure IV-9).

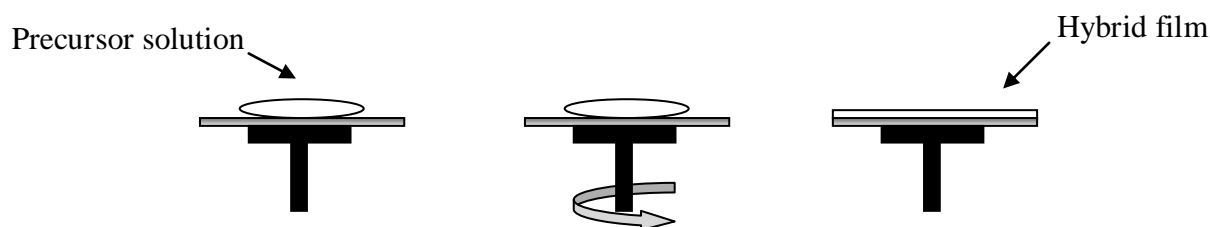
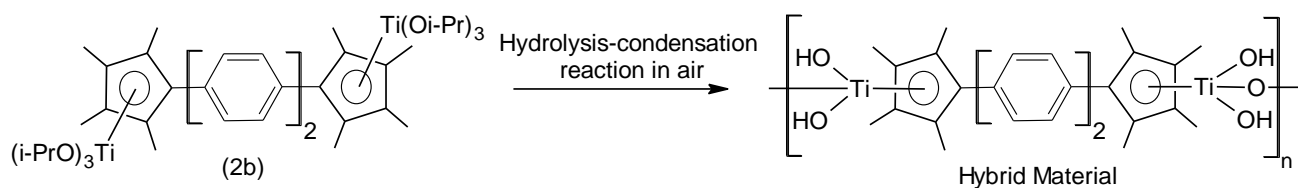


Figure IV-9: Preparation of hybrid film by spin-coating

Due to high moisture sensitivity of the precursor, the solution was prepared under nitrogen and about 150 μL of it was dropped on the glass slide via syringe. After spin-coating,

the prepared films were left in air for a few hours and then were stored in the glove box. It was anticipated that the hydrolysis of the precursor should take place in air without the addition of water (Scheme IV-4).



Scheme IV-4: Schematic representation of preparation of hybrid film (**XPh2OR-F**)

The thickness of the films was determined with a profilometer. Smooth films of about 1 μm thickness were obtained after single coating (Figure IV-10). Attempts to increase the thickness of the films either by increasing the concentration of the solution or by applying multilayers were unsuccessful as they led to rough films with large grains on the surface.

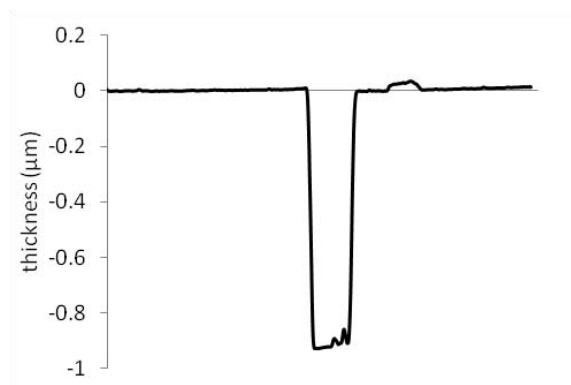


Figure IV-10: Profilometer picture showing the thickness of the film

The prepared film was studied by various techniques to check the completion of hydrolysis-condensation reactions before thermal treatment.

III.1.1. Infrared Spectroscopy

The infrared spectrum of the prepared film (**XPh2OR-F**) was recorded to ensure the completion of hydrolysis. As the glass slides give strong absorption bands below 2000 cm^{-1} , it was not possible to observe the presence or absence of isopropoxy groups that give bands around $1000\text{-}1300\text{ cm}^{-1}$. In order to overcome this difficulty, the films were scratched and the obtained powder was then analyzed in the form of KBr pellet. The resulting spectrum was compared to the infrared spectrum of the precursor (Figure IV-11). The absence of two strong doublets around 1022 cm^{-1} and 1160 cm^{-1} attributed to the skeletal C-C vibrations of isopropoxy groups³⁹ was observed in the spectrum of **XPh2OR-F**. Similarly a characteristic doublet at $1360\text{-}1375\text{ cm}^{-1}$ corresponding to the symmetric deformation of the gem-dimethyl structure of isopropoxy groups in the precursor disappeared in the final material indicating a complete hydrolysis of the isopropoxy groups. Several strong bands were observed around 780.0 cm^{-1} owing to the formation of a Ti-O-Ti network³⁴. These results indicate that the

hydrolysis-condensation reactions have taken place in air even without the direct addition of water to the precursor. The retention of bands at 2972, 2930, and 2864 cm^{-1} assigned to $\nu(\text{C}_{\text{aryl}}\text{-H})$, $\nu_{\text{s}}(\text{C-H})$ and $\nu_{\text{as}}(\text{C-H})$ respectively shows that the spacer is still present in the final material as expected.

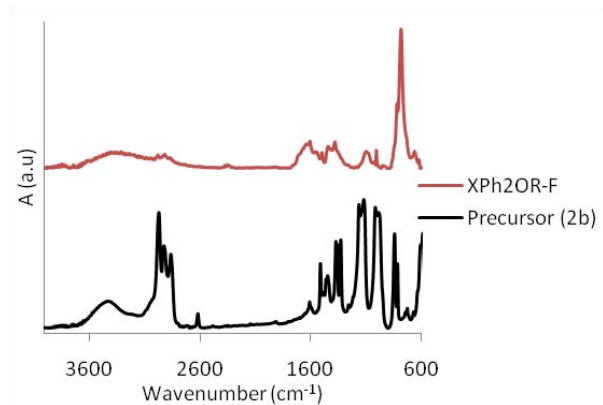


Figure IV-11: Infrared spectra of hybrid film (XPh2OR-F) and the precursor (2b)

III.1.2. Atomic force microscopy (AFM)

The surface of the film was studied by atomic force microscopy (AFM). Due to rather rough surface of the glass slides even before deposition, the surface study was carried out on a hybrid film prepared on a silicon wafer. The microscopic images showed a homogeneous film with a smooth surface (Figure IV-12). No cracks or big clusters were observed on the surface. For a $4 \mu\text{m}^2$ area of the film, the root mean square (RMS) surface roughness of 0.29 nm was obtained. The value is quite low indicating a smooth film without imperfections (cracks, holes, etc.) and that it is suitable for the preparation of TiO_2 films in the next step.

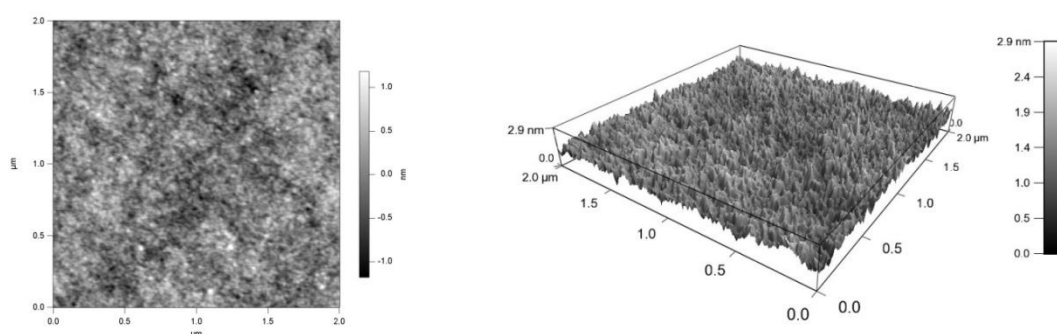


Figure IV-12: AFM images of the hybrid film (XPh2OR-F)

III.2. Preparation of titanium dioxide films

Once the required hybrid films with reasonable thickness were formed, the next step was their thermal treatment to remove the organic groups leading to pure titanium dioxide films. In order to study the effect of annealing temperature on the properties of the resulting films, the hybrid films were heated for four hours at 400°C (T_1), 500°C (T_2) or 600°C (T_3), in air leading to **F-TiO₂-400°C**, **F-TiO₂-500°C**, and **F-TiO₂-600°C** respectively. The thickness

of the films measured with a profilometer was about 180 nm after thermal treatment. The prepared films were characterized by Raman spectroscopy, XPS and X-ray diffraction analysis.

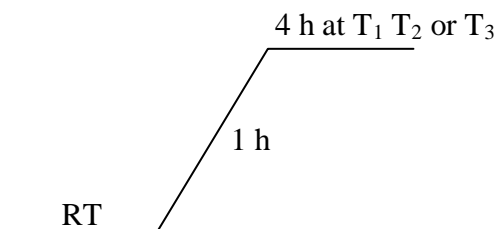


Figure IV-13: Thermal program used for the calcination of the films

III.2.1. X-ray photoelectron spectrometry (XPS)

The X-ray photoelectron spectrometry was performed to determine the nature of elements present in the films. Three expected elements, titanium (Ti2p), oxygen (O1s) and carbon (C1s) were detected in the hybrid film (**XPh2OR-F**) (Figure IV-14). A small amount of silicon (Si2s, Si2p) impurity was detected as well that came from silicone grease pollution. The very prominent peak corresponding to carbon (C1s) was reduced to a greater extent in the calcinated films indicating the decomposition of the organic part. However, the retention of this small peak indicates that all the organic matter has not been completely removed and a small amount of carbon is still present even after heating to 600°C. The remaining two peaks corresponding to titanium (Ti2p) and oxygen (O1s) were retained in the calcinated films.

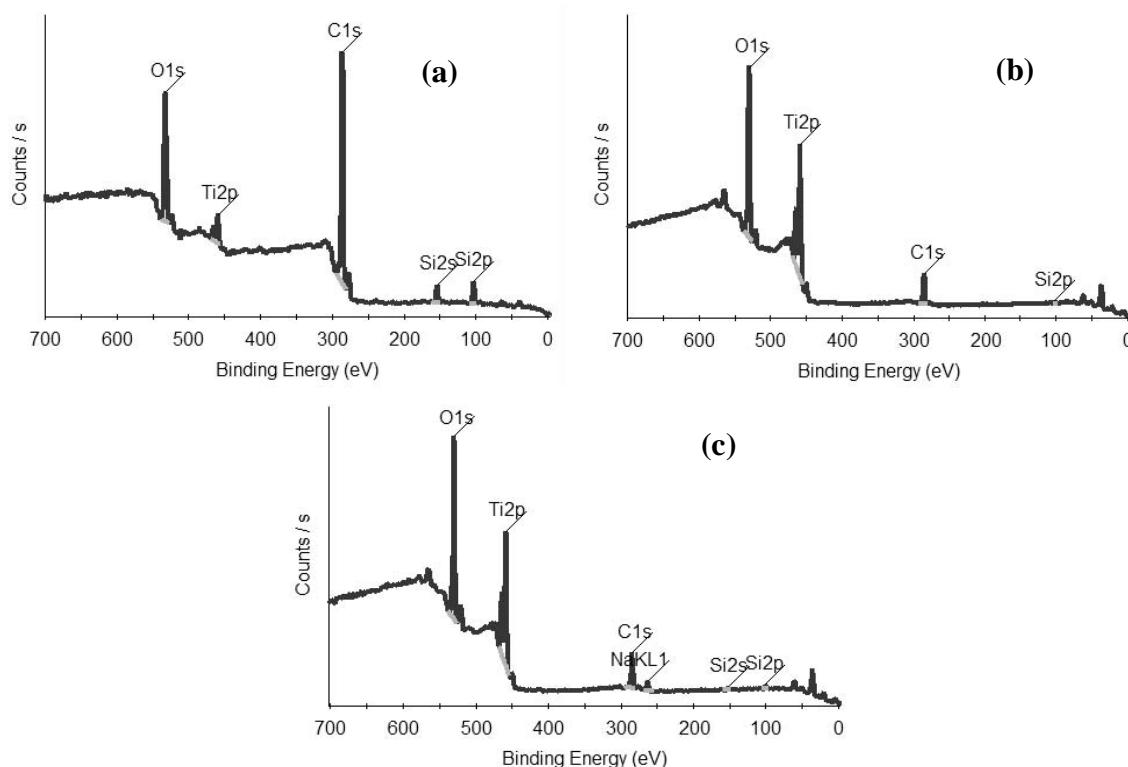


Figure IV-14: XPS spectrum of (a) hybrid film (**XPh2OR-F**) (b) **F-TiO₂-400°C** and (c) **F-TiO₂-600°C**

The oxygen core level spectra of **F-TiO₂-400°C** and **F-TiO₂-600°C** are shown in Figure IV-15. Both spectra show a prominent peak at 530 eV with a shoulder that can be deconvoluted to two smaller peaks at 531.6 and 532.8 eV. The peak at 530 eV can be attributed to O²⁻ as expected while the other corresponds to the surface carbonyl impurities and hydroxyl groups^{40,41}. The presence of these groups is not surprising as their existence was observed in the TiO₂ powders as well explained in the previous part of the chapter.

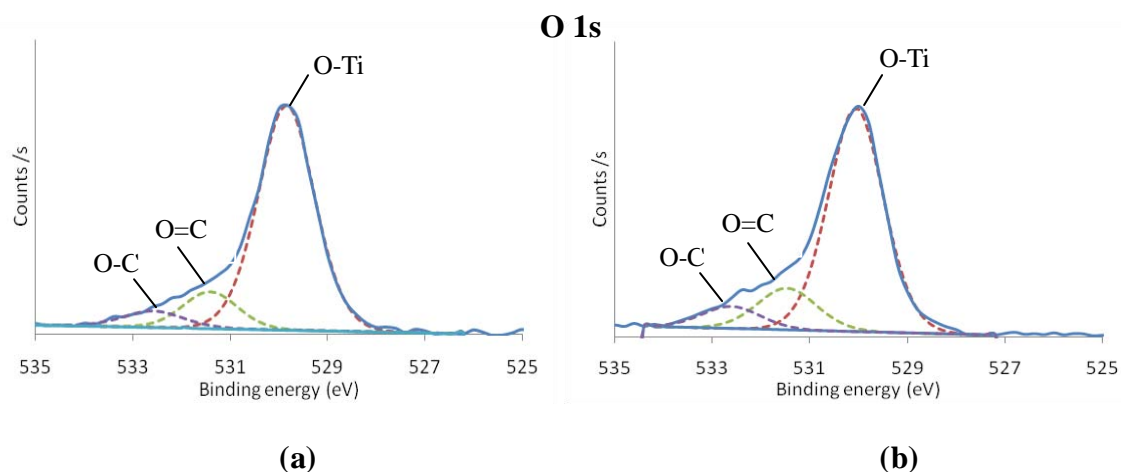


Figure IV-15: O 1s spectra of the calcinated films (a) **F-TiO₂-400°C** and (b) **F-TiO₂-600°C**

The carbon core shell spectra of both calcinated films show a single peak at 285 eV corresponding to carbon impurities mainly as Csp³ coming from pollution with some contribution of Csp² as well that is likely originated from the organic spacer (Figure IV-16). Some smaller peaks at higher binding energy values were detected that were assigned to the surface carbonyl groups observed in the O1s spectra. A decrease in the amount of these carbonyl species was observed in the film prepared at 600°C.

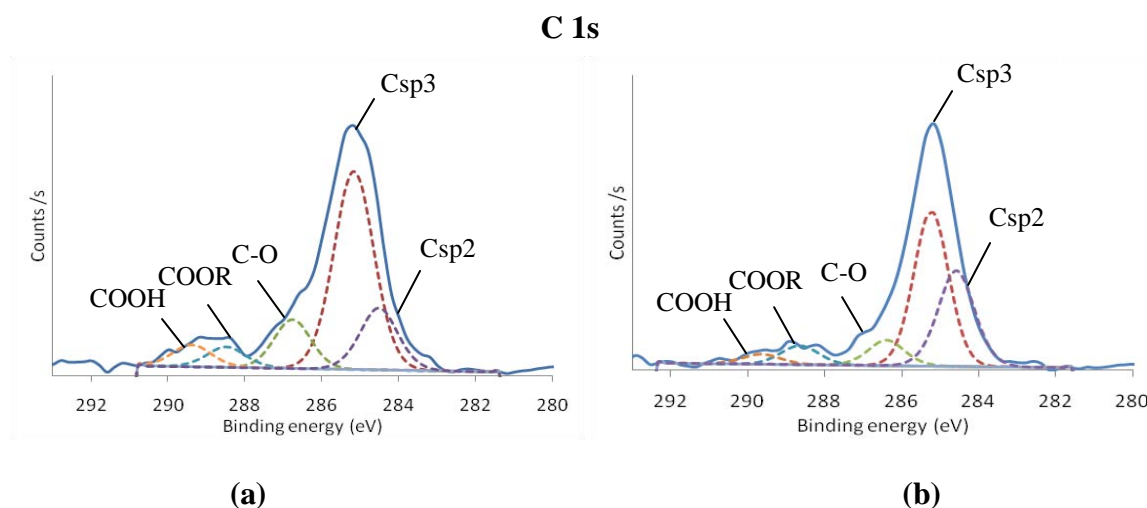


Figure IV-16: C 1s spectra of the calcinated films (a) **F-TiO₂-400°C** and (b) **F-TiO₂-600°C**

These results indicate that both films calcinated at 400°C and 600°C are constituted of mainly TiO₂ along with some surface hydroxyl groups and carbon species.

III.2.2. Optical Properties

The UV-visible spectra of the titanium dioxide films, **F-TiO₂-400°C** and **F-TiO₂-600°C**, were obtained by subtraction of the glass substrates background. Both films were quite transparent and the absorption edge was observed at about 350 nm²⁸ (Figure IV-17). Broad absorption bands observed between 400-600 nm can be associated with carbon impurities on the surface^{11e,41}.

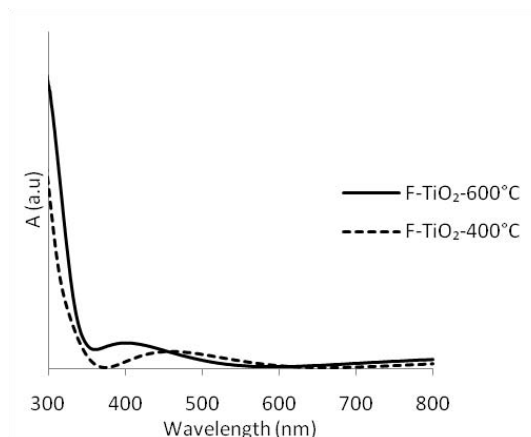


Figure IV-17: UV-visible spectra of **F-TiO₂-400°C** and of **F-TiO₂-600°C**

III.2.3. Raman Spectroscopy

The Raman spectra of the titanium dioxide films were taken in order to determine the crystalline nature of titanium dioxide. No peak was detected in the spectrum of TiO₂ film prepared at 400°C indicating a completely amorphous material (Figure IV-18). After treatment at higher temperature (500°C) the appearance of a small peak at 147 cm⁻¹ revealed the beginning of crystallization. Further increase in the temperature to 600°C led to the emergence of four prominent peaks at 147, 403, 521, and 643 cm⁻¹ indicating a crystalline titanium dioxide film in anatase phase³⁵. Unlike the titanium dioxide powders reported in the previous section, no rutile or brookite phase was detected on the film.

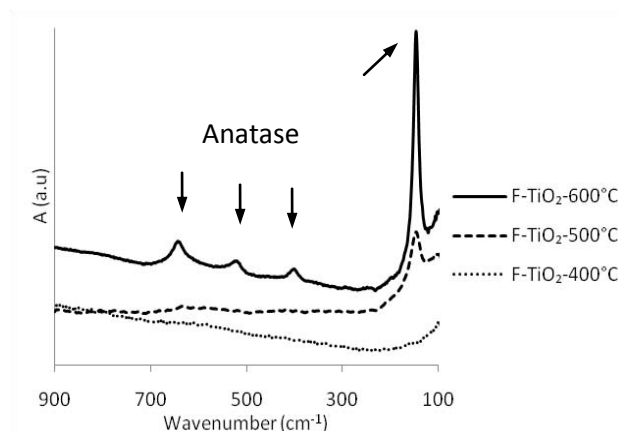


Figure IV-18: Raman spectra of TiO₂ films

In the case of TiO_2 powders described in the earlier part of the chapter, a reasonably crystalline material was obtained after heating at 450°C or 500°C . On films, however, a higher temperature (600°C) was required to induce crystallinity. This difference would come from the more oxidizing atmosphere used for the preparation of powders (oxygen) than for the film (air) that would allow an easier oxidation and decomposition of organics.

The crystallite size for **F-TiO₂-600°C** estimated by the phonon confinement model³⁶ is about 6.7 ± 1 nm.

III.2.4. X-ray diffraction analysis

The x-ray diffraction analysis allowed us to study the organization of the hybrid as well as the calcinated material on films. A very broad peak was obtained at 8.1° in the diffractogram of **XPh2OR-F** which indicates that the material is weakly organized at the nanometric level (Figure IV-19). The nature of organization looks similar to the organization of the material in powder. However, the domain size is 2.1 nm that corresponds to only two associated dimers. The hybrid material is thus better organized as powder than as film.

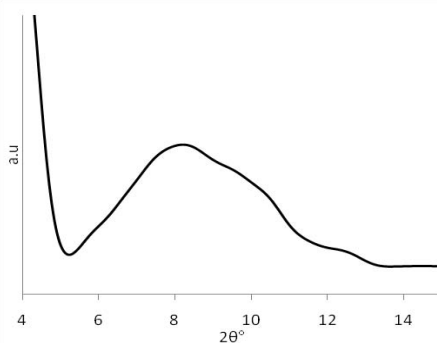


Figure IV-19: X-ray diffractogram of hybrid film (**XPh2OR-F**)

The X-ray diffractogram of the films after thermal treatment at 400°C or 500°C showed only a small peak at 31.7° . The peak could be associated with crystal lattice orientation (121) of brookite^{11c}. No other peak corresponding to anatase or rutile phase was observed. The film prepared at 600°C , however, exhibited the characteristic peaks of anatase phase [(101), (004), (200), (204) etc.] (Figure IV-20). This observation is consistent with the results obtained from Raman spectroscopy discussed before. The average crystallite size for **F-TiO₂-600°C** film calculated by the Scherrer equation is 5.7 nm.

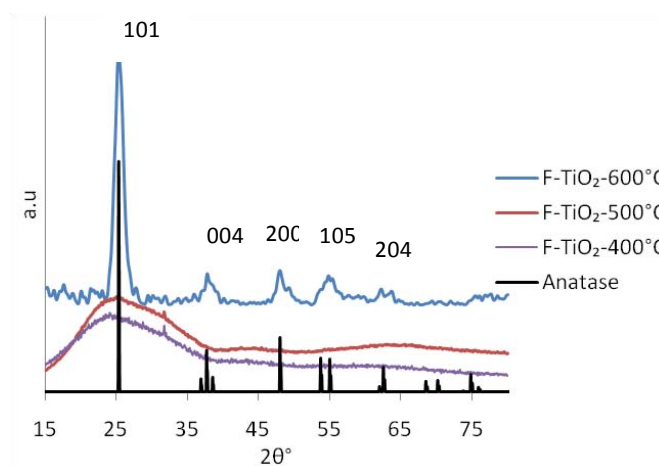


Figure IV-20: X-ray diffractograms of titanium dioxide films prepared at different temperatures along with the expected peaks for anatase

IV. Conclusion

The thermolysis of the prepared titanium-based hybrid materials led to the formation of mesoporous anatase titanium dioxide. Depending on the calcination temperatures, the preparation of materials with surface areas ranging from 65.2 to 158.0 m²/g, average pore size between 5.1 and 7.0 nm, and mean particle size ranging from 5.4 to 6.7 nm was achieved. In each case, a porous network of aggregated nanoparticles was detected, mesoporosity being attributed to the inter-particle space. For the films, a calcination temperature of 600°C was necessary to produce dense anatase titanium dioxide with an average crystallite size of 5.7 nm.

- ¹ (a) Pfaff, G.; Reynders, P. *Chem. Rev.* **1999**, *99*, 1963 (b) Thiele, E. S.; French, R. H. *J. Am. Ceram. Soc.* **1998**, *81*, 469 (c) Feldmann, C. *Adv. Mater.* **2001**, *13*, 1301 (d) Feldmann, C.; Jungk, H. O. *Angew. Chem. Int. Ed.* **2001**, *40*, 359
- ² (a) Salvador, A.; Pascual-Marti, M. C.; Adell, J. R.; Requeni, A.; March, J. G. *J. Pharm. Biomed. Anal.* **2000**, *22*, 301
- ³ Yuan, S. A.; Chen, W. H.; Hu, S. S. *Mater. Sci. Eng. C* **2005**, *25*, 479
- ⁴ (a) Mills, A.; Davies, R. *J. Photochem. Photobiol. A* **1995**, *85*, 173 (b) Vindogopal, K. *Environ. Sci. Technol.* **1995**, *29*, 841
- ⁵ Tanaka, K.; Harada, K.; Murata, S. *Sol. Energy.* **1986**, *36*, 159
- ⁶ (a) Bard, A. J.; Fox, M. A. *Acc. Chem. Res.* **1995**, *28*, 141 (b) Henderson, M. A. *Langmuir* **1996**, *12*, 5093
- ⁷ (a) O'Regan, B.; Grätzel, M. *Nature* **1991**, *353*, 737 (b) Nazeeruddin, M. K.; De Angelis, F.; Fantacci, S.; Selloni, A.; Viscardi, G.; Liska, P.; Ito, S.; Takeru, B.; Grätzel, M. *J. Am. Chem. Soc.* **2005**, *127*, 16835 (c) Grätzel, M. *Acc. Chem. Res.* **2009**, *42*, 1788
- ⁸ Jiang, K. J.; Kitamura, T.; Yin, H.; Ito, S.; Yanagida, S. *Chem. Lett.* **2002**, *31*, 872
- ⁹ Kim, K. J.; Benkstein, K. D.; van de Lagemaat, J.; Frank, A. J. *Chem. Mater.* **2002**, *14*, 1042 (b) Byun, H. Y.; Vittal, R.; Kim, D. Y.; Kim, K. J. *Langmuir* **2004**, *20*, 6853
- ¹⁰ Chen, X.; Mao, S. S. *Chem. Rev.* **2007**, *107*, 2891
- ¹¹ (a) Oskam, G.; Nellore, A.; Penn, R. L.; Searson, P. C. *J. Phys. Chem. B* **2003**, *107*, 1734 (b) Bessekhoud, Y.; Robert, D.; Weber, J. V. *J. Photochem. Photobiol. A* **2003**, *157*, 47 (c) Kuznetsova, I. N.; Blaskov, V.; Stambolova, I.; Znaidi, L.; Kanaev, A. *Mater. Lett.* **2005**, *59*, 3820 (d) Lee, J. H.; Yang, Y. S. *Mater. Chem. Phys.* **2005**, *93*, 237 (e) Reddy, K. M.; Reddy, C. V. G.; Manorama, S. V. *J. Solid State Chem.* **2001**, *158*, 180 (f) Manorama, S. V.; Reddy, K. M.; Reddy, C. V. G.; Narayanan, S.; Raja, P. R.; Chatterji, P. R. *J. Phys. Chem. Solids* **2002**, *63*, 135 (g) Sugimoto, T.; Okada, K.; Itoh, H. *J. Colloid Interface Sci.* **1997**, *193*, 140 (h) Sugimoto, T.; Zhou, X. *J. Colloid Interface Sci.* **2002**, *252*, 347
- ¹² Li, Y.; White, T. J.; Lim, S. H. *J. Solid State Chem.* **2004**, *177*, 1372
- ¹³ Moritz, T.; Reiss, J.; Diesner, K.; Su, D.; Chemseddine, A. *J. Phys. Chem. B* **1997**, *101*, 8052
- ¹⁴ (a) Chemseddine, A.; Moritz, T. *Eur. J. Inorg. Chem.* **1999**, 235 (b) Moritz, T.; Reiss, J.; Diesner, K.; Su, D.; Chemseddine, A. *J. Phys. Chem. B* **1997**, *101*, 8052
- ¹⁵ Lin, J.; Lin, Y.; Liu, P.; Meziani, M. J.; Allard, L. F.; Sun, Y. -P. *J. Am. Chem. Soc.* **2002**, *124*, 11514 (b) Lim, K. T.; Hwang, H. S.; Ryoo, W.; Johnston, K. P. *Langmuir* **2004**, *20*, 2466
- ¹⁶ Zhang, D.; Qi, L.; Ma, J.; Cheng, H. *J. Mater. Chem.* **2002**, *12*, 3677
- ¹⁷ (a) Mutin, P. H.; Vioux, A. *Chem. Mater.* **2009**, *21*, 582 (b) Niederberger, M.; Bartl, M. H.; Stucky, G. D. *Chem. Mater.* **2002**, *14*, 4364 (c) Parala, H.; Devi, A.; Bhakta, R.; Fischer, R. A. *J. Mater. Chem.* **2002**, *12*, 1625 (d) Arnal, P.; Corriu, R. J. P.; Leclercq, D.; Mutin, P. H.; Vioux, A. *Chem. Mater.* **1997**, *9*, 694 (e) Hay, J. N.; Raval, H. M. *J. Sol-Gel Sci. Technol.* **1998**, *13*, 109 (f) Lafond, V.; Mutin, P. H.; Vioux, A. *Chem. Mater.* **2004**, *16*, 5380 (g) Trentler, T. J.; Denler, T. E.; Bertone, J. F.; Agrawal, A.; Colvin, V. L. *J. Am. Chem. Soc.* **1999**, *121*, 1613

- ¹⁸ (a) Andersson, M.; Oesterlund, L.; Ljungstroem, S.; Palmqvist, A. *J. Phys. Chem. B* **2002**, *106*, 10674 (b) Chae, S. Y.; Park, M. K.; Lee, S. K.; Kim, T. Y.; Kim, S. K.; Lee, W. I. *Chem. Mater.* **2003**, *15*, 3326. (c) Yang, J.; Mei, S.; Ferreira, J. M. F. *Mater. Sci. Eng., C* **2001**, *15*, 183 (d) Yang, J.; Mei, S.; Ferreira, J. M. F. *J. Colloid Interface Sci.* **2003**, *260*, 82 (e) Feng, X.; Zhai, J.; Jiang, L. *Angew. Chem., Int. Ed.* **2005**, *44*, 5115
- ¹⁹ (a) Li, X. L.; Peng, Q.; Yi, J. X.; Wang, X.; Li, Y. D. *Chem. Eur. J.* **2006**, *12*, 2383 (b) Wang, X.; Zhuang, J.; Peng, Q.; Li, Y. D. *Nature* **2005**, *437*, 121
- ²⁰ (a) Wu, J. M.; Zhang, T. W.; Zeng, Y. W.; Hayakawa, S.; Tsuru, K.; Osaka, A. *Langmuir* **2005**, *21*, 6995 (b) Wu, J. M.; Hayakawa, S.; Tsuru, K.; Osaka, A. *Scripta Mater.* **2002**, *46*, 101 (c) Wu, J. M.; Hayakawa, S.; Tsuru, K.; Osaka, A. *Scripta Mater.* **2002**, *46*, 705 (d) Wu, J. M.; Zhang, T. W. *J. Photochem. Photobiol., A* **2004**, *162*, 171
- ²¹ (a) Huang, W.; Tang, X.; Wang, Y.; Kolytyn, Y.; Gedanken, A. *Chem. Commun.* **2000**, 1415 (b) Xia, H.; Wang, Q. *Chem. Mater.* **2002**, *14*, 2158 (c) Yu, J. C.; Zhang, L.; Yu, J. *Chem. Mater.* **2002**, *14*, 4647 (d) Yu, J. C.; Zhang, L.; Li, Q.; Kwong, K. W.; Xu, A. W.; Lin, J. *Langmuir* **2003**, *19*, 7673 (e) Zhu, Y.; Li, H.; Kolytyn, Y.; Hacothen, Y. R.; Gedanken, A. *Chem. Commun.* **2001**, 2616
- ²² (a) Gressel-Michel, E.; Chaumont, D.; Stuerge, D. *J. Colloid Interface Sci.* **2005**, *285*, 674 (b) Uchida, S.; Tomiha, M.; Masaki, N.; Miyazawa, A.; Takizawa, H. *Sol. Energy Mater. Sol. Cells* **2004**, *81*, 135 (c) Wu, X.; Jiang, Q. Z.; Ma, Z. F.; Fu, M.; Shangguan, W. F. *Solid State Commun.* **2005**, *136*, 513 (d) Yamamoto, T.; Wada, Y.; Yin, H.; Sakata, T.; Mori, H.; Yanagida, S. *Chem. Lett.* **2002**, 964.
- ²³ Wu, J. M. *J. Cryst. Growth* **2004**, *269*, 347
- ²⁴ Sakatani, Y.; Grosso, D.; Nicole, L.; Boissiere, C.; Soler-Illia, G. J. D. A.; Sanchez, C. *J. Mater. Chem.* **2006**, *16*, 77 (b) Martinez-Ferrero, E.; Sakatani, Y.; Boissiere, C.; Grosso, D.; Fuertes, A.; Fraxedas, J.; Sanchez, C. *Adv. Funct. Mater.* **2007**, *17*, 3348
- ²⁵ Guliants, V. V.; Carreon, M. A.; Lin, Y. S. *J. Membr. Sci.* **2004**, *235*, 53
- ²⁶ Bass, J. D.; Grosso, D.; Boissiere, C.; Belamie, E.; Coradin, T.; Sanchez, C. *Chem. Mater.* **2007**, *19*, 4349
- ²⁷ Bosc, F.; Edwards, D.; Keller, N.; Keller, V.; Ayrat, A. *Thin Solid Films* **2006**, *495*, 272
- ²⁸ Que, W.; Uddin, A.; Hu, X. *J. Power Sources* **2006**, *159*, 353
- ²⁹ Huang, C. -Y.; Hsu, Y. -C.; Chen, J. -G.; Suryanarayanan, V.; Lee, K-M.; Ho, K. -C. *Sol. Energy Mater. Sol. Cells*, **2006**, *90*, 2391
- ³⁰ (a) Wilson, G. J.; Matijasevich, A. S.; Mitchell, D. R. G.; Schulz, J. C.; Will, G. D. *Langmuir* **2006**, *22*, 2016 (b) Hart, J. N.; Cervini, R.; Cheng, Y. -B.; Simon, G. P.; Spiccia, L. *Sol. Energy Mater. Sol. Cells*, **2004**, *84*, 135
- ³¹ Chevalier, P.; Corriu, R. J. P.; Delord, P.; Moreau, J. J. E.; Wong Chi Man, M. *New J. Chem.* 1998, 423
- ³² Toupance, T.; Elhamzaoui, H.; Jousseume, B.; Riague, H.; Saadeddin, I.; Campet, G.; Brötz, J. *Chem. Mater.* **2006**, *18*, 6364
- ³³ (a) Connor, P. A.; Dobson, K. D.; McQuillan, A. J. *Langmuir* **1999**, *15*, 2402 (b) Dobson, K. D.; McQuillan, A. J. *Langmuir* **1997**, *13*, 3392 (c) Yates, D. J. C. *J. Phys. Chem.* **1961**, 746

(d) Tebby, Z.; Babot, O.; Toupance, T.; Park, D. -H.; Campet, G.; Delville, M. -H. *Chem. Mater.* **2008**, *20*, 7260

³⁴ Léaustic, A.; Babonneau, F.; Livage, J. *Chem. Mater.* **1989**, *1*, 248

³⁵ Djaoued, Y.; Badilescu, S.; Ashrit, P. V.; Robichaud, J. *Int. J. Vibr. Spec.* **2001**, *5*, 4 (b)

Lottici, P. P.; Bersani, D.; Braghini, M.; Montenero, A. *J. Mater. Sci.* **1993**, *28*, 177 (c)

Bersani, D.; Antonioli, G.; Lottici, P. P.; Lopez, T. *J. Non-Cryst. Solids* **1998**, *232-234*, 175

³⁶ Balaji, S.; Djaoued, Y.; Robichaud, J. *J. Raman Spec.* **2006**, *37*, 1416

³⁷ (a) Sing, K. S. W.; Everett, D. H.; Haul, R. A. W.; Moscou, L.; Pierotti, R. A.; Rouquerol, J.; Siemieniewska, T. *Pure Appl. Chem.* **1985**, *57*, 603 (b) Brunauer, S.; Deming, L. S.; Deming, W. E.; Teller, E. *J. Am. Chem. Soc.* **1940**, *62*, 1723

³⁸ Jhang, H.; Banfield, J. F. *J. Phys. Chem. B.* **2000**, *104*, 3481

³⁹ (a) Burgos, M.; Langlet, M. *Thin Solid Films* **1999**, *349*, 19 (b) Lynch, C. T.; Mazdiyasi, K. H.; Smith, J. S.; Crawford, W. J. *Anal. Chem.* **1964**, *36*, 2332

⁴⁰ Isley, S. L. ; Penn, R. L. *J. Phys. Chem. C* **2008**, *112*, 4469

⁴¹ Nagaveni, K.; Hegde, M. S.; Ravishankar, N.; Subbanna, G. N.; Madras, G. *Langmuir*, **2004**, *20*, 2900



GENERAL CONCLUSION

This work concerns the preparation of titanium-based organic-inorganic hybrid materials. So far these materials have been developed the most with silicon and recently some examples have been reported with tin as well. A literature review of silicon-based and tin-based materials has been given in the first chapter of the thesis. The synthetic route for their preparation i.e., the sol-gel process, has also been described to understand the nature of the reactions involved during the process. So far the chemistry of hybrid materials has only been very little explored with transition metals due to synthetic problems. Our project proposes a new methodology to prepare transition metal-based class II hybrid materials having a stable metal-carbon bond.

The first step of the project involves the synthesis of suitable precursors for hybrid materials. Various di(cyclopentadienyltitanium) derivatives where the cyclopentadienyl groups are linked by different spacers and where the titanium atoms bear hydrolysable groups were synthesized and are mentioned in detail in the second chapter. The nature of the spacer was varied from linear aromatics to spacers containing long lateral chains in order to study their effect on the organization of the resulting materials. Complexes with spacers including heteroatoms were prepared as well. The hydrolysable groups on titanium were also changed from isopropoxy to methyl and benzyl groups due to the same reason.

The next step of the conversion of these precursors to the hybrid materials in a sol-gel process was carried out successfully. Various self-assembled titanium-based hybrid materials have been prepared in which the inorganic network is connected to the organic network through stable titanium-carbon π -bonds. The retention of this bond was ensured by a combined study of infrared and Raman spectroscopies along with a chemical derivatization of the xerogel. The nature of the spacer between the cyclopentadienyl groups governed the mode of organization of the nanostructures. Linear aromatic spacers led to materials with stair-like structures in which the organic groups are arranged by stacking interactions. The length of the spacer had no effect on the organization mode. The materials containing lateral chains showed a completely different organization based on the grafted chains. Changing the nature of the hydrolysable groups modified the organization of the nanostructures in some cases. Formation of only one Ti-O-Ti bridge per titanium atom was deduced from the microanalysis results. Each titanium atom is thus equipped with two hydroxyl groups. The result is the formation of a loosely bound structure that can facilitate the self-assembly of the organic spacers. The materials showed dense structures with low specific areas. Thermogravimetric analysis showed that the materials are thermally stable until about 300°C after which the decomposition of organic groups starts. Hence a variety of stable titanium-based organic-inorganic hybrid materials organized at nanoscale were prepared by sol-gel route. The resulting materials have a potential to be used as catalysts in various organic chemistry reactions like esterification, epoxidation, alkene polymerization, etc. and in the production of nanocrystalline titanium dioxide.

One application of hybrid materials for the production of nanocrystalline titanium dioxide was investigated. The thermal treatment of a hybrid material under oxygen led to mesoporous nanocrystalline titanium dioxide. The surface area and crystallinity of the resulting TiO₂ powders depend on the calcination temperature. A reasonably crystalline TiO₂ in anatase phase with average crystallite size of 5.4 nm and surface area as high as 158 m²/g was obtained by calcinating the xerogel at 450°C. Increasing the calcination temperature to 500°C increased the crystallite size to 6.7 nm but reduced its surface area (65.2 m²/g). Titanium dioxide thin films were also prepared by the pyrolysis of hybrid thin films at high temperature. In this case, a higher temperature (600°C) was required to achieve the crystallization of titanium dioxide in anatase phase, with crystallite size being 5.7 nm. The UV-visible spectrum of the films showed a high degree of transparency while XPS studies revealed the presence of surface hydroxyl groups.

CHAPTER V. EXPERIMENTAL SECTION

Apparatus and experimental techniques

Solvents and chemicals

All the starting chemicals were purchased from Aldrich, Acros and Alfa-Aesar and were used without further purification unless mentioned otherwise. Most of the solvents were dried and distilled before use by standard procedures: pentane, THF, toluene and diethyl ether were distilled from sodium benzophenone ketyl while acetonitrile and dichloromethane were distilled over CaH_2 .

Nuclear Magnetic Resonance Spectroscopy

^1H , and ^{13}C NMR spectra were recorded on a Bruker AC 200, AC 250 or DPX 300 spectrometer. The choice of the deuterated solvents was done on the basis of solubility and in some cases stability of the products and is described for each product. The chemical shifts are given in ppm with respect to tetramethylsilane (TMS). The abbreviations used to describe peaks are following: s (singlet), d (doublet), t (triplet), (q = quadruplet), (m = multiplet).

Vibrational studies

Infrared spectra were recorded on Perkin-Elmer Spectrum 100 FT-IR and Nicolet 6700 FT-IR Spectrometer. The samples were analyzed in the form of KBr or CsI pellets with about 2% sample by weight. The Raman spectra were taken on Labram 1B. Due to sensitive nature of the samples, they were analyzed in sealed tubes under nitrogen.

X-Ray diffraction analysis

XRD investigations of films were performed by a Seifert PTS 3003 using a Cu anode, an X-ray mirror, a long soller slit and a secondary monochromator. XRD analysis on powders was done using Nanostar Bruker.

Elemental analysis

Elemental analyses were performed by the “Service d’analyse du CNRS” at Vernaison, France.

Nitrogen adsorption-desorption (BET)

Nitrogen sorption analyses (BET) to determine the specific area were carried out by standard volumetric method using Micromeritics ASAP 2010. Before each analysis, the sample was degassed overnight at 100°C . The calculations were done by Micromeritics software applying Harkins and Jura equation for multilayers.

Thermogravimetric analysis

The thermogravimetric analyses were recorded on Netzsch STA 409. All the measurements were done under a continuous air flow.

SEM

The SEM images were captured on microscope SEM Philips XL-30 FEG. The samples were covered with gold particles by sputtering.

AFM

AFM images of the films were taken on Asylum Research MFP-3D™ AFM.

TEM

High resolution TEM images were recorded on FEI TEM CM20. The resolution of the machine was 0.23 nm.

Profilometer

The films were scratched by a spatula and their thickness was measured by profilometer KLA Tencor, Alfa-step IQ.

XPS

The XPS analyses were performed on VG Escalab 220i XL. Fitting of the high resolution spectra were provided through the AVANTAGE software from ThermoFischer Scientific.

Experimental section related to chapter II

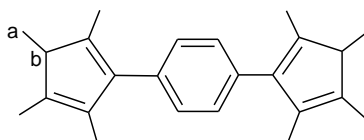
Synthesis of 1,4-bis(2,3,4,5-tetramethylcyclopentadienyl)benzene (1a)¹

In a dry Schlenk under nitrogen, a solution of n-BuLi (20 mL, 50 mmol) was added dropwise to a slurry of p-dibromobiphenyl (8.53 g, 36.2 mmol) in diethyl ether (150 mL). The reaction mixture was stirred for 20 min to form white precipitates and 2,3,4,5-tetramethylcyclopent-2-enone (5.0 g, 36 mmol) was added slowly via syringe. The mixture was refluxed for 1 h and then was allowed to cool down to room temperature. Again a solution of n-BuLi (20 mL, 50 mmol) was added, forming white precipitates. The reaction mixture was stirred for 1 h and 2,3,4,5-tetramethylcyclopent-2-enone (5.0 g, 36 mmol) was added. The precipitates dissolved. After the solution was stirred for 1 h at room temperature and then refluxed for 30 min, it was cooled down to room temperature and quenched with 200 mL of aqueous saturated NH₄Cl. The aqueous phase was extracted twice with diethyl ether (30 mL), and the combined ether fractions were dried over MgSO₄. The solution was concentrated to 30 mL (roughly) via rotary evaporation, and p-toluenesulfonic acid (1.57 g) was added. After 10 min of stirring, precipitates were observed. The stirring was continued for 2 h, after which sufficient ether was added to dissolve all of the precipitate. The ether solution was washed three times with water (200 mL) and then was dried over MgSO₄. The solvent was evaporated under vacuum to give the required product as yellow solid.

Yield = 85%

¹H NMR (300 MHz, CDCl₃, ppm) : 0.98 (d, J = 7.5 Hz, 6H, H^a), 1.87 (s, 6H, CH₃ on Cp), 1.94 (s, 6H, CH₃ on Cp), 2.08 (s, 6H, CH₃ on Cp), 3.20 (q, J = 7.5 Hz, 2H, H^b), 7.24 (s, 4H, H^{aromatic})

¹³C NMR (75.4 MHz, CDCl₃, ppm) : 11.1 (CH₃ on Cp), 11.9 (CH₃ on Cp), 12.9 (CH₃ on Cp), 15.0 (C^a), 49.9 (C^b), 128.0 (C^{aromatic}), 134.0 (C^{quat.}), 135.1 (C^{quat.}), 136.9 (C^{quat.}), 140.5 (C^{quat.}), 142.5 (C^{quat.})



Synthesis of 1,4-phenylenebis(2,3,4,5-tetramethylcyclopentadienyl)di(triisopropoxytitanium) (1b)

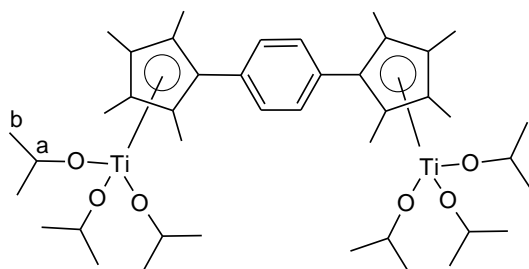
In a dry Schlenk under nitrogen, a solution of n-BuLi (7.19 mL, 17.98 mmol) in pentane was added dropwise to a solution of 1,4-bis(2,3,4,5-tetramethylcyclopentadienyl)benzene (**1a**) (2.86 g, 8.99 mmol) in THF (50 mL) at 0°C. The reaction mixture was stirred at room temperature overnight. A solution of chlorotriisopropoxytitanium (4.68 g, 17.99 mmol) in THF (30 mL) was added to the reaction mixture at 0°C and the resulting mixture was refluxed for 3 days. The solvent was evaporated under vacuum and the residue was extracted with pentane. A yellow solid was obtained after

evaporation of the solvent which was then washed 3 times with pentane to give the required product.

Yield : 67%

^1H NMR (250 MHz, CDCl_3 , ppm) : 1.06 (d, $J = 6.1$ Hz, 36H, H^b), 2.06 (s, 12H, CH_3 on Cp), 2.12 (s, 12H, CH_3 on Cp), 4.48 (m, $J = 6.1$ Hz, 6H, H^a), 7.36 (s, 4H, $\text{H}^{\text{aromatic}}$)

^{13}C NMR (62.9 MHz, CDCl_3 , ppm) : 11.5 (CH_3 on Cp), 12.5 (CH_3 on Cp), 26.5 (C^b), 75.4 (C^a), 121.7 ($\text{C}^{\text{quat.}}$), 122.1 ($\text{C}^{\text{quat.}}$), 124.6 ($\text{C}^{\text{quat.}}$), 130.0 ($\text{C}^{\text{aromatic}}$), 133.4 ($\text{C}^{\text{quat.}}$)



Elemental analysis for $\text{C}_{42}\text{H}_{70}\text{Ti}_2\text{O}_6$

Calculated : %C : 65.79 %H : 9.20

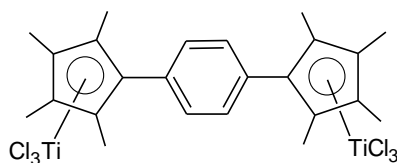
Found : %C : 62.80 %H : 8.96

Synthesis of 1,4-phenylenebis(2,3,4,5-tetramethylcyclopentadienyl)di(trichlorotitanium) (1c)

In a dry Schlenk under nitrogen, chlorotrimethylsilane (5.09 g, 46.99 mmol) was added slowly to a solution of 1,4-phenylenebis(2,3,4,5-tetramethylcyclopentadienyl)di(triisopropoxytitanium) (**1b**) (2 g, 2.61 mmol) in dichloromethane (20 mL) at 0°C . The reaction mixture was stirred at room temperature for 24 h. A slow formation of red precipitates was observed. The precipitates were allowed to settle down and the solvent was decanted off. The red compound was washed several times with a mixture of pentane and dichloromethane (3:1) and dried in vacuum. The required product was obtained as red crystals. Due to the very low solubility of the compound in CDCl_3 and other solvents, it was not possible to obtain a good ^{13}C NMR spectrum.

Yield : 84%

^1H NMR (250 MHz, CDCl_3 , ppm) : 2.45 (s, 12H, CH_3 on Cp), 2.52 (s, 12H, CH_3 on Cp), 7.47 (s, 4H, $\text{H}^{\text{aromatic}}$)



Elemental analysis for $C_{24}H_{28}Ti_2Cl_6$

Calculated : %C : 46.13 %H : 4.52 %Ti : 15.32

Found : %C : 45.59 %H : 4.56 %Ti : 14.77

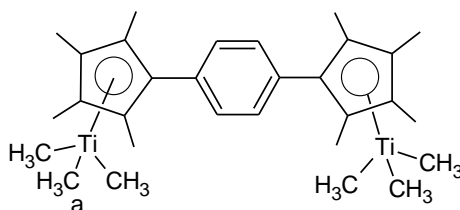
Synthesis of 1,4-phenylenebis(2,3,4,5-tetramethylcyclopentadienyl)di(trimethyltitanium) (1d)

In a dry Schlenk under nitrogen, covered with an aluminium foil, a solution of MeLi (8.16 mL, 13.05 mmol) in diethyl ether was added slowly to a solution of 1,4-phenylenebis(2,3,4,5-tetramethylcyclopentadienyl)di(trichlorotitanium) (**1c**) (1.36 g, 2.17 mmol) in diethyl ether (30 mL) at -78°C . The reaction mixture was stirred at this temperature for 1 h and then at room temperature for 2 h. The solvent was removed under vacuum and the residue was extracted with toluene. The required product was obtained as a yellowish green powder after the evaporation of the solvent.

Yield : 62%

^1H NMR (250 MHz, CDCl_3 , ppm): 0.90 (s, 18H, H^a), 2.01 (s, 12H, CH_3 on Cp), 2.07 (s, 12H, CH_3 on Cp), 7.11 (s, 4H, $\text{H}^{\text{aromatic}}$)

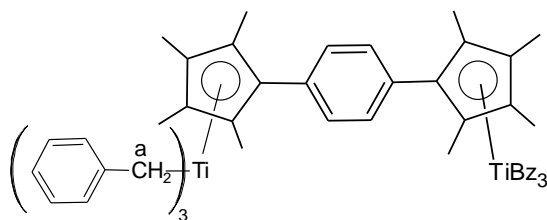
^{13}C NMR (62.5 MHz, CDCl_3 , ppm): 12.4 (CH_3 on Cp), 13.3 (CH_3 on Cp), 63.4 (C^a), 120.3 ($\text{C}^{\text{quat.}}$), 124.1 ($\text{C}^{\text{quat.}}$), 129.7 ($\text{C}^{\text{aromatic}}$), 130.1 ($\text{C}^{\text{quat.}}$), 134.1 ($\text{C}^{\text{quat.}}$)

**Synthesis of 1,4-phenylenebis(2,3,4,5-tetramethylcyclopentadienyl)di(tribenzyltitanium) (1e)**

In a dry Schlenk under nitrogen, covered with an aluminium foil, a solution of benzylmagnesium chloride (9.6 mL, 9.6 mmol) in diethyl ether was added slowly to a solution of 1,4-phenylenebis(2,3,4,5-tetramethylcyclopentadienyl)di(trichlorotitanium) (**1c**) (1 g, 1.6 mmol) in diethyl ether (20 mL) at -78°C . The reaction mixture was stirred at this temperature for 1 h and then at room temperature for 3 h. The solvent was removed under vacuum and the residue was extracted with toluene. The required product was obtained as a red powder after the evaporation of the solvent. The NMR spectrum of the sample showed the presence of some degradation products along with the required hexabenzyltitanium compound. The compound could not be purified by washing and was used as such for the preparation of the material in the next step.

Yield = 91%

^1H NMR (300 MHz, CDCl_3 , ppm): 1.65 (s, 12H, CH_3 on Cp), 1.83 (s, 12H, CH_3 on Cp), 2.97 (s, 12H, H^a), 6.76-7.22 (m, 34H, $\text{H}^{\text{aromatic}}$)



Synthesis of 4,4'-bis(2,3,4,5-tetramethylcyclopentadienyl)biphenyl (2a)²

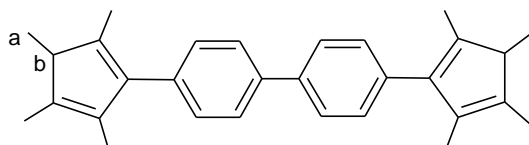
In a dry Schlenk under nitrogen, a solution of *n*-BuLi (24 mL, 60 mmol) was added dropwise to a slurry of 4,4'-dibromobiphenyl (9.36 g, 30 mmol) in diethyl ether (40 mL) at -30°C . The reaction mixture was stirred for 30 min at 0°C and then 2 h at room temperature. The colorless solution on top of the white precipitates was decanted off and THF (30 mL) was added to the dilithiated compound. The reaction mixture was cooled again to -78°C and a solution of 2,3,4,5-tetramethylcyclopent-2-enone (8.29 g, 60 mmol) in THF (20 mL) was added slowly via cannula. It was stirred overnight at room temperature and the reaction was stopped by the addition of a saturated solution of NH_4Cl . The organic phase was separated and washed with water till neutral. After drying with MgSO_4 (anhydrous) and evaporation of the solvent, a colorless liquid was obtained which was redissolved in dichloromethane (20 mL). A small amount of *p*-toluenesulfonic acid (approx. 0.1 g) was added at room temperature and the reaction mixture was stirred for 30 minutes. The solvent was evaporated until wet and petroleum ether (30 mL) was added to precipitate out the product. After filtration and washing of the precipitates with diethyl ether and petroleum ether, the required product was obtained as a yellow powder.

Yield : 58 %

^1H NMR (250 MHz, CDCl_3 , ppm) : 1.02 (d, 6H, $J = 7.5$ Hz, H^a), 1.91 (s, 6H, CH_3 on Cp), 1.98 (s, 6H, CH_3 on Cp), 2.11 (s, 6H, CH_3 on Cp), 3.26 (q, 2H, $J = 7.5$ Hz, H^b), 7.34 (d, $J = 8.2$ Hz, 4H, $\text{H}^{\text{aromatic}}$), 7.64 (d, $J = 8.2$ Hz, 4H, $\text{H}^{\text{aromatic}}$)

^{13}C NMR (62.9 MHz, CDCl_3 , ppm) : 11.3 (CH_3 on Cp), 12.2 (CH_3 on Cp), 13.1 (CH_3 on Cp), 15.1 (C^a), 50.1 (C^b), 126.7 ($\text{C}^{\text{aromatic}}$), 128.9 ($\text{C}^{\text{aromatic}}$), 135.3–142.5 (C^{quat})

MS : *m/e* 394



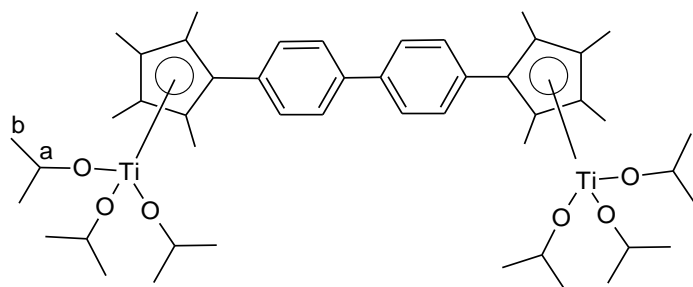
Synthesis of 4,4'-biphenylenebis(2,3,4,5-tetramethylcyclopentadienyl)di(triisopropoxytitanium) (2b)²

In a dry Schlenk under nitrogen, a solution of n-BuLi (4.0 mL, 10.0 mmol) in pentane was added dropwise to a solution of 4,4'-bis(2,3,4,5-tetramethylcyclopentadienyl)biphenyl (**2a**) (1.97 g, 5.0 mmol) in THF (60 mL) at 0°C. The reaction mixture was stirred overnight at room temperature. A solution of chlorotriisopropoxytitanium (2.61 g, 10.0 mmol) in THF (30 mL) was added to the reaction mixture at 0°C and the resulting mixture was refluxed for 3 days. The solvent was evaporated under vacuum and the residue was extracted with pentane. A yellow solid was obtained after evaporation of the solvent that was then washed 3 times with pentane to give the required product.

Yield : 73%

¹H NMR (250 MHz, CDCl₃, ppm) : 1.12 (d, J = 6.0 Hz, 36H, H^b), 2.10 (s, 12H, CH₃ on Cp), 2.16 (s, 12H, CH₃ on Cp), 4.55 (m, J = 6.0 Hz, 6H, H^a), 7.50 (d, J = 8.3 Hz, 4H, H^{aromatic}), 7.70 (d, J = 8.3 Hz, 4H, H^{aromatic})

¹³C NMR (62.9 MHz, CDCl₃, ppm) : 11.5 (CH₃ on Cp), 12.5 (CH₃ on Cp), 26.5 (C^b), 75.5 (C^a), 121.9 (C^{aromatic}), 122.0 (C^{aromatic}), 126.0 (C^{quat.}), 126.4 (C^{quat.}), 131.2 (C^{quat.}), 134.9 (C^{quat.}), 138.4 (C^{quat.})

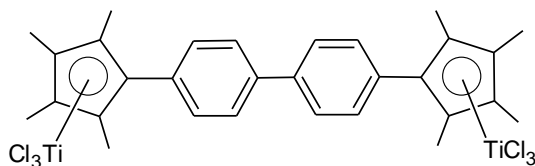


Synthesis of 4,4'-biphenylenebis(2,3,4,5-tetramethylcyclopentadienyl)di(trichlorotitanium) (2c)²

In a dry Schlenk under nitrogen, chlorotrimethylsilane (4.64 g, 42.75 mmol) was added slowly to a solution of 4,4'-biphenylenebis(2,3,4,5-tetramethylcyclopentadienyl)di(triisopropoxytitanium) (**2b**) (2 g, 2.37 mmol) in dichloromethane (20 mL) at 0°C. The reaction mixture was stirred at room temperature for 24 h. A slow formation of red precipitates was observed. The precipitates were allowed to settle down and the solvent was decanted off. The red compound was washed several times with a mixture of pentane and dichloromethane (3:1) and dried in vacuum. The required compound was obtained as red crystals. Due to very low solubility of the compound in CDCl₃ and other solvents, it was not possible to obtain a good ¹³C NMR spectrum.

Yield : 65%

^1H NMR (250 MHz, CDCl_3 , ppm): 2.46 (s, 12H, CH_3 on Cp), 2.53 (s, 12H, CH_3 on Cp), 7.46 (d, $J = 8.2$ Hz, 4H, $\text{H}^{\text{aromatic}}$), 7.70 (d, $J = 8.2$ Hz, 4H, $\text{H}^{\text{aromatic}}$)



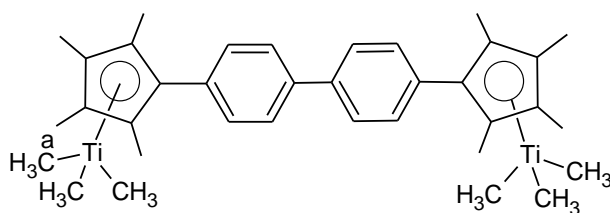
Synthesis of 4,4'-biphenylenebis(2,3,4,5-tetramethylcyclopentadienyl)di(trimethyltitanium) (2d)

In a dry Schlenk under nitrogen, covered with an aluminium foil, a solution of MeLi (10.69 mL, 17.12 mmol) in diethyl ether was added slowly to a solution of 4,4'-biphenylenebis(2,3,4,5-tetramethylcyclopentadienyl)di(trichlorotitanium) (**2c**) (2 g, 2.85 mmol) in diethyl ether (30 mL) at -78°C . The reaction mixture was stirred at this temperature for 1 h and then at room temperature for 3 h. The solvent was removed under vacuum and the residue was extracted with toluene. The required product was obtained as a yellowish green powder after the evaporation of the solvent.

Yield : 71%

^1H NMR (300 MHz, CDCl_3 , ppm): 0.89 (s, 18H, H^{a}), 1.99 (s, 12H, CH_3 on Cp), 2.06 (s, 12H, CH_3 on Cp), 7.16 (d, $J = 8.1$ Hz, 4H, $\text{H}^{\text{aromatic}}$), 7.55 (d, $J = 8.1$ Hz, 4H, $\text{H}^{\text{aromatic}}$)

^{13}C NMR (62.5 MHz, CDCl_3 , ppm): 12.4 (CH_3 on Cp), 13.2 (CH_3 on Cp), 63.4 (C^{a}), 120.3 ($\text{C}^{\text{quat.}}$), 124.1 ($\text{C}^{\text{quat.}}$), 126.5 ($\text{C}^{\text{aromatic}}$), 129.8 ($\text{C}^{\text{quat.}}$), 130.7 ($\text{C}^{\text{aromatic}}$), 134.9 ($\text{C}^{\text{quat.}}$), 138.8 ($\text{C}^{\text{quat.}}$)



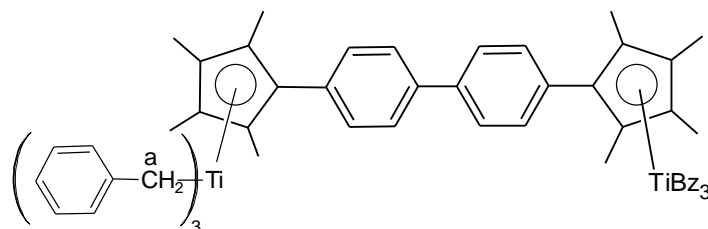
Synthesis of 4,4'-biphenylenebis(2,3,4,5-tetramethylcyclopentadienyl)di(tribenzyltitanium) (2e)

In a dry Schlenk under nitrogen, covered with an aluminium foil, a solution of benzylmagnesium chloride (8.56 mL, 8.56 mmol) in diethyl ether was added slowly to a solution of 4,4'-biphenylenebis(2,3,4,5-tetramethylcyclopentadienyl)di(trichlorotitanium) (**2c**) (1 g, 1.43 mmol) in diethyl ether (20 mL) at -78°C . The reaction mixture was stirred at this temperature for 1 h and then at room temperature for 3 h. The solvent was removed under vacuum and the residue was extracted with toluene. The required product was obtained as a red powder after the evaporation of the solvent.

Yield : 95%

^1H NMR (250 MHz, CDCl_3 , ppm): 1.96 (s, 12H, CH_3 on Cp), 2.03 (s, 12H, CH_3 on Cp), 2.81 (s, 12H, H^a), 6.62 – 7.70 (m, 38H, $\text{H}^{\text{aromatic}}$).

^{13}C NMR (62.5 MHz, CDCl_3 , ppm): 12.4 (CH_3 on Cp), 13.3 (CH_3 on Cp), 96.7 (C^a), 122.5 ($\text{C}^{\text{quat.}}$), 122.7 ($\text{C}^{\text{aromatic}}$), 125.7 ($\text{C}^{\text{quat.}}$), 126.8 ($\text{C}^{\text{aromatic}}$), 128.4 ($\text{C}^{\text{aromatic}}$), 128.6 ($\text{C}^{\text{quat.}}$), 130.9 ($\text{C}^{\text{aromatic}}$), 134.2 ($\text{C}^{\text{quat.}}$), 139.3 ($\text{C}^{\text{quat.}}$), 139.8 ($\text{C}^{\text{quat.}}$), 150.1 ($\text{C}^{\text{aromatic}}$)

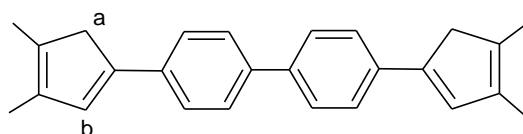


Synthesis of 4,4'-bis(3,4-dimethylcyclopentadienyl)biphenyl (3a)

In a dry Schlenk under nitrogen, a solution of n-BuLi (25.6 mL, 64.1 mmol) was added dropwise to a slurry of 4,4'-dibromobiphenyl (10 g, 32.0 mmol) in diethyl ether (40 mL) at -30°C . The reaction mixture was stirred for 30 min at 0°C and then 2 h at room temperature. The colorless solution on top of the white precipitates was decanted off and THF (30 mL) was added to the dilithiated compound. The reaction mixture was cooled again to -78°C and a solution of 3,4-dimethylcyclopent-2-enone (7.05 g, 64.1 mmol) in THF (20 mL) was added slowly via cannula. It was stirred at room temperature for overnight and the reaction was stopped by the addition of a saturated solution of NH_4Cl . The organic phase was separated and washed with water till neutral. After drying with MgSO_4 (anhydrous) and evaporation of the solvent, a colorless liquid was obtained which was redissolved in dichloromethane (20 mL). A small amount of p-toluenesulfonic acid (aprox. 0.1 g) was added at room temperature resulting in the formation of precipitates. The reaction mixture was stirred for 30 minutes followed by the removal of solvent till wet. A small amount of pentane (about 30 mL) was added to precipitate out the product. After filtration and washing of the precipitates with diethyl ether and petroleum ether, the required product was obtained as a yellow powder. Due to the very low solubility of the compound in most of the solvents, the ^1H NMR spectrum was taken at 120°C in $\text{C}_2\text{D}_2\text{Cl}_4$. It was not possible to get a good ^{13}C NMR spectrum due to the same reason.

Yield : 57%

^1H NMR (400 MHz, $\text{C}_2\text{D}_2\text{Cl}_4$, ppm): 2.02 (s, 6H, CH_3 on Cp), 2.09 (s, 6H, CH_3 on Cp), 3.39 (s, 4H, H^a), 6.7 (s, 2H, H^b), 7.57 (m, 8H, $\text{H}^{\text{aromatic}}$)

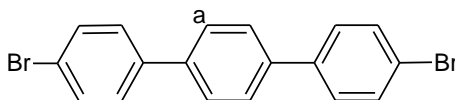


High resolution mass spectrumCalculated for $C_{26}H_{26}Na = 361.192$

Found = 361.192

Synthesis of 4,4''-dibromoterphenyl³

In a round bottom flask equipped with a magnetic stirrer, separatory funnel, and a reflux condenser, a solution of p-terphenyl (15 g, 65.1 mmol) in bromobenzene (100 mL) was heated to 130°C. Few crystals of iodine were added as a catalyst followed by the dropwise addition of bromine (7.0 mL, 128.1 mmol). When the reaction mixture became clear (after about 1.5 h) some more iodine crystals and bromine (4.5 mL, 82.8 mmol) were added. The reaction mixture was stirred at 130°C for 2 days. The excess of iodine and bromine was removed by vacuum and the solid was filtered. The light brown solid was washed with a sodium thiosulfate solution followed by its recrystallization in bromobenzene. The required product was obtained as white crystals.

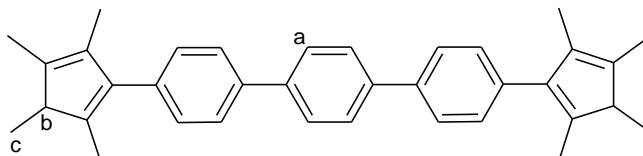
Yield : 67%**¹H NMR (300 MHz, CDCl₃, ppm)** : 7.48 (d, 4H, J = 8.5 Hz, H^{aromatic}), 7.57 (d, 4H, J = 8.5 Hz, H^{aromatic}), 7.63 (s, 4H, H^a)**Synthesis of 4,4''-bis(2,3,4,5-tetramethylcyclopentadienyl)terphenyl (4a)**

In a dry Schlenk under nitrogen, a solution of t-BuLi (22 mL, 37.12 mmol) was added dropwise to a slurry of 4,4''-dibromoterphenyl (3.6 g, 9.28 mmol) in diethyl ether (75 mL) at -78°C. The reaction mixture was stirred for 4 h at this temperature and then 1 h at room temperature. It was again cooled to -78°C and a solution of 2,3,4,5-tetramethyl-cyclopent-2-enone (2.56 g, 18.56 mmol) in THF (60 mL) was added dropwise. The reaction mixture was stirred for two days at room temperature. A saturated solution of NH₄Cl was added to stop the reaction and both layers were separated. The aqueous phase was further extracted with diethyl ether and the combined organic phase was dried over MgSO₄. The solvent was evaporated and the white oil was redissolved in dichloromethane (30 mL). A catalytic amount of p-toluenesulfonic acid was added to the reaction mixture changing the color of the solution to yellow. After stirring at room temperature for 30 min, the solvent was removed till wet and a small amount of petroleum ether was added to precipitate out the product. After filtration and washing of the precipitates with diethyl ether and petroleum ether, the required product was obtained as a yellow powder.

Yield : 45%

^1H NMR (300 MHz, CDCl_3 , ppm) : 1.00 (d, $J = 7.5$ Hz, 6H, H^c), 1.89 (s, 6H, CH_3 on Cp), 1.96 (s, 6H, CH_3 on Cp), 2.10 (s, 6H, CH_3 on Cp), 3.25 (q, $J = 7.5$ Hz, 2H, H^b), 7.33 (d, $J = 8.1$ Hz, 4H, $\text{H}^{\text{aromatic}}$), 7.65 (d, $J = 8.1$ Hz, 4H, $\text{H}^{\text{aromatic}}$), 7.71 (s, 4H, H^a)

^{13}C NMR (75.4 MHz, CDCl_3 , ppm) : 11.4 (CH_3 on Cp), 12.2 (CH_3 on Cp), 13.1 (CH_3 on Cp), 15.1 (C^c), 50.2 (C^b), 126.8 ($\text{C}^{\text{aromatic}}$), 127.4 ($\text{C}^{\text{aromatic}}$), 128.9 ($\text{C}^{\text{aromatic}}$), 135.4 ($\text{C}^{\text{quat.}}$), 136.3 ($\text{C}^{\text{quat.}}$), 137.7 ($\text{C}^{\text{quat.}}$), 137.9 ($\text{C}^{\text{quat.}}$), 139.8 ($\text{C}^{\text{quat.}}$), 141.3 ($\text{C}^{\text{quat.}}$), 142.5 ($\text{C}^{\text{quat.}}$)



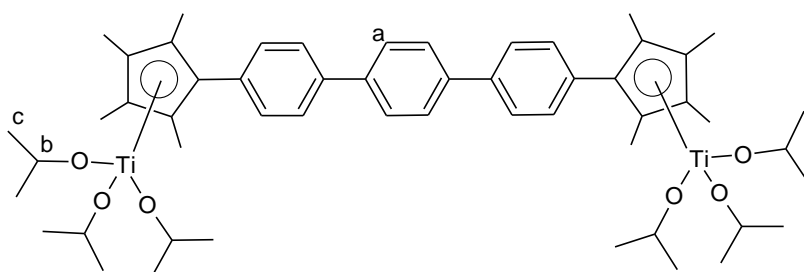
Synthesis of 4,4''-terphenylbis(2,3,4,5-tetramethylcyclopentadienyl)di(triisopropoxytitanium) (4b)

In a dry Schlenk under nitrogen, a solution of $n\text{-BuLi}$ (4.0 ml, 10.0 mmol) in pentane was added dropwise to a solution of 4,4''-bis(2,3,4,5-tetramethylcyclopentadienyl)terphenyl (**4a**) (1.97 g, 5.0 mmol) in THF (60 mL) at 0°C . The reaction mixture was stirred overnight at room temperature. A solution of chlorotriisopropoxytitanium (2.61 g, 10.0 mmol) in THF (30 mL) was added to the reaction mixture at 0°C and the resulting mixture was refluxed for 3 days. The solvent was evaporated under vacuum and the residue was extracted with pentane. A yellow solid was obtained after evaporation of the solvent which was then washed 3 times with pentane to give the required product.

Yield : 42%

^1H NMR (300 MHz, CDCl_3 , ppm) : 1.00 (d, $J = 6.0$ Hz, 36H, H^c), 1.99 (s, 12H, CH_3 on Cp), 2.06 (s, 12H, CH_3 on Cp), 4.44 (m, $J = 6.0$ Hz, 6H, H^b), 7.40 (d, $J = 8.3$ Hz, 4H, $\text{H}^{\text{aromatic}}$), 7.58 (d, $J = 8.3$ Hz, 4H, $\text{H}^{\text{aromatic}}$), 7.67 (s, 4H, H^a)

^{13}C NMR (75.4 MHz, CDCl_3 , ppm) : 11.5 (CH_3 on Cp), 12.5 (CH_3 on Cp), 26.5 (C^c), 75.6 (C^b), 121.8 ($\text{C}^{\text{quat.}}$), 122.0 ($\text{C}^{\text{quat.}}$), 124.0 ($\text{C}^{\text{quat.}}$), 126.1 ($\text{C}^{\text{aromatic}}$), 127.4 ($\text{C}^{\text{aromatic}}$), 131.3 ($\text{C}^{\text{aromatic}}$), 135.3 ($\text{C}^{\text{quat.}}$), 138.1 ($\text{C}^{\text{quat.}}$), 139.9 ($\text{C}^{\text{quat.}}$)



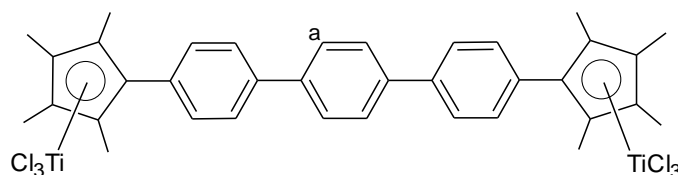
Synthesis of 4,4''-terphenylenebis(2,3,4,5-tetramethylcyclopentadienyl)di(trichlorotitanium) (4c)

In a dry Schlenk under nitrogen, chlorotrimethylsilane (4.25 g, 39.21 mmol) was added slowly to a solution of 4,4''-terphenylenebis(2,3,4,5-tetramethylcyclopentadienyl)di(triisopropoxytitanium) (**4b**) (2 g, 2.18 mmol) in dichloromethane (20 mL) at 0°C. The reaction mixture was stirred at room temperature for 24 h. A slow formation of red precipitates was observed. The precipitates were allowed to settle down and the solvent was decanted off. The red compound was washed several times with a mixture of pentane and dichloromethane (3:1) and dried in vacuum. The required compound was obtained as red crystals.

Yield : 87%

¹H NMR (250 MHz, CDCl₃, ppm): 2.46 (s, 12H, CH₃ on Cp), 2.54 (s, 12H, CH₃ on Cp), 7.47 (d, J = 8.3 Hz, 4H, H^{aromatic}), 7.73 (d, J = 8.3 Hz, 4H, H^{aromatic}), 7.75 (s, 4H, H^a)

¹³C NMR (62.9 MHz, CDCl₃, ppm): 14.9 (CH₃ on Cp), 15.8 (CH₃ on Cp), 127.1 (C^{aromatic}), 127.8 (C^{aromatic}), 131.1 (C^{aromatic}), 132.4 (C^{quat.}), 136.4 (C^{quat.}), 139.0 (C^{quat.}), 139.7 (C^{aromatic}), 140.9 (C^{quat.})



Elemental analysis for C₃₆H₃₆Ti₂Cl₆

Calculated : %C : 55.64 %H : 4.67 %Ti : 12.32

Found : %C : 55.32 %H : 4.92 %Ti : 11.41

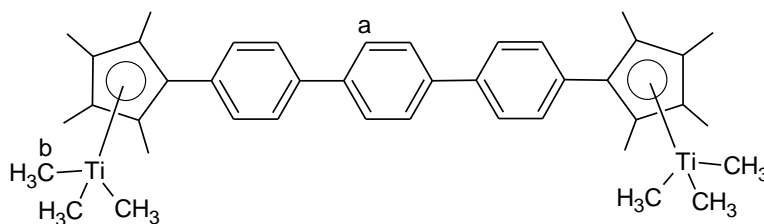
Synthesis of 4,4''-terphenylenebis(2,3,4,5-tetramethylcyclopentadienyl)di(trimethyltitanium) (4d)

In a dry Schlenk under nitrogen, covered with an aluminium foil, a solution of MeLi (4.83 mL, 7.72 mmol) in diethyl ether was added slowly to a solution of 4,4''-terphenylenebis(2,3,4,5-tetramethylcyclopentadienyl)di(trichlorotitanium) (**4c**) (1 g, 1.29 mmol) in diethyl ether (30 mL) at -78°C. The reaction mixture was stirred at this temperature for 1 h and then at room temperature for 3 h. The solvent was removed under vacuum and the residue was extracted with toluene. The required product was obtained as a yellowish green powder after evaporation of the solvent.

Yield = 50%

¹H NMR (250 MHz, CDCl₃, ppm): 0.94 (s, 18H, H^b), 2.03 (s, 12H, CH₃ on Cp), 2.11 (s, 12H, CH₃ on Cp), 7.22 (d, J = 8.3 Hz, 4H, H^{aromatic}), 7.63 (d, J = 8.3 Hz, 4H, H^{aromatic}), 7.71 (s, 4H, H^a)

^{13}C NMR (62.9 MHz, CDCl_3 , ppm): 12.4 (CH_3 on Cp), 13.2 (CH_3 on Cp), 63.5 (C^{b}), 120.4 ($\text{C}^{\text{quat.}}$), 124.2 ($\text{C}^{\text{quat.}}$), 126.6 ($\text{C}^{\text{aromatic}}$), 127.5 ($\text{C}^{\text{aromatic}}$), 129.8 ($\text{C}^{\text{quat.}}$), 130.8 ($\text{C}^{\text{aromatic}}$), 135.0 ($\text{C}^{\text{quat.}}$), 138.9 ($\text{C}^{\text{quat.}}$), 139.7 ($\text{C}^{\text{quat.}}$)



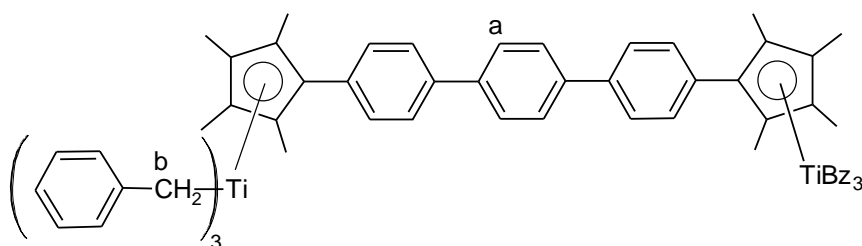
Synthesis of 4,4''-terphenylenebis(2,3,4,5-tetramethylcyclopentadienyl)di(tribenzyltitanium) (4e)

In a dry Schlenk under nitrogen, covered with an aluminium foil, a solution of benzylmagnesium chloride (7.72 mL, 7.72 mmol) in diethyl ether was added slowly to a solution of 4,4''-terphenylenebis(2,3,4,5-tetramethylcyclopentadienyl)di(trichlorotitanium) (**4c**) (1 g, 1.28 mmol) in diethyl ether (20 mL) at -78°C . The reaction mixture was stirred at this temperature for 1 h and then at room temperature for 3 h. The solvent was removed under vacuum and the residue was extracted with toluene. The required product was obtained as a red powder after the evaporation of the solvent.

Yield : 92%

^1H NMR (250 MHz, CDCl_3 , ppm): 1.96 (s, 12H, CH_3 on Cp), 2.03 (s, 12H, CH_3 on Cp), 2.81 (s, 12H, H^{b}), 6.62 – 7.72 (m, 38H, $\text{H}^{\text{aromatic}}$), 7.78 (s, 4H, H^{a}).

^{13}C NMR (62.9 MHz, CDCl_3 , ppm): 12.4 (CH_3 on Cp), 13.4 (CH_3 on Cp), 96.7 (C^{b}), 122.5 ($\text{C}^{\text{quat.}}$), 122.7 ($\text{C}^{\text{aromatic}}$), 125.7 ($\text{C}^{\text{quat.}}$), 126.8 ($\text{C}^{\text{aromatic}}$), 127.6 ($\text{C}^{\text{aromatic}}$), 128.5 ($\text{C}^{\text{aromatic}}$), 130.9 ($\text{C}^{\text{aromatic}}$), 134.2 ($\text{C}^{\text{quat.}}$), 139.3 ($\text{C}^{\text{quat.}}$), 139.8 ($\text{C}^{\text{quat.}}$), 150.1 ($\text{C}^{\text{aromatic}}$)



Synthesis of 4,4''-bis(3,4-dimethylcyclopentadienyl)terphenyl (5a)

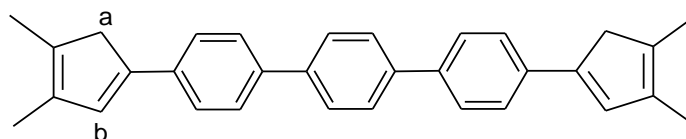
In a dry Schlenk under nitrogen, a solution of *t*-BuLi (64.43 mL, 103.09 mmol) was added dropwise to a slurry of 4,4''-dibromoterphenyl (10 g, 25.77 mmol) in diethyl ether (200 mL) at -78°C . The reaction mixture was stirred for 4 h at this temperature and then 1 h at room temperature. It was again cooled to -78°C and a solution of 3,4-dimethylcyclopent-2-enone (5.67 g, 51.54 mmol) in THF (30 mL) was added dropwise. The reaction mixture was stirred for two days at room temperature. A saturated solution of NH_4Cl was added to stop the reaction and both layers were separated. The aqueous phase was further extracted with diethyl

ether and the combined organic phase was dried over MgSO_4 . The solvent was evaporated and the yellow solid was redissolved in dichloromethane (30 mL). A catalytic amount of p-toluenesulfonic acid was added to the reaction mixture. After stirring at room temperature for 30 min, the solvent was removed till wet and a small amount of petroleum ether was added to precipitate out the product. After filtration and washing of the precipitates with diethyl ether and petroleum ether, the required product was obtained as a yellow powder.

Due to the very low solubility of the compound in practically all the solvents it was not possible to take its ^{13}C NMR. The product was characterized by ^1H NMR in $\text{C}_2\text{D}_2\text{Cl}_4$ at 120°C and high resolution mass spectrum.

Yield : 43%

^1H NMR (400 MHz, $\text{C}_2\text{D}_2\text{Cl}_4$, ppm) : 2.02 (s, 6H, CH_3 on Cp), 2.1 (s, 6H, CH_3 on Cp), 3.41 (s, 4H, H^a), 6.7 (s, 2H, H^b), 7.42-7.74 (m, 12H, $\text{H}^{\text{aromatic}}$)



High resolution mass spectrum

Calculated = 414.234

Found = 414.234

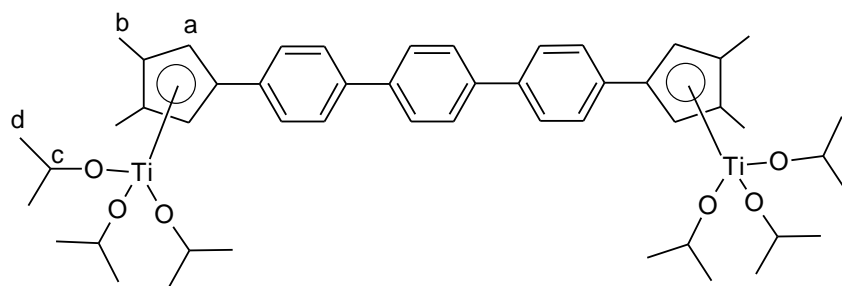
Synthesis of 4,4''-terphenylenebis(3,4-dimethylcyclopentadienyl)di(triisopropoxytitanium) (5b)

In a dry Schlenk under nitrogen, a solution of n-BuLi (9.66 mL, 24.15 mmol) in pentane was added dropwise to a solution of 4,4''-bis(3,4-dimethylcyclopentadienyl)-terphenyl (5 g, 12.07 mmol) in THF (100 mL) at 0°C . The reaction mixture was stirred overnight at room temperature. A solution of chlorotriisopropoxytitanium (6.29 g, 24.15 mmol) in THF (30 mL) was added to the reaction mixture at 0°C and the resulting mixture was refluxed for 3 days. The solvent was evaporated under vacuum and the residue was extracted with dichloromethane. A yellow solid was obtained after evaporation of the solvent which was then washed several times with pentane to give the required product.

Yield : 42%

^1H NMR (250 MHz, CDCl_3 , ppm) : 1.02 (d, $J = 6.1$ Hz, 36H, H^d), 2.14 (s, 12H, H^b), 4.46 (m, $J = 6.1$ Hz, 6H, H^c), 6.39 (s, 4H, H^a), 7.61 (s, 8H, $\text{H}^{\text{aromatic}}$), 7.70 (s, 4H, $\text{H}^{\text{aromatic}}$)

^{13}C NMR (62.9 MHz, CDCl_3 , ppm) : 13.38 (C^b), 26.19 (C^d), 76.98 (C^c), 109.66 (C^a), 126.0 ($\text{C}^{\text{aromatic}}$), 126.9 ($\text{C}^{\text{aromatic}}$), 127.3 ($\text{C}^{\text{aromatic}}$), 134.6 ($\text{C}^{\text{quat.}}$), 138.3 ($\text{C}^{\text{quat.}}$), 139.8 ($\text{C}^{\text{quat.}}$)



Elemental analysis for $C_{50}H_{70}Ti_2O_6$

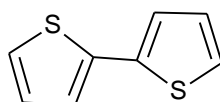
Calculated :	%C : 69.60	%H : 8.12	%Ti : 11.13
Found :	%C : 67.33	%H : 7.47	%Ti : 11.22

Synthesis of 2,2'-bithiophene

In a three necked round bottom flask under nitrogen, equipped with a reflux condenser and a dropping funnel, a solution of 2-bromothiophene (15.86 g, 97.3 mmol) in diethyl ether (50 mL) was added dropwise to preactivated magnesium (2.96 g) in 20 mL of diethyl ether. The reaction mixture was refluxed for 1 h and then was allowed to cool down to room temperature. The black supernatant was transferred via cannula to another three necked round bottom flask under nitrogen containing a mixture of 2-bromothiophene (13.2 g, 80.98 mmol), Ni catalyst ($NidppCl_2$, 0.42 g), and diethyl ether (40 mL). The addition was done very slowly, preferably using a dropping funnel as the reaction was very exothermic. The resulting mixture was refluxed for 15 h and then was cooled down to room temperature. The reaction was stopped by the addition of 1 M HCl (30-40 mL) and the resulting two layers were separated. The organic layer was washed with water, dried over anhydrous $MgSO_4$ and evaporated to give a black oily product. It was purified by column chromatography using pentane as the eluent. The required product was obtained as colorless oil that converted to solid after staying at room temperature for some time.

Yield : 96 %

1H NMR (300 MHz, $CDCl_3$, ppm) : 7.01 (dd, 2H), 7.18(dd, 2H) 7.21 (dd, 2H)



Synthesis of 5,5'-bis(2,3,4,5-tetramethylcyclopentadienyl)bithiophene (6a)

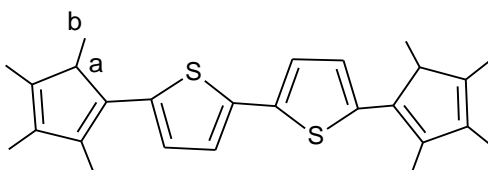
In a dry Schlenk under nitrogen, a solution of n-BuLi (24.09 mL, 60.24 mmol) was added dropwise to a slurry of 2,2'-bithiophene (5 g, 30.12 mmol) in diethyl ether (40 mL) at $-30^\circ C$. The reaction mixture was stirred for 30 min at $0^\circ C$ and then 2 h at room temperature. The colorless solution on top of the white precipitates was decanted off and THF (20 mL) was added to the dilithiated compound. The reaction mixture was cooled again to $-78^\circ C$ and a solution of 2,3,4,5-tetramethylcyclopent-2-enone (8.31 g, 60.24 mmol) in THF (20 mL) was

added slowly via cannula. It was stirred at room temperature overnight and the reaction was stopped by the addition of a saturated solution of NH_4Cl . The organic phase was separated and washed with water till neutral. After drying with MgSO_4 (anhydrous) and evaporation of the solvent, a green viscous liquid was obtained which was redissolved in dichloromethane (20 mL). A small amount of p-toluenesulfonic acid (approx. 0.1 g) was added at room temperature and the reaction mixture was stirred for 30 minutes. A quick appearance of precipitates was observed while changing the color of the reaction mixture to green. The solvent was evaporated till wet and pentane (30 mL) was added to precipitate out the product. After filtration and washing of the precipitates with ethanol, diethyl ether, and pentane, the required product was obtained as a yellow powder.

Yield : 49 %

^1H NMR (300 MHz, CDCl_3 , ppm) : 1.14 (d, 6H, $J=7.5$ Hz, H^b), 1.85 (s, 6H, CH_3 on Cp), 1.93 (s, 6H, CH_3 on Cp), 2.15 (s, 6H, CH_3 on Cp), 3.06 (q, 2H, $J = 7.5$ Hz, H^a), 6.76 (d, $J = 3.7$ Hz, 2H, $\text{H}^{\text{aromatic}}$), 7.09 (d, $J = 3.7$ Hz, 2H, $\text{H}^{\text{aromatic}}$)

^{13}C NMR (75.4 MHz, CDCl_3 , ppm) : 11.3 (CH_3 on Cp), 12.3 (CH_3 on Cp), 13.5 (CH_3 on Cp), 16.6 (C^b), 50.6 (C^a), 123.2 ($\text{C}^{\text{aromatic}}$), 124.3 ($\text{C}^{\text{aromatic}}$), 135.2 ($\text{C}^{\text{quat.}}$), 135.5 ($\text{C}^{\text{quat.}}$), 136.3 ($\text{C}^{\text{quat.}}$), 138.4 ($\text{C}^{\text{quat.}}$), 138.8 ($\text{C}^{\text{quat.}}$), 141.8 ($\text{C}^{\text{quat.}}$)



Elemental analysis for $\text{C}_{26}\text{H}_{30}\text{S}_2$

Calculated :	%C : 76.84	%H : 7.38	%S : 15.76
Found :	%C : 76.47	%H : 7.49	%S : 16.05

High resolution mass spectrum

Calculated = 406.178

Found = 406.175

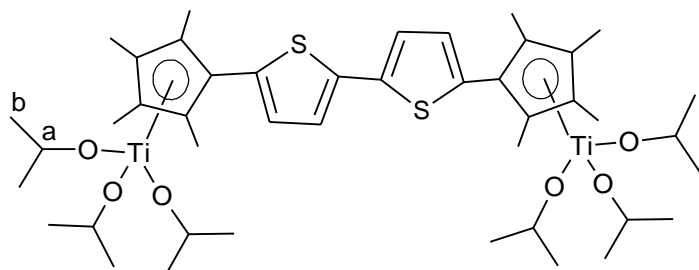
Synthesis of 5,5'-bithiophenebis(2,3,4,5-tetramethylcyclopentadienyl)di(triisopropoxytitanium) (6b)

In a dry Schlenk under nitrogen, a solution of n-BuLi (5.91 ml, 14.78 mmol) in pentane was added dropwise to a solution of 5,5'-bis(2,3,4,5-tetramethylcyclopentadienyl)-bithiophene (**6a**) (3.0 g, 7.39 mmol) in THF (60 mL) at 0°C . The reaction mixture was stirred overnight at room temperature. A solution of chlorotriisopropoxytitanium (3.85 g, 14.78 mmol) in THF (30 mL) was added to the reaction mixture at 0°C and the resulting mixture was refluxed for 2 days. The solvent was evaporated under vacuum and the residue was extracted with pentane. A yellow solid was obtained after evaporation of the solvent which was then washed 3 times with pentane to give the required product.

Yield: 40%.

^1H NMR (300 MHz, CDCl_3 , ppm) : 1.11 (d, $J = 6.0$ Hz, 36H, H^b), 2.03 (s, 12H, CH_3 on Cp), 2.18 (s, 12H, CH_3 on Cp), 4.55 (m, $J = 6.0$ Hz, 6H, H^a), 6.90 (d, $J = 3.8$ Hz, 2H, $\text{H}^{\text{thiophenic}}$), 7.11 (d, $J = 3.8$ Hz, 2H, $\text{H}^{\text{thiophenic}}$)

^{13}C NMR (75.4 MHz, CDCl_3 , ppm) : 11.5 (CH_3 on Cp), 12.7 (CH_3 on Cp), 26.5 (C^b), 75.8 (C^a), 116.4, 122.2, 122.4, 122.6, 127.9, 136.4, 136.9 ($\text{C}^{\text{quat.}}$ and thiophenic)



Elemental analysis for $\text{C}_{44}\text{H}_{70}\text{S}_2\text{Ti}_2\text{O}_6$

Calculated : %C : 61.82 %H : 8.19 %S : 7.49

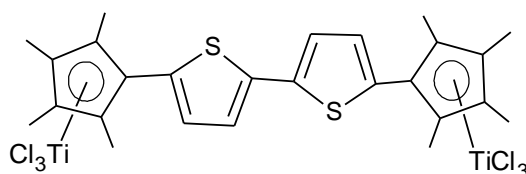
Found : %C : 59.25 %H : 8.25 %S : 7.26

Synthesis of 5,5'-bithiophenylenebis(2,3,4,5-tetramethylcyclopentadienyl)di(trichlorotitanium) (6c)

In a dry Schlenk under nitrogen, dichlorodimethylsilane (6.03 g, 46.79 mmol) was added slowly to a solution of 5,5'-bithiophenylenebis(2,3,4,5-tetramethylcyclopentadienyl)di(triisopropoxytitanium) (**6b**) (2.2 g, 2.59 mmol) in dichloromethane (20 mL) at 0°C . The reaction mixture was stirred at room temperature for 48 h. A color change from yellow to red and then purple was observed with the passage of time. The resulting precipitates were allowed to settle down and the solvent was decanted off. The purple compound was washed several times with acetonitrile and dried in vacuum. Due to very low solubility of the compound in most of the solvents, it was not possible to get a good ^{13}C NMR spectrum.

Yield: 78%.

^1H NMR (300 MHz, CD_2Cl_2 , ppm): 2.42 (s, 12H, CH_3 on Cp), 2.64 (s, 12H, CH_3 on Cp), 7.22 (d, $J = 3.8$ Hz, 2H, $\text{H}^{\text{thiophenic}}$), 7.30 (d, $J = 3.8$ Hz, 2H, $\text{H}^{\text{thiophenic}}$)



Anal. Calcd. for $\text{C}_{26}\text{H}_{28}\text{S}_2\text{Ti}_2\text{Cl}_6$:

Calculated : %C : 43.94 %H : 3.94 %S : 9.01 %Cl : 29.58 %Ti : 13.52

Found : %C : 44.90 %H : 4.09 %S : 8.93 %Cl : 29.43 %Ti : 12.89

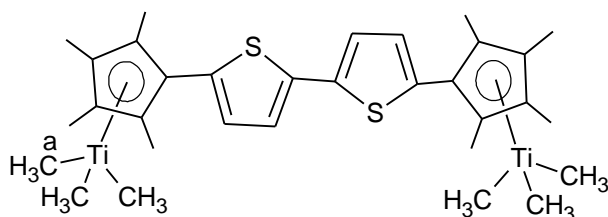
Synthesis of 5,5'-bithiophenylenebis(2,3,4,5-tetramethylcyclopentadienyl)di(trimethyltitanium) (6d)

In a dry Schlenk under nitrogen, covered with an aluminium foil, a solution of MeLi (4.73 mL, 7.57 mmol) in diethyl ether was added slowly to a solution of 5,5'-bithiophenylenebis(2,3,4,5-tetramethylcyclopentadienyl)di(trichlorotitanium) (**6c**) (0.9 g, 1.26 mmol) in diethyl ether (30 mL) at -78°C. The reaction mixture was stirred at this temperature for 2 h and then was slowly allowed to warm up to room temperature. The solvent was removed under vacuum and the residue was extracted with toluene. The required product was obtained as a yellowish green powder after the evaporation of the solvent. It was very sensitive to light and heat and long staying at room temperature either during the reaction or afterwards resulted in degradation of the product.

Yield: 95%.

¹H NMR (300 MHz, CDCl₃, ppm): 0.94 (s, 18H, H^a), 2.00 (s, 12H, CH₃ on Cp), 2.18 (s, 12H, CH₃ on Cp), 6.78 (d, 4H, J = 3.7 Hz, H^{thiophenic}), 7.07 (d, J = 3.7 Hz, 4H, H^{thiophenic})

¹³C NMR (50.3 MHz, CDCl₃, ppm): 12.4 (CH₃ on Cp), 13.5 (CH₃ on Cp), 64.4 (C^a), 120.4 (C^{quat.}), 121.7 (C^{quat.}), 123.2 (C^{thiophenic}), 124.4 (C^{quat.}), 127.8 (C^{thiophenic}), 129.2 (C^{quat.}), 136.5 (C^{quat.})



Synthesis of 1,4-bis(cyclopentadienylmethyl)benzene (7a)⁴

In a dry Schlenk under nitrogen, a solution of sodium cyclopentadienide (67 mL, 134 mmol) in THF was added dropwise to a solution of 1,4-bis(bromomethyl)benzene (17.68 g, 66.96 mmol) in THF (200 mL) at -78°C. The reaction mixture was stirred at 0°C for 1 h, filtered through celite and the solvent was removed under vacuum. The solid residue was extracted with benzene followed by evaporation of the solvent at low temperature (3 - 4°C) under vacuum. The resulting crude product was purified by column chromatography using petroleum ether (80%) and chloroform (20%).

Yield : 30%

NMR spectrum of the sample showed the presence of two isomers.

Isomer (7a) :

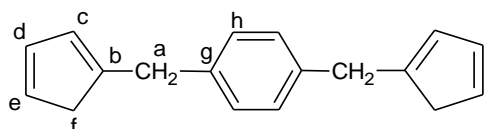
¹H NMR (250 MHz, CDCl₃, ppm) : 3.07 (d, J = 1.5 Hz, 4H, H^f), 3.81 (s, 4H, H^a), 6.10 (s, 2H, H^c), 6.37 (s, 2H, H^c), 6.51 (s, 2H, H^d), 7.24 (s, 4H, H^h)

^{13}C NMR (62.9 MHz, CDCl_3 , ppm) : 36.1 (C^a), 41.4 (C^f), 127.5 (C^e), 128.8 (C^h), 131.5 (C^c), 134.1 (C^d), 137.9 (C^g), 146.1 (C^b)

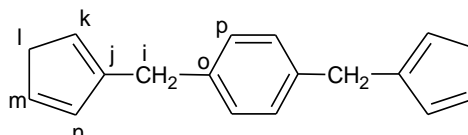
Isomer (7b) :

^1H NMR (250 MHz, CDCl_3 , ppm) : 2.95 (d, $J = 1.2$ Hz, 4H, H^l), 3.78 (s, 4H, H^i), 6.26 (s, 2H, H^k), 6.35 (s, 2H, H^m), 6.51 (s, 2H, H^n), 7.23 (s, 4H, H^p)

^{13}C NMR (62.9 MHz, CDCl_3 , ppm) : 37.1 (C^i), 43.2 (C^l), 128.0 (C^k), 128.8 (C^p), 132.4 (C^m), 134.1 (C^n), 138.6 (C^o), 148.7 (C^j)



(7a)



(7b)

MS : m/e 234

Synthesis of 1,4-phenylenebis(cyclopentadienylmethyl)di(triisopropoxytitanium) (7b)

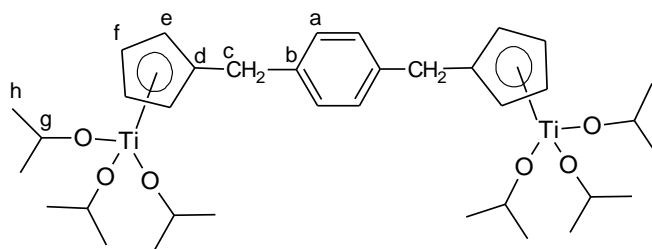
In a dry Schlenk under nitrogen, a solution of n-BuLi (5.7 mL, 2.5 mmol) in pentane was added dropwise to a solution of bis(cyclopentadienylmethyl)benzene (**7a**) (1.67 g, 7.13 mmol) in pentane (25 mL) at 0°C. The reaction mixture was stirred at this temperature for 1h and then overnight at room temperature. The white precipitates formed were washed with pentane and then suspended in THF (40 mL).

A solution of chlorotriisopropoxytitanium (3.71 g, 14.2 mmol) in THF (20 mL) was added to the reaction mixture at -78°C and the resulting mixture was stirred at room temperature for 24 h. The solvent was evaporated under vacuum and the residue was extracted with pentane. A yellow liquid was obtained after evaporation of the solvent.

Yield: 77%

^1H NMR (250 MHz, CDCl_3 , ppm) : 1.16 (d, $J = 5.8$ Hz, 36H, H^h), 3.92 (s, 4H, H^c), 4.56 (m, $J = 5.8$ Hz, 6H, H^g), 6.02 (s, 4H, H^f), 6.16 (s, 4H, H^e), 7.19 (s, 4H, H^a)

^{13}C RMN (62.9 MHz, CDCl_3 , ppm) : 26.1 (C^h), 35.4 (C^c), 77.4 (C^g), 111.2 (C^f), 112.0 (C^e), 129.0 (C^a), 131.5 (C^b), 138.5 (C^d)



Synthesis of 4,4'-bis(cyclopentadienylmethyl)biphenyl (8a)⁵

In a dry Schlenk under nitrogen, sodium cyclopentadienide (32 mL, 2M in THF) was added dropwise to a solution of 4,4'-bis(chloromethyl)biphenyl in THF (60 mL) at -78°C. The reaction mixture was stirred at room temperature for 1 h, filtered through celite and the solvent was removed under vacuum. The solid residue was extracted with benzene followed by the evaporation of benzene at low temperature (3-4°C) under vacuum. The resulting crude product was purified by column chromatography using petroleum ether (80%) and chloroform (20%). A white solid was obtained that was characterized by NMR and mass spectrum.

Yield: 9%

NMR spectrum of the sample showed the presence of two isomers.

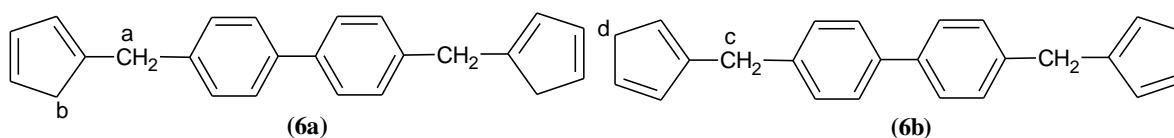
Isomer (6a) : ¹H NMR (250 MHz, CDCl₃, ppm) : 3.03 (s, 4H, H^b), 3.78 (s, 4H, H^a), 6.08-6.47 (m, 12H, CH of Cp), 7.30 (d, J = 7.5 Hz, H^{aromatic}), 7.54 (d, J = 7.5 Hz, H^{aromatic})

¹³C NMR (75.4 MHz, CDCl₃, ppm) : 36.2 (C^a), 41.5 (C^b), 127.1 (H^{aromatic}), 129.4 (H^{aromatic}), 128.3-134.7 (CH of Cp), 138.9-148.4 (C^{quat.})

Isomer (6b) :

¹H NMR (250 MHz, CDCl₃, ppm) : 2.92 (s, 4H, H^d), 3.80 (s, 4H, H^c), 6.08-6.47 (m, 12H, CH of Cp), 7.30 (d, J = 7.5 Hz, H^{aromatic}), 7.54 (d, J = 7.5 Hz, H^{aromatic})

¹³C NMR (75.4 MHz, CDCl₃, ppm) : 37.2 (C^c), 43.3 (C^d), 127.1 (C^{aromatic}), 129.4 (C^{aromatic}), 128.3-134.7 (CH of Cp), 138.9 - 148.4 (C^{quat.})

**Synthesis of 4,4'-biphenylenebis(cyclopentadienylmethyl)di(triisopropoxytitanium) (8b)**

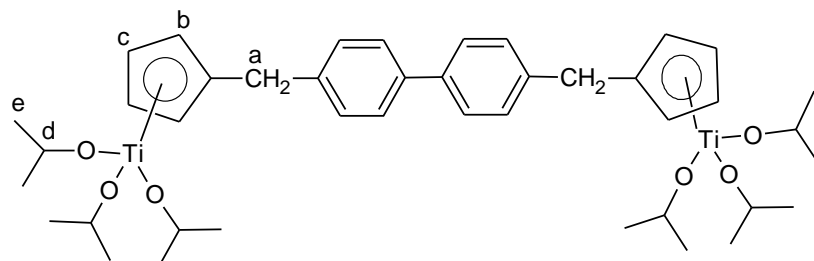
In a dry Schlenk under nitrogen, a solution of n-BuLi (2.3 mL, 5.6 mmol) in pentane was added dropwise to a solution of 4,4'-bis(cyclopentadienylmethyl)biphenyl (8a) (0.88 g, 2.8 mmol) in pentane (30 mL) at 0°C. The reaction mixture was stirred at this temperature for 1h and then overnight at room temperature. The white precipitates were formed which were washed with pentane and then suspended in THF (40 mL).

A solution of chlorotriisopropoxytitanium (1.48 g, 5.6 mmol) in THF (20 mL) was added to the reaction mixture at -78° and the resulting mixture was stirred at room temperature for 24 h. The solvent was evaporated under vacuum and the residue was extracted with pentane. The required product was obtained as a yellow solid after evaporation of the solvent.

Yield : 85%

^1H NMR (250 MHz, CDCl_3 , ppm) : 1.18 (d, $J = 5.0$ Hz, 36H, H^e), 3.99 (s, 4H, H^a), 4.60 (m, $J = 5.0$ Hz, 6H, H^d), 6.06 (s, 4H, H^c), 6.18 (s, 4H, H^b), 7.31 (d, $J = 7.5$ Hz, $\text{H}^{\text{aromatic}c}$), 7.49 (d, $J = 7.5$ Hz, $\text{H}^{\text{aromatic}b}$)

^{13}C NMR (62.9 MHz, CDCl_3 , ppm) : 26.1 (C^e), 35.4 (C^a), 77.4 (C^d), 111.3 (C^c), 112.1 (C^b), 126.9 ($\text{C}^{\text{aromatic}c}$), 129.4 ($\text{C}^{\text{aromatic}b}$), 131.2 ($\text{C}^{\text{quat.}}$), 138.8 ($\text{C}^{\text{quat.}}$), 139.8 ($\text{C}^{\text{quat.}}$)



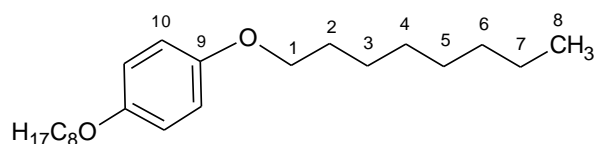
Synthesis of 1,4-bis(octyloxy)benzene⁶

In a 500 ml round bottom flask equipped with a pressure equilibrating dropping funnel and a reflux condenser, a solution of hydroquinone (15.1 g, 137 mmol) in ethanol (200 mL) was added to a solution of potassium hydroxide (15.3 g, 272 mmol) in ethanol (200 mL). After stirring at room temperature for 1.5 h 1-bromooctane (55.42 g, 287 mmol) was added and the reaction mixture was stirred at 50°C for 24 h. The green suspension was allowed to cool to room temperature and then distilled water (1 L) was added. After extraction with dichloromethane and drying with MgSO_4 (anhydrous) the solvents were evaporated and a brown solid was obtained. Recrystallization of the crude product in methanol gave the white crystals of the required product.

Yield : 66 %

^1H NMR (300 MHz, CDCl_3 , ppm) : 0.93 (t, 6H, H^8), 1.25 - 1.6 (m, 20H, H^{3-7}), 1.78 (m, 4H, H^2), 3.92 (t, 4H, H^1), 6.85 (s, 4H, H^{10})

^{13}C NMR (75.4 MHz, CDCl_3 , ppm) : 14.2 (C^8), 22.8, 26.2, 29.4, 29.61, 29.63, 32.0 (C^{2-7}), 68.8 (C^1), 115.5 (C^{10}), 153.4 (C^9)



Synthesis of 2,5-dibromo-1,4-bis(octyloxy)benzene⁶

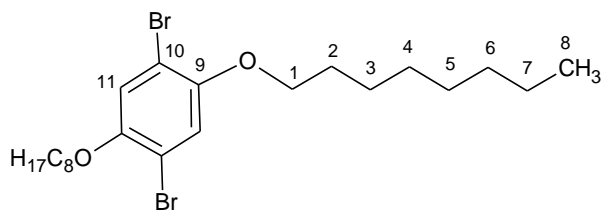
In a two necked round bottom flask equipped with a dropping funnel, a solution of bromine (26.8 g, 168 mmol) in dichloromethane (20 mL) was added dropwise to a solution of 1,4-bis(octyloxy)benzene (22.4 g, 67 mmol) in dichloromethane (500 mL). The reaction mixture was stirred at room temperature for 48 h. An aqueous solution of 20% potassium hydroxide (300 mL) was added followed by the extraction with dichloromethane. The organic

phase was dried with MgSO_4 (anhydrous) and the solvents were evaporated to give a yellow solid. The crude product was recrystallized in ethanol to give white crystals of the required product.

Yield : 79%

^1H NMR (250 MHz, CDCl_3 , ppm) : 0.90 (t, 6H, H^8); 1.28 - 1.50 (m, 20H, H^{3-7}); 1.80 (q, 4H, H^2); 3.94 (t, 4H, H^1); 7.08 (s, 2H, H^{11})

^{13}C NMR (62.9 MHz, CDCl_3 , ppm) : 14.3 (C^8), 22.8, 26.1, 29.3, 29.42, 29.46, 31.9 (C^{2-7}), 70.4 (C^1), 111.3 (C^9), 118.6 (C^{11}), 150.2 (C^{10})



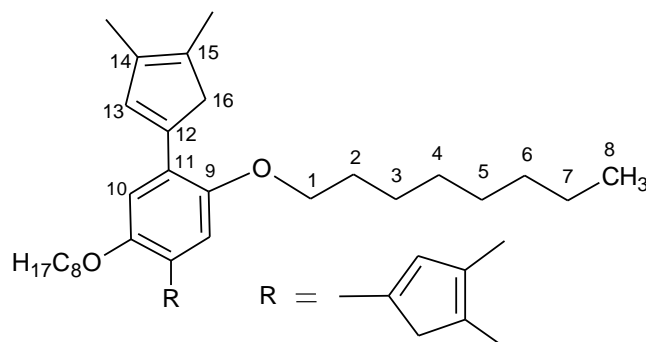
Synthesis of 2,5-bis(3,4-dimethylcyclopentadienyl)-1,4-bis(octyloxy)benzene (9a)

In a two necked round bottom flask equipped with a reflux condenser and a dropping funnel, a solution of $t\text{-BuLi}$ (10.16 mL, 16.26 mmol) in hexane was added dropwise to a solution of 2,5-dibromo-1,4-bis(octyloxy)benzene (2 g, 4.06 mmol) in diethyl ether (75 mL) at -78°C . The reaction mixture was stirred at this temperature for 4 h and then at room temperature for 1 h. It was again cooled to -78°C and a solution of 3,4-dimethylcyclopent-2-enone (0.89 g, 8.13 mmol) in THF (20 mL) was added slowly. The reaction mixture was stirred at this temperature for 1 h and then at room temperature for 48 h. A saturated solution of NH_4Cl was added to stop the reaction and both layers were separated. The aqueous phase was further extracted with diethyl ether and the combined organic phase was dried over MgSO_4 . The solvent was evaporated and the white solid was redissolved in dichloromethane. A catalytic amount of $p\text{-toluenesulfonic acid}$ was added to the reaction mixture changing the color of the solution to yellow. After stirring at room temperature for 30 min, the solvent was removed till wet and a small amount of petroleum ether was added to precipitate out the product. The yellow solid was filtered and washed several times with petroleum ether and diethyl ether followed by recrystallization in toluene to give the required product as yellow crystals.

Yield : 45%

^1H NMR (300 MHz, CDCl_3 , ppm) : 0.88 (t, $J = 6.5$ Hz, 6H, H^8), 1.29-1.50 (m, 20H, H^{3-7}), 1.87 (m, 4H, H^2), 1.90 (s, 6H, CH_3 on Cp), 1.98 (s, 6H, CH_3 on Cp), 3.36 (s, 4H, H^{16}), 3.98 (t, $J = 6.5$ Hz, 4H, H^1), 6.90 (s, 2H, H^{10}), 6.94 (s, 2H, H^{13})

^{13}C NMR (62.9 MHz, CDCl_3 , ppm) : 12.9 (CH_3 on Cp), 13.6 (CH_3 on Cp), 14.3 (C^8), 22.9, 26.5, 29.5, 29.6, 29.8, 32.0 (C^{2-7}), 47.6 (C^{16}), 69.1 (C^1), 111.8 (C^{10} or 13), 123.8 ($\text{C}^{\text{quat.}}$), 135.5 (C^{10} or 13), 135.6 ($\text{C}^{\text{quat.}}$), 136.9 ($\text{C}^{\text{quat.}}$), 139.4 ($\text{C}^{\text{quat.}}$), 150.4 ($\text{C}^{\text{quat.}}$)



Elemental analysis for $\text{C}_{36}\text{H}_{54}\text{O}_2$

Calculated : %C : 83.34 %H : 10.49

Found : %C : 82.91 %H : 10.56

High resolution mass spectrum

Calculated = 518.411

Found = 518.409

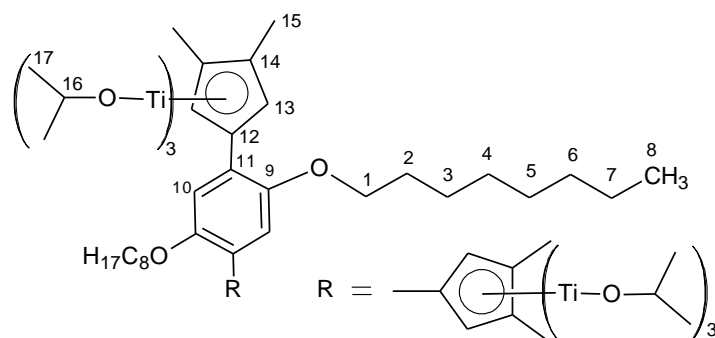
Synthesis of 1,4-bis(octyloxy)phenylene-2,5-bis(3,4-dimethylcyclopentadienyl)di(triisopropoxytitanium) (9b)

In a dry Schlenk under nitrogen, a solution of *n*-BuLi (3.08 mL, 7.7 mmol) in pentane was added dropwise to a solution of 2,5-bis(3,4-dimethylcyclopentadienyl)-1,4-bis(octyloxy)benzene (**9a**) (2 g, 3.86 mmol) in THF (80 mL) at 0°C. The reaction mixture was stirred at room temperature for overnight. A solution of chlorotriisopropoxytitanium (2.01 g, 7.72 mmol) in THF (30 mL) was added to the reaction mixture at 0°C and the resulting mixture was refluxed for 4 days. The solvent was evaporated under vacuum and the residue was extracted with pentane. A yellow solid was obtained after evaporation of the solvent which was then washed several times with pentane to give the required product.

Yield : 95%

^1H NMR (250 MHz, CDCl_3 , ppm) : 0.87 (t, J = 6.5 Hz, 6H, H^8), 1.03 (d, J = 6.0 Hz, 36H, H^{17}), 1.21-1.89 (m, 24H, H^{2-7}), 2.12 (s, 12H, H^{15}), 3.99 (t, J = 6.5 Hz, 4H, H^1), 4.5 (m, J = 6.0 Hz, 6H, H^{16}), 6.56 (s, 4H, H^{13}), 7.11 (s, 2H, H^{10})

^{13}C NMR (62.5 MHz, CDCl_3 , ppm) : 13.3 (C^{15}), 14.3 (C^8), 22.9, 26.2, 26.5, 29.6, 29.8, 32.0 (C^{2-7}), 26.2 (C^{17}), 69.4 (C^1), 76.6 (C^{16}), 112.8 (C^{10}), 113.1 ($\text{C}^{\text{quat.}}$), 121.1 ($\text{C}^{\text{quat.}}$), 122.8 ($\text{C}^{\text{quat.}}$), 125.2 (C^{13}), 150.4 ($\text{C}^{\text{quat.}}$)



Elemental analysis for $C_{54}H_{92}O_8Ti_2$

Calculated : %C : 67.21 %H : 9.54 %Ti : 9.95

Found : %C : 66.42 %H : 9.79 %Ti : 9.57

Synthesis of 1,4-bis(octyloxy)phenylene-2,5-bis(3,4-dimethylcyclopentadienyl)di(tri-chlorotitanium) (9c)

In a dry Schlenk under nitrogen, dichlorodimethylsilane (2.40 g, 18.63 mmol) was added slowly to a solution of 1,4-bis(octyloxy)phenylene-2,5-bis(3,4-dimethylcyclopentadienyl)di(triisopropoxytitanium) (**9b**) (1.0 g, 1.03 mmol) in dichloromethane (20 mL) at 0°C. The reaction mixture was stirred at room temperature for 2 days. A slow formation of purple precipitates was observed. The solvent was evaporated and the crude product was washed several times with dry acetonitrile. The purple product was dried in vacuum and characterized.

Yield : 65%

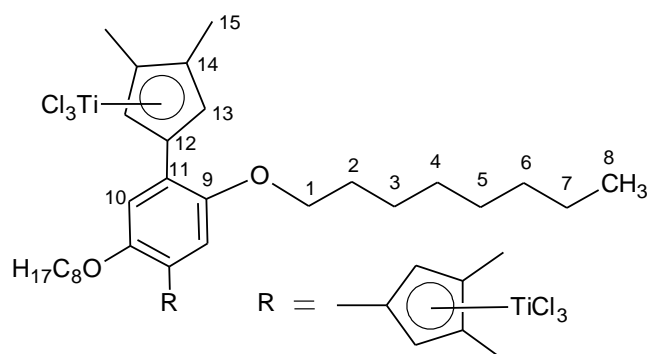
1H NMR (250 MHz, $CDCl_3$, ppm) : 0.87 (t, 6H, H^8), 1.30 - 1.99 (m, 24H, H^{2-7}), 2.49 (s, 12H, H^{15}), 4.13 (t, 4H, H^1), 7.29 (s, 2H, H^{10}), 7.41 (s, 4H, H^{13})

^{13}C NMR (62.9 MHz, $CDCl_3$, ppm) : 14.3 (C^8), 16.2 (C^{15}), 22.8, 26.5, 29.4, 29.5, 29.6, 32.0 (C^{2-7}), 69.6 (C^1), 113.0 (C^{10}), 122.9 (C^{13}), 124.3 ($C^{quat.}$), 136.9 ($C^{quat.}$), 139.4 ($C^{quat.}$), 150.5 ($C^{quat.}$)

Elemental analysis for $C_{36}H_{52}O_2Ti_2Cl_6$

Calculated : %C : 52.55 %H : 6.32

Found : %C : 53.68 %H : 6.87



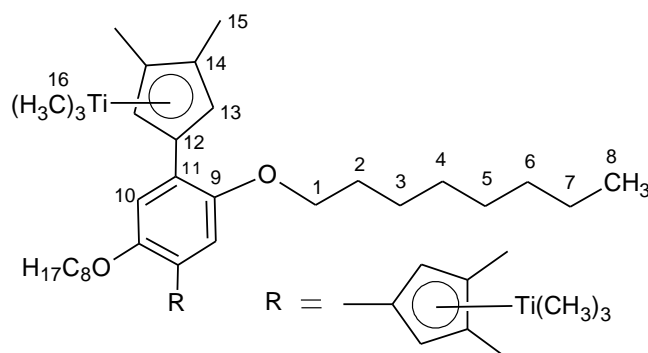
Synthesis of 1,4-bis(octyloxy)phenylene-2,5-bis(3,4-dimethylcyclopentadienyl)di(trimethyltitanium) (9d)

In a dry Schlenk under nitrogen, covered with an aluminium foil, a solution of MeLi (4.54 mL, 7.27 mmol) in diethyl ether was added slowly to a solution of 1,4-bis(octyloxy)phenylene-2,5-bis(3,4-dimethylcyclopentadienyl)di(trichlorotitanium) (**9c**) (1.0 g, 1.21 mmol) in diethyl ether (20 mL) at -78°C . The reaction mixture was stirred at this temperature for 2 h and then was slowly allowed to reach room temperature. A color change from purple to yellow/green was observed during the course of the reaction. The solvent was removed under vacuum and the residue was extracted with toluene. The required product was obtained as a yellowish green powder after the evaporation of the solvent. It was very sensitive to light and heat and decomposed after staying long time at room temperature even in the glove box.

Yield : 87%

^1H NMR (300 MHz, CDCl_3 , ppm) : 0.89 (t, 6H, H^8), 0.91 (s, 18H, H^{16}), 1.29 - 1.84 (m, 24H, H^{2-7}), 2.06 (s, 12H, H^{15}), 3.94 (t, 4H, H^1), 6.60 (s, 4H, H^{13}), 6.92 (s, 2H, H^{10})

^{13}C NMR (75.4 MHz, CDCl_3 , ppm) : 14.0, 14.3, 22.9, 26.5, 29.5, 29.6, 29.7, 32.0 ($\text{C}^{2-8, 15}$), 62.5 (C^{16}), 69.0 (C^1), 111.9 (C^{quat}), 112.2 (C^{10}), 123.2 (C^{quat}), 124.9 (C^{quat}), 125.3 (C^{13}), 149.9 (C^{quat})

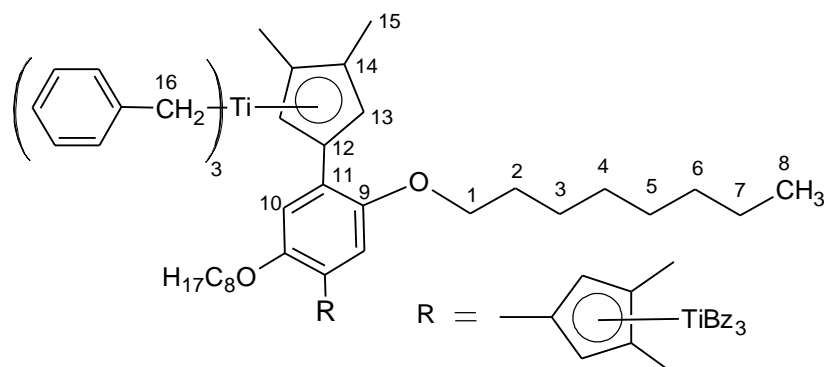


Synthesis of 1,4-bis(octyloxy)phenylene-2,5-bis(3,4-dimethylcyclopentadienyl)di(trimethyltitanium) (9e)

In a dry Schlenk under nitrogen, covered with an aluminium foil, a solution of benzylmagnesium chloride (5.82 mL, 5.82 mmol) in diethyl ether was added slowly to a solution of 1,4-bis(octyloxy)phenylene-2,5-bis(3,4-dimethylcyclopentadienyl)di(trichlorotitanium) (**9c**) (0.8 g, 0.97 mmol) in diethyl ether (20 mL) at -78°C . The reaction mixture was stirred at this temperature for 2 h and then was allowed to warm to room temperature. The color of the solution changed from purple to red during the course of the reaction. The solvent was removed under vacuum and the residue was extracted with toluene. The required product was obtained as a red powder after the evaporation of the solvent.

Yield : 92%

^1H NMR (300 MHz, CDCl_3 , ppm) : 1.02 (t, 6H, H^8), 1.37-1.93 (m, 24H, H^{2-7}), 1.89 (s, 12H, H^{15}), 3.14 (s, 12H, H^{16}), 3.97 (t, 4H, H^1), 6.79-7.27 (m, 36H, $\text{H}^{\text{aromatic}}$)



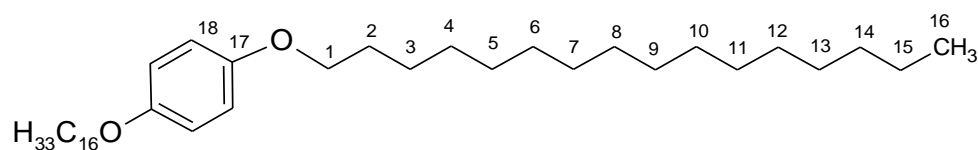
Synthesis of 1,4-bis(hexadecyloxy)benzene⁶

In a 500 ml round bottom flask equipped with a pressure equilibrating dropping funnel and a reflux condenser, a solution of hydroquinone (8.61 g, 78.2 mmol) in ethanol (75 ml) was added to a solution of potassium hydroxide (8.72 g, 155.4 mmol) in ethanol (150 ml). After stirring at room temperature for 1.5 hr 1-bromohexadecane (50.0 g, 163.7 mmol) was added and the reaction mixture was stirred at 50°C for 24 hr. The green suspension was allowed to cool to room temperature and then distilled water (1 L) was added. After extraction with dichloromethane and drying over MgSO_4 (anhydrous) the solvents were evaporated and a brown solid was obtained. Recrystallization of the crude product in ethanol gave the white crystals of the required product.

Yield : 48%

^1H NMR (300 MHz, CDCl_3 , ppm): 0.88 (t, 6H, H^{16}); 1.25-1.43 (m, 52H, H^{3-15}); 1.72 (m, 4H, H^2); 3.89 (t, 4H, H^1); 6.81 (s, 4H, H^{18})

^{13}C NMR (75.4 MHz, CDCl_3 , ppm): 14.3 (C^{16}), 22.9, 26.3, 29.6, 29.6, 29.6, 29.8, 29.9, 32.1 (C^{2-15}), 68.8 (C^1), 115.5 (C^{18}), 153.4 (C^{17})



Synthesis of 2,5-dibromo-1,4-bis(hexadecyloxy)benzene⁶

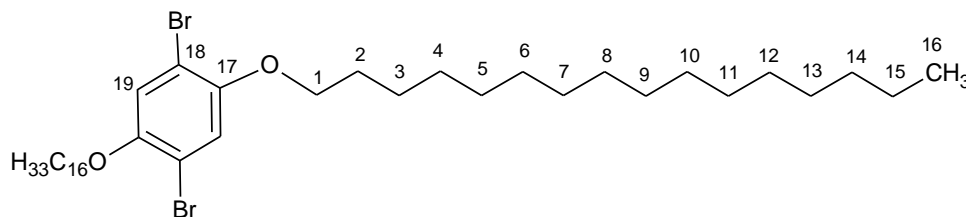
In a two necked round bottom flask equipped with a dropping funnel, a solution of bromine (7.16 g, 44.75 mmol) in dichloromethane (10 mL) was added dropwise to a solution of 1,4-bis(hexadecyloxy)benzene (10.0 g, 17.9 mmol) in dichloromethane (120 mL). The reaction mixture was stirred at room temperature for 48 h. An aqueous solution of 20% potassium hydroxide (100 mL) was added followed by the extraction with dichloromethane. The organic phase was dried with MgSO_4 (anhydrous) and the solvents were evaporated to

give a yellow solid. The crude product was recrystallized in ethanol to give white crystals of the required product.

Yield : 92 %

^1H NMR (250 MHz, CDCl_3 , ppm): 0.88 (t, 6H, H^{16}); 1.15-1.6 (m, 56H, H^{3-15}); 1.80 (q, 4H, H^2); 3.95 (t, 4H, H^1); 7.01 (s, 2H, H^{19})

^{13}C NMR (62.9 MHz, CDCl_3 , ppm): 14.3 (C^{16}), 22.9, 26.1, 29.3, 29.51, 29.58, 29.77, 29.80, 29.87, 29.92 (C^{3-15}), 32.1 (C^2), 70.5 (C^1); 111.3 (C^{17}); 118.6 (C^{19}); 150.2 (C^{18})

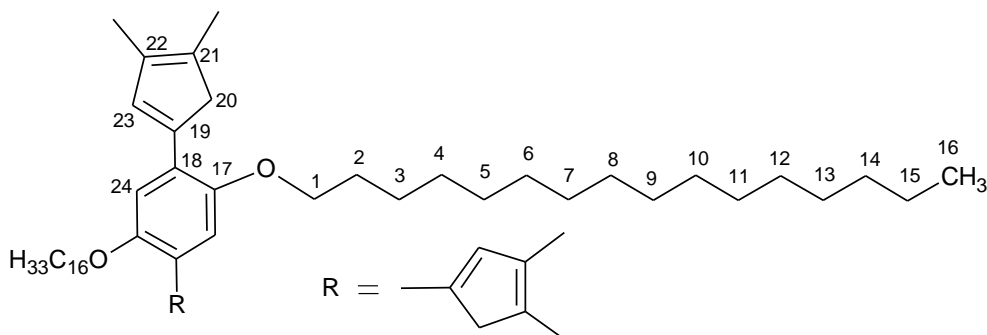


Synthesis of 2,5-bis(3,4-dimethylcyclopentadienyl)-1,4-bis(hexadecyloxy)benzene (10a)

In a two necked round bottom flask equipped with a reflux condenser and a dropping funnel, a solution of *t*-BuLi (6.98 mL, 11.17 mmol) in hexane was added dropwise to a solution of 2,5-dibromo-1,4-bis(hexadecyloxy)benzene (2 g, 2.79 mmol) in diethyl ether (75 mL) at -78°C . The reaction mixture was stirred at this temperature for 4 h and then at room temperature for 1 h. It was again cooled to -78°C and a solution of 3,4-dimethylcyclopent-2-enone (0.92 g, 8.38 mmol) in THF (20 mL) was added slowly. The reaction mixture was stirred at this temperature for 1 h and then at room temperature for 48 h. A saturated solution of NH_4Cl was added to stop the reaction and both layers were separated. The aqueous phase was further extracted with diethyl ether and the combined organic phase was dried over MgSO_4 . The solvent was evaporated and the white solid was redissolved in dichloromethane. A catalytic amount of *p*-toluenesulfonic acid was added to the reaction mixture changing the color of the solution to yellow. After stirring at room temperature for 30 min, the solvent was removed till wet and a small amount of pentane was added to precipitate out the product. The yellow solid was filtered and washed several times with petroleum ether and diethyl ether followed by recrystallization in toluene to give the required product as yellow crystals. Due to low solubility of the compound in CDCl_3 at room temperature, ^1H NMR spectrum was taken at high temperature (55°C). It was not possible to record a ^{13}C NMR spectrum due to the same reason.

Yield : 48%

^1H NMR (200 MHz, CDCl_3 , ppm): 0.89 (t, $J = 6.5$ Hz, 6H, H^{16}), 1.28 - 1.45 (m, 52H, H^{3-15}), 1.85 (m, 4H, H^2), 1.90 (s, 6H, CH_3 on Cp), 1.98 (s, 6H, CH_3 on Cp), 3.36 (s, 4H, H^{20}), 3.99 (t, $J = 6.5$ Hz, 4H, H^1), 6.90 (s, 2H, H^{23}), 6.91 (s, 2H, H^{24})



Elemental analysis for $C_{52}H_{86}O_2$

Calculated : %C : 84.03 %H : 11.66

Found: %C : 83.98 %H : 11.88

High resolution mass spectrum

Calculated : 742.662

Found : 742.663

Synthesis of dimethyl(phenyltetramethylcyclopentadienyl)silane (11a)

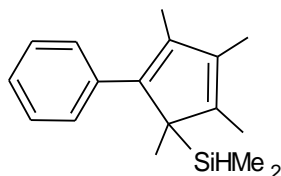
To a solution of phenyltetramethylcyclopentadiene (2g, 10 mmol) in diethyl ether (50 mL) in a Schlenk at 0 °C, a solution of n-butyllithium (4.5 mL, 11.2 mmol) was added dropwise. An immediate precipitation was observed. The suspension was stirred for 1 h at RT. The supernatant liquid was removed with a canula equipped with a filter and the solid was washed with about 30 mL of diethylether. THF (50 mL) was added to the solid followed by the dropwise addition of chlorodimethylsilane (1.2 mL, 12.6 mmol). The mixture was warmed at 50 °C for 1 h. After cooling to room temperature and evaporation of the solvent, the residu was taken up in 60 mL of pentane. Filtration followed by the evaporation of the solvent gave 2.4 g of dimethyl(phenyltetramethylcyclopentadienyl)silane.

Yield : 94%

$^1\text{H NMR}$ (200 MHz, C_6D_6 , ppm): -0.15 (s, 6H, CH_3 on Si), 1.78 (m, 12H), 4.05 (m, $J = 3.4$ Hz, 1H), 7.49-7.30 (m, 5H)

$^{13}\text{C NMR}$ (50.3 MHz, $CDCl_3$, ppm): -6.7, 12.2, 12.4, 126.2, 128.1, 129.8, 138.2, 141.4

$^{129}\text{Si NMR}$ (39.7 MHz, $CDCl_3$, ppm) : -4.2



Synthesis of trichloro(phenyltetramethylcyclopentadienyl)titanium (11b)

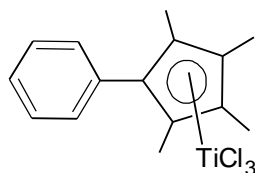
To a solution of dimethyl(phenyltetramethylcyclopentadienyl)silane (4.8 g, 19 mmol) in pentane (100 mL) in a Schlenk at -78 °C, titanium tetrachloride (3.5 g, 18.4 mmol) was

added dropwise. The solution was stirred for 1.5 h at room temperature. The red crystalline precipitate was filtered, washed with 20 mL of pentane and dried.

Yield: 76%

^1H NMR (200 MHz, CDCl_3 , ppm): 2.46 (s, 6H, CH_3 on Cp), 2.50 (s, 6H, CH_3 on Cp), 7.42-7.45 (m, 5H, $\text{H}^{\text{aromatic}}$)

^{13}C NMR (75.4 MHz, CDCl_3 , ppm): 14.8 (CH_3 on Cp), 15.7 (CH_3 on Cp), 128.5 ($\text{C}^{\text{aromatic}}$), 128.8 ($\text{C}^{\text{aromatic}}$), 130.5 ($\text{C}^{\text{aromatic}}$), 133.1 (C^{q}), 136.4 (C^{q}), 138.9 (C^{q}), 141.1 (C^{q})



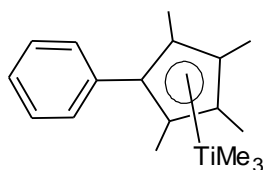
Synthesis of trimethyl(phenyltetramethylcyclopentadienyl)titanium (11c)

A 1.6 M solution of methyllithium in diethylether (25 mL, 40 mmol) was added to a Schlenk charged with a suspension of trichloro(phenyltetramethylcyclopentadienyl)titanium (4.5 g, 12.8 mmol) in 100 mL of diethyl ether at $-78\text{ }^\circ\text{C}$. The mixture was allowed to reach RT and stirred for 2 h. After evaporation of the solvent, the solids were extracted with 150 mL of pentane. Filtration on Celite followed by evaporation of the solvent gave a yellow-green oil which solidified on standing.

Yield : 81%

^1H NMR (200 MHz, C_6D_6 , ppm): 1.13 (s, 9H, CH_3 on Ti), 1.71 (s, 6H, CH_3 on Cp), 1.88 (s, 6H, CH_3 on Cp), 7.22-7.08 (m, 5H, $\text{H}^{\text{aromatic}}$)

^{13}C NMR (50.3 MHz, C_6D_6 , ppm): 11.6 (CH_3 on Cp), 12.5 (CH_3 on Cp), 63.1 (CH_3 on Ti), 126.5, 127.0, 127.5, 128.0, 130.0, 135.7



Elemental analysis for $\text{C}_{18}\text{H}_{26}\text{Ti}$

Calculated : %C : 74.47 %H : 9.03

Found: %C : 73.57 %H : 8.77

Synthesis of tetramethyl- μ -oxobis(phenyltetramethylcyclopentadienyl)ditanium (11d)

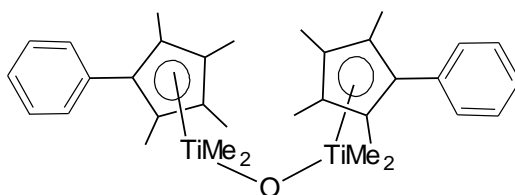
A Schlenk charged with a solution of trimethyl(phenyltetramethylcyclopentadienyl)-titanium (0.72 g, 2.5 mmol) in 50 mL of pentane was linked to a flask containing 20 mL of

water. After 72 h the yellow-green solution was concentrated to give 0.60 g of tetramethyl- μ -oxobis(phenyltetramethylcyclopentadienyl)ditanium as green crystals upon cooling at -20°C .

Yield: 86%

^1H NMR (300 MHz, C_6D_6 , ppm): 0.95 (s, 12H, CH_3 on Ti), 2.04 (s, 12H, CH_3 on Cp), 2.07 (s, 12H, CH_3 on Cp), 7.19-7.38 (m, 10H, $\text{H}^{\text{aromatic}}$)

^{13}C NMR (50.3 MHz, CDCl_3 , ppm): 11.2 (CH_3 on Cp), 12.2 (CH_3 on Cp), 54.8 (CH_3 on Ti), 120.5 (C^{q}), 123.5 (C^{q}), 126.4 (C^{q}), 127.5 ($\text{C}^{\text{aromatic}}$), 127.7 (C^{q}), 128.4 (C^{q}), 130.3 ($\text{C}^{\text{aromatic}}$), 135.3 (C^{q})



Elemental analysis for $\text{C}_{34}\text{H}_{46}\text{TiO}$

Calculated : %C : 72.08 %H : 8.13

Found: %C : 72.82 %H : 8.62

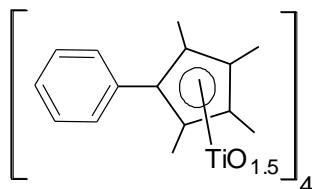
Synthesis of hexa- μ -oxotetrakis(phenyltetramethylcyclopentadienyl)tetratitanium (11e)

To a solution of trimethyl(phenyltetramethylcyclopentadienyl)titanium (0.50 g, 1.7 mmol) in 200 mL of THF was added excess of water (0.30 g, 16.6 mmol). After 48 h, the solvent was evaporated to give a yellow solid which was recrystallized in dichloromethane.

Yield : 71%

^1H NMR (200 MHz, CDCl_3 , ppm): 1.92 (s, 6H, CH_3 on Cp), 1.97 (s, 6H, CH_3 on Cp), 7.22-7.51 (m, 5H, $\text{H}^{\text{aromatic}}$)

^{13}C NMR (50.3 MHz, CDCl_3 , ppm): 11.2 (CH_3 on Cp), 12.2 (CH_3 on Cp), 122.3, 123.1, 127.7, 128.1, 130.7, 130.9, 135.8



Experimental section related to chapter III

I. Preparation of hybrid materials with linear spacers

I.1. Hybrid materials from di(cyclopentadienyltriisopropoxytitanium) precursors

I.1.1. Hydrolysis in homogeneous medium

In a dry Schlenk under nitrogen, a solution of 4,4'-biphenylenebis(2,3,4,5-tetramethylcyclopentadienyl)di(triisopropoxytitanium) (**2b**) (1.0 g, 1.19 mmol) in THF (15 mL) was cooled down to -80°C. A mixture of water (129 μ L, 7.14 mmol) and THF (5 mL) was added slowly to the stirring solution slowly via a syringe. The reaction mixture was allowed to stir for 10 min and then was left untouched for gelification. The resulting yellow gel was aged for 3 weeks. It was then washed with THF, diethyl ether and petroleum ether after centrifugation to remove the oligomers. The resulting powder was dried overnight under vacuum and the required xerogel was obtained as a yellow powder. The same procedure was used to prepare all other xerogels in homogeneous medium. The only difference was in the reaction temperature that has been discussed previously in chapter III.

Elemental Analysis

Xerogel	%C		%H		%O*		%Ti	
	Cal.	Exp.	Cal.	Exp.	Cal.	Exp.	Cal.	Exp.
XPh2OR	62.9	62.1	6.3	6.0	14.0	15.8	16.8	16.2
XPh3OR1	66.7	64.4	6.2	6.0	12.3	13.5	14.8	16.1
XPh3OR2	64.9	62.3	5.4	5.6	13.5	19.1	16.2	13.0
XTh2OR	53.4	53.2	5.5	5.2	13.7	-	16.4	16.2
XBz2OR	59.0	53.9	4.9	4.5	16.4	23.8	19.7	17.8

*Obtained by difference

I.1.2. Hydrolysis in heterogeneous medium

To a solution of 4,4'-biphenylenebis(2,3,4,5-tetramethylcyclopentadienyl)di(triisopropoxytitanium) (**2b**) (1.0 g, 1.19 mmol) in toluene (20 mL) in a dry Schlenk under nitrogen, water (129 μ L, 7.14 mmol) was added slowly at room temperature with constant stirring. The resulting mixture was stirred for 20 min and then was left untouched for gelification for 3 weeks. A yellow powder was obtained after washing and drying of the gel. The same procedure was used for other xerogels prepared in biphasic medium.

Elemental analysis

Xerogel	%C		%H		%O*		%Ti	
	Cal.	Exp.	Cal.	Exp.	Cal.	Exp.	Cal.	Exp.
XPh2OR-Tol	62.9	63.7	6.3	6.2	14.0	14.6	16.8	15.5
XPh3OR1-Tol	66.7	61.8	6.2	5.9	12.3	18.9	14.8	13.3
XBz2OR-Tol	59.0	51.2	4.9	4.5	16.4	26.5	19.7	17.8

*Obtained by difference

I.2. Hybrid materials from di(cyclopentadienyltrimethyltitanium) precursors

The previously described procedure used to prepare hybrid materials in homogeneous medium was used. The only difference was in the solvent/precursor ratio which was kept 40/1 (w/w) in this case due to low solubility of the methylated complexes in THF.

Elemental analysis

Xerogel	%C		%H		%O*		%Ti	
	Cal.	Exp.	Cal.	Exp.	Cal.	Exp.	Cal.	Exp.
XPh1Me	58.1	60.6	6.5	6.5	16.1	15.7	19.4	17.2
XPh2Me	62.9	64.4	6.3	6.0	14.0	13.5	16.8	16.1
XPh3Me	66.7	66.6	6.2	6.1	12.3	13.6	14.8	13.7
XTh2Me	53.4	41.3	5.5	5.2	13.7	-	16.4	10.0

* Obtained by difference

I.3. Hybrid materials from di(cyclopentadienyltribenzyltitanium) precursors

The previously described procedure was used here as well.

Elemental analysis

Xerogel	%C		%H		%O*		%Ti	
	Cal.	Exp.	Cal.	Exp.	Cal.	Exp.	Cal.	Exp.
XPh1Bz	58.1	54.2	6.5	6.0	16.1	23.0	19.4	16.2
XPh2Bz	62.9	62.2	6.3	6.3	14.0	17.1	16.8	14.4

* Obtained by difference

II. Preparation of hybrid materials with lateral chains

The hydrolysis procedure used to prepare hybrid materials in homogeneous medium carrying linear spacers was used here as well.

Elemental analysis

Xerogel	%C		%H		%O*		%Ti	
	Cal.	Exp.	Cal.	Exp.	Cal.	Exp.	Cal.	Exp.
XPhC8OR	62.1	63.0	8.0	8.0	16.1	16.2	13.8	12.8
XPhC8Me	62.1	22.2	8.0	4.5	16.1	53.8	13.8	19.4
XPhC8Bz	62.1	58.2	8.0	7.1	16.1	23.0	13.8	11.7

* Obtained by difference

Experimental section related to chapter IV

Preparation of TiO₂ powders

The xerogel **XPh2Me** was introduced in a quartz chamber and was placed in the oven. The temperature was increased to 450°C or 500°C and the sample was heated for 5 h (1 h to reach the required temperature + 4 h) under a constant flow of oxygen. White powders were obtained after pyrolysis and were characterized.

Preparation of TiO₂ films

The substrate for the films was chosen to be microscopic glass films although for surface studies silicon wafer was used as well. The films (glass or silicon wafer) were washed by immersing in boiling chloroform (analytical grade) for 15 min followed by a UV treatment for 30 min each side.

In a dry Schlenk under nitrogen, a solution of 4,4'-biphenylenebis(2,3,4,5-tetramethylcyclopentadienyl)di(triisopropoxytitanium) (**2b**) (650 mg) was prepared in dry chloroform (2.5 mL). About 150 µL of it was dropped on the glass substrate via a syringe and was rotated at a speed of 2000 tr/min for 20 seconds. The prepared films were allowed to dry in air for 4-5 h and then were stored in the glove box.

The hybrid material films were analyzed by various techniques to determine the completion of hydrolysis-condensation reactions. They were then treated at 400°C, 500°C or 600°C for 5 h (1 h to reach that temperature and 4 h heating at the specified temperature) in oven.

-
- ¹ (a) Meng, X.; Sabat, M.; Grimes, R. N. *J. Am. Chem. Soc.* **1993**, *115*, 6143 (b) Bunel, E. E.; Campos, P.; Ruz, J.; Valle, L.; Chadwick, I.; Ana, M. S.; Gonzalez, G.; Manriquez, J. M. *Organometallics* **1988**, *7*, 474
- ² Lee, M. H.; Kim, S. K.; Do, Y. *Organometallics* **2005**, *24*, 3618
- ³ Wang, Z. ; Heising, J. M. ; Clearfield, A. *J. Am. Chem. Soc.* **2003**, *125*, 10375
- ⁴ Liu, X.; Sun, J.; Zhang, H.; Xiao, X.; Lin, F., *Eur. Polym. J.*, **2005**, *41*, 1519
- ⁵ Sun, J.; Zhang, H.; Liu, X.; Xiao, X.; Lin, F. *Eur. Polym. J.* **2006**, *42*, 1259
- ⁶ (a) Tamura, H.; Watanabe, T.; Imanishi, K.; Sawada, M. *Synth. Met.* **1999**, *107*, 19 (b) Lightowler, S. ; Hird, M. *Chem. Mater.* **2004**, *16*, 3963 (c) Elhamzaoui, H.; Jousseume, B.; Toupance, T.; Allouchi, H. *Organometallics* **2007**, *26*, 3908



Préparation et caractérisation de matériaux hybrides organiques-inorganiques à base de cyclopentadienyltitanes

Résumé

Ce mémoire rapporte la préparation et l'étude de matériaux hybrides organiques-inorganiques à base de titane où les deux réseaux sont liés par des liaisons titane-carbone stables. Différents précurseurs dans lesquels deux groupes cyclopentadienyltitane sont reliés par des espaceurs variés ont été préparés. Ces espaceurs comprennent des groupes aromatiques et hétéroaromatiques linéaires ainsi que des groupes aromatiques disubstitués par des chaînes alkyle. Ces complexes dimétalliques, où le titane est aussi lié à trois groupes labiles, ont été ensuite hydrolysés dans les conditions du procédé sol-gel pour conduire à des hybrides de classe II. Le réseau organique y est lié au réseau inorganique par des liaisons stables titane-carbone. Ces matériaux sont organisés et leur mode d'organisation dépend de la nature de l'espaceur reliant les groupes cyclopentadienyle. Les espaceurs linéaires conduisent à des matériaux à structure en escalier dans lesquels les ligands sont associés par des liaisons π . La longueur des espaceurs n'a pas d'effet sur cette organisation. Par contre, les matériaux à espaceurs substitués latéralement sont organisés par les chaînes alkyle. La calcination de ces matériaux hybrides sous oxygène conduit à la formation de dioxyde de titane nanoporeux sous forme d'anatase dont la cristallinité et la surface spécifique dépendent de la température de calcination. D'une façon similaire des films de dioxyde de titane de même type sont obtenus par la calcination de films minces d'hybrides préparés par spin-coating.

Mots Clef : Matériaux hybrides, sol-gel, organotitane, cyclopentadienyltitane, xérogels, auto-assemblage, dioxyde de titane, mésoporeux, films.

Preparation and characterization of cyclopentadienyltitanium-based organic-inorganic hybrid materials

Abstract

This work aimed to the preparation of titanium-based organic-inorganic hybrid materials where both networks are linked through stable titanium-carbon bonds. The preparation of various di(cyclopentadienyltitanium) precursors in which various organic groups serve as a bridge between the two cyclopentadienyl groups while each titanium atom is equipped with three hydrolysable groups was first achieved. Then, these complexes were hydrolyzed in a sol-gel process that led to new self-assembled titanium-based class II hybrid materials in which the inorganic network is connected to the organic network through stable titanium-carbon bonds. The mode of organization of the nanostructures depends on the spacer bridging the cyclopentadienyl groups. Linear aromatic spacers led to materials having a stair-like structure in which the organic ligands are arranged via π -stacking. The length of the spacer has a little effect on the organization of the nanostructures. The structure of the materials obtained with spacers endowed with long lateral chains is governed by the side chains. The calcination of these materials under oxygen led to the formation of nanoporous anatase titanium dioxide the crystallinity and surface area of which depend on the calcination temperature. Similarly titanium dioxide thin films were prepared by the calcination of hybrid thin films prepared by spin coating.

Key-words: Hybrid materials, sol-gel, organotitanium, cyclopentadienyltitanium, xerogels, self-assembly, titanium dioxide, mesoporous, films.

